Palestine Polytechnic University

College of Engineering and Technology

Electrical and Computer Engineering Department

Communication and Electronic Engineering

Graduation project

''Channel Models for MIMO Systems in 4G Networks''

Project Team

Ahmad Mujahed Mohammed Jaber

Suzan Al-Hroub Narmin Al-Dawadeh

Project Supervisor

Dr.Khaled Hijjeh

Hebron-Palestine

2010-2011

Dedication

This project is dedicated to our parents, who have always encouraged us to be in such a position;

Sisters, brothers and friends, for their love;

To our homeland, where our hearts belong…

Our lovely Palestine;

We love you all!

Acknowledgments

We would like to express our greatest gratitude to the following people who help us to accomplish this work. Without their guidance and help the work presented in this project would not have been possible.

The first person who comes to mind is Dr.Khaleed Hijjeh, with his patience, guidance, deep vision, support, and constant encouragement, this work has been done what it is today. We are very glad and it has been an honor to work with him over this year.

In particular, we owe gratitude to all instructors in the electrical and computer engineering department of Palestine polytechnic university. Specifically, to Dr.Ghandi Manasra, Dr.Murad Abu Sbaih, Dr.Osama Ata,Eng.Ahmad Qudaimat for their guidance which was extremely helpful.

Thanks go out to our parents, brothers, sisters, and friends for their love, support, and encouragement. They were really always there.

Abstract

This project attempts to study the behavior of bad urban and rural macro-cells channel models for (4x2) and (2x2) MIMO multipath fading channel. The channel behavior is investigated for (8x2) MIMO system under indoor propagation environment as well. The fading envelops for the multipath components are observed and analyzed manipulating different parameters; changing the symbol rate, doppler shift, and antennas spacing in order to understand the behavior of the MIMO channel so as to ease the deployment of the entire MIMO system. The simulation results shows that the channel behavior is getting better and becomes more stable when increasing the symbol rate and antennas spacing, and at the same time reducing the Doppler shift. The operation frequency's influence on the path-loss that the propagating signals suffer is investigated.

Table of contents:

List of figures:

List of tables:

List of abbreviations:

Abbreviation	Definition
3G	**3rd Generation**
3GPP	3rd Generation Partnership Project
4G	4th Generation
ADD	Antenna Division Duplexing
AOA	Angle-of-Arrival
AP	Access Point
ATM	Automated Teller Machine
BER	Bit Error Rate
BF	Beam-Forming
BS	Base Station
CRC	Communications Research Centre Canada
DC-HSDPA	Dual Carrier- High Speed Downlink Packet Access
DC-HSUPA	Dual Carrier- High Speed Uplink Packet Access
E-DCH	Enhanced Dedicated Channel (also known as HSUPA)
EDGE	Enhanced Data for GSM Evolution
EPC	Evolved Packet Core
FDD	Frequency Division Duplex
GPRS	Global Packet Radio System
GSM	Global System for Mobile communications
HO	Homogeneous channels
HSDPA	High Speed Downlink Packet Access
HS-DSCH	High Speed-Downlink Shared Channel
HSPA	High Speed Packet Access (HSDPA + HSUPA)
HSPA +	High Speed Packet Access Plus (also known as HSPA Evolution or Evolved HSPA)
HSUPA	High Speed Uplink Packet Access
IMS	IP Multimedia Subsystem
IMT	International Mobile Telecommunications
IP	Internet Protocol
ITU	International Telecommunication Union
LOS	Line-of-sight
LTE	Long Term Evolution
M2M	Machine-to-Machine
Mb	Megabit or Mb
Mbps	Megabits per Second
MCSSS	Multi-Carrier Spread Spectrum Signal
MIMO	Multiple-Input Multiple-Output
MISO	Multiple-Input Single-Output
MMS	Multimedia Messaging Service
MR	Multi Receiver
MS	Mobile Station
MT	Multi Transmitter

MU-MIMO	Multi-User Multiple-Input Multiple-Output
NLOS	Non Line-of-Sight
OFDM	Orthogonal Frequency Division Multiplexing
OFDMA	Orthogonal Frequency Division Multiple Access
PDF	Probability density function
PN	Pseudo Noise
PoC	Push-to-Talk over Cellular
QAM	Quadrature Amplitude Modulation
Rel-X	Release 99, Release 4, Release 5, etc. from 3GPP standardization
RF	Radio Frequency
SC-FDMA	Synchronization Channel-Frequency Division Multiple Access
SIMO	Single Input Multiple Output
SISO	Single Input Single Output
SM	Spatial Multiplexing
SMS	Short Message Service
SNR	Signal to noise ratio
ST	Space-Time
STP	Space-Time Processing
SUI	Stanford University Interim
SVD	Singular value decomposition
TDD	Time Division Duplex
TDL	Tapped delay lines
TUI	Technical University of Ilmenue.
UE	User Equipment
UMTS	Universal Mobile Telecommunication System, also known as WCDMA
US	Uncorrelated scattering
UTRAN	UMTS Terrestrial Radio Access Network
VoIP	Voice over Internet Protocol
W-CDMA	Wideband Code Division Multiple Access
WiMAX	Worldwide interoperability for Microwave Access based on IEEE 802.16 standard
WINNER	Wireless world Initiative New Radio
WLOS	Wall Line-of-sight
WNLOS	Wall Non Line-of-Sight
WSS	Wide Sense Stationary
WSSUS-HO	Wide Sense Stationary Uncorrelated scattering Homogeneous

Chapter 1

Introduction

Chapter contents:

1.1. An overview.

In this chapter, a general idea about the project, its objectives, the simulation process's path-loss equations, and the work procedure is to be discussed and further analyzed.

1.1.1. Review for wireless technologies.

Wireless communications have gained enormous popularity since it offers an attractive option for many personal as well as organizational communication needs because of flexibility, cost effectiveness, and mobility. Accordingly there is a growing number of different wireless technologies and standards that are being used such as 3GPP cellular system (2G, 3G, and 4G), WiMAX, Wi-Fi, and Bluetooth. So it's clear that wireless communication is naturally suitable for mobile applications. Thus, the need of wireless communications can't be overestimated.

1.1.2. Limitations facing wireless systems.

The major problems that the wireless communications suffer are mainly the limited spectrum available, propagation channel environment, fading, path-loss, interference and noise.

Since the signal may reach the destination from multipath at the receiver side producing many copies of the signal with different attenuations and with different delays. The multipath environment causes the fading problem in the channel resulted from scattering, reflections, refractions and diffractions.

Despite the fact that multipath arrival of a signal was harmful to the conventional communication system that uses one transmitter and one receiver , multi antenna systems has benefited from this multipath propagation phenomena to enhance the system's capacity, coverage, and quality. But for now the available bandwidth will be the most limiting factor that faces wireless communication systems, thus, all recent research related to wireless field focus on how to efficiently use the bandwidth.[1]

1.1.3. 4G systems.

The approaching 4G mobile communication systems are projected to solve still-remaining problems of third generation systems and to provide a wide variety of new services, from high-quality voice to high-definition video to high-data-rate wireless channels. One of the terms used to describe 4G is MAGIC—Mobile multimedia, anytime anywhere, Global mobility support, integrated wireless solution, and

customized personal service. Technically, 4G stands for one integrated, IP-based environment for all telecommunications requirements including voice, video, broadcasting media and Internet that utilizes both fixed and wireless networks. The fourth generation promises to offer high data rates everywhere over a wireless network.[2]

1.1.4. Channel models in 4G systems.

A generic channel modeling approach can be thought as a channel model framework that can be applied in different scenarios. Each scenario has scenario specific distributions and parameters. By changing the scenario specific distributions in angle and delay domains as well as the scenario specific parameters, we can have different channel models for different scenarios under the same framework of the channel model. It has been widely understood that radio propagation has a significant impact on the performance of wireless communication systems. The impact on future broadband systems is even more important due to increased data rate, bandwidth, mobility, adaptivity, quality of service (QoS), etc. Because of the major influence on the system performance and complexity, radio channel models and simulations have to be more versatile and accurate than in earlier systems.[3]

1.2. General idea of this project.

Limitation of the bandwidth is one of the biggest problems that faces the wireless communications, therefore, multiple-input and multiple-output, or MIMO systems have been developed since it offers significant increases in data throughput and link range without additional bandwidth or transmit power. The MIMO technology depends on using many antennas at the transmitter and many antennas at the receiver to transmit and receive different data streams simultaneously, thus higher data rates are achieved by using MIMO system as shown in figure 1.1.

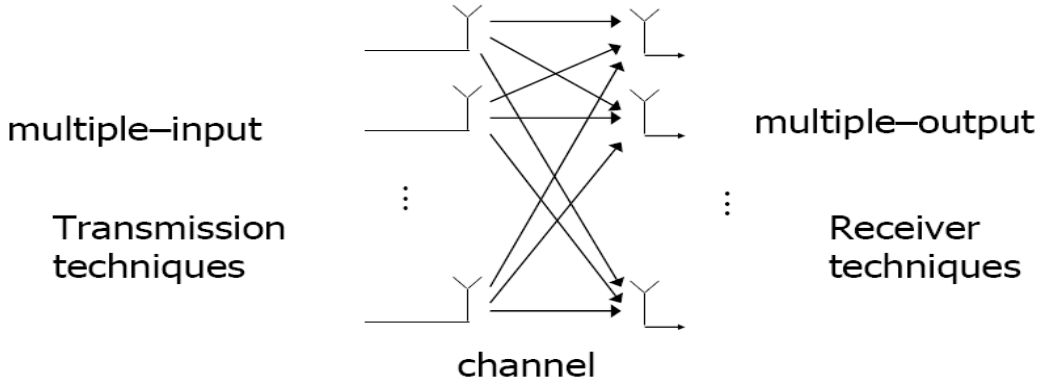

Figure 1.1: MIMO technology

This project attempts to model the channel for MIMO antennas that will be applied in 4G systems. Accurate modeling of MIMO channels is an important

requisite for MIMO system design, simulation and deployment. In channel modeling for MIMO systems there are many parameters that must be considered such as number of transmitter and receiver antennas which plays an important role in designing a good channel model, and the number of multipath fading channels which is the most important factor in building a channel model in MIMO systems.

1.3.Project objectives.

In this project there are four main objectives:

1. Study and perform deep analysis for the channel models of 2X1 MIMO systems through Matlab simulation.
2. Develop 2X2 and 4X2 MIMO channel models that analyze the behavior of bad urban and rural MIMO multipath fading channel.
3. Simulate an indoor propagation environment for 8x2 MIMO configuration.
4. Observing the frequency of operation influence on the path loss.

1.4. Introduction to wireless channels.

Wireless channels operate through electromagnetic radiation from the transmitter to the receiver. In principle, one could solve the electromagnetic field equations, in conjunction with the transmitted signal, to find the electromagnetic field impinging on the receiver antenna. This would have to be done taking into account the obstructions caused by ground, buildings, vehicles, etc. These obstacles between transmitter and receiver will influence the signals propagated through the wireless channel till they reach the destination along different paths, causing random fluctuations on the received channel's signal strengths.

The main impairment factors resulting on these fluctuations are: path loss, fading and shadowing.[4]

1.4.1. Path loss

Path loss or path attenuation is the reduction in power density (attenuation) of an electromagnetic wave as it propagates through space. Path loss is a major component in the analysis and design of the link budget of a telecommunication system.

This term is commonly used in wireless communications and signal propagation. Path loss results due to many factors, such as free-space loss, refraction, diffraction, reflection, aperture-medium coupling loss, and absorption. Path loss is also influenced by terrain contours, urban or rural, propagation medium (dry or moist air), the

distance between the transmitter and the receiver, and the height and location of antennas.

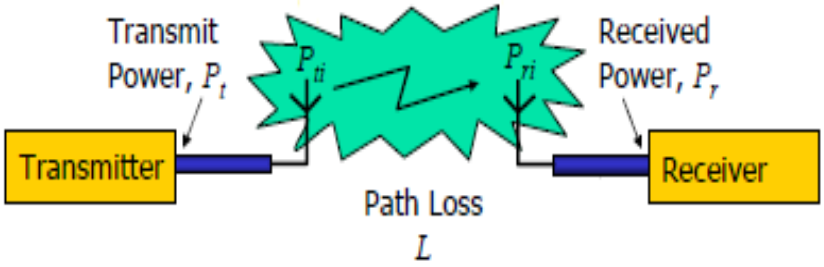

Figure1.2: path loss

Path loss is usually expressed in dB. In its simplest form, the path loss can be calculated using the formula:

$$L = 10n\log_{10}(d) + C \quad \text{(1.1)}$$

Where L is the path loss, n is the path loss exponent, d is the distance between the transmitter and the receiver, and C is a constant which accounts for system losses.[5]

The following are the path-loss models used to formulate the response of the channel throughout the simulation process in this project. More illustration of the path-loss related environments can be found in chapter two. These path-loss models are taken from [6].

- **Bad urban macro-cell:**

Two path-loss models are defined for this scenario; one for the ling of sight (LOS) case and another for the non-line of sight (NLOS).

$$PL(LOS) = 40\log_{10}(d) + 13.47 - 14\log_{10}(h_{BS}) - 14\log_{10}(h_{MS}) + 6\log_{10}\left(\frac{f[GHZ]}{5}\right) + 6 \quad \text{(1.2)}$$

$$PL(NLOS) = 44.9 - 6.55\,log_{10}(h_{BS}[m])]\,log_{10}(d[m]) + 34.46 + 5.83\,log_{10}(h_{MS}[m]) + 20\,log_{10}\left(\frac{f[GHZ]}{5.0}\right) + 8 \quad \text{(1.3)}$$

Where $h_{BS}[m]$ and $h_{MS}[m]$ are the heights of the base station and the mobile station in meters respectively, d is the distance between the T_x and R_x antennas. f is the center frequency.

- **Rural macro-cell:**

$$PL(LOS) = 10.5 + 40\log_{10}(d) + 18.5\log_{10}(h_{BS}) - 18.5\log_{10}(h_{MS}) + 1.5\log_{10}\left(\frac{f[GHZ]}{5}\right) + 4 \quad \text{..... (1.4)}$$

$$PL(NLOS) = \max\left(\left(55.4 + 25.1\log_{10}(d) - 0.13\log_{10}(h_{BS} - 25)\left(\frac{\log_{10}(d)}{100}\right)\right) - 0.9(h_{MS} - 1.5) + 21.3\log_{10}\left(\frac{f[GHZ]}{5}\right), PL_{free}\right) \quad \text{..... (1.5)}$$

Where $PL_{free} = 46.4 + 20\log_{10}(d) + 20\log_{10}\left(\frac{f[GHZ]}{5}\right)$ ..... (1.6)

Where h_{BS} and h_{MS} are the heights of the base station and the mobile station respectively, d is the distance between the T_x and R_x antennas. f is the center frequency.

- **Suburban macro-cell:**

$$PL(LOS) = 23.8\log_{10}(d) + 41.2 + 20\log_{10}\left(\frac{f[GHZ]}{5}\right) + 4 \quad \text{..... (1.7)}$$

$$PL(NLOS) = (44.9 - 6.55\log_{10}(h_{BS})\log_{10}(d)) + 31.46 + 5.83\log_{10}(h_{MS}) + 20\log_{10}\left(\frac{f(GHZ)}{5}\right) + 8 \quad \text{..... (1.8)}$$

Where h_{BS} and h_{MS} are the heights of the base station and the mobile station respectively, d is the distance between the T_x and R_x antennas. f is the center frequency.

- **Indoor small office:**

$$PL(LOS) = 18.7\log_{10}(d) + 46.8 + 20log_{10}\left(\frac{f[GHZ]}{5.0}\right) + 3 \quad \text{..... (1.9)}$$

$$PL(NLOS) = 36.8\log_{10}(d) + 43.8 + 20log_{10}\left(\frac{f[GHZ]}{5.0}\right) + 4 \quad \text{..... (1.10)}$$

Where h_{BS} and h_{MS} are the heights of the base station and the mobile station respectively, d is the distance between the T_x and R_x antennas. f is the center frequency.

- **Fixed Stationary Feeder: Roof-top to Roof-top:**

$$PL(LOS) = \max(23.5\log_{10}(d) + 42.5 + 20\log_{10}(f[GHz]/5.0), PL_{free}) + 4 \ldots \quad (1.11)$$

$$PL(NLOS) = 23.5\log_{10}(d) + 57.5 + 20log_{10}(f[GHz]/5.0) + 8 \ldots \quad (1.12)$$

Where h_{BS} and h_{MS} are the heights of the base station and the mobile station respectively, d is the distance between the T_x and R_x antennas. f is the center frequency. PL_{free} is defined previously.

- **Moving networks:**

$$PL(LOS) = \max(41.1\log_{10}(d) + 17.2 + 20\log_{10}(f[GHz]/5.0), PL_{free}) + 3 \ldots \quad (1.13)$$

Where PL_{free} is as defined previously.

- **Indoor to outdoor:**

The outdoor environment of this scenario is urban, its path-loss model is given by

$$PL = PL_b + PL_{tw} + PL_{in} \quad (1.14)$$

Where

$$PL_b = \max(22.7\log_{10}(d) + 41.0 + 20\log_{10}(f[GHz]/5.0), PL_{free}) + 3$$
$$PL_{tw} = 14 + 15(1 - \cos(\theta))^2$$
$$PL_{in} = 0.5d_{in}$$

Where PL is the path loss equation, PL_b is the urban path-loss, din is the distance from wall to the inside terminal, and θ is the angle between the outdoor path and the normal of the wall.

More details about all equations above can be found in [6].

1.4.2. Fading.

In wireless communications, fading is deviation of the attenuation that a carrier-modulated signal experiences over certain propagation media. The fading may vary with time, geographical position and/or radio frequency.

The presence of reflectors in the environment surrounding a transmitter and receiver create multiple paths that a transmitted signal can traverse. As a result, the receiver sees the superposition of multiple copies of the transmitted signal, each traversing a different path. Each signal copy will experience differences in attenuation, delay and phase shift while travelling from the source to the receiver. This can result in either constructive or destructive interference, amplifying or attenuating the signal power seen at the receiver. Strong destructive interference is frequently referred to as a deep fade and may result in temporary failure of communication due to a severe drop in the channel signal-to-noise ratio.[7]

A more detailed information about fading can be found in chapter two.

1.4.3. Shadowing.

Shadowing is the effect that the received signal power fluctuates due to objects obstructing the propagation path between transmitter and receiver. Shadowing occurs when objects block line of sight between the transmitter and the receiver causes random variations of the received power at a given distance.[1]

1.5. Procedures.

First of all, a literature review were prepared about what has been done in channel modeling for MIMO systems; more than thirty IEEE papers and about ten textbooks have been studied and summarized. Matlab program is the main tool by which the channel models for MIMO system are developed. A comprehensive analysis for channel model that applied two transmitters and one receiver (2x1) MIMO system had been firstly done. The following steps summarize the procedure that we followed throughout this project:

1. Making a literature review about what has been done in channel modeling for MIMO systems.

2. Become familiar with all Matlab tools, demos, and functions that are related to our project.

3. A comprehensive analysis for channel model that applied two transmitters and one receiver 2x1 MIMO system.

4. Finally, channel models that deals (4x2), (2x2), and (8x2) MIMO configurations under different propagation environments have been developed.

Figure1.3 illustrates the scenario of the project.

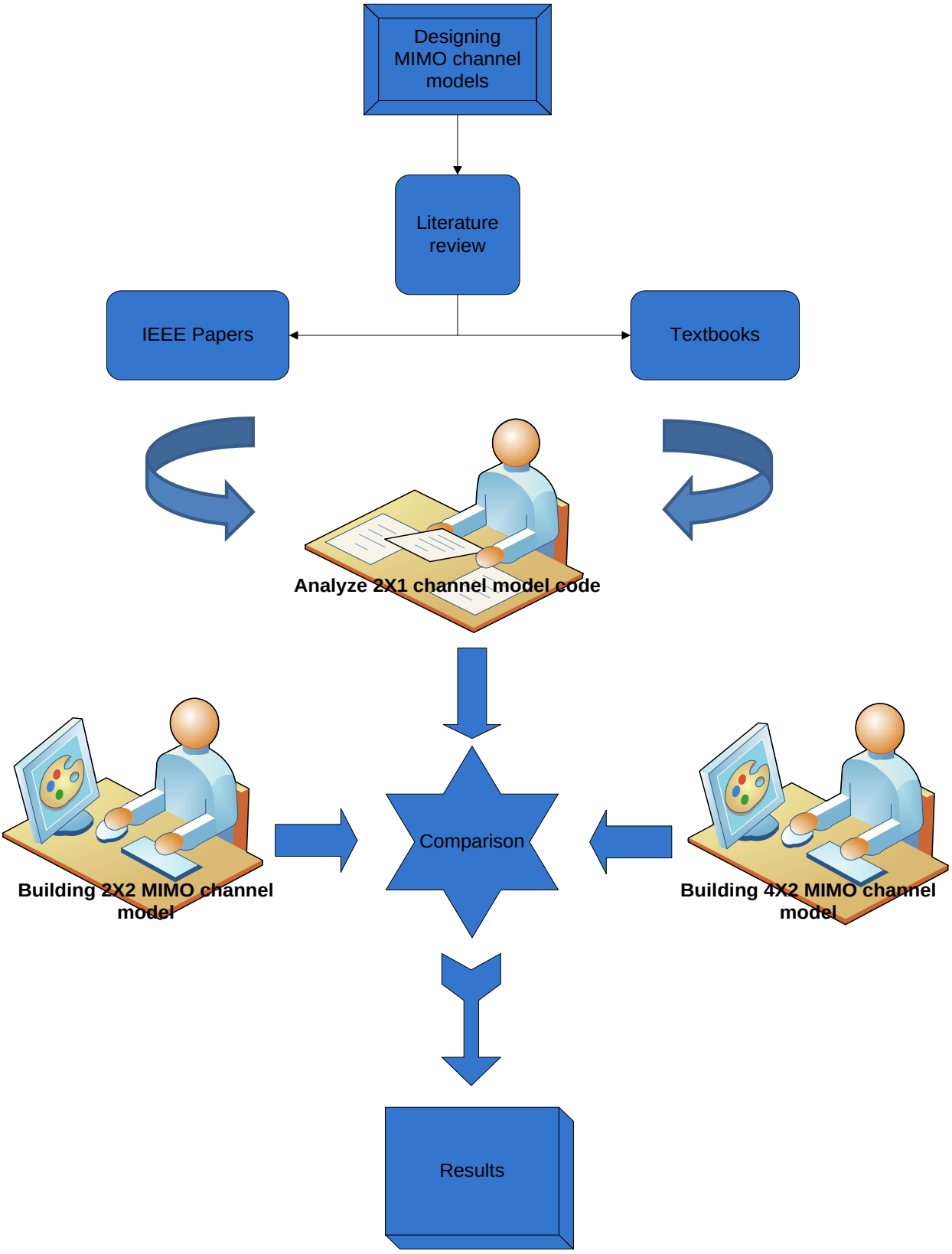

Figure 1.3 : project scenario.

Chapter 2

Literature review

Chapter contents:

2.7. Statistical properties of channel matrix H.

2.7.1. Singular value of H.

2.7.2. Squared Frobenius.

2.8. Channel estimation.

2.8.1. Estimating the ST channel at the receiver.

2.8.2. Estimating the ST channel at the transmitter.

2.8.2.1. Channel estimation at transmitter using feedback.

2.8.2.2. Channel estimation at transmitter using reciprocity.

2.9. Channel dependency.

2.9.1. Environment dependence.

2.9.2. System dependence.

2.9.3. Path loss.

2.10. Summary of channel modeling related IEEE papers.

2.1. Introduction.

The rapid progress in wireless communication systems aims to provide ever higher data rates and greater reliability to the increasing number of users all over the world. Wireless system designing faces a number of challenges including the limited availability of the radio frequency spectrum and a complex time-varying wireless environment; fading and multipath. The use of multiple antennas at the receiver and/or at the transmitter, popularly known as space-time (ST) wireless or multi antenna communications or smart antennas is an emerging technology that promises significant improvements in wireless communications.[8]

Channel modeling has a great influence on wireless systems performance. A MIMO channel is mathematically denoted by a channel matrix which provides an elegant, compact, and unified way to represent physical channels of completely different nature.

This chapter introduces the basic concept of the space time channel for SISO, SIMO, MISO, and MIMO systems. Moreover, this chapter will cover space time propagation concept. Channel modeling approach for MIMO system will be discussed in details. In addition this chapter gives an overview of release 9 and release 10 of 3GPP mobile broadband innovation which is the path to 4G.

2.2. 3GPP broadband mobile evolution.

Wireless data usage is increasing faster now than ever before. So the usage of wireless applications leads to an increasing demand of higher data rate and the need for continued innovations in wireless data technologies to provide more capacity and higher quality of service. 3GPP technologies have evolved from GSM-EDGE to UMTS-HSPA-HSPA+ to provide increased capacity and user experience, and the evolution will continue in the coming years with further enhancements to HSPA+ and the introduction of LTE.[9]

Significant growth in HSDPA and HSUPA deployments occurred recently as well as the introduction of HSPA+. The HSPA is the combination of HSUPA and HSDPA which provided spectrally efficient wireless solution for operators. HSPA+, also referred to as Evolved HSPA, consists of 3GPP Rel-7 enhancements to HSPA that provide improved support and performance for real-time conversational and interactive services such as Push-to-Talk over Cellular (PoC), picture and video sharing and Voice and Video over IP through the introduction of features like MIMO antennas and Higher Order Modulations. Since the Evolved HSPA enhancements are fully backwards compatible with Rel-99/Rel-5/Rel-6, the evolution to Evolved HSPA has been smooth and simple for operators. 3GPP completed the Rel-8 specifications

in March of 2009, which provide further enhancements to the HSPA+ technology and defines a new OFDMA-based technology through the Long Term Evolution (LTE) work item.[9]

With the completion of Rel-8, focus in 3GPP has turned to Rel-9 and Rel-10. Rel-9 is targeted to be complete by 2009 and will add feature functionality and performance enhancements to both HSPA and LTE. For HSPA, additional multi-carrier and MIMO options are introduced. For LTE, additional features and enhancements to support emergency services, location services and broadcast services are the focus. 3GPP has already submitted proposals for the IMT-Advanced evaluation and certification process led by the International Telecommunication Union (ITU). The ITU has defined requirements that will officially define and certify technologies as IMT-Advanced or "4G".[9]

2.2.1. Progress of release 99, release 5, release 6, and release 7.

3GPP Rel-99 UMTS specifications provide the evolutionary path for GSM, General Packet Radio Service (GPRS) and Enhanced Data Rates for GSM Evolution (EDGE) technologies, Rel-99 enabled more spectrally efficient and better performing voice and data services.[9]

Rel-4 introduced call and bearer separation in the Core Network, and Rel-5 introduced some significant enhancements to UMTS, including HSDPA, IMS and IP UTRAN.6 Rel-6 introduced further enhancements to UMTS including HSUPA (or E-DCH), and Advanced Receivers. HSUPA increases data throughput and reduces latency, resulting in an improved user experience for applications such as gaming, VoIP, etc.[9]

Currently, the 3GPP standard supports the 850, 900, 1700, 1800, 1900, 2100, 1700/2100 and 2600 MHz frequency bands .Additionally, the standard will be expanded for use in the 700 MHz bands. There will be further opportunities for introducing 3GPP technologies in frequency bandwidths smaller than 5 MHz.[9]

Rel-7 features were commercially introduced as HSPA+ and trials of HSPA+ began. Rel-7 HSPA+ networks are sometimes also deployed with MIMO antenna systems providing yet another upgrade in performance benefits.[9]

2.2.2. The growing demands for wireless data applications.

The wireless ecosystem, from carriers to handset manufacturers, to network providers, to operating system providers, to application developers is evolving before our eyes and this is not the same market that it was even three years ago. In this industry, innovation is everywhere. With the success factors of high-speed mobile

broadband networks, Internet-friendly handheld devices (smartphones) and a wide variety of applications. It's expected that video will represent 91 percent of all global consumer traffic. Mobile data will increase by 66 times, doubling each year from 2008 to 2013. As the wireless industry prepares for the deluge of IP data traffic brought on by coming 4G networks, mobile core vendor Cisco prophesized that the flood will come long before Long Term Evolution (LTE) and WiMAX networks become common.[9]

2.2.3. 3G devices.

Smartphones are evolving quickly and still compete on hardware features that support key applications like photography or video viewing, but software and applications that enable a user's preferred mobile uses have an increasing influence on device selection**.** Currently, the most compelling applications for 3G mobile broadband include mobile TV, a light version of video conferencing, simple games and multimedia, MMS, SMS, email, and Internet browsing. The long-term future of mobile networks promises to create a premium experience with applications such as telemedicine, mobile virtual presence, mobile to mobile applications such as telematics, enriched navigation experience, interactive gaming, remote sensing applications, mobile education systems, mobile emergency management systems, and far richer advertising opportunities for mobile advertising and entertainment. According to Cisco, "4G" may be the rainmaker to make this happen.[9]

The data traffic for a single subscriber will grow 450 times from 2005 to 2015, in other words it will increase from 30 MB to 14,275 MB by 2015. The number of non-handset mobile devices is set to grow dramatically including products such as data cards, laptops, game consoles, eBooks, ATMs and a host of other M2M applications. Within each of these devices is a wireless data module providing a connection to a wide-area network.[9]

2.2.4. Femto-cells.

Femto-cells are small cellular base stations using broadband connections which intended to extend coverage in home and small office environments. Mobile phone user's desire for improved 3G network coverage in their homes will be the main driving force behind femto-cell deployments in the next few years, with subscriptions predicted to surpass the 15 million mark worldwide during 2012. By 2014, there will be almost six femto-cells per macro base station and the number of users that connect to a femto-cell on a regular basis is estimated to surpass 70 million.[9]

2.2.5. Status and highlights of release 8: HSPA+ and LTE/EPC.

3GPP Rel-8 provided significant new capabilities, not only through enhancements to the W-CDMA technology but also the addition of OFDM technology through the introduction of LTE. By using WCDMA Rel-8 provided the capability to perform 64QAM modulation with 2x2 MIMO on HSPA+, as well as the capability to perform dual carrier operation for HSPA+. These enhancements enabled the HSPA+ technology to reach peak rates of 42 Mbps. Rel-8 also introduced Evolved Packet System consisting of a new flat-IP core network called the Evolved Packet Core (EPC) coupled with a new air interface based on OFDM called Long Term Evolution (LTE). In Rel-8, LTE defined new physical layer specifications consisting of an OFDMA based downlink and SC-FDMA based uplink that is used to improving battery life by reducing peak-to-average power. Moreover, Rel-8 also defined a suite of MIMO capabilities supporting open and closed loop techniques, Spatial Multiplexing (SM), Multi-User MIMO (MU-MIMO) schemes and beam-forming.[9]

2.2.6. Status of release 9: HSPA+ enhancements.

3GPP Rel-9 focuses on enhancements to HSPA+ and LTE.

2.2.6.1. Non-contiguous dual-cell HSDPA (DC-HSDPA).

In deployments where multiple downlink carriers are available, multi-carrier HSDPA operation offers an attractive way of increasing coverage for high bit rates. Dual-carrier (or dual-cell) HSDPA operation enables a base station to schedule HSDPA transmissions over two adjacent 5 MHz carriers simultaneously to the same user, which gives a rate of 42 Mbps for 64QAM.[9]

In order to provide the benefits of dual-carrier HSDPA where two adjacent carriers cannot be made available to the user, Rel-9 introduces dual-band HSDPA operation, where in the downlink the primary serving cell resides on a carrier in one frequency band and the secondary serving cell on a carrier in another frequency band . In the uplink transmission takes place only on one carrier, which can be configured by the network on any of the two frequency bands.[9]

In Rel-9, dual-band HSDPA operation is introduced for three different band combinations, one for each ITU region :

- Band I (2100MHz) and Band VIII (900MHz).
- Band II (1900MHz) and Band IV (2100/1700MHz).
- Band I (2100MHz) and Band V (850MHz).

In Dual-band HSDPA operation the user can be scheduled in the primary serving cell as well as in a secondary serving cell over two parallel HS-DSCH transport

channels. All non-HSDPA-related channels are transmitted from the primary serving cell only, and all physical layer procedures are essentially based on the primary serving cell.[9]

2.2.6.2. MIMO plus DC-HSDPA.

Rel-8 introduced two ways to achieve a theoretical peak rate of 42 Mbps :dual-carrier HSDPA and 2x2 MIMO in combination with 64QAM. Rel-9 combines dual-carrier HSDPA operation with MIMO .The peak downlink rate is thus doubled to 84 Mbps and the spectral efficiency is boosted significantly compared to dual-carrier HSDPA operation without MIMO. In order to provide maximum deployment flexibility for the operator, the MIMO configuration is carrier-specific, meaning that, if desired, one carrier can be operated in non-MIMO mode and the other carrier in MIMO mode.[9]

2.2.6.3. Contiguous dual-cell HSUPA (DC-HSUPA).

The data rate improvements in the downlink call for improved data rates also in the uplink. Therefore, support for dual-carrier HSUPA operation on adjacent uplink carriers is introduced in Rel-9. This doubles the uplink peak rate to 23 Mbps for the highest modulation scheme (64QAM). Dual-carrier HSUPA operation can only be configured together with dual-carrier HSDPA operation and the secondary uplink carrier can only be active when the secondary downlink carrier is also active.[9]

2.2.6.4. Transmit diversity extension for non-MIMO UEs.

The 2x2 MIMO operation for HSDPA specified in Rel-7 allows transmission of up to two parallel data streams to a MIMO UE over a single carrier. If and when the HSDPA scheduler in the base station decides to only transmit a single stream to the UE for any reason the two transmit antennas in the base station will be used to improve the downlink coverage by single-stream transmission using BF. As MIMO is being deployed in more and more networks, single-stream transmission using BF also towards non-MIMO UEs that reside in MIMO cells becomes an increasingly attractive possibility.[9]

2.2.7. Release 10 (LTE-Advanced).

3GPP LTE Rel-10 and beyond, LTE-Advanced, is intended to meet the diverse requirements of advanced applications. LTE-Advanced will be an evolution of LTE,

which will provide for backward compatibility with LTE and will meet or exceed all IMT-Advanced requirements.[9]

These are some of the current agreements on the requirements for LTE-Advanced: [10]

- Peak data rate of 1 Gbps for downlink (DL) and 500 Mbps for uplink (UL).
- The system should support downlink peak spectral efficiency up to 30 bps/Hz and uplink peak spectral efficiency of 15bps/Hz with an antenna configuration of 8×8 or less in DL and 4×4 or less in UL.
- Average user spectral efficiency in DL must be 2.4 bps/Hz/cell with MIMO 2×2, 2.6 bps/Hz/cell with MIMO 4×2 and 3.7 bps/Hz/cell with MIMO 4×4, whereas in UL the target average spectral efficiency is 1.2 bps/Hz/cell and 2.0 bps/Hz/cell with SIMO 1×2 and MIMO 2×4, respectively.
- The mobility and coverage requirements are identical to LTE Release 8. There are only differences with indoor deployments that need additional care in LTE-Advanced.
- In terms of spectrum flexibility, the LTE-Advanced system will support scalable bandwidth and spectrum aggregation with transmission bandwidths up to100MHz in DL and UL.

There are also some of the LTE-Advanced technical proposals:

- **Supporting of wider bandwidth:** a significant underlying feature of LTE-Advanced will be the flexible spectrum usage. The framework for the LTE-Advanced air-interface technology is mostly determined by the use of wider bandwidths, potentially even up to 100 MHz, noncontiguous spectrum deployments, also referred to as spectrum aggregation, and a need for flexible spectrum usage. In general OFDM provides a simple means to increase bandwidth by adding additional subcarriers.[9] [10]
- **Enhanced multiple-input multiple-output transmission:** another significant element of the LTE-Advanced technology framework is MIMO, as in theory it offers a simple way to increase the spectral efficiency. The combination of higher order MIMO transmission, beam-forming or Multi-User. [10]

2.3. Space-time channel propagation.

This section gives an overview of the wireless channel behavior, the focus being on outdoor macro-cellular environments. It also describes the wireless channel, and scattering and fading models for such channels.

2.3.1. The wireless channel.

A signal propagating through the wireless channel arrives at the destination along multi different paths which arise from scattering (deviation of waves from a straight trajectory as passing through the channel), reflection (wave propagating in one medium impinges upon another medium having different electrical properties, so the wave is partially reflected and partially transmitted) and diffraction (occurs when the radio path between the transmitter and receiver is obstructed by a surface that has sharp irregularities) of radiated energy by objects in the environment. The power of the signal drops off due to three effects; path loss (is a measure of attenuation based only on the distance to the transmitter), macroscopic fading and microscopic fading. The first which is the mean propagation loss is a range dependent, in microcellular environments comes from inverse square law power loss, and the effect of ground reflection. In free space propagation, the inverse square law power loss and received signal power is given by [1] [8]

$$P_r = P_t \left(\frac{\lambda_c}{4\pi d}\right)^2 G_t G_r \quad \text{.....} \quad (2.1)$$

Where P_t and P_r are the transmitted and received powers respectively, λ_c is the wave-length, G_t, G_r are the power gains of transmit and receive antennas respectively, and d is the range separation. In cellular environments the received power can be approximated by

$$P_r = P_t \left(\frac{h_t h_r}{d^2}\right)^2 G_t G_r \quad \text{.....} \quad (2.2)$$

Where h_t, h_r are the effective heights of transmit and receive antennas respectively, with assumption that $d^2 >> h_t\, h_r$, so the effective path loss follows an inverse fourth power low. In real environments the path loss exponent varies from 2.5 to 6. Also there are several path loss models such as Okumura and Hate models. [8]

- **Okumura model:** it is one of the most widely used models for signal prediction in urban areas, which based totally on measurements and it's given by

$$L_{50}(dB) = L_F + A_{mn}(f,d) - G(h_{re}) - G(h_{te}) - G_{AREA} \quad \text{.....} \quad (2.3)$$

Where L_{50} is the median path loss (50%), L_F is the free space path loss, $A_{mn}(f, d)$ is the median attenuation relative to free space, $G(h_{re})$ and $G(h_{te})$ are antenna height gain factors, G_{AREA} is the gain due to the type of environment.[1]

- **Hata model:** it is a developed version of the Okumura Model, which incorporates the graphical information from Okumura model and develops it further to realize the effects of diffraction, reflection and scattering caused by city structures and it is given by

$$L_{50}(dB) = 69.55 + 26.16 \log f_c - 13.82 \log h_{te} - a(h_{re}) + (44.9 - 6.55 \log h_{te}) \log d \quad \text{(2.4)}$$

Where f_c is the frequency (in MHz), h_{te} and h_{re} is the effective transmitter and receiver antenna height respectively, d is the separation between the transmitter and receiver (in Km), and $a(h_{re})$ is the correlation factor for effective receiver antenna height. [1]

The second effect that cause signal power drops is macroscopic fading (long term fading or shadowing), this results from blocking effect by buildings and natural features where the received signal power level fluctuate slowly. This fading is determined by the local mean of a fast fading signal the probability density function (PDF): [10]

$$f(x) = \frac{1}{\sqrt{2\pi\sigma}} e^{\frac{-(x-\mu)2}{2\sigma 2}} \quad \text{(2.5)}$$

Where μ and σ are respectively the mean and standard deviation of the signal power .

The third effect is Microscopic fading (fast fading), this results from the constructive and destructive combination of multipath, and the envelope of the received signal has a Rayleigh density function:

$$f(x) = \frac{2x}{\Omega} e^{-\frac{x^2}{\Omega}} u(x) \quad \text{(2.6)}$$

Where Ω is the average received power. If there is direct Line-of-sight (LOS) path present, the signal envelope is Rician. There are also three additional types of fading such that: [8]

1. Doppler spread or time selective fading which is time varying fading due to scattered or transmitter/receiver motion. The selective fading can be characterized by the coherence time (T_c) which is the time over which the channel remains not varying.
2. Delay spread or frequency selective fading present the span of path delays, and is caused by delay spread, it's characterized by the coherence bandwidth

(it is a statistical measure of the range of frequencies over which the channel can be considered flat).

3. Angle spread or space selective fading which refers to the spread in AOA's of multipath components at receiver antenna array. The space selective fading caused by angle spread where the signal amplitude depends on the spatial location of the antenna, it characterized by the coherence distance d_c (Antenna spacing must be such that the fading at each antenna is independent). [8]

2.3.2. Fading models.

In wireless communications, fading is deviation of the attenuation that a carrier-modulated telecommunication signal experiences over certain propagation media. The fading may vary with time, geographical position and/or radio frequency.

The presence of reflectors in the environment surrounding a transmitter and receiver create multiple paths that a transmitted signal can travel. As a result, the receiver sees the superposition of multiple copies of the transmitted signal, each traveling a different path. Each signal copy will experience differences in attenuation, delay and phase shift while travelling from the source to the receiver. This can result in either constructive or destructive interference, amplifying or attenuating the signal power seen at the receiver. Strong destructive interference is frequently referred to as a deep fade and may result in temporary failure of communication due to a severe drop in the channel signal-to-noise ratio.[1] [11]

Fading channel models are often used to model the effects of electromagnetic transmission of information over the air in cellular networks and broadcast communication. Mathematically, fading is usually modeled as a time-varying random change in the amplitude and phase of the transmitted signal.[11]

There are two main types of fading, small scale fading and large scale fading:

a) **Small scale fading** (rapid fluctuations in the signal's envelope) is a characteristic of radio propagation resulting from the presence of the reflectors and scatters that cause multiple versions of the transmitted signal to arrive at the receiver, each distorted in amplitude, phase and angle of arrival.[1]

Small scale fading has the following forms:

1. **Slow fading** occurs when the coherence time (is a measure of the minimum time required for the magnitude change of the channel to become uncorrelated from its previous value) of the channel is large relative to the delay constraint of the channel. In this case, the amplitude and phase change imposed by the channel can be considered roughly constant over the period of use. Slow fading can be caused by

a large obstruction such as a hill or large building obscures the main signal path between the transmitter and the receiver.[1] [11]

2. **Fast fading** occurs if the channel impulse response changes rapidly within the symbol duration. In other words, fast fading occurs when the coherence time of the channel is smaller than the symbol period of the transmitted signal. This causes frequency dispersion or time selective fading due to Doppler spreading. Fast fading is due to reflections of local objects and the motion of the objects relative to those objects.[11]

3. **Flat fading** occurs when the coherence bandwidth (is the range of frequencies over which two frequency components have a strong potential for amplitude correlation) of the channel is larger than the bandwidth of the signal. Therefore, all frequency components of the signal will experience the same magnitude of fading.[1]

4. **Frequency-selective fading** occurs when the coherence bandwidth of the channel is smaller than the bandwidth of the signal. Different frequency components of the signal therefore experience uncorrelated fading.[1]

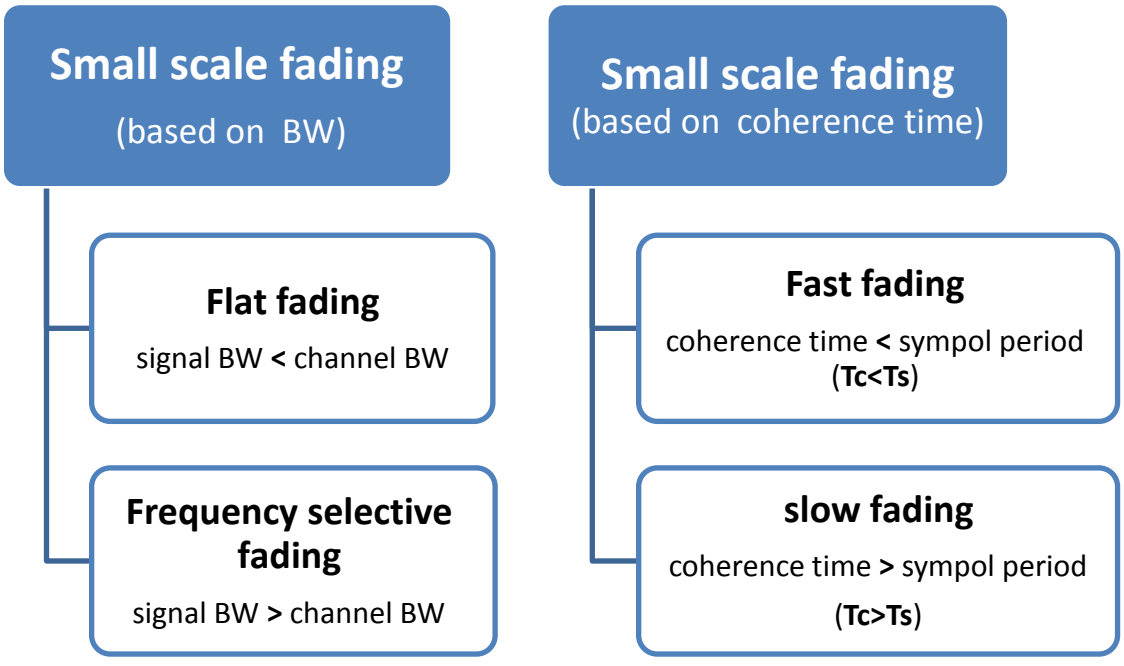

Figure 2.1: small scale fading.

b) **Large scale fading** (slow fluctuations in the signal's envelope) is explained by the gradual loss of received signal power (since it propagates in all directions) with transmitter-receiver separation distance.[1]

Several fading models have been developed, here are the most used:

1. **Rayleigh fading** is a statistical model for the effect of a propagation environment on a radio signal, such as that used by wireless devices. Rayleigh fading models assume that the magnitude of a signal that has passed through a communications channel will vary randomly, or fade, according to a Rayleigh distribution . Rayleigh fading is most applicable when there is no dominant propagation along a line of sight between the transmitter and receiver. The Rayleigh distribution has a probability density function given by: [1]

$$p(r) = \begin{cases} \frac{r}{\sigma^2} exp\left(-\frac{r^2}{2\sigma^2}\right) & 0 \le r < \infty \\ 0 & r < 0 \end{cases} \quad \text{..... (2.7)}$$

Where σ is the rms of the received voltage signal before envelope detection, and σ^2 is the time-average power of the received signal before envelope detection.

2. **Rician fading** whenever there is a dominant stationary signal component present, such as a line-of-site propagation path, the small-scale fading envelope is Rician. In such a situation, random multipath components arriving at different paths are superimposed on a stationary dominant signal. The Rician distribution degenerates to a Rayleigh distribution when the dominant component fades away. The Rician distribution is given by:

$$p(\mathrm{r}) = \begin{cases} \frac{\mathrm{r}}{\sigma^2} \mathrm{e}^{-\frac{(\mathrm{r}^2+\mathrm{A}^2)}{2\sigma^2}} \mathrm{I}_0\left(\frac{\mathrm{Ar}}{\sigma^2}\right) & \mathrm{A} \ge 0, \mathrm{r} \ge 0 \\ 0 & \mathrm{r} < 0 \end{cases} \quad \text{..... (2.8)}$$

Where the parameter (A) denotes the peak amplitude of the dominant signal. The Rician distribution is often described of a parameter k which is defined as the ratio between the deterministic signal power and the variance of the multipath.[1]

2.3.3. Scattering in macro-cells.

Scatters between the terminal and base station can be categorized as local to terminal scatters, remote scatters, or local to base scatters. Local to terminal scatters is caused by building or other scatters. remote scatters results from remote dominant scatters and it causes delay and angle spread, and local to base scatters where there is no contribution from outside scatters and this effect is modeled with a scatters exclusion zones around the bas-station.[8]

2.4. Propagation scenarios.

A set of multidimensional channel models are developed in wireless communication systems that cover wide scope of propagation scenarios and environments, and based on generic channel modeling approach, this approach enables the use of the same channel data in different link level and system level simulations without changing the basic propagation model. A wide variety of radio propagation models for different wireless services that specifically address varying propagation environments and operating frequency bands are generally known, a large number of propagation prediction models have been developed for various terrain irregularities, urban streets and buildings, earth curvature, etc. In many projects such as the generic WINNER II interim channel model follows a geometric-based stochastic channel modeling approach which allows creating of virtually unlimited double directional radio channel model. The following will present some of the propagation scenarios.[6]

- **Indoor small office**.

This scenario is defined for both LOS and NLOS cases, Base stations (Access Points) in this scenario are assumed to be in corridor, thus LOS case is corridor-to-corridor and NLOS case is corridor-to-room. In the NLOS case the basic path-loss is calculated into the rooms adjacent to the corridor where the AP is situated. For rooms farther away from the corridor wall-losses must be applied for the walls parallel to the corridors. The Floor Loss is constant for the same distance between floors, but increases with the floor separation and has to be added to the path-loss calculated for the same floor. The indoor environment is local area here.[6]

In [12], the indoor measurements performed using network analyzer at 2 and 5 and 17 GHz, the RF bandwidth was 500 MHz. The environment of the measurement locations was composed of a corridor of length 21.7 m, width 2 m and height 3 m and a room with dimensions 7x8x2.8 m. Both antennas were mounted on stands at a height of 1.8 m.

It was found that in LOS cases, the path-loss exponents are 1.5, 1.7, and 1.6 respectively at the three frequency bands. There is almost no difference and one cannot find how the path-loss exponents change with frequencies. However, for NLOS cases, the path-loss exponents were increased with the center frequencies.

- **Indoor to outdoor.**

For the propagation in this scenario there exist some different sub-scenarios. The indoor to outdoor environment is somewhat more complex than the single scenarios. Normally it has been sufficient to model LOS and NLOS conditions. This scenario

defines the paths BS-wall (indoors), penetration through the exterior wall and path from the wall to the MS. The BS-wall path can be LOS or NLOS depending on the BS location. The penetration through the wall depends on the wall. Eventually the wall-MS path can be either LOS or NLOS. In addition, the floor affects also the propagation.[6]

The four sub-scenarios Indoor to outdoor propagation are:

1. BS near the exterior wall, MS in WLOS (Wall in LOS towards MS).
2. BS near exterior wall, MS in WNLOS (Wall in NLOS towards the MS) behind one corner.
3. BS near the exterior wall, MS in WNLOS on the opposite side of the building (wing).
4. BS far from the exterior wall, MS in WLOS.

- **Urban micro-cell.**

For microcells the base station is placed well below the average rooftop where the height of the antenna at the BS and MS is assumed to be below the tops of surrounding buildings. Both antennas are assumed to be outdoors in an area. The streets in the coverage area are classified to the Main Street, perpendicular streets, and parallel streets. This scenario is defined for LOS and NLOS cases. The Cell shapes are defined by the surrounding building in local and metropolitan area.[6]

- **Bad Urban micro-cell.**

This scenario is the same in layout to Urban Micro-cell scenarios but here with long delays. The propagation characteristics are such that multipath energy from distant objects can be received at some locations. This energy has significant power, and exhibits long excess delays. Such situations typically occur when there are clear radio paths across open areas, such as large squares and parks.[6]

- **Indoor hotspot.**

This scenario represents the propagation conditions pertinent to operation in a typical indoor hotspot, with wide but non-ubiquitous coverage and low mobility. Traffic of high density would be expected in such scenarios, as in factories, train stations and airports, where the ranges between a BS and a MS or between two MS can be significant. In this scenario, LOS and NLOS propagation conditions could exist.[6]

- **Outdoor to indoor.**

In outdoor-to-indoor scenario the MS antenna height is assumed to be at 1 – 2 m (plus the floor height), and the BS antenna height below roof-top, at 5 - 15 m

depending on the height of surrounding buildings. Outdoor environment is metropolitan area, typical urban microcell where the user density and the requirements for system throughput and spectral efficiency are high.

In[6], a propagation loss model for LOS outdoor to indoor scenario is proposed. Measurements to test the validity of this model were carried out at 2.385 and 5.184 GHz in three different U.K. cities and the proposed model is said to be in agreement with the measurements.

In[13], this paper proposes an outdoor-to-indoor path loss model that considers the paths through wall openings. The measurements were conducted at a department store at 8.45 GHz and the transmitting antenna was at a height of 14 meters. The path loss model assumes that the loss is a sum of outdoor propagation loss, wall opening penetration loss, and indoor propagation loss. The measurements show that the penetration loss of wall openings ranges from 5 to 28 dB with a mean value of 17.2 dB. The indoor attenuation coefficient was measured to be 0.348 dB/m.

- **Suburban macro-cell.**

In this scenario base stations are located above the rooftops to allow wide area coverage, and mobile stations are outdoors at street level. Buildings are typically low residential detached houses with one or two floors, or blocks of flats with a few floors. Occasional open areas such as parks, both LOS and NLOS conditions exist.[6]

- **Urban macro-cell.**

In macro-cells, the base station is often placed above an average rooftop where the mobile station is located outdoors at street level and fixed base station clearly above surrounding building height. As for propagation conditions, obstructed or non-line of sight is a common case, since street level is often reached by a single diffraction over the rooftop. Buildings height and density in typical urban macro-cell are mostly homogenous.[6]

- **Bad urban macro-cell.**

Bad urban macro-cell has frequency range from (2-6) GHz and defined for both LOS and NLOS cases. It describes the cities with buildings with inhomogeneous building heights or densities. The inhomogeneous is caused due to large water areas that separate the building or due to the high-rise skyscrapers or by mountainous surrounding the city. This urban causes dispersive propagation in delay and angular domain and it is differs from urban macro-cell by an additional far scatter cluster. [6]

- **Rural macro-cell.**

It represents radio propagation in large areas with low building density. LOS conditions can be expected to be in most of the coverage area because of the height of the AP antenna is much higher than the average building height. The channel has frequency range (2–6) GHz and used different antenna heights for BS and MS with fixed location for the AP antenna. An extra loss is achieved when the UE is inside a building and the UE antenna has a velocity range from 0 to 200 km/h**.**[6]

- **Moving networks.**

Rural Moving Network represents radio propagation in a rural area where both the AP and the UE are moving with very high speed, it occurs in high-speed trains where wireless coverage is provided by so-called moving relay stations. The link between the fixed network and the moving network is typically a LOS wireless link which propagation characteristics are represented by rural macro-cell propagation scenario**.**[6]

2.5. Radio channel measurement tools.

Different radio channel measurement system can be used in the propagation measurements, here are some of them.

- **Propsound.**

It is a multi-dimensional radio channel sounder based on the spread spectrum sounding method in the delay domain, Which is suitable for determining the radio channel measurements for both the time-domain and spatial-domain. It uses a time-domain switching with optional super-resolution techniques to cover the polarizations, FDD frequencies or spatial dimensions across antenna arrays and give accurate measurements for SISO, SIMO, and MIMO.[6]

- **TUI sounder.**

The channel sounder RUSK TUI-FAU, is a real-time radio channel measurement system that supports MIMO. The channel sounder measures the channel response matrix between all transmitting and receiving antenna by switching between different antennas, which means that the sounder uses only one transmitter and receiver channel to cause a reduction in the sensitivity to channel**.** The channel sounder (RUSK) uses multi-carrier spread spectrum signal (MCSSS) with rectangular shape in frequency domain in order to concentrate the signal energy into the band of interest.[6]

- **CRC sounder.**

It is a fourth generation of a PN sounder design with 20 MHz bandwidth and operates over the range 69 dBm to 89 dBm, where the transmitter and receiver for a CRC have two RF sections with bandwidths centered on 2.25 GHz and 5.8 GHz. The transmitter transmits in both bands. CRC sounder depends on bread-board style in its construction which includes semi-rigid cables connecting various modules (such as power splitters, mixers, and amplifiers) this construction keep maintained to allow reconfiguration for different measurement.[6]

2.6. ST channel models.

A typical ST wireless system uses one or more antennas at the transmitter and/or the receiver with a certain narrow band-width. This section discusses the SISO, SIMO, MISO and MIMO channel models, and the developed techniques that are used for constructing channels from channel description and from capturing macro cellular effect on ST channel.

2.6.1. SISO channel.

SISO is a radio channel standard where the transmitter uses one antenna as does the receiver. There is no diversity and no additional processing required. The advantage of a SISO system is its simplicity. However, the SISO channel is limited in its performance. Interference and fading will impact the system more than a MIMO system using some form of diversity, and the channel bandwidth is limited by Shannon's law; that is the throughput being dependent upon the channel bandwidth and the signal to noise ratio.[8] [14]

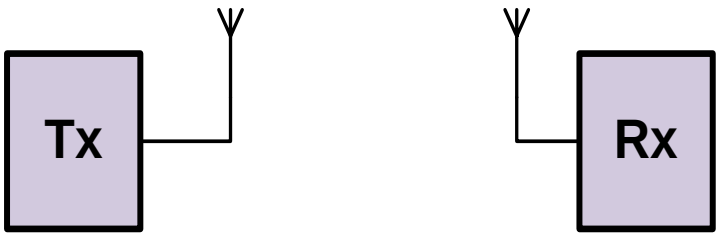

Figure 2.2: SISO system.

Consider $h(\tau,t)$ as the time varying channel impulse response that comes from the input of filter at the transmitter which is called pulse shaping filter $g(\tau)$, in another

meaning it is the channel from transmitter to the receiver antenna and it is the complex envelope of the band pass impulse response function.

If a signal s(t) is transmitted the received signal y(t) is given by

$$y(t) = \int_0^{\tau_{total}} h(\tau, t)s(t-\tau)d\tau = h(\tau, t) * s(t) \quad \text{.....} \quad (2.14)$$

Where $*$ denotes the convolution operator and assuming a causal channel impulse response of duration τ_{total}.

2.6.2. SIMO channel.

The SIMO or Single Input Multiple Output version of MIMO occurs where the transmitter has a single antenna and the receiver has multiple antennas. This is also known as receiving diversity. It is often used to enable a receiver system that receives signals from a number of independent sources to combat the effects of fading. SIMO has the advantage that it is relatively easy to implement although it does have some disadvantages in that the processing is required in the receiver. The use of SIMO may be quite acceptable in many applications, but where the receiver is located in a mobile device such as a cellphone handset, the levels of processing may be limited by size, cost and battery drain. There are two forms of SIMO that can be used; Switched diversity SIMO that looks for the strongest signal and switches to that antenna, and Maximum ratio combining SIMO that takes both signals and sums them to give a combination. In this way, the signals from both antennas contribute to the overall signal.[8] [14]

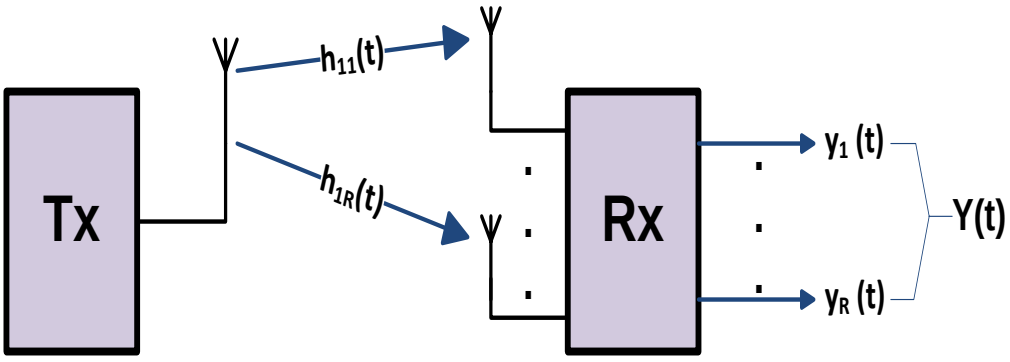

Figure 2.3: SIMO system.

Consider a SIMO channel with M_R receive antennas. The SIMO channel can be considered as an M_R SISO channels in which the impulse response between the transmit antenna and the *i*th (i = 1,2,…, M_R) receive antenna, is $h_i(\tau, t)$. Then the channel $h(\tau, t)$ is given by:

$$\mathbf{h}(\tau, t) = \left[h_1(\tau, t) h_2(\tau, t) \dots h_{M_R}(\tau, t)\right]^T \quad \text{(2.15)}$$

If the signal s (t) is transmitted, then the received signal at the *i*th receive antenna $y_i(t)$ is given by:

$$y_i(t) = h_i(\tau, t) * s(t), \qquad i = 1,2, \dots, M_R \quad \text{(2.16)}$$

And $$y(t) = \left[y_1(t) y_2(t) \dots y_{M_R}(t)\right]^T \quad \text{(2.17)}$$

Finally y (t) is expressed as

$$y(t) = \mathbf{h}(\tau, t) * s(t) \quad \text{(2.18)}$$

2.6.3. MISO channel.

Multiple-input single-output (MISO) has multiple transmitting antennas and one receive antenna. If the channel is known to the multiple antenna transmitters, the transmitter will weight the transmission with weights, depending on the channel coefficients, so that there is coherent combining at the single antenna receiver.[8] [15]

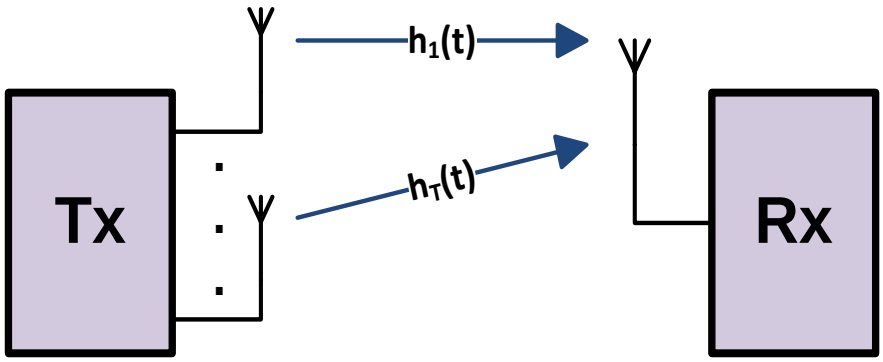

Figure 2.4: MISO system.

The MISO channel comprises M_T SISO links, denoting the impulse response between the *j*th (j =1,2,…,M_T) transmit antenna and the receive antenna by $h_j(\tau, t)$, the MISO channel may be represented by a 1 x M_T vector $\mathbf{h}(\tau, t)$ given by

$$\mathbf{h}(\tau, t) = \left[h_1(\tau, t) h_2(\tau, t) \dots h_{M_T}(\tau, t)\right] \quad \text{(2.19)}$$

If a signal $s_j(t)$ is transmitted from the *j*th transmit antenna, then the received signal is y(t), where y(t) can be expressed as

$$y(t) = \sum_{j=1}^{M_T} h_j(\tau, t) * s_j(t) \quad \text{.....} \quad (2.20)$$

2.6.4. MIMO channel.

Multiple-input multiple-output (MIMO) radio communications based on transmit/receive diversity are attracting increasing interest, due to the enhanced capacity or radio link robustness they promise in comparison with conventional SISO or SIMO techniques.[16]

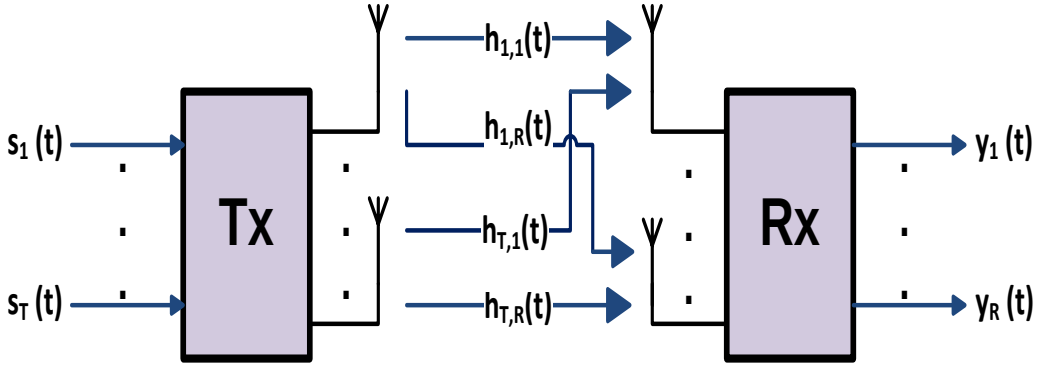

Figure 2.5: MIMO system.

The basic concept of MIMO is that the transmitted signals from all transmit antennas are combined at each receive antenna element in such a way as to improve the Bit Error Rate (BER) performance or the data rate of the transmission. Both the network's Quality of Service and the operator's revenues can be increased significantly. Space-Time Processing (STP) is the core concept of MIMO systems. Time is the natural dimension of digital communication data. Space refers to the spatial dimension inherent in the use of multiple spatially distributed antennas.[8] [17]

MIMO systems with MT transmit antennas and MR receive antennas. Denoting the impulse response between the *j*th (*j* =1,2,…, MT) transmit antenna and the *i*th (*i* =1,2,…,MR) receive antenna by $h_{i,j}(\tau, t)$ the MIMO channel is given by:

$$H(\tau, t) = \begin{bmatrix} h_{1,1}(\tau,t) & h_{1,2}(\tau,t) & \cdots & h_{1,M_T}(\tau,t) \\ h_{2,1}(\tau,t) & h_{2,2}(\tau,t) & & h_{2,M_T}(\tau,t) \\ \vdots & & \ddots & \vdots \\ h_{M_R,1}(\tau,t) & h_{M_R,2}(\tau,t) & \cdots & h_{M_R,M_T}(\tau,t) \end{bmatrix} \quad \text{.....} \quad (2.21)$$

The vector $\left[h_{1,j}(\tau,t)h_{2,j}(\tau,t)\ldots h_{M_R,j}(\tau,t)\right]^T$ is the channel introduced by the *j*th transmit antenna across the receive antenna array. Further, given that signal $s_j(t)$ is launched from the *j*th transmit antenna, the received signal at the *i*th received antenna, $y_i(t)$ is given by

$$y_i(t) = \sum_{j=1}^{M_T} h_{i,j}(\tau,t) * s_j(t), \qquad i = 1,2,\ldots.,M_R \quad \ldots\ldots\ldots\ldots\ldots\ldots\ldots\ldots\ldots\ldots \quad (2.22)$$

The input-output relation for the MIMO channel may be expressed in matrix notation as

$$y(t) = \mathbf{H}(\tau,t) * s(t) \quad \ldots\ldots\ldots\ldots\ldots\ldots\ldots\ldots\ldots\ldots\ldots\ldots\ldots\ldots\ldots\ldots \quad (2.23)$$

Where $s(t) = \left[s_1(t)s_2(t)\ldots s_{M_T}(t)\right]^T$ is an M_T x1 vector, and y(t) is a vector of dimension M_R x 1, in which $y(t) = \left[y_1(t)y_2(t)\ldots y_{M_R}(t)\right]^T$.[8]

2.7. Statistical properties of channel matrix H.

In particular the statistical properties of the channel matrix are the singular values and the squared Frobenius norm. MIMO channel can be decomposed to several parallel SISO channels called Eigen-channels or Eigen-modes via singular value decomposition (SVD). [8][18]

2.7.1. Singular values of H.

Channel matrix Eigen values is essential to the effectiveness of MIMO and the communication, distribution of singular values is a measure of the relative usefulness of various spatial paths through the channel.[8] [19]

The M_R x M_T channel matrix **H**, with rank r, has singular value decomposition

$$\mathbf{H} = U\sum V^H \quad \ldots\ldots\ldots\ldots\ldots\ldots\ldots\ldots\ldots\ldots\ldots\ldots\ldots\ldots\ldots\ldots\ldots\ldots \quad (2.24)$$

Where **U** and **V** are M_R x r and M_T x r unitary matrices respectively, and satisfy $\mathbf{U}^H\mathbf{U}=\mathbf{V}^H\mathbf{V}=\mathbf{I}_r$, and $\sum$=diag{σ_1, σ_2,..., σ_r } with $\sigma_i \geq 0$ and $\sigma_i \geq \sigma_{i+1}$, where σ_i is the *i*th singular value of the channel. The columns of **V** and **U** are also known as the input and output singular vectors respectively. $\mathbf{HH}^H$ is an M_R x M_R positive semi-defined Hermitian matrix. Letting the Eigen-decomposition of $\mathbf{HH}^H$ be $\mathbf{Q\Lambda Q}^H$, where **Q** is an M_R x M_R matrix satisfying $\mathbf{Q}^H\mathbf{Q} = \mathbf{QQ}^H = \mathbf{I}_{MR}$ and **Λ**= diag{ λ_1 λ_2 …. λ_{MR}}with $\lambda_i \geq 0$. Assuming the Eigen values λ_i are ordered so that $\lambda_i \geq \lambda_{i+1}$. Then,

$$\lambda_i = \begin{cases} \sigma_i^2 , & if\ i = 1,2, \ldots.., r \\ 0, & if\ = r+1, r+2, \ldots., M_R \end{cases} \quad \text{.. (2.25)}$$

2.7.2. Squared frobenius norm of H.

The squared Frobenius norm of **H**, $||\boldsymbol{H}||_F^2$, is defined as

$$||H||_F^2 = Tr(HH^H) = \sum_{i=1}^{M_R} \sum_{j=1}^{M_T} \left|h_{i,j}\right|^2 \quad \text{.. (2.26)}$$

$||\boldsymbol{H}||_F^2$ May be interpreted as the total power gain of the channel and satisfies

$$||\boldsymbol{H}||_F^2 = \sum_{i=1}^{M_R} \lambda_i \quad \text{.. (2.27)}$$

Where λ_i (i=1,2,…..,M_R) are the eigenvalues of $\mathbf{HH}^{\boldsymbol{H}}$

2.8. Channel estimation.

The need to estimate the parameters of a communication channel in order to improve decoder performance and communication reliability is present in many communication applications. Some of present techniques use a training phase, in which the transmitter sends a known signal to the receiver, allowing the latter to estimate the channel based on the received signal.[20]

2.8.1. Estimating the ST channel at the receiver.

In a real MIMO communication system an exact MIMO channel estimate is required. In comparison to a single antenna system with only one channel to be estimated, in a MIMO system with four transmit and four receive antennas, 16 channels from every transmitter to every receiver antenna have to be estimated simultaneously and not consecutively. The increased number of required training symbols may reduce the higher data rate of a MIMO system.[8] [21]

The channel is estimated by the receiver using training signals sent by the transmitter. A number of training techniques are specified to each modulation scheme. Depending on the SNR at the receiver and the desired signal estimation accuracy, the energy of the training signal has to be selected. The desired channel estimation accuracy depends on the modulation order used. If the channel has delay spread, more channel parameters have to be estimated and additional training signal energy has to be expanded to estimate the channel.[8]

In Channel estimation for blind techniques no explicit training signals are used, instead the receiver estimates the channel from the signals received during normal data transmission. But this will take too much time.

2.8.2. Estimating the ST channel at the transmitter.

The channel estimation at the transmitter is used for adapting the modulation rate or for power control, which only needs the gain of the forward channel. In MISO and MIMO channels, knowledge of the channel H can be achieved in additional ways, such as beam-forming, to provide significant value. In MIMO-MU channel knowledge is necessary to steer signals selectively at users.[8]

In channel estimation at the transmitter, two general techniques are used. In the first technique the forward channel is estimated at the receiver after the signal has traveled through the channel and then sent back (feedback) to the base station on the reverse link. In the second technique, the base station first estimates the reverse link channel, and uses this estimate for the forward link channel.[8]

2.8.2.1.Channel estimation at the transmitter using feedback.

Feedback in a communications system can enable the transmitter to exploit channel conditions and avoid interference. In the case of a multiple-input multiple-output channel, feedback can be used to specify a pre-coding matrix at the transmitter, which activates the strongest channel modes. In situations where the feedback is severely limited, important issues are how to quantize the information needed at the transmitter and how much improvement in associated performance can be obtained as a function of the amount of feedback available.[22]

In this technique the forward link ST channel is estimated at the terminal and is sent to the base station on the reverse link. Some delay (δ_{lag}) will result from feedback, since wireless channels are time varying.

The delay must be much smaller than coherence time ($\delta_{lag} << T_c$). Therefore, (δ_{lag} / T_c) determines channel accuracy at the transmitter. A fast changing channel needs more frequent estimation and feedback.

An overhead can be occurred on the reverse channel, at this point two approaches can be used to reduce the feedback overhead, one of them is to send a slow changing statistic of the channel such as the correlation matrices R_t or R_r, second is to feedback only partial channel information such as channel condition number.[8]

2.8.2.2.Channel estimation at transmitter using reciprocity.

The use of channel reciprocity is usually suggested for Time-Division Duplex (TDD) systems. The reciprocity principle is based on the property that electromagnetic waves traveling in both directions will undergo the same physical perturbations (i.e. reflection, refraction, diffraction, etc. . .). Therefore, if the link operates on the same frequency band in both directions, the impulse response of the channel observed between any two antennas should be the same regardless of the direction. Application of the reciprocity principle lifts the requirement for a continuous feedback of the channel estimates.[8] [23]

Let $h_f(t_f,f_f,i_f)$ be the forward channel from the transmitter to receiver and $h_r(t_r,f_r,i_r)$ be the reverse channel, t_f, f_f and i_f refers to time, frequency and antenna index on the forward channel. t_r, f_r and i_r refers to time, frequency and antenna index on the reverse channel. The antenna index specifies the antenna used at the transmitter.

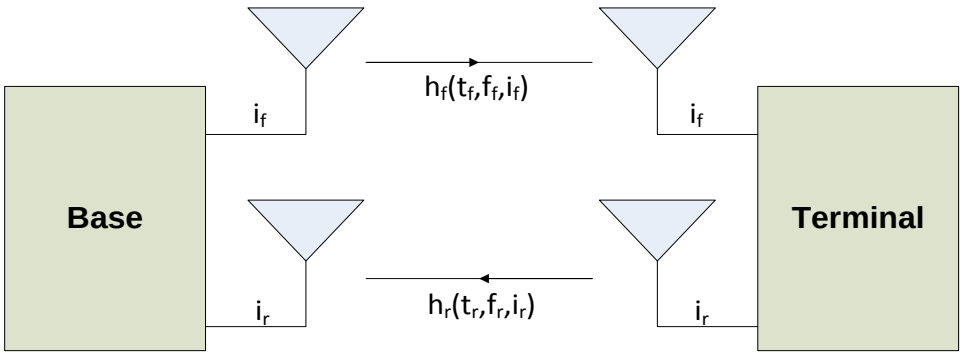

Figure 2.6: duplexing in ST channels.

The principle of reciprocity is that if the time, frequency and antenna for channel are the same **(**$t_f = t_r$, $f_f = f_r$, $i_f = i_r$), then the forward and reverse channel are identical. In order to isolate simultaneous two way links (duplexing scheme), we need to force some difference in time, or frequency and/or spatial parameters.[8]

In time division duplexing (TDD), the forward and reverse channels use the same frequency and antenna, but use different time slots to communicate. Let $\delta_t = t_f - t_r$ be the duplexing time delay. It follows that the forward and reverse channels can be equated only if

$\delta_t << T_c$ ……..……(2.28)

Where T_c is the coherence time of the channel. The more stringent the requirements of accuracy in channel estimates, the smaller δ_t / T_c will be needed.

In frequency division duplexing (FDD), the forward and reverse channels use the same time and antennas to communicate, but uses different frequencies on the links. Let $\delta_f = f_f - f_r$ be the duplexing frequency difference. It follows that the forward and reverse channels can be equated only if

$\delta_f << B_c$ ……...……..……..(2.29)

Where B_c is the coherence bandwidth of the channel. In practice, due to physical limits on duplexing filters that isolate the forward and reverse links, δ_f is about 5% of the operating frequency v_c. this usually means that $\delta_f >> B_c$. therefore the reciprocity principle in general cannot be exploited in FDD for transmit estimation.

In antenna division duplexing (ADD), the forward and reverse channels use the same frequency and time, but use different antennas (or beams) on each link to communicate. Let δ_d be the separation between the antennas indexed by i_f and i_r. It follows that the forward and reverse channels can be equated if

$\delta_d << D_c$ ……...……(2.30)

Were D_c is the coherence distance of the channel. This may be impossible to meet physically when D_c is itself as small as $\lambda_c / 2$. ADD does not provide sufficient isolation between the two links and is almost never used directly as a duplexing scheme.[8]

Many communication systems use a combination of time / frequency / antenna separation in the duplex links, making reciprocity infeasible.[8]

2.9. Channel dependency.

There are two ways for modeling a channel, either empirically which based on measurements or by simulation.

2.9.1. Environment dependence.

Different radio-propagation environments would cause different radio-channel characteristics. Channel models can be generated by using propagation parameters measured in different environments. A generic channel model after analyzing those parameters can be used to model all scenarios or environments. The existence of the LOS component, even for the same scenario, can influence the control parameters so it's important to differentiate LOS and NLOS conditions. Therefore, transition

between LOS and NLOS cases in an appropriate scenario modeling have to be described.[6]

2.9.2. System dependence.

Path-loss models, usually, depend on the carrier frequency. On the other hand model parameters; delay spread, azimuth spread, and Ricean K-factor don't show significant frequency dependence. For modeling of systems with time-division-duplex (TDD) all models are using same parameters for both uplink and downlink. If system is using different carriers for duplexing (FDD), then random phases of scatter contributions between uplink and downlink are independent.[6]

2.9.3. Path loss.

Path loss is a measure of attenuation based only on the distance to the transmitter. Path loss depends on distance between transmitter and receiver, LOS clearance between the receiving and transmitting antennas, and Antenna height. These models can be obtained from complex analytical or empirical measurements. Sometimes simple models are convenient, since complex models are anyway approximations. Details about the path-loss models used in this project can be found in chapter one.

The fixed parameters path-loss models have usually the form of

$$PL = A\log_{10}(d[m]) + B \quad \text{(2.31)}$$

Where d is the distance between transmitter and receiver, the fitting parameter A Includes the path-loss exponent.

Free space attenuation can be modeled as

$$PL_{free} = 46.4 + 20\log_{10}(d[m]) + 20\log_{10}(f[GHz]/5) \quad \text{(2.32)}$$

2.10. Summary of channel modeling related IEEE papers.

In [24], this paper considered frequency-flat fading MIMO channels with m transmit and n receive antennas where each single realization of the channel can be described by the n×m channel matrix H. The number of envisaged antennas plays an important role in designing a good channel model. The appropriate model has to be chosen according to the considered application. Therefore, Accurate modeling of

MIMO channels is an important prerequisite for MIMO system design, simulation, and deployment.

In [25], this paper proposes a general scattering geometry-based channel model for the analysis and design of MIMO systems in mobile fading channels. Every channel models requires two steps, first, setting up a generic channel model and identifying the parameters that have to be determined, then performing the measurement campaigns and extracting the parameters. The channel model within this paper includes the layout of the channel, location of the scatters and parameters setting. This model takes into account the scattering near BS and MS as well as scattering by far clusters.

In [26], this paper presents a stochastic 2x2 MIMO wideband channel modeling method that uses tapped delay lines (TDL) and a single channel spatial correlation matrix that represents a novel simplification with respect to other wideband MIMO models. The resulting model is accurate and also easy to implement, it leads to a correct fitting of the channel in the time and the frequency domain, and it requires a low number of parameters. The response of the channels generated with the model fits closely the behavior of the real measured channels. Although the model is based in a limited number of measurements, it provides insight with respect to the characteristics of the broadband 2x2 MIMO channels in the outdoor-indoor environment.

In [27], this paper deals with the theoretical derivation of a channel model for the communication link between the platform and mobile users or stations, a propagation model suited to the stratospheric platform case is presented in this paper, keeping in account the fading effects due to the presence of scatters on the ground. The small scale fading effects are analyzed. The simulation results show the dispersive effects of the channel and demonstrate that generic models of the channel that do not considering multipath effects of scatters on the ground can yield to too optimistic results. Besides, the novel model presented in this paper can be essential for the design of future communication systems.

In [28], this paper focuses on MIMO channel characterization and optimization. The Characterization of the MIMO channel in different scenarios and operating-frequency bands is a crucial factor in the design of new systems and standards. In contrast to the conventional communication systems with one transmit and one receive antenna, MIMO system are equipped with multiple antennas at both link ends. So MIMO channel has to be described for all transmit and receive antenna pairs. By knowing several methods such as the MIMO channel modeling, MIMO channel estimation, channel diversity and channel capacity, the channel will be easy for characterization.

In [29], in this work, the authors derive precise PDFs as well as good Gaussian approximations for various MIMO wireless channels. This statistical characterization

helps to understand and predict the capacity gain expected from the MIMO technique, in terms of system parameters and channel dimension. It also helps to design space-time modulation schemes that can take full advantage of the MIMO link for various wireless channels.

In [30], MIMO systems are aversion for future wireless communications systems. Where MIMO channel is radio propagation channel that determines the characteristics of the entire MIMO system. this paper examine the accuracy of MIMO channel models by using some different measures of quality, the authors used three different metrics In an indoor environment to analyze MIMO models which are double directional angular power spectrum, average mutual information, and the Diversity measure. As a conclusion the Weichsel Berger's model performance is the best with respect to the analyzed metrics, and the Kronecker model used only for limited antenna numbers, such as 2x2 and the virtual channel representation used only for modeling the joint APS for very large antenna numbers.

Chapter 3

Analyzing the SUI-1 channel model

Chapter contents:

3.1. Preface.

This channel model is proposed to simulate MIMO multipath fading channels for fixed wireless applications, two transmit antennas and one receive antenna are used.

This channel model has three paths. Each path is characterized by a relative delay with respect to the first path delay, a relative power, a Rician K-factor, and a maximum Doppler shift. This channel model specifies statistical parameters effects (tapped delay line, fading, antenna directivity). To complete the channel model, these statistics have to be combined with macroscopic channel effects such as path loss and shadowing. SUI-1 channel model considers a flat terrain with light tree density.

The three paths are classified as; the first path is Rician while the remaining two are Rayleigh. Each path has a rounded Doppler spectrum for its diffuse component; the parameters are as specified in the default Doppler Rounded object.

Figure 3.1 shows the previous points:

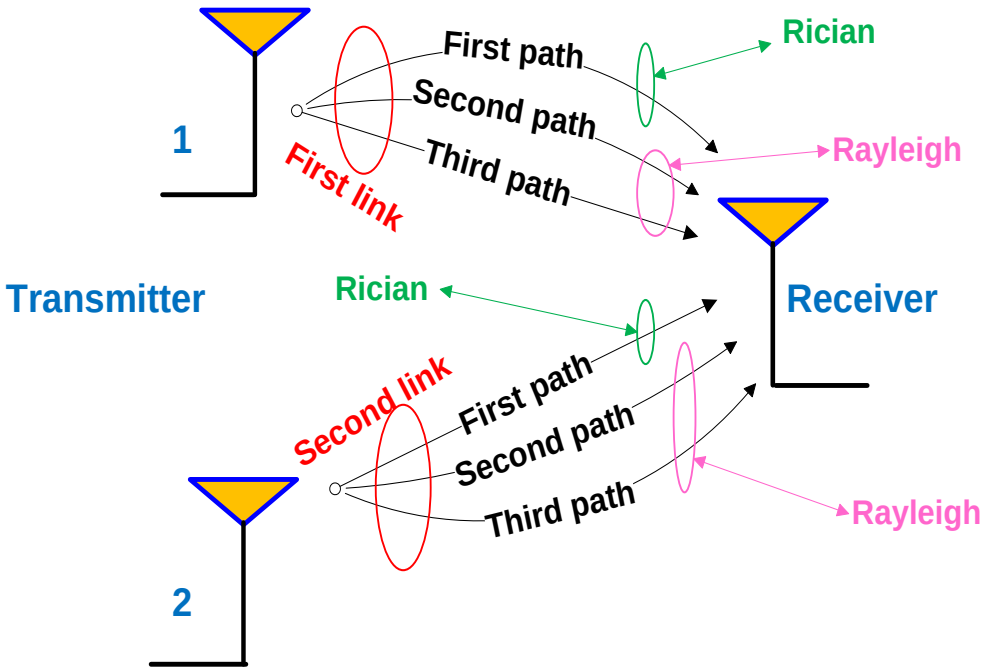

Figure 3.1: SUI-1 channel model illustration.

The generic structure for the SUI channel model is given in figure 3.2:

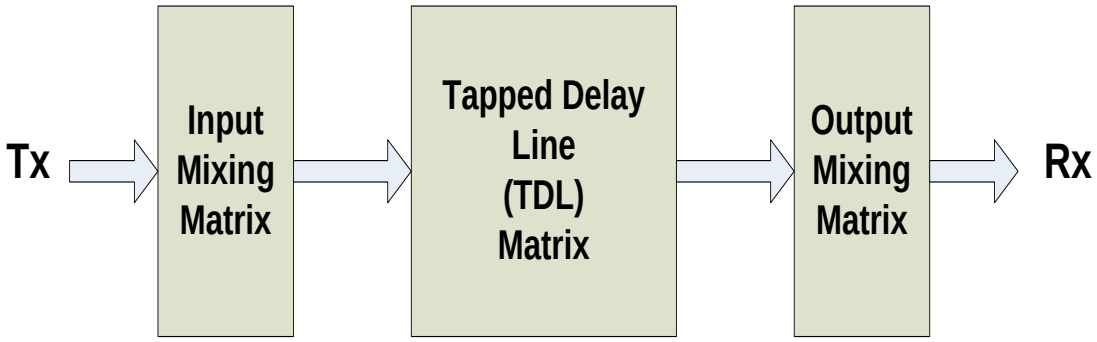

Figure 3.2: generic structure for the SUI channel model.

This structure is general for MIMO channel and includes the other configurations; MISO, SIMO, and SISO. The input mixing matrix models the correlation between transmitted signals when multiple antennas are used. Multipath fading is modeled as a taped delay line with three taps and non-uniform delays. The gain associated with each tap is characterized by a fading distribution (Rician with K > 0 or Rayleigh with K = 0) and Doppler frequency. The output mixing matrix specifies the correlation between signals at the output.

3.2. SUI-1 channel model parameters.

The table below summarizes the SUI-1 channel model parameters.

Correlation(rho)=0.7	Path 1	Path 2	Path 3	Unit
Delay (tau)	0	0.4	0.9	µs
Power (pdb)	0	-15	-20	dB
K-factor	4	0	0	
Doppler (fd)	0.4	0.3	0.5	Hz

Table 3.1: SUI-1 channel model parameters.

3.3. Code flow chart.

The following flow chart shows the main stages of the code:

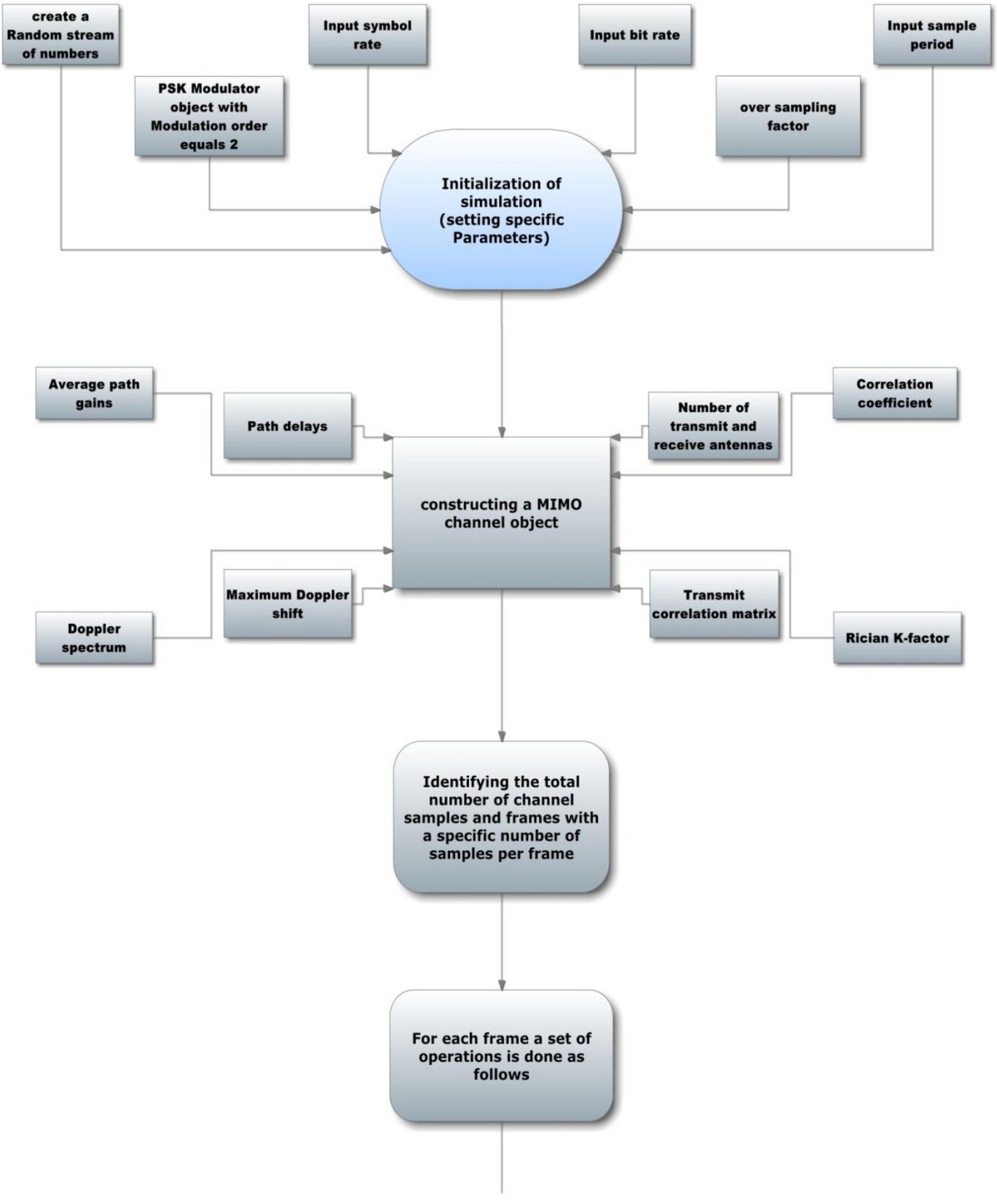

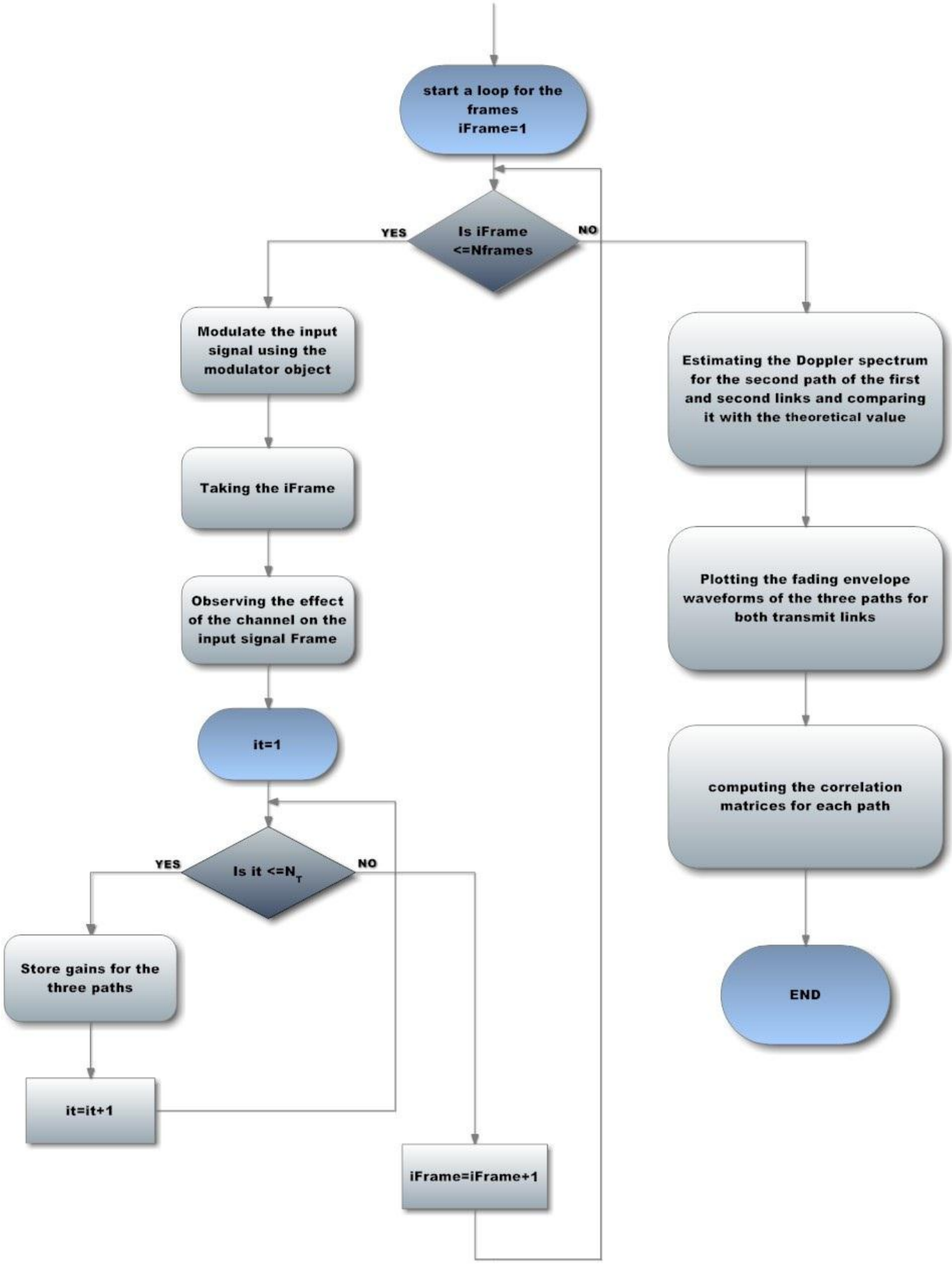

Figure 3.3: code flow chart.

3.4. Main code stages explanation.

1. Initialization of simulation: the simulation sampling rate is specified, and kept the same for the remainder of the code. The input to the channel simulator is oversampled by a factor of four. A psk modulation object is defined with modulation order equals 2.

2. Constructing a MIMO channel object: a MIMO channel object according to the modified SUI-1 channel model is constructed, mimochan (nt, nr, ts, fd, tau, pdb) constructs a MIMO fading channel object with a frequency selective multipath link that models each discrete path as an independent Rayleigh fading process with the same average gain, tau represents a row vector of path delays each specified in seconds and pdb is a row vector of average path gains each in dB. The Doppler Rounded function creates a rounded Doppler spectrum object with default polynomial coefficients (a_0 = 1, a_2 = -1.75, a_3 = 0.785). h.kfactor defines the k-factor (the power ration between the direct path component and the power of the multipath component) of the first path because it's Rician

3. Simulation of SUI-1 channel model: after each frame is processed, the channel is not reset; this is necessary to preserve continuity across frames. h.ResetBeforFiltering is set to zero in order to make the filter uses the existing state information in the channel when starting the filtering operation. h.StorePathGains is set to one so as to store the complex path gain vector while the channel filter function processes the signal, h.pathgains holds a 4-D array of complex path gains of size $N_S \; x \; L \; x \; N_T \; x \; N_R$, where N_S is the number of samples , N_T is the number of transmitters, N_R is the number of receivers, and L is the number of paths. $modulate(h, x)$ Function is used for signal modulation, it modulates the input signal x using modulator object h. The Matlab function $y = filter(chan, x)$ passes a signal x through the multipath MIMO channel, where x is the input signal of size $N_S x N_T$.

4. Estimating the Doppler spectrum for the second path of the first link: the Doppler spectrum is estimated from the complex path gains. Welch power is used for estimating a power of a signal versus frequency and implicitly reducing the noise in the data sequence. The power spectral density function $psd(H_S, x)$ returns an object containing the power spectral density estimate of the discrete signal x using the spectrum object H_S , power spectral density is the distribution of power per unit frequency. A rounded Doppler spectrum is proposed as an approximation to the measured Doppler spectrum for the scatter component of fixed wireless channels, the normalized rounded Doppler spectrum is given analytically by a polynomial of order four in the frequency

domain that is $S(f) = C_r[a_0 + a_2(f/f_d)^2 + a_4(f/f_d)^4], |f| \leq f_d$, and C_r is given by$\left(1/2f_d\left[a_0 + \frac{a_2}{3} + \frac{a_4}{5}\right]\right)$.

5. Plotting the fading envelope waveforms of the three paths for both transmit links: a correlation between the fading envelops can be observed.

6. Computing the correlation matrices for each path: the Matlab corrcoef can be improved by increasing the number of samples.

3.5. Results of changing the SUI-1 channel model parameters.

Through this part, we will change the code parameters, obtain new results and compare them to the original states. The following three figures are related to the original code which parameters are specified in table 3.1.

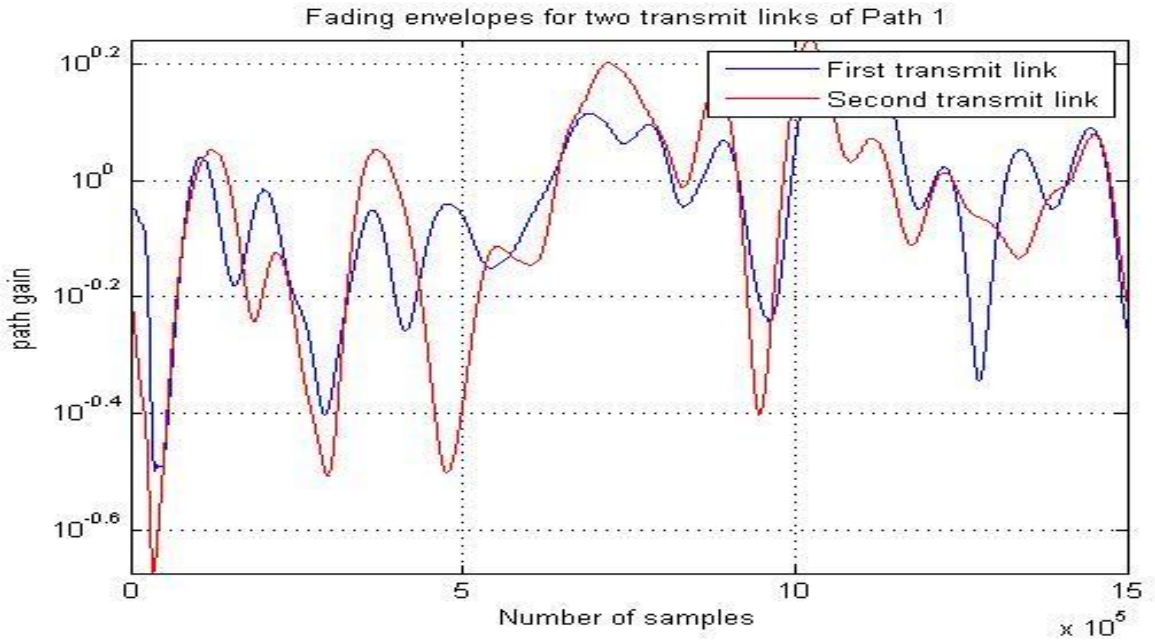

Figure 3.4: Fading envelopes for path 1.

The above figure shows the fading envelop of the first Rician path through the two transmit links, it's clear that there is good fitness between the two paths. This case could be considered as a real case. The following two figures are for the Rayleigh paths:

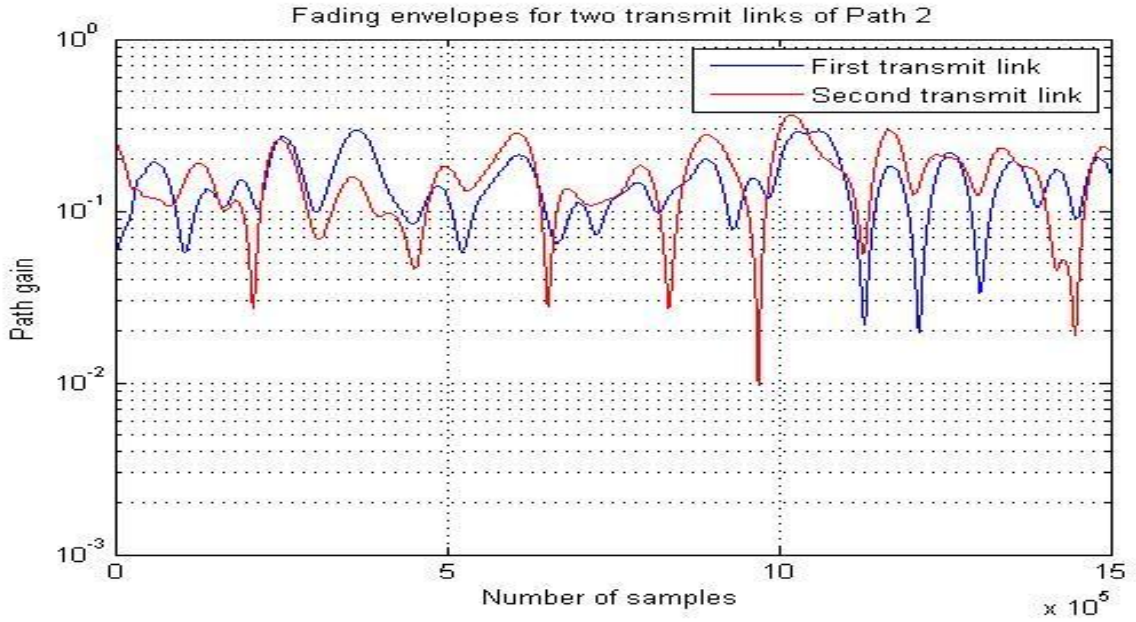

Figure 3.5: Fading envelopes for path 2.

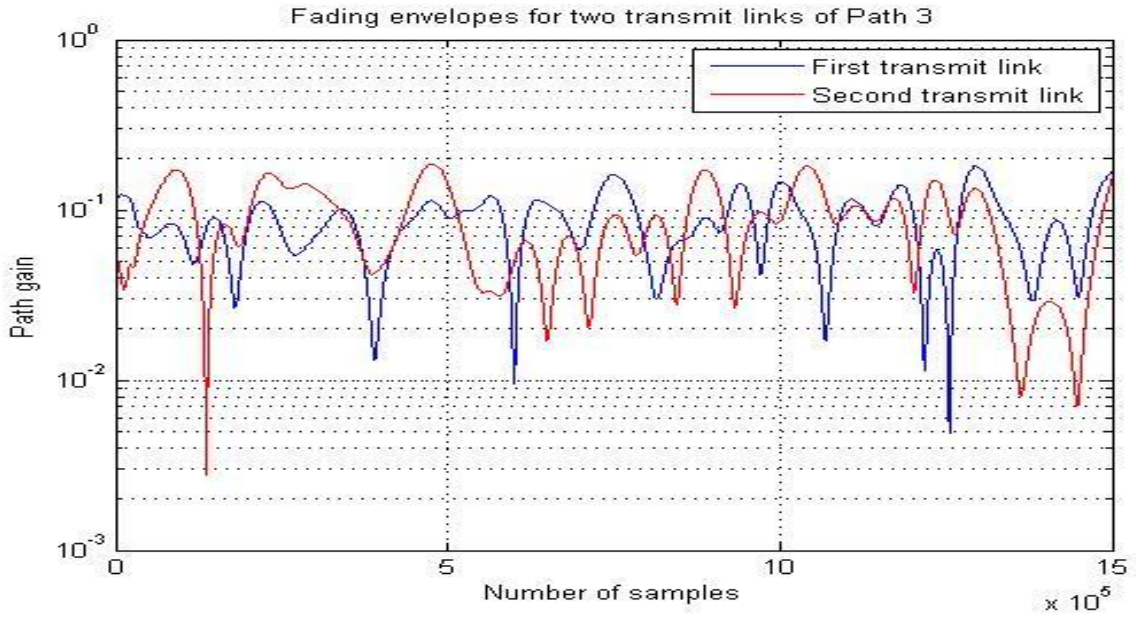

Figure 3.6: Fading envelopes for path 3.

By comparing the Rician path with the Rayleigh paths, one can say that the Rayleigh paths have faster fading than the Rician does, this sounds logical since there is a LOS component in the Rician case where there is no any line of sight components in Rayleigh cases. However, there still a good match between the envelpoes of the Rayleigh paths from the two links.

Case1: changing the correlation coefficient.

- Correlation coefficient (rho) = 0.4:

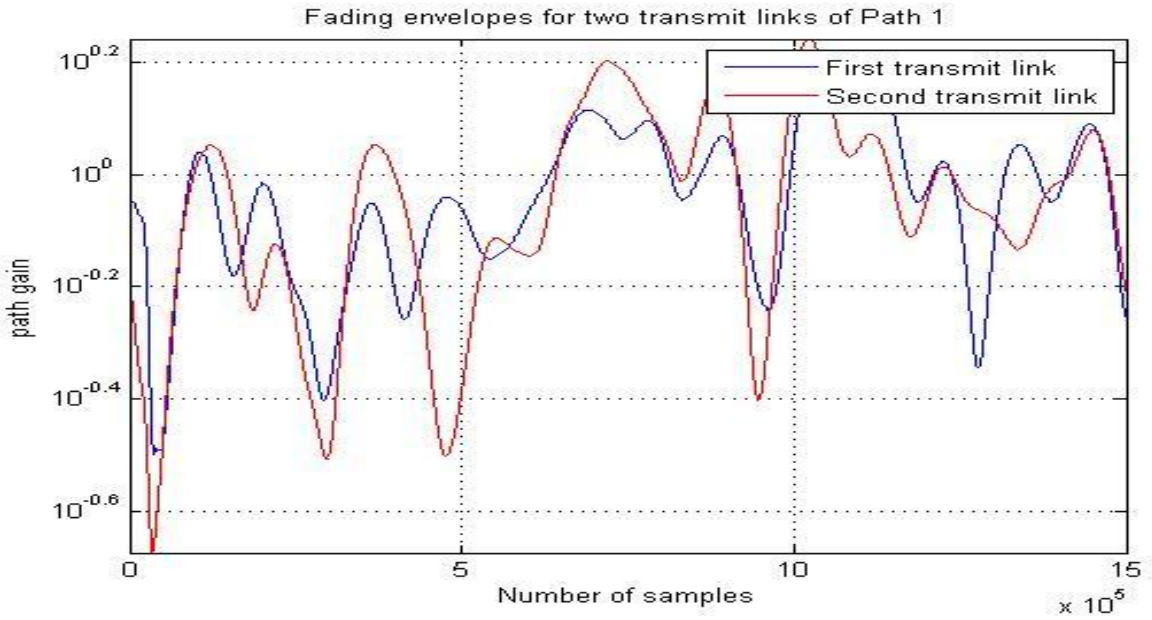

Figure 3.7: Fading envelopes for path 1 when (rho = 0.4).

This figure illustrates the effect of reducing the correlation coefficient on the Rician path, it's obvious that the less correlation coefficent, the more miss correlation between links we get. It should be noted that the correlation coefficient indicates the similarity between the fading envelopes of the propagating signals in the channel.

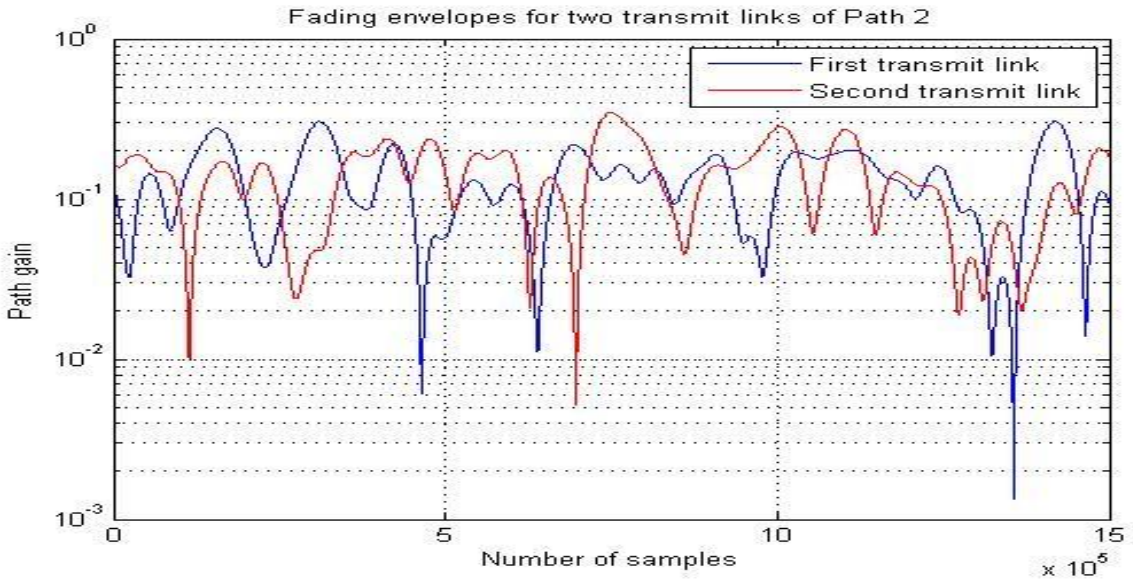

Figure 3.8: Fading envelopes for path 2 when (rho = 0.4).

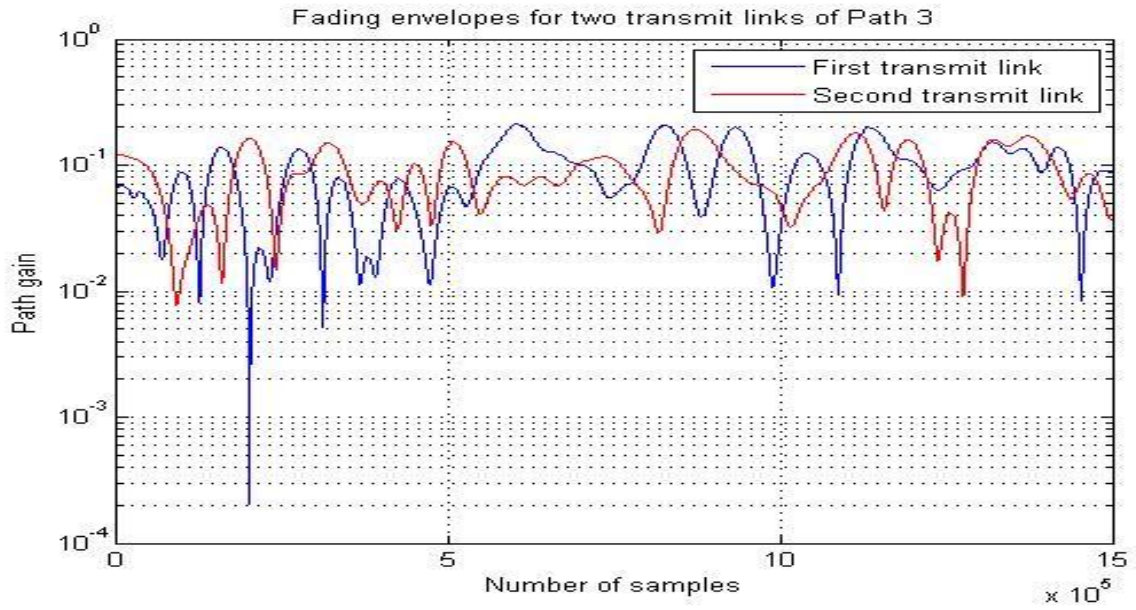

Figure 3.9: Fading envelopes for path 3 when (rho = 0.4).

The above two figures show the effect of reducing the correlation coefficient from 0.7 to 0.4 on Rayliegh. It can be noticed that there is a large miss correlation between the paths in Rayliegh case compared to Rician.

- Correlation coefficient (rho) = 0.9:

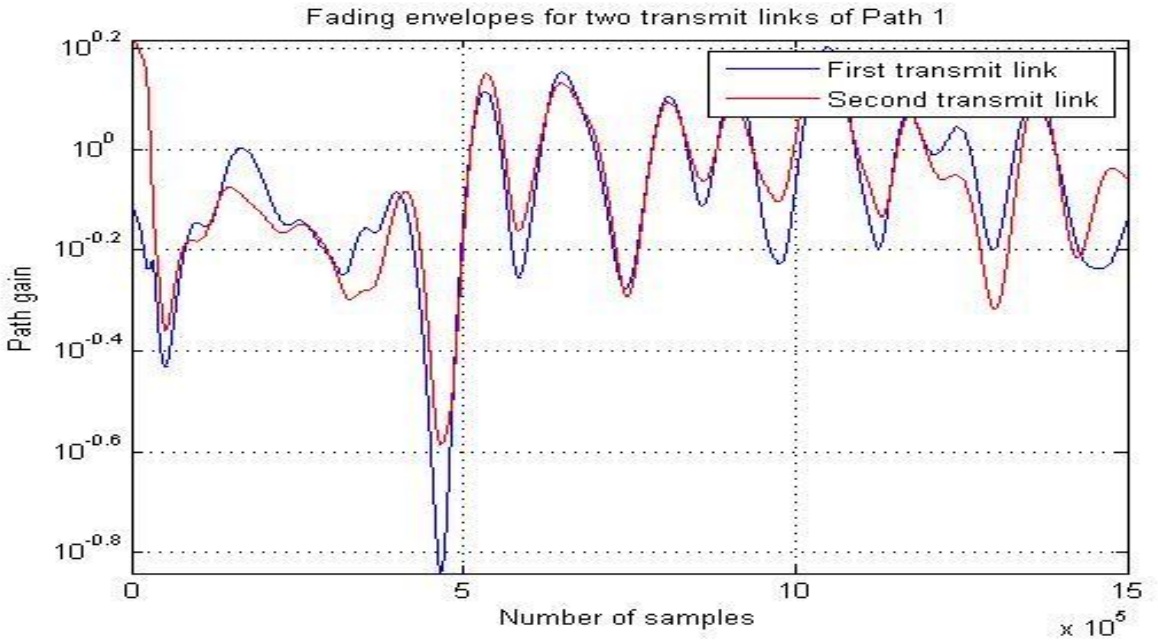

Figure 3.10: Fading envelopes for path 1 when (rho = 0.9).

The previous figure shows the effect of increasing the correlation coefficient from 0.7 to 0.9 on the Rician path, it can be noticed that there is a high match between the two links.

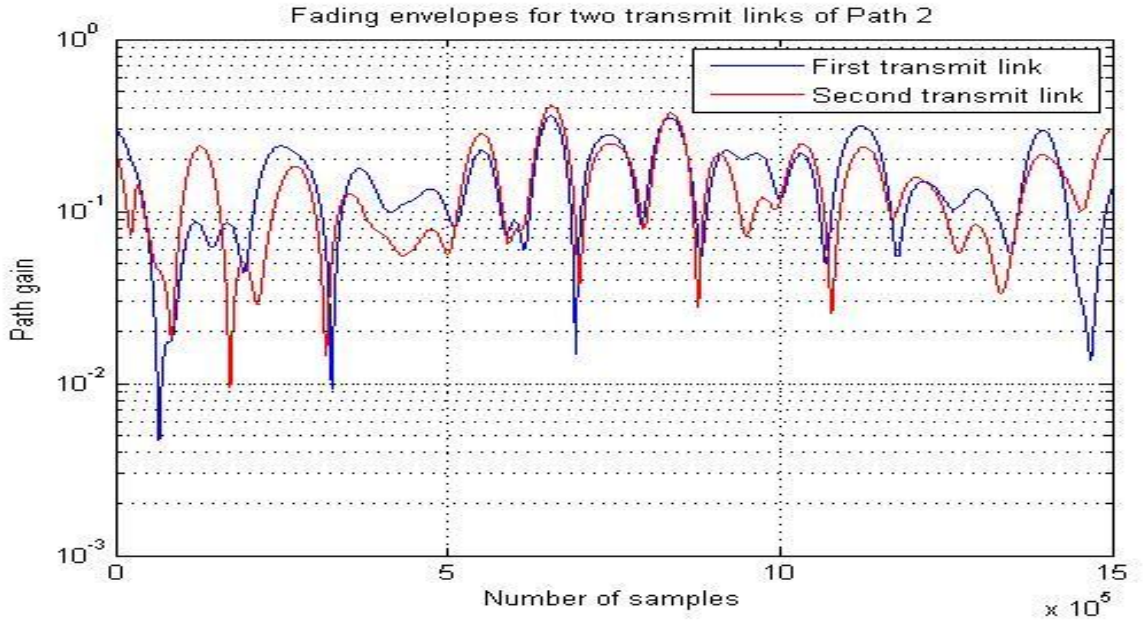

Figure 3.11: Fading envelopes for path 2 when (rho = 0.9).

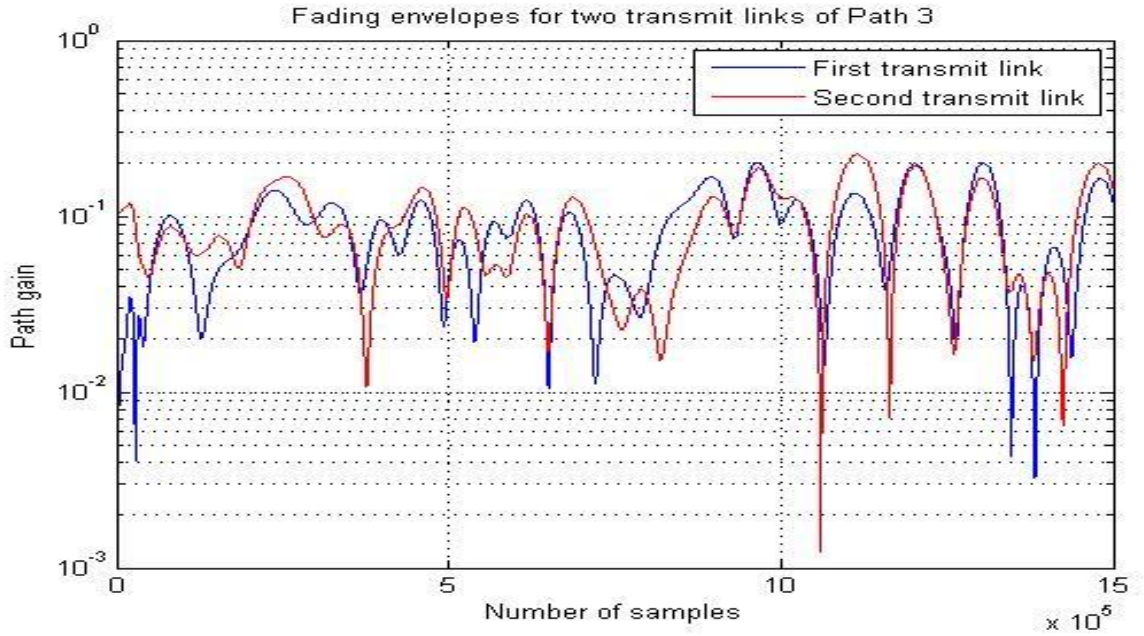

Figure 3.12: Fading envelopes for path 3 when (rho = 0.9).

The last two figures show the effect of changing the correlation coefficient from 0.7 to 0.9, it's obvious that the correlation between the Rayleigh paths has highly increased and they are almost completely matched.

As a result of changing the correlation coefficient, increasing the correlation coefficient to be more than 0.7 results in a high and approximately full match between the different paths in both Rician and Rayleigh case, that is the paths examine the same channel conditions. On other hand, reducing the correlation coefficient to 0.4 will result in a miss correlation between the paths.

Case2: changing the doppler shift.

- Doppler shift (fd) = 0.1:

The follwing three figures show the effect of reducing the doppler shift from 0.5 to 0.1 in both Rician and Rayleigh cases:

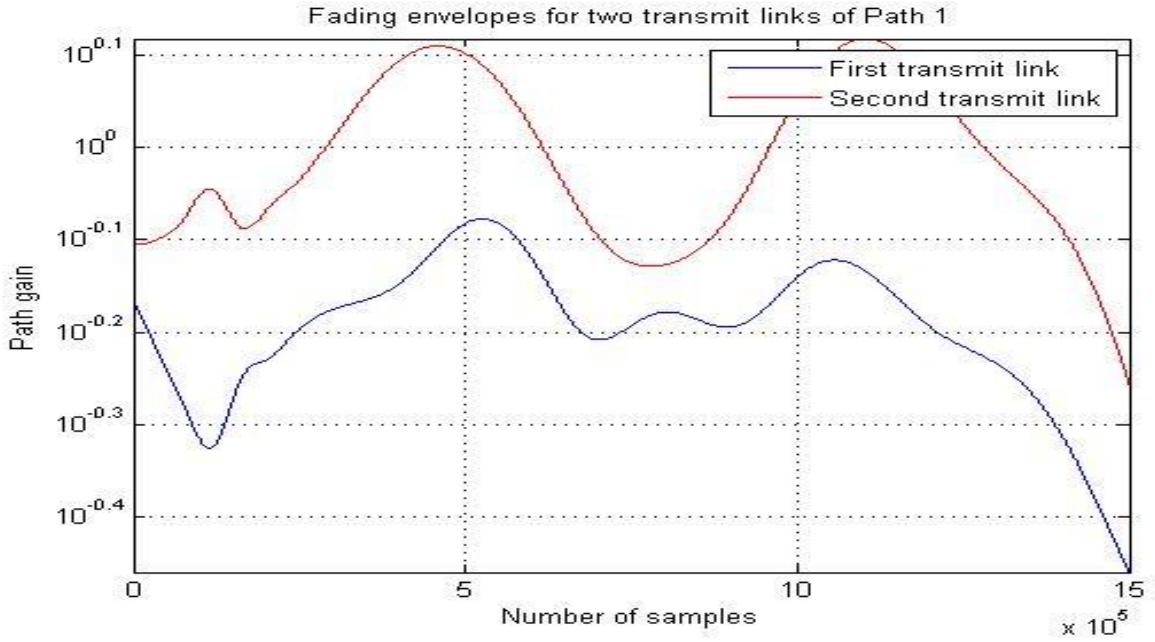

Figure 3.13: Fading envelopes for path 1 when (fd = 0.1).

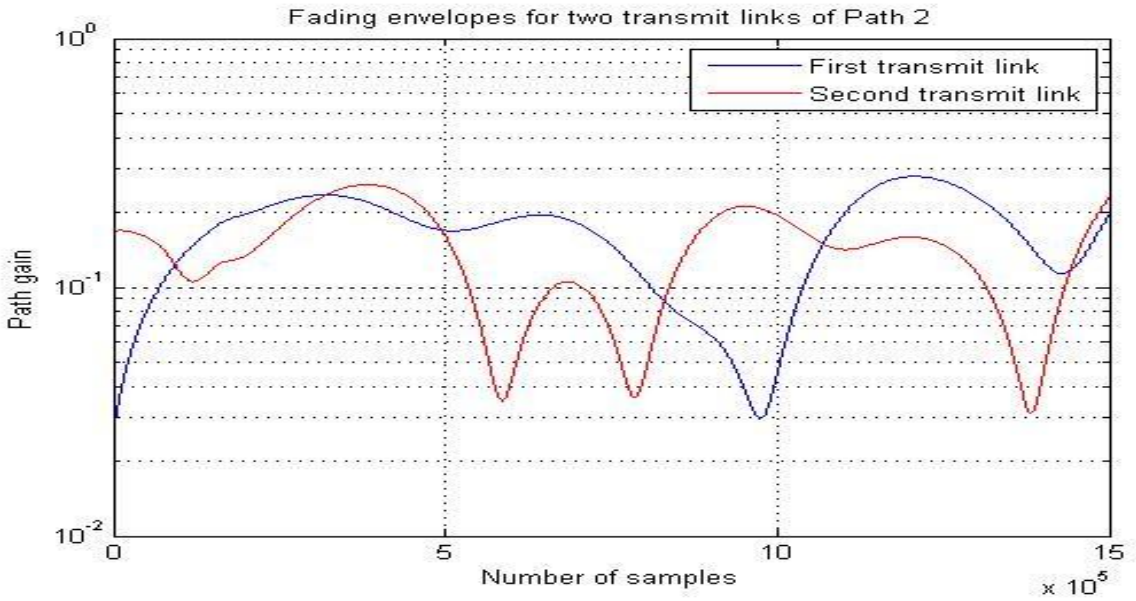

Figure 3.14: Fading envelopes for path 2 when (fd = 0.1).

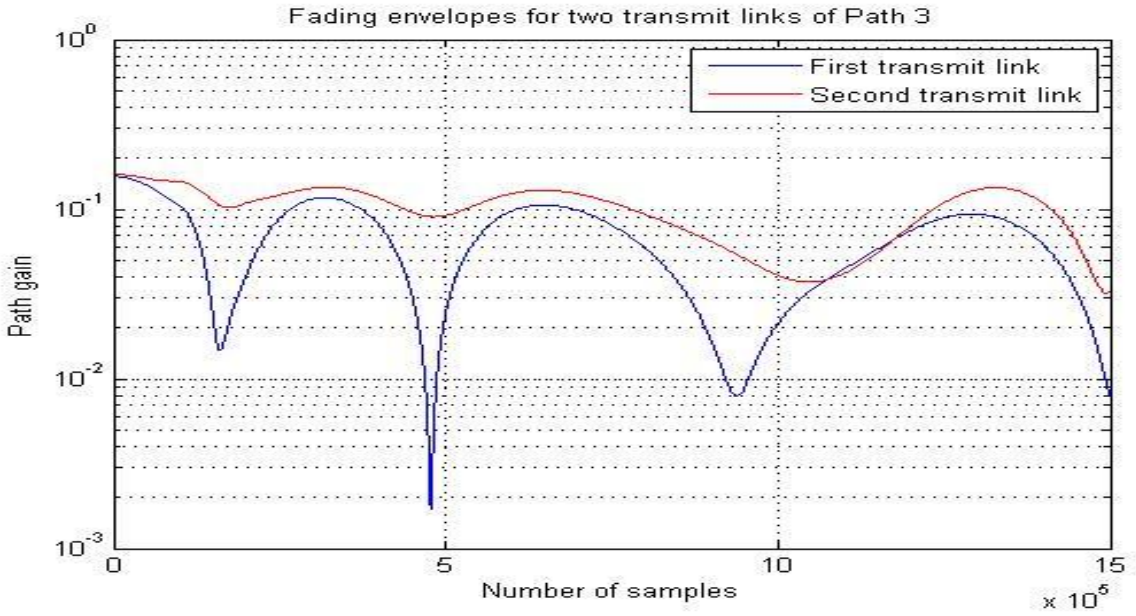

Figure 3.15: Fading envelopes for path 3 when (fd = 0.1).

Reducing the Doppler shift from 0.5 to 0.1 results in slow variations in the fading envelopes, so more smooth envelopes are found to occur. In reality, this indicates the slowly movements of the transmitter and the receiver, they may be considered almost fixed. Moreover, the probability of line of sight between the transmitter and the receiver implicitly increases. It should be noted that the Doppler shift value (fd=0.5) in the SUI channel model is extracted based on carried measurements that take on consideration the propagation environment, the velocity of the wind, and the scatters caused by obstacles between Tx and Rx.

- Doppler shift (fd) = 0.8:

The follwing three figures show the effect of increasing the doppler shift from 0.5 to 0.8 in both Rician and Rayleigh cases:

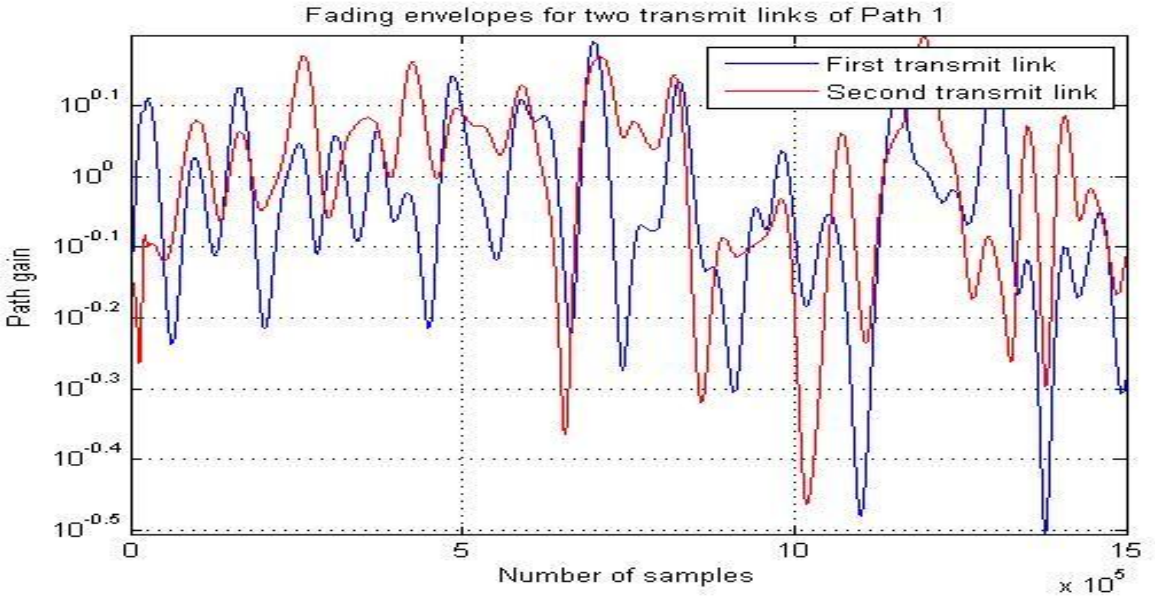

Figure 3.16: Fading envelopes for path 1 when (fd = 0.8).

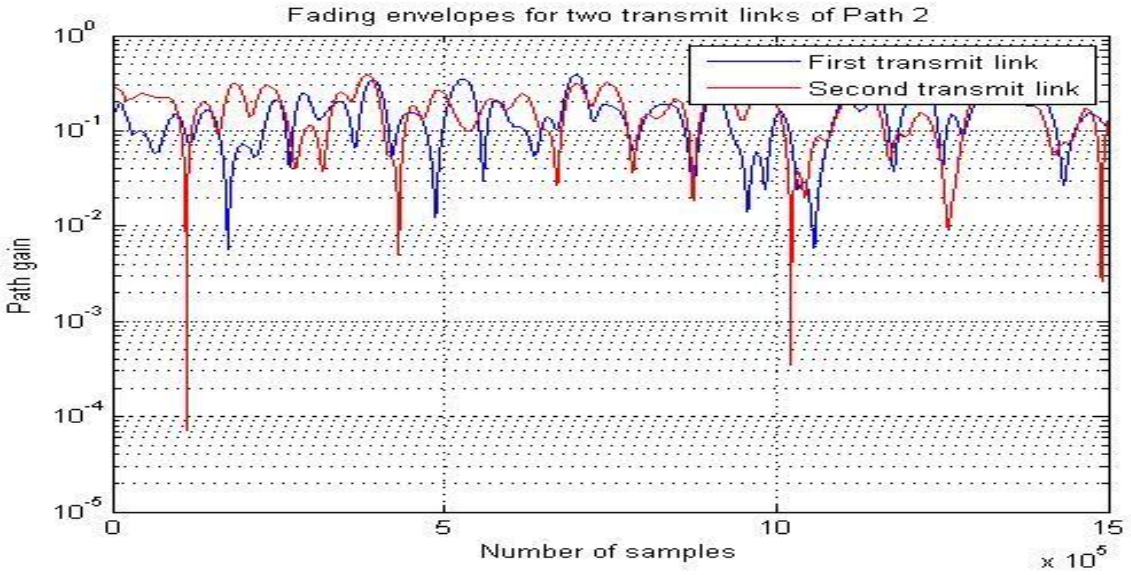

Figure 3.17: Fading envelopes for path 2 when (fd = 0.8).

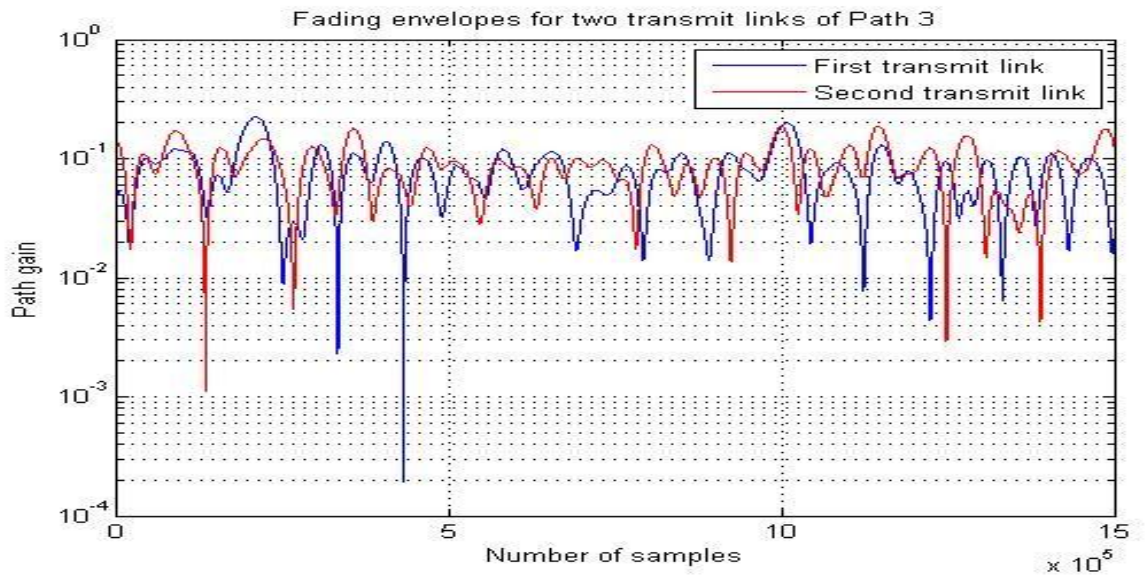

Figure 3.18: Fading envelopes for path 3 when (fd = 0.8).

Increasing the Doppler shift from 0.5 to 0.8 results in so rapid fluctuations in the fading envelopes, this could be caused by the high speed movement of the receiver and/or the transmitter.

Case3: changing the average path gains.

- Average path gains (pdb) = [0 -30 -60]:

The follwing three figures show the effect of changing the average path gains from [0 -15 -20] to [0 -30 -60] in both Rician and Rayleigh cases:

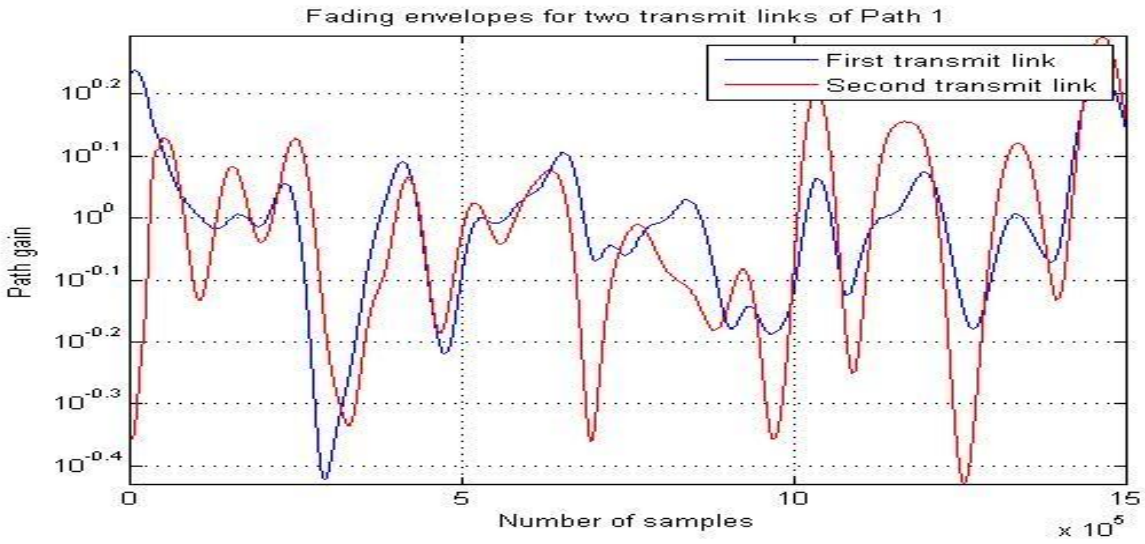

Figure 3.19: Fading envelopes for path 1 when (pdb = [0 -30 -60]).

Figure 3.19 shows that there is no change on the fading envelopes since they examine again the same value of the path gain (0 dB), there is a considrable correlation between them.

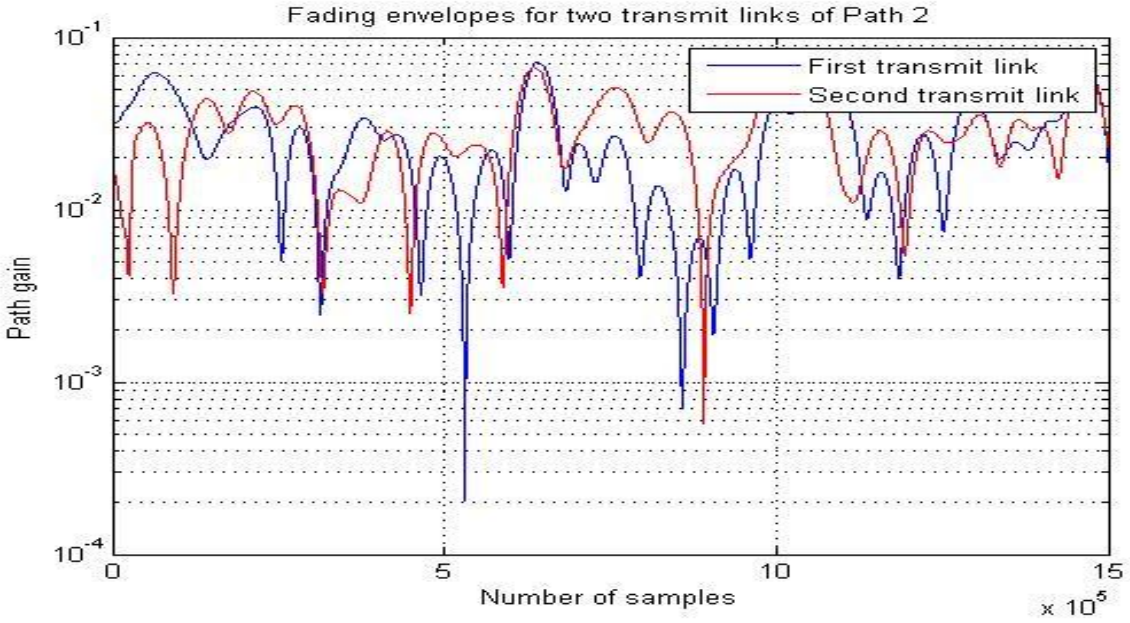

Figure 3.20: Fading envelopes for path 2 when (pdb = [0 -30 -60]).

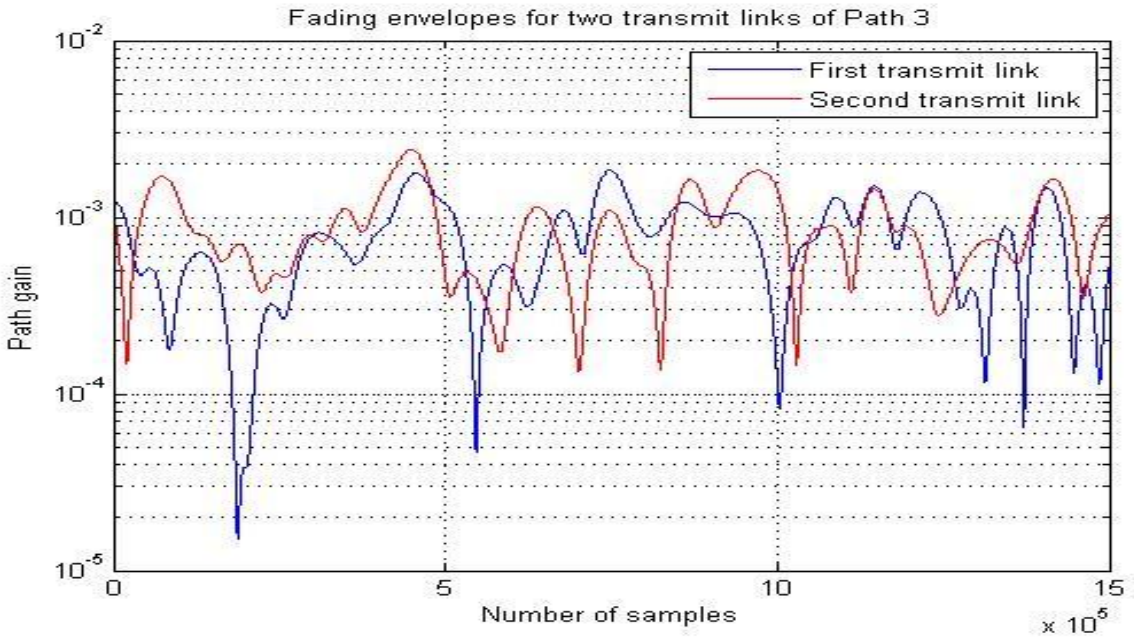

Figure 3.21: Fading envelopes for path 3 when (pdb = [0 -30 -60]).

Figures 3.20 and 3.21 show the envelpoes of the Rayleigh paths, it is clear that the level of the envelopes reaches a less gain levels than the orginal levels. In other words, the signal to noise ratio has been decreased.

- Average path gains (pdb) = [0 -5 -10]:

The follwing three figures show the effect of changing the average path gains from [0 -15 -20] to [0 -5 -10] in both Rician and Rayleigh cases:

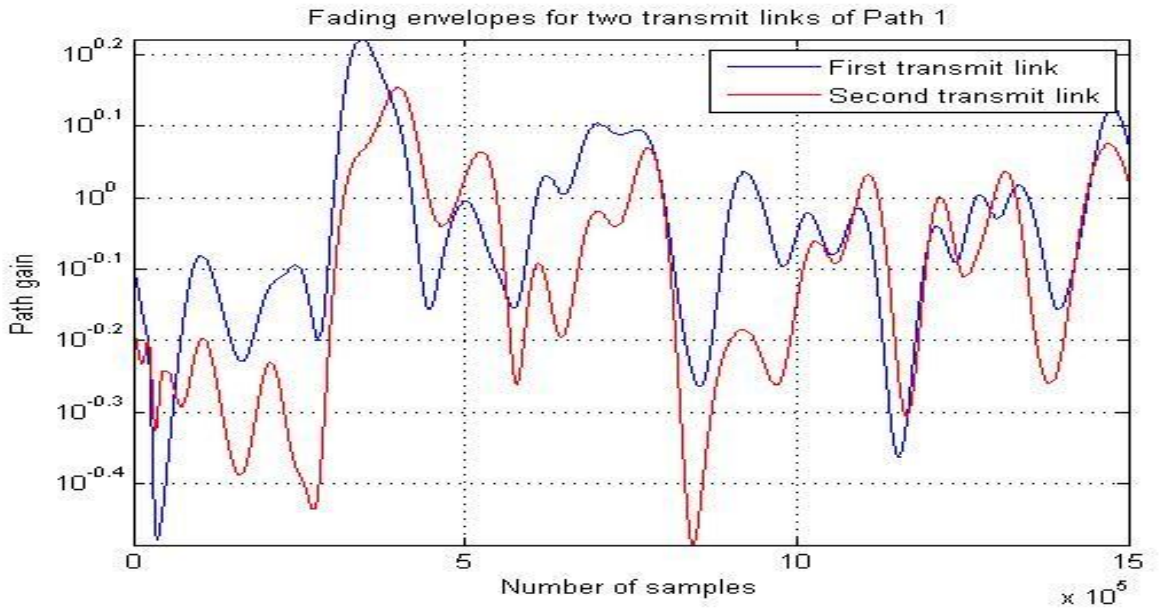

Figure 3.22: Fading envelopes for path 1 when (pdb = [0 -5 -10]).

Figure 3.22 shows that there is no change on the fading envelopes since they examine again the same value of the path gain (0 dB), there is a considrable correlation between them.

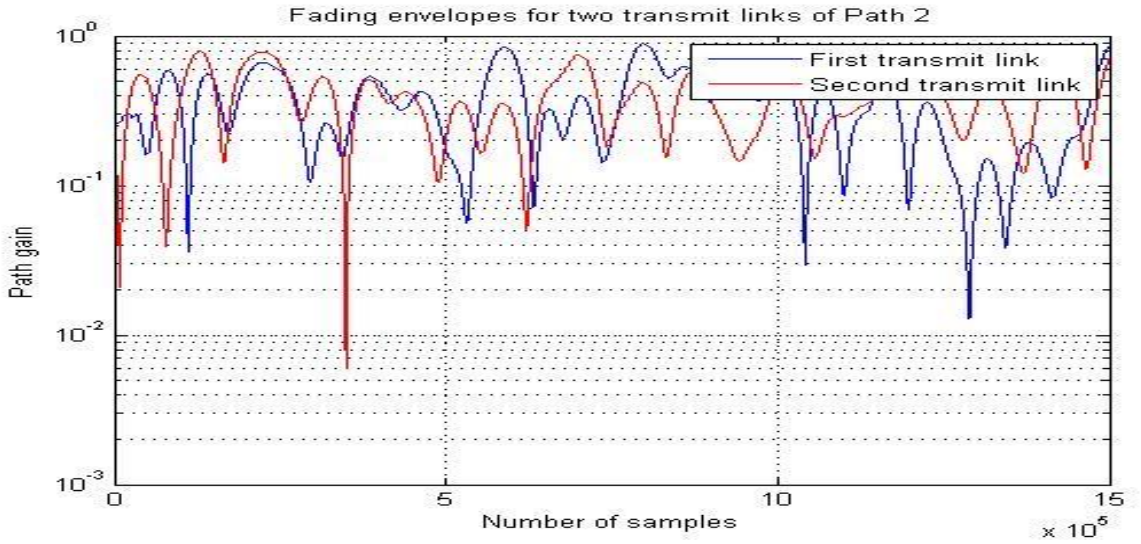

Figure 3.23: Fading envelopes for path 2 when (pdb = [0 -5 -10]).

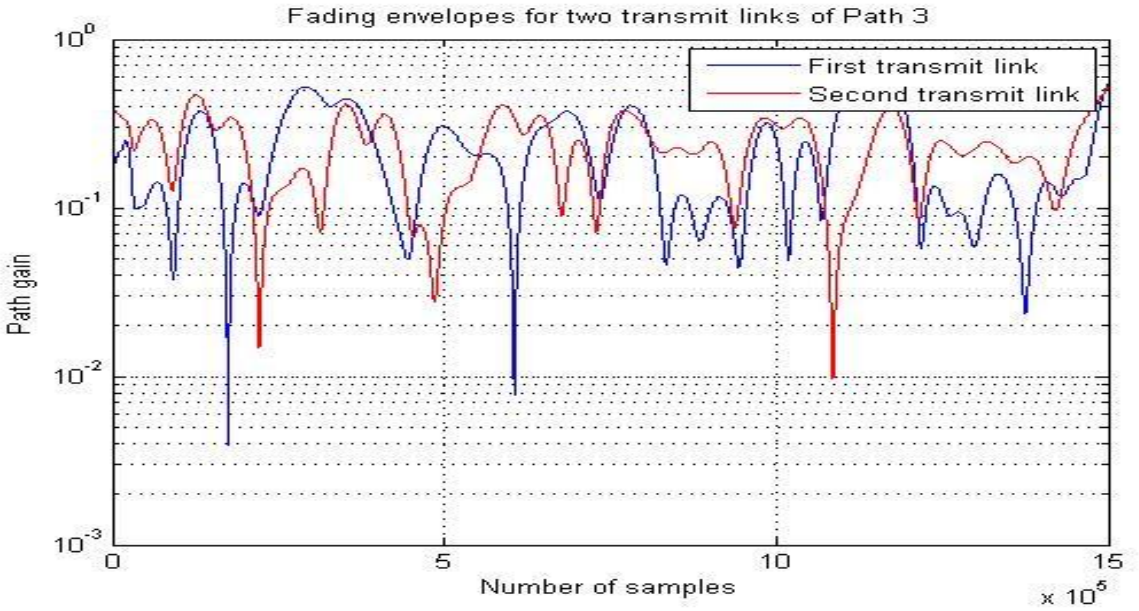

Figure 3.24: Fading envelopes for path 3 when (pdb = [0 -5 -10]).

Figures 3.23 and 3.24 show the envelpoes of the Rayleigh paths, it is clear that the level of the envelopes reaches a higher gain levels than the orginal levels. In other words, the signal to noise ratio has been increased. Furthermore, there are less fluctuations in the envelopes.

Case4: changing the path delays.

- path delays (tau) = $[0 \ \ 0.4 \ \ 0.9] \times 10^{-4}$:

The following three figures show the effect of increasing the path delays from $[0 \ \ 0.4 \ \ 0.9] \times 10^{-6}$ to $[0 \ \ 0.4 \ \ 0.9] \times 10^{-4}$in both Rician and Rayleigh cases:

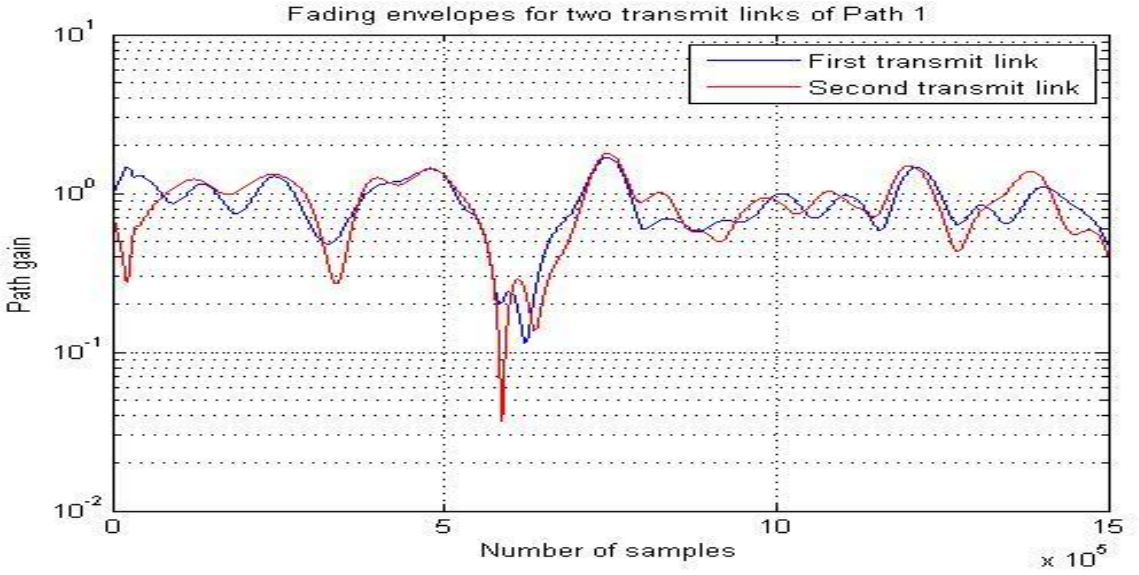

Figure 3.25: Fading envelopes for path 1 when ($tau = [0 \ \ 0.4 \ \ 0.9] \times 10^{-4}$).

Figure 3.25 shows the effect of nicreasing the path delays on the Rician paths from the two transmit links, it could be noticed that the fading is reduced. Increasing the delay will reduce the inter symbol interference at the receiver and as a result the fading will be reduced. Additionally, there is a high correlation between the envelopes.

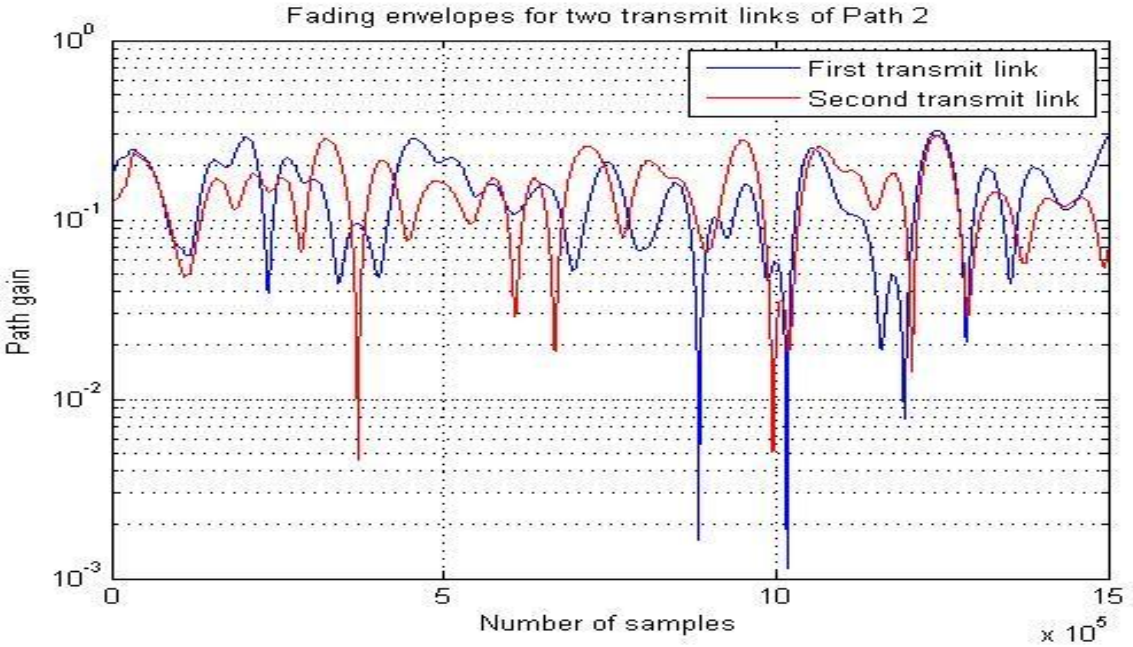

Figure 3.26: Fading envelopes for path 2 when ($tau = [0 \ \ 0.4 \ \ 0.9] \times 10^{-4}$).

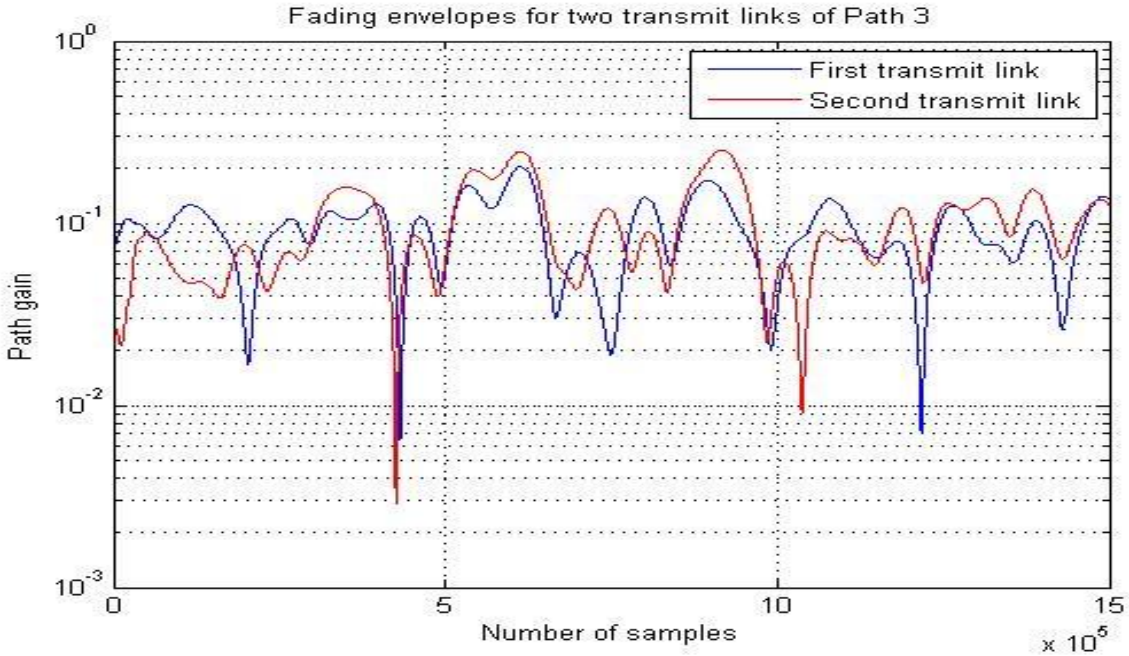

Figure 3.27: Fading envelopes for path 3 when ($tau = [0 \ \ 0.4 \ \ 0.9] \times 10^{-4}$).

Figures 3.26 and 3.27 show the envelopes of the Rayleigh paths after increasing the path delays, it can be observed that the fading is reduced due to the decreasing in the inter symbol interference but with a ratio less than Rician paths. Also, there is a good match between the paths.

- path delays (tau) = $[0\ \ 0.4\ \ 0.9] \times 10^{-8}$:

The following three figures show the effect of decresing the path delays from $[0\ \ 0.4\ \ 0.9] \times 10^{-6}$ to $[0\ \ 0.4\ \ 0.9] \times 10^{-8}$ in both Rician and Rayleigh cases:

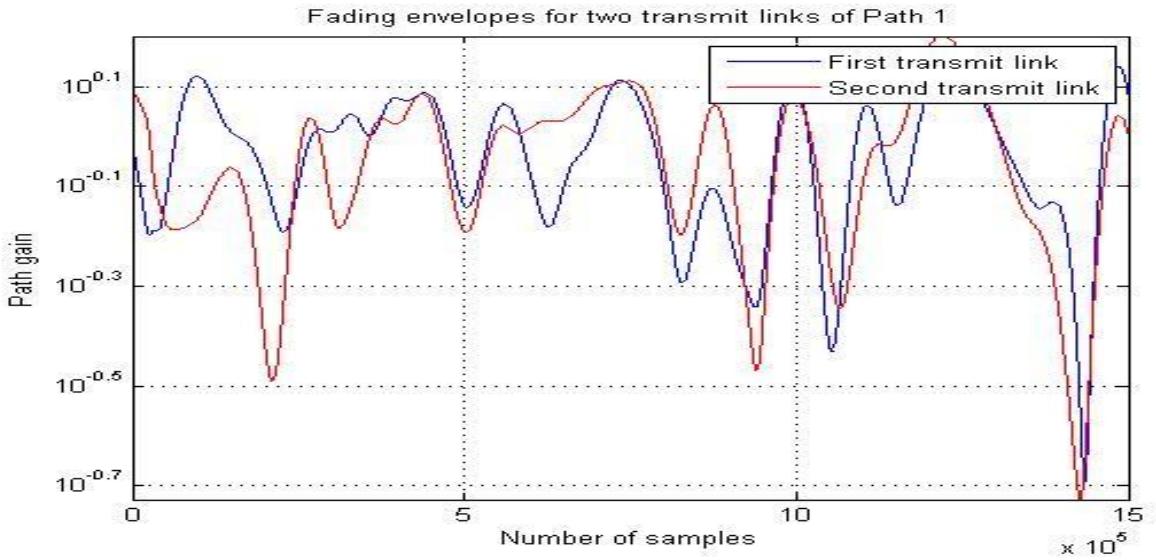

Figure 3.28: Fading envelopes for path 1 when ($tau = [0\ \ 0.4\ \ 0.9] \times 10^{-8}$).

The above figure shows the effect of reducing the path delays on the Rician paths from the two transmit links, it could be noticed that the fading is approximately increased. Reducing the delay will increase the inter symbol interference at the receiver and as a result the fading will be increased.

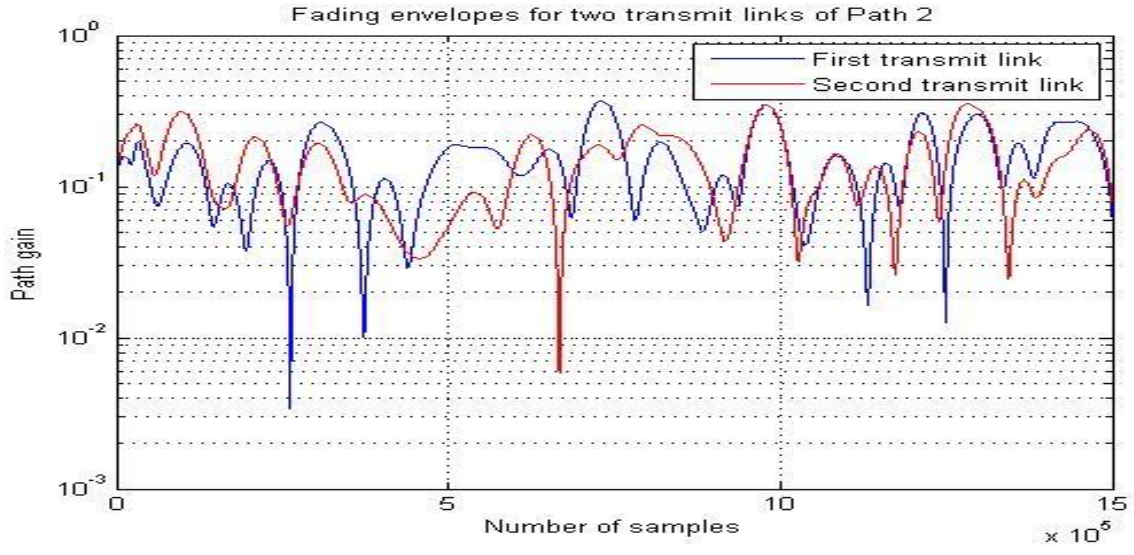

Figure 3.29: Fading envelopes for path 2 when ($tau = [0\ \ 0.4\ \ 0.9] \times 10^{-8}$).

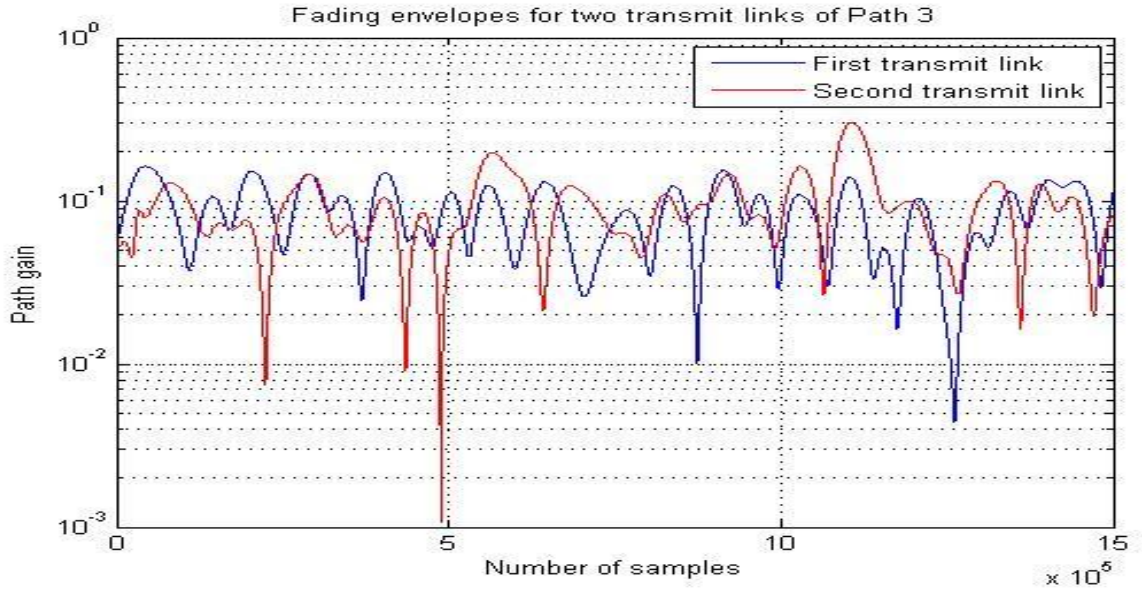

Figure 3.30: Fading envelopes for path 3 when ($tau = [0 \ \ 0.4 \ \ 0.9] \times 10^{-8}$).

Figures 3.29 and 3.30 show the envelopes of the Rayleigh paths after reducing the path delays, it can be observed that the fading is incresed due to the increasing in the inter symbol interference but with a ratio more than Rician paths.

Case 5: changing all parameters together.

In this case the correlation coefficient, Doppler shift, average path gains, and the path delays are considered to be at there perfect values that is (rho = 0.9, fd = 0.1, pdb = [0 -30 -60], $tau = [0 \ \ 0.4 \ \ 0.9] \times 10^{-4}$).:

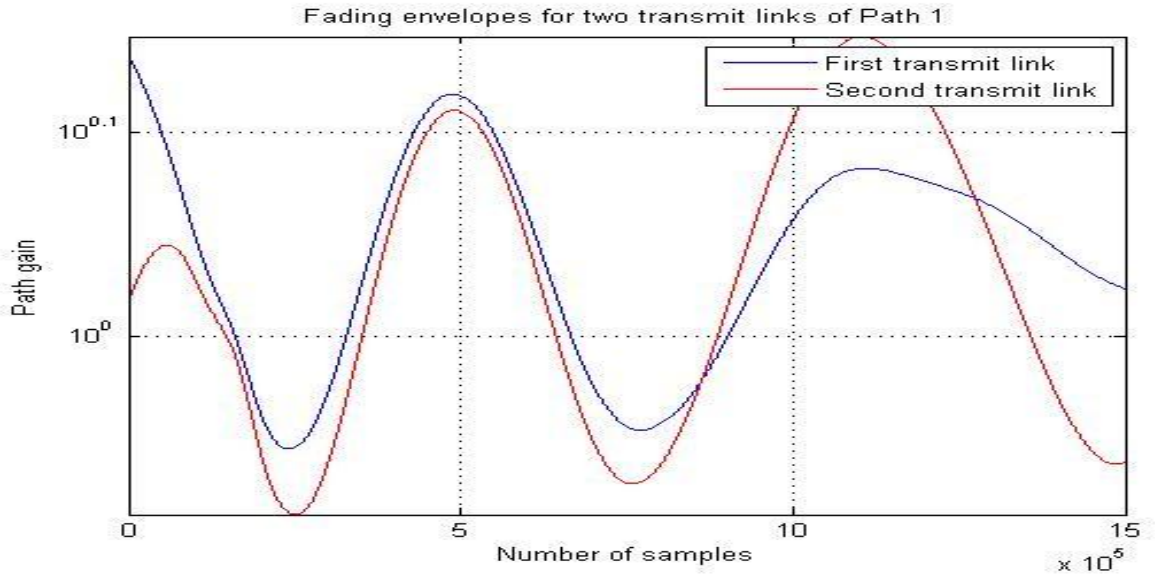

Figure 3.31: Fading envelopes for path 1 with changing all parameters.

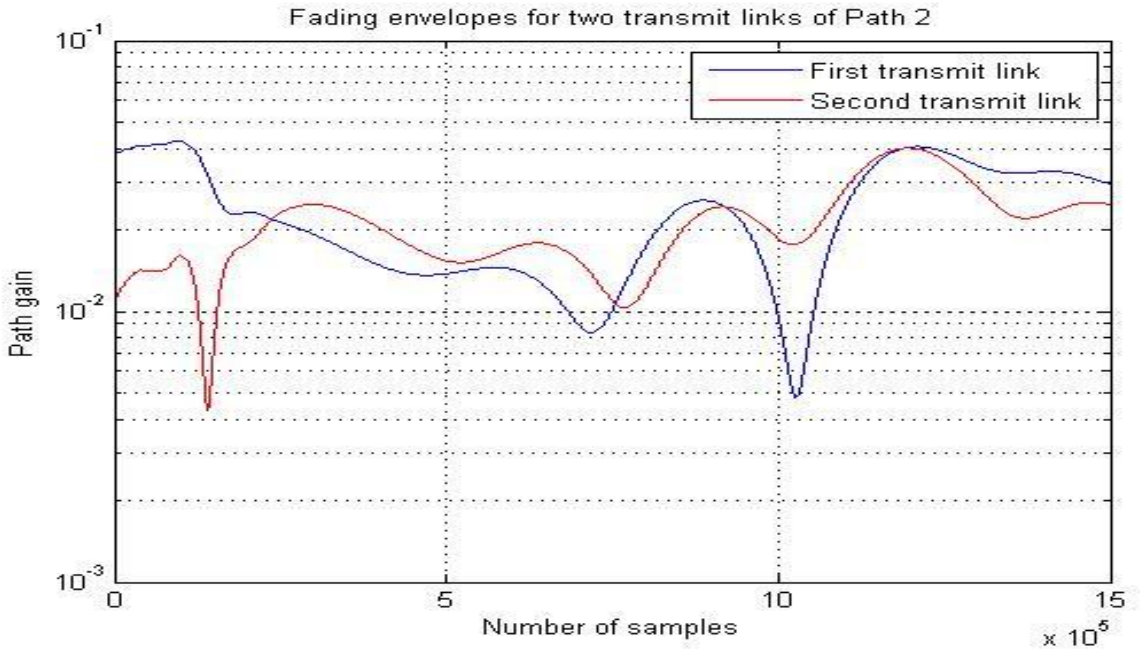

Figure 3.32: Fading envelopes for path 2 with changing all parameters.

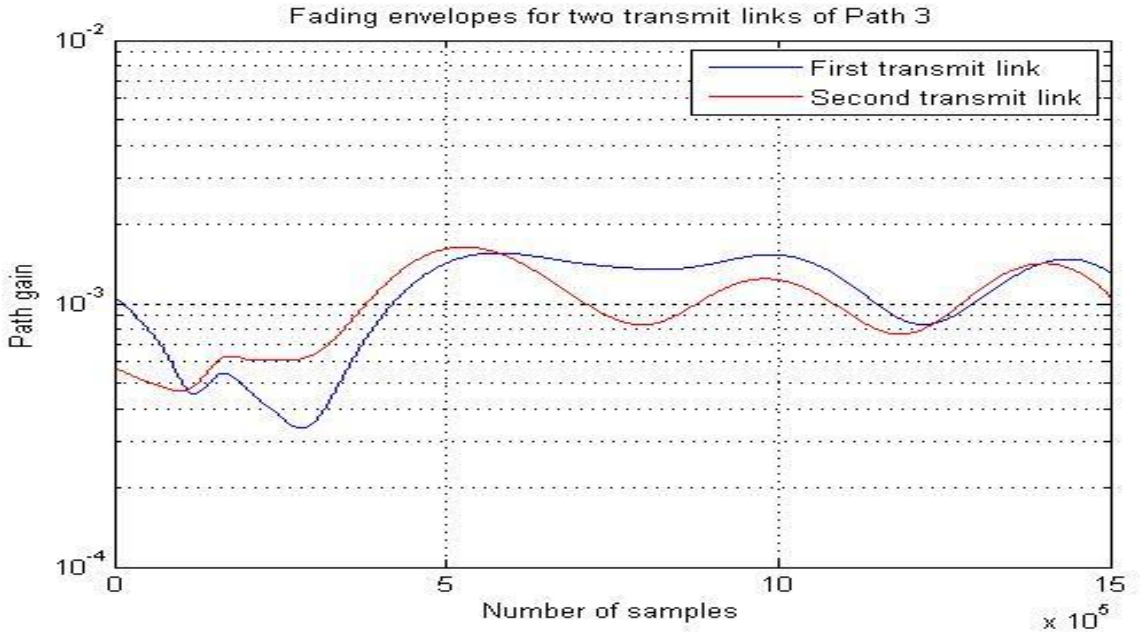

Figure 3.33: Fading envelopes for path 3 with changing all parameters.

The above three figures show an ideal channel conditions. slow variation of the signal and a low fading levels are found to occur.

Case 6: when all paths are Rayleigh:

The following three figures show the fading envelopes when all paths are considered to be Rayleigh; there is no line of sight between the transmitter and the receiver.

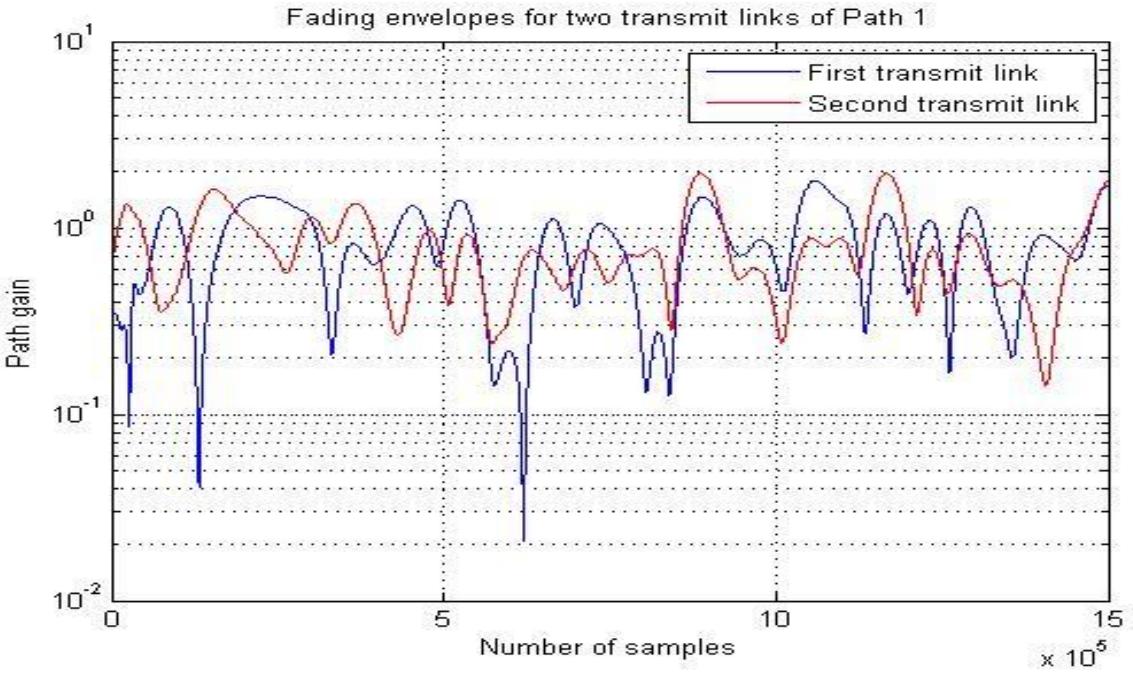

Figure 3.34: Fading envelopes for path 1 when all paths are Rayleigh.

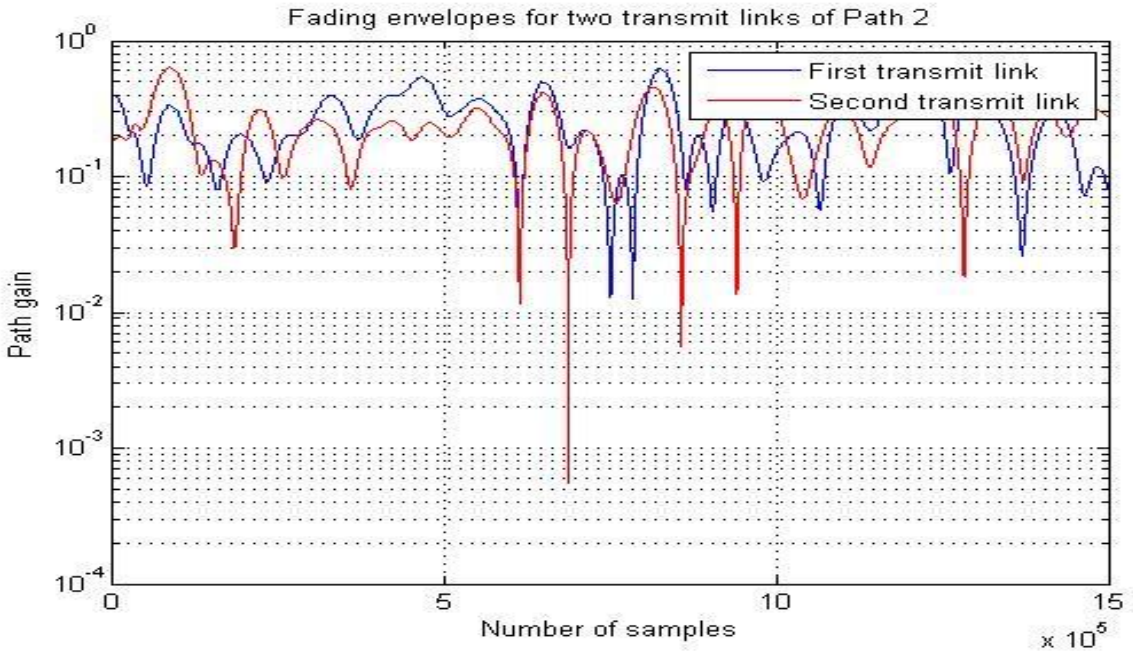

Figure 3.35: Fading envelopes for path 2 when all paths are Rayleigh.

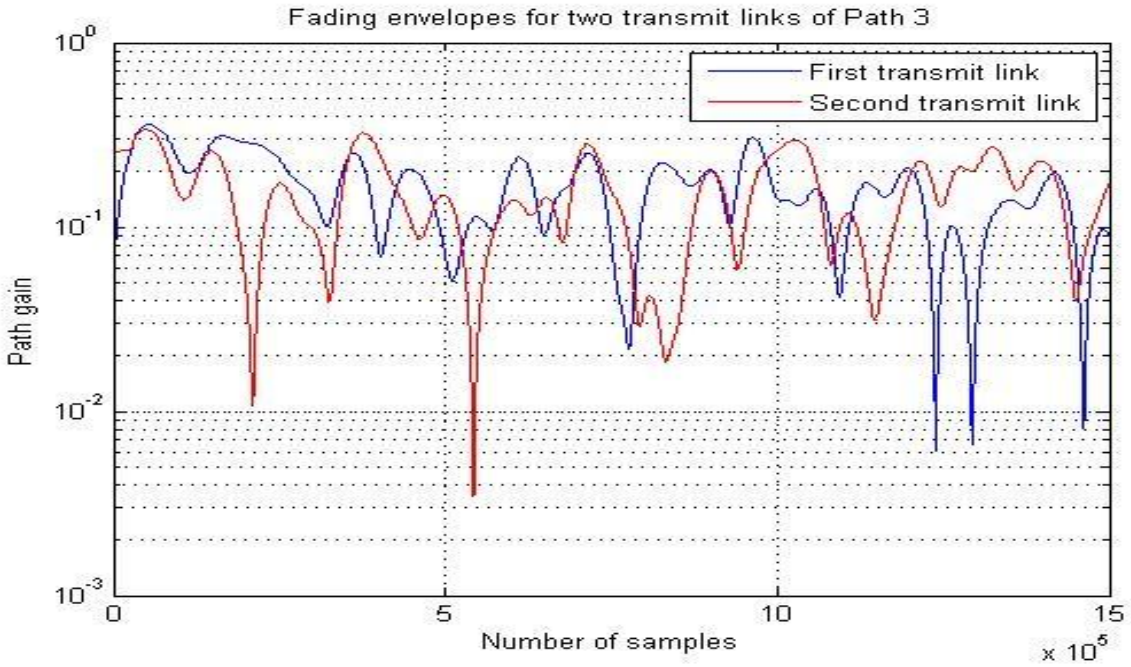

Figure 3.36: Fading envelopes for path 3 when all paths are Rayleigh.

Figure 3.34 shows the envelopes of the first two paths from the two transmit links, a high miss match between the paths has occurred.

Case 7: when all paths are Rician:

The following three figures show the fading envelopes when all paths are considered to be Rician; there is line of sight between the transmitter and the receiver.

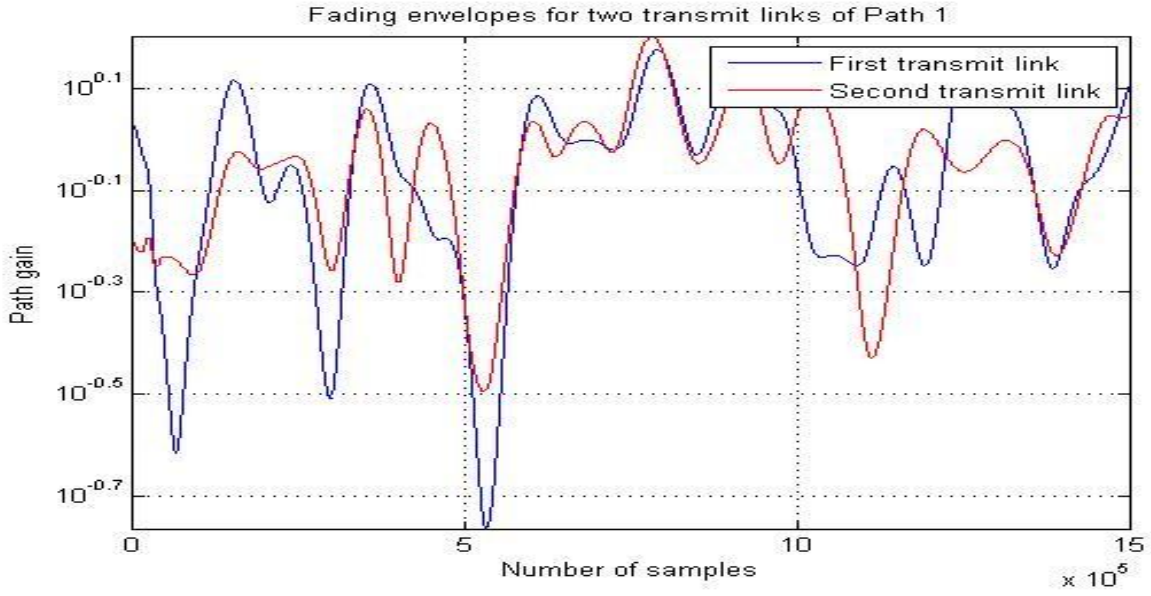

Figure 3.37: Fading envelopes for path 1 when all paths are Rician.

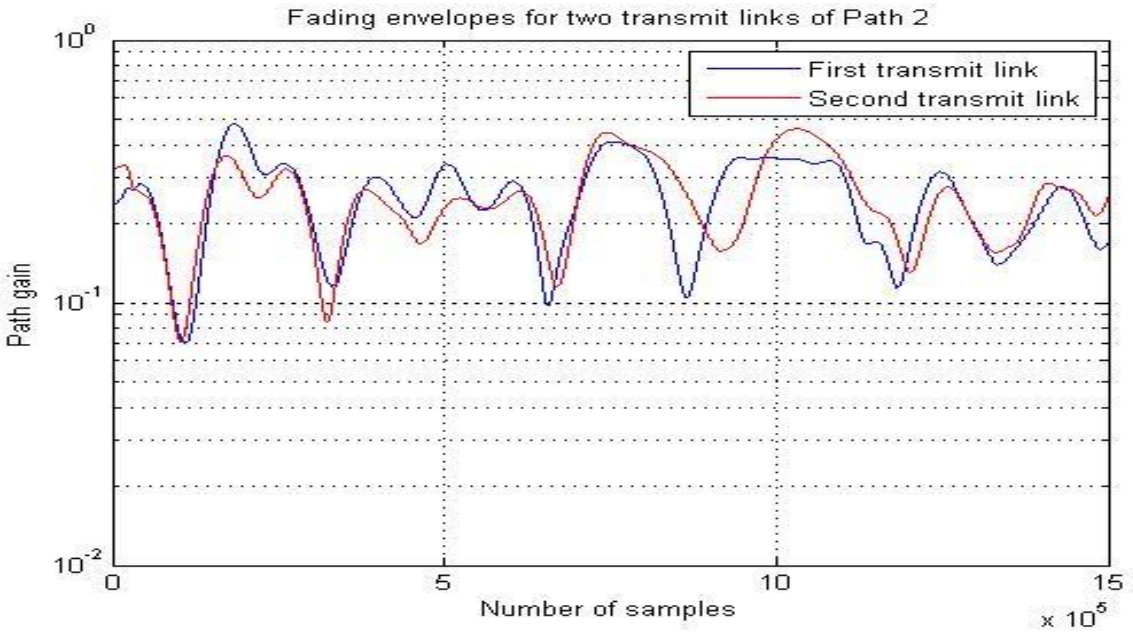

Figure 3.38: Fading envelopes for path 2 when all paths are Rician.

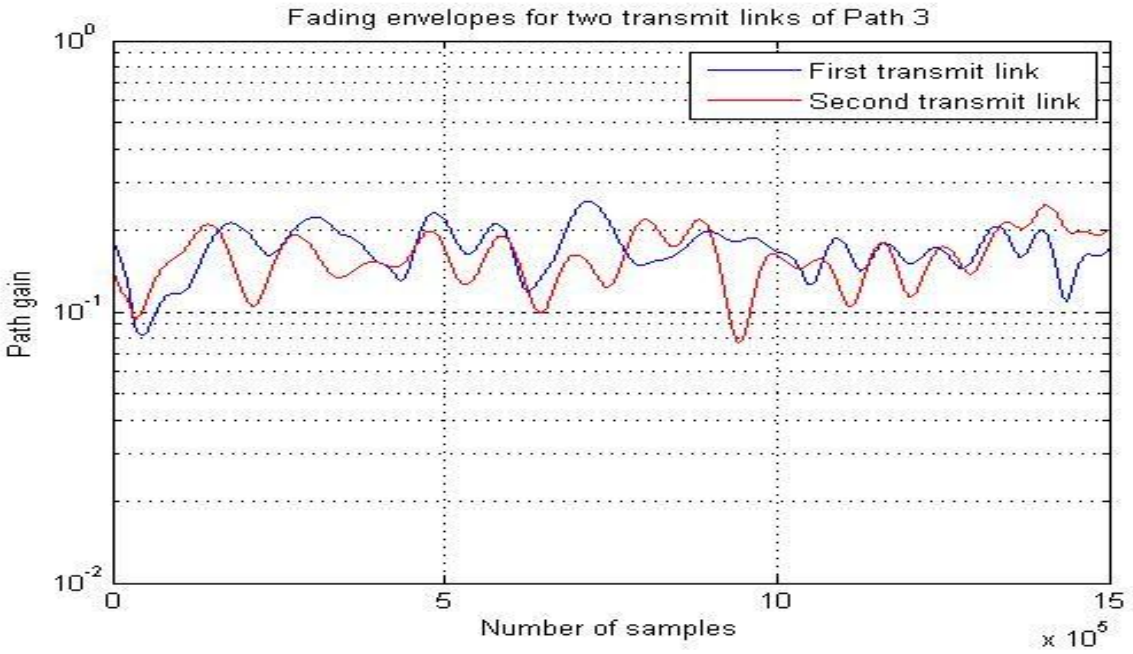

Figure 3.39: Fading envelopes for path 3 when all paths are Rician.

Figures 3.38 and 3.39 show Rician fading envelopes of path2 and path3 respectively, a more correlation between the paths can be noticed compared to the original case where they were Rayliegh, the fading also has been decreased.

Case 8: changing the symbol rate.

The following figures show the fading envelopes of all paths when increasing the symbol rate from 1×10^3 to 1×10^4.

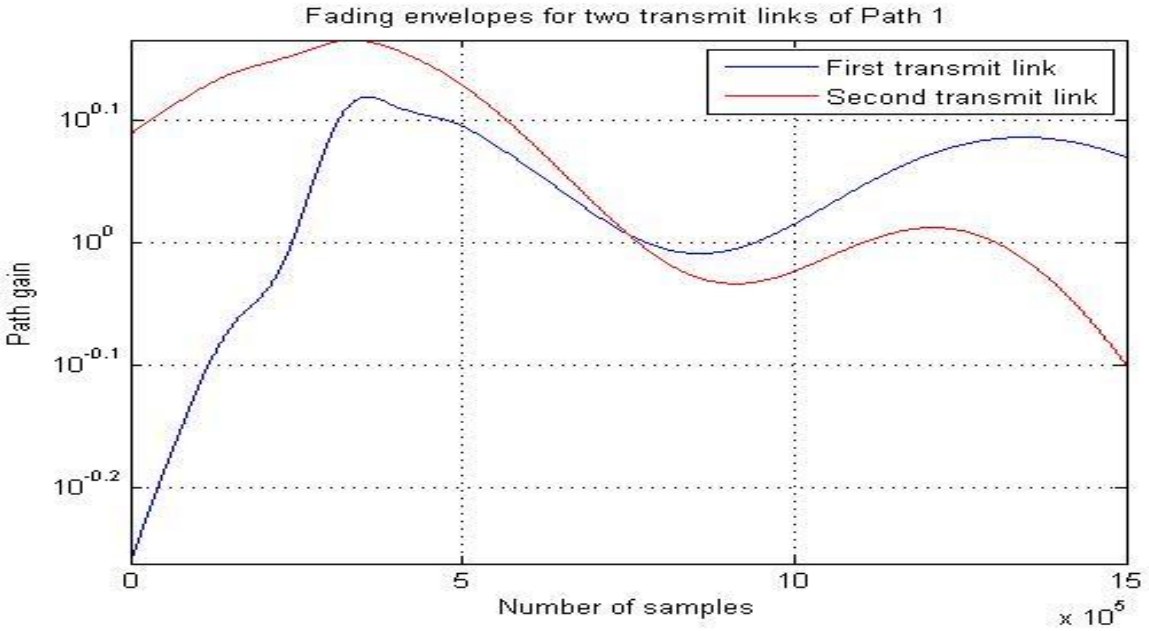

Figure 3.40: Fading envelopes for path 1 when symbol rate = 1×10^4 .

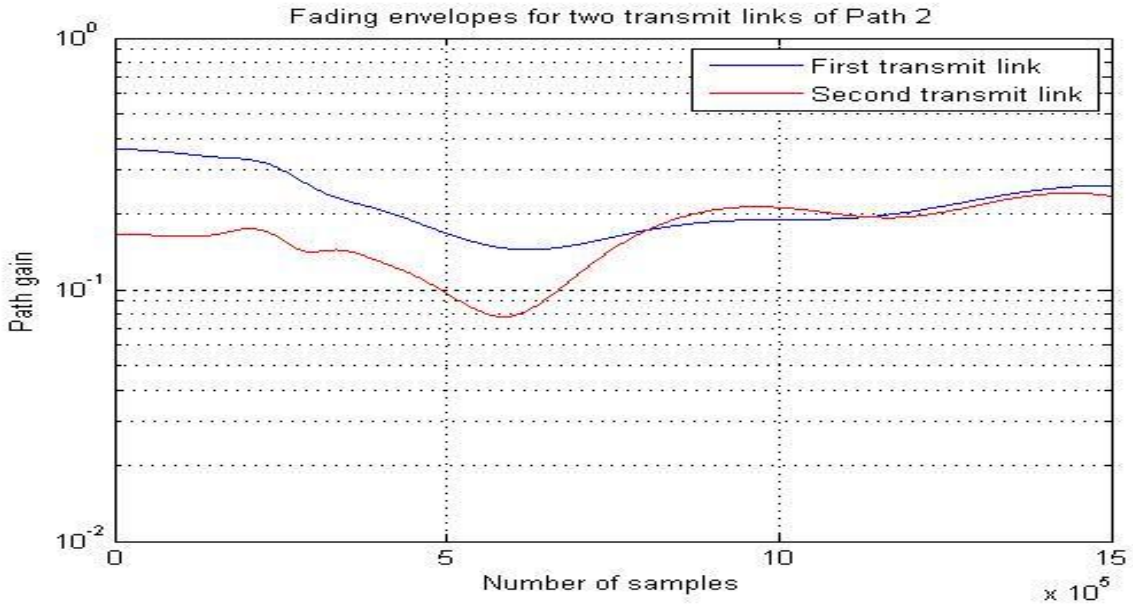

Figure 3.41: Fading envelopes for path 2 when symbol rate = 1×10^4 .

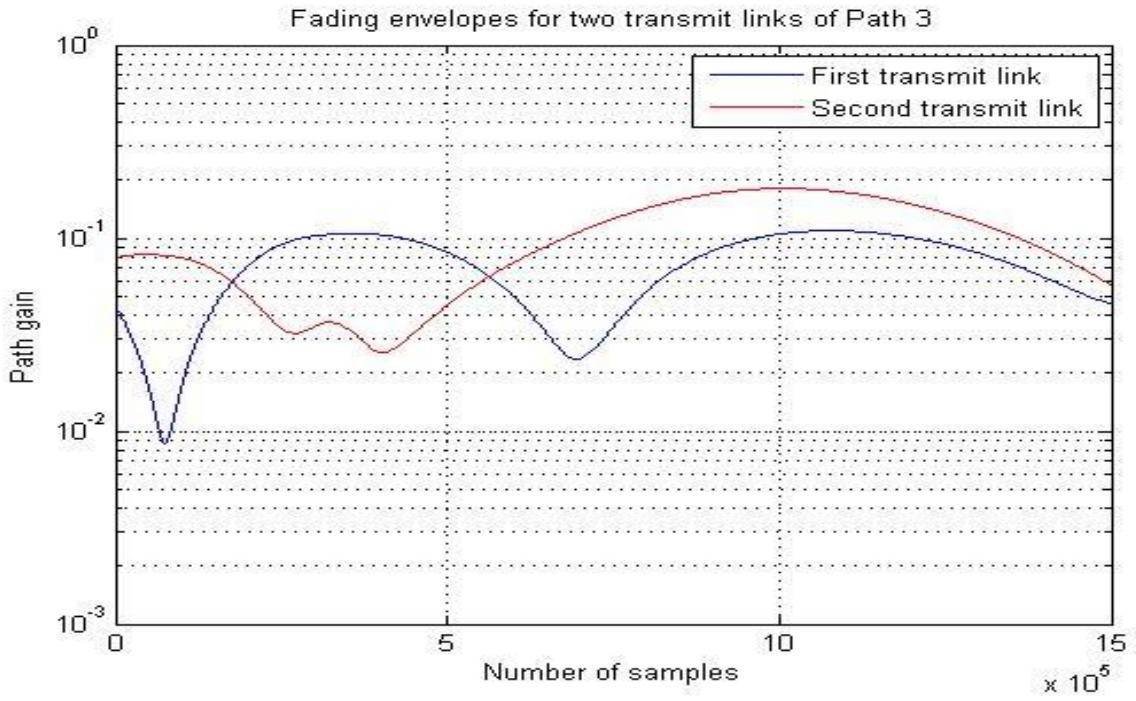

Figure 3.42: Fading envelopes for path 3 when symbol rate = 1×10^4 .

The above three figures show the effect of increasing the symbol rate on the fading envelopes, increasing the symbol rate leads to reducing the symbol period and as a result the probability of the symbol's transmission within the coherence time will increase, that's the symbol will travel through the channel while it is not varying ,which means the variations of the channel that the symbol will examine will be less.

The following table sumurizes the main results:

parameter		Results
Correlation Coefficient (rho)	0.4	Miss correlation between the links.
	0.9	A high and approximately full match between the links, which means they examine the same channel conditions.
Doppler Shift (fd)	0.1	Slow variations in the fading envelopes due to the slow movement of Tx and Rx
	0.8	Rapid fluctuations in the fading envelopes (high speed mobility)
Path gains (pdb) in dB	[0 -30 -60]	The level of the envelopes reaches a less gain levels (SNR has been decreased)
	[0 -5 -10]	The level of the envelopes reaches a higher gain levels (SNR has been increased)
Path delays (tau) in seconds	[0 0.4 0.9]x10^{-4}	The fading is reduced as a result of ISI reduction
	[0 0.4 0.9]x10^{-8}	The fading is increased as a result of ISI increment
Symbol rate in symbol/second	1x10^{4}	A low fluctuation in the fading envelopes and a high correlation between them, since the probability of the symbol's transmission within the coherence time has been increased.

Table 3.2: Results of changing main channel parameters.

Chapter 4

Simulation results

Chapter contents:

4.1. An overview.

This chapter introduces the simulation results for simulating the MIMO 4x2 and 2x2 bad urban and rural macro-cells, the 8x2 simulation results for indoor scenario as well, and finally the impact of the frequency of operation on the path-loss model.

4.2. Main simulation stages.

The following are the main steps through which the simulation process is accomplished:

- **An initializing phase:**

During which parameters of the set-up are read and initialized. Parameters such as; angles of arrival and angles of departure (AoA/AoD), path gains (pbd), the spacing between the transmitters and receivers, transmitters and receivers numbers ….etc, are firstly defined.

- **A processing phase:**

During which the actual simulation runs. In the simulation it is assumed that the multipath components are divided into three clusters each with five paths that is similar in the AoA, AoD, AS. Line of sight (LOS) and non-line of sight (NLOS). Then, the impulse response of the channel is extracted for each of the defined propagation scenario after defining a set of the path-loss equations for the considered environments. Thereafter, transmit and receive correlation matrices for the different MIMO configurations are constructed.

- **A post-processing Phase:**

To exploit simulation results; the channel behavior being observed for each path while manipulating the scenarios-dependent parameters. Two ways for plotting the impulse response are used; either plotting all of the impulse responses for each defined link between the transmitter and the receiver, or plotting the impulse response for one path through all the links among the transmitters and receivers.

For details on the path-loss equation that this simulation make use of, you can kindly refer to chapter one of this project or to [6] for more details.

The communication system illustration is shown in figure 4.1.

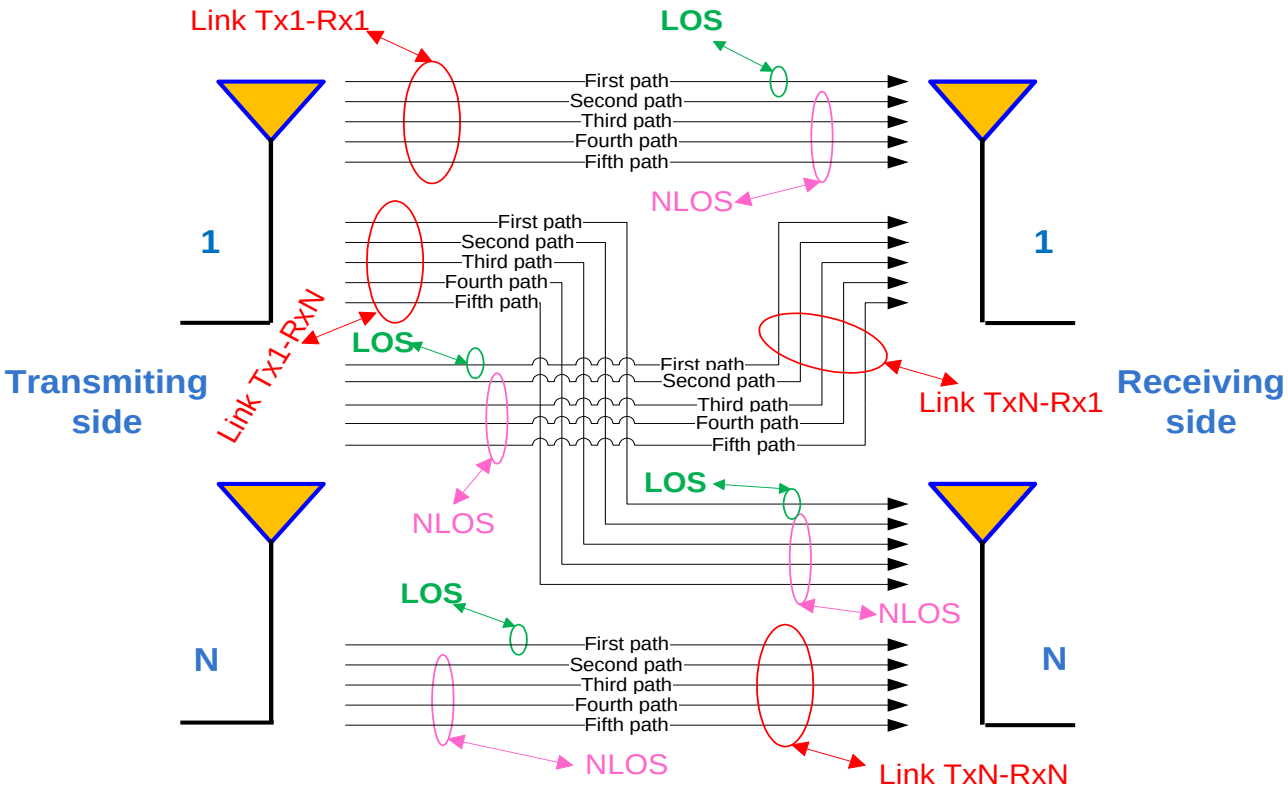

Figure 4.1: The communication system illustration.

It should be noticed that the values of the parameters in table 4.1 are one of the simulation's assumptions. Moreover the paths delays were assumed to be random, and the path gains were derived from the path loss equations of chapter 1.

Cluster number	Parameters	Path 1	Path 2	Path 3	Path 4	Path 5
Cluster 1	AoD	120	120	120	120	120
	AoA	170	170	170	170	170
	AS	14.4	14.4	14.4	14.4	14.4
Cluster 2	AoD	150	150	150	150	150
	AoA	250	250	250	250	250
	AS	25.4	25.4	25.4	25.4	25.4
Cluster 3	AoD	200	200	200	200	200
	AoA	130	130	130	130	130
	AS	29.5	29.5	29.5	29.5	29.5

Table 4.1: clusters parameters.

The following flow chart shows the simulation process of extracting the channel response:

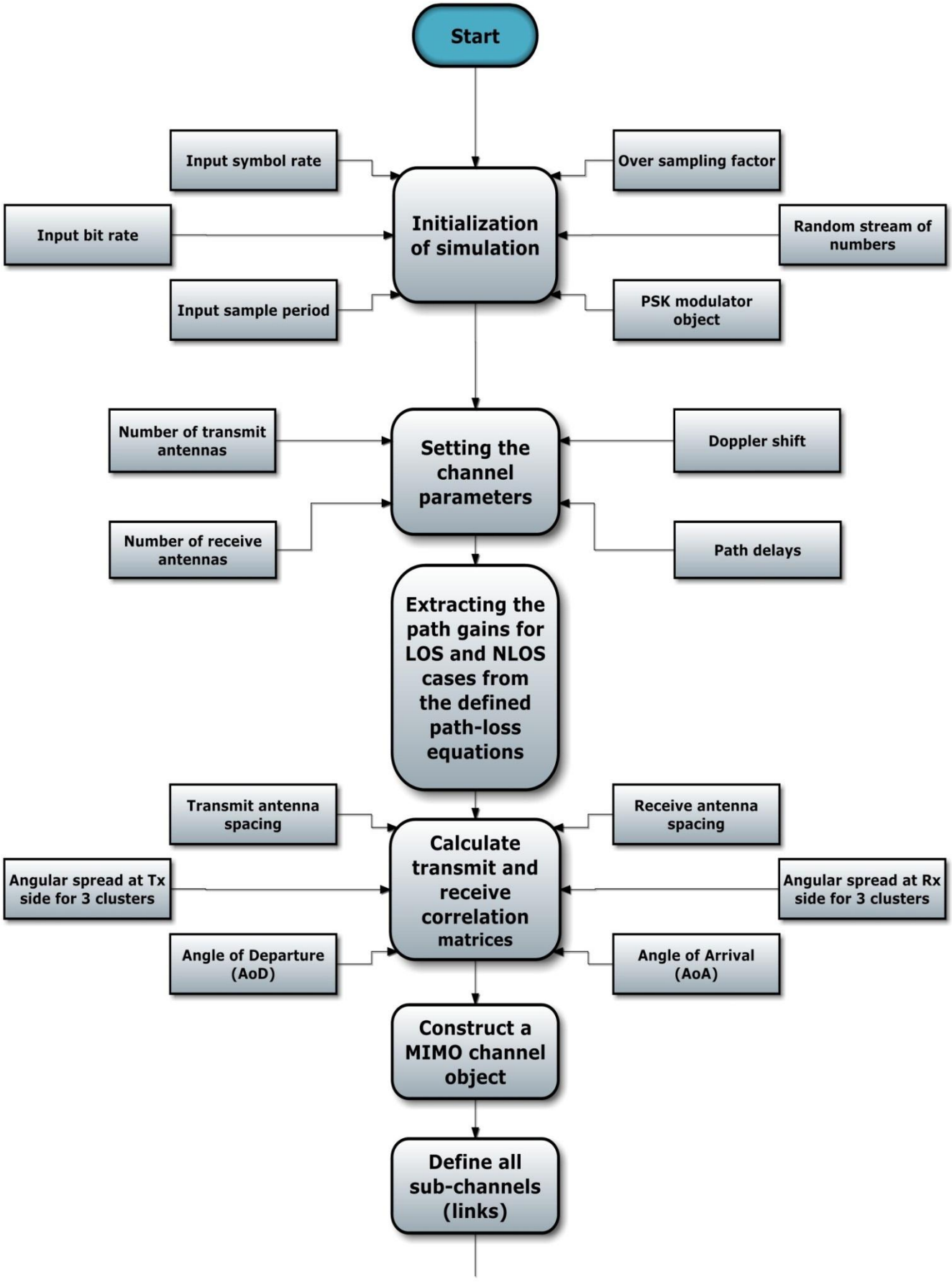

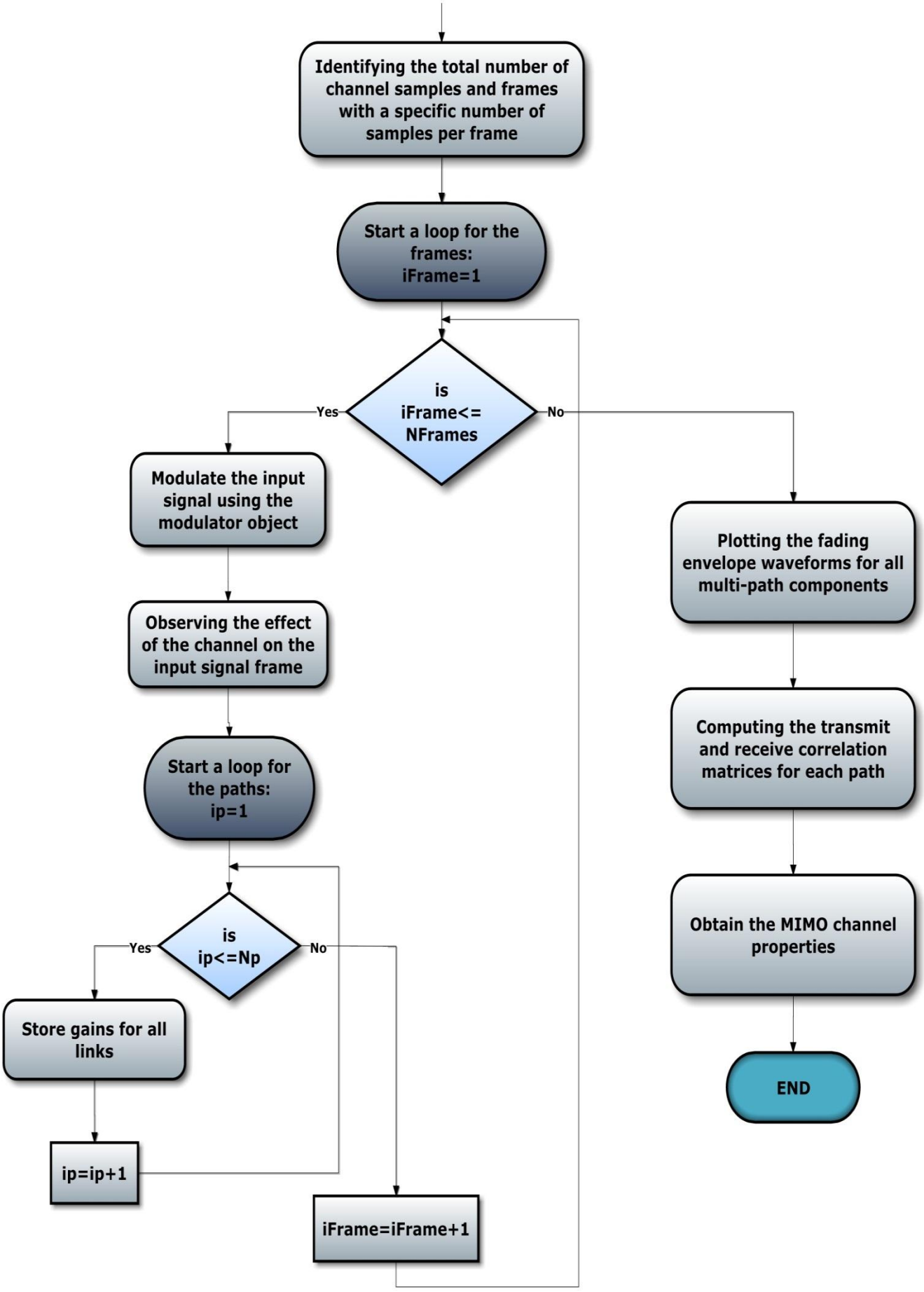

Figure 4.2: simulation process flowchart

4.3. Simulation results for 2x2 MIMO channel model under bad urban macro-cell and rural macro-cell environments.

In this section, the simulation results for both bad urban and rural environments are introduced.

- **Bad urban macro-cell:**

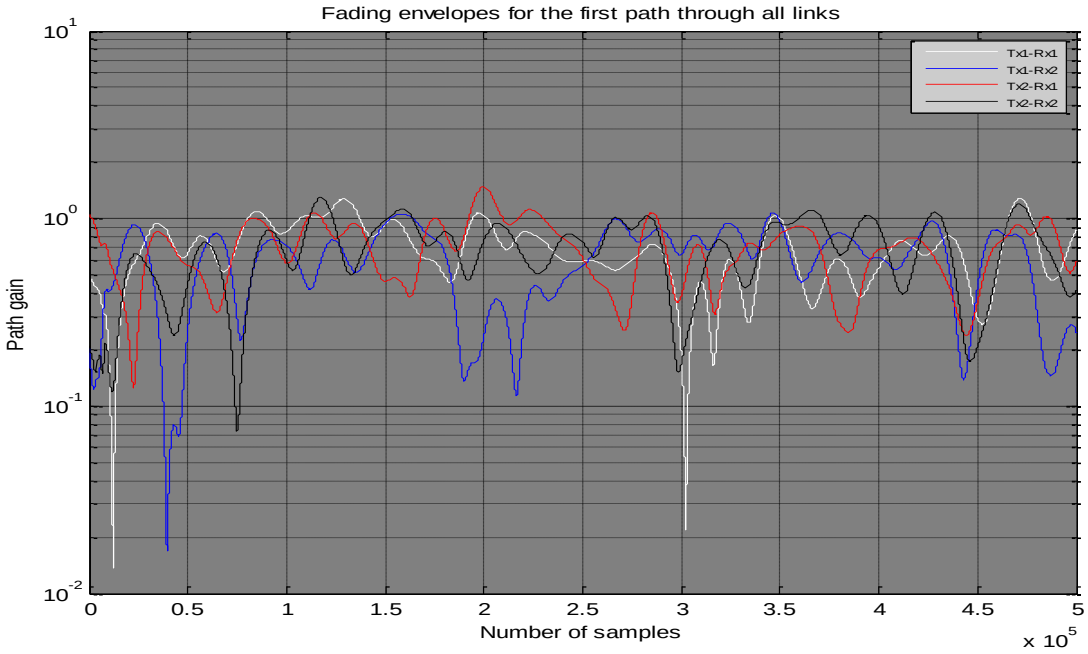

Figure 4.3: Fading envelopes for path1 through all links (2x2Bad urban).

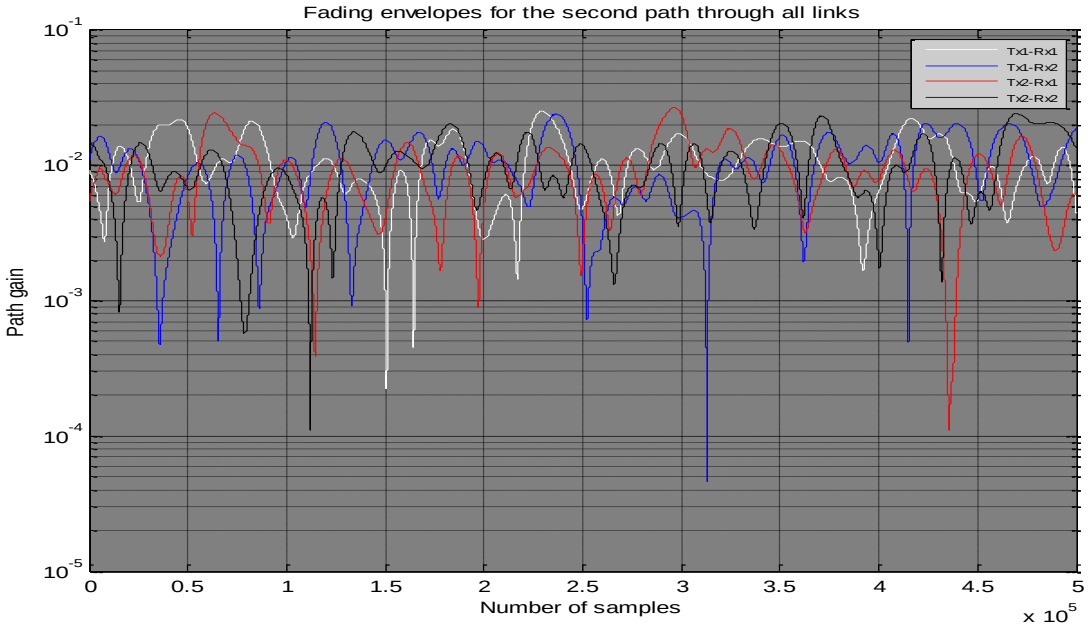

Figure 4.4: Fading envelopes for path2 through all links (2x2Bad urban).

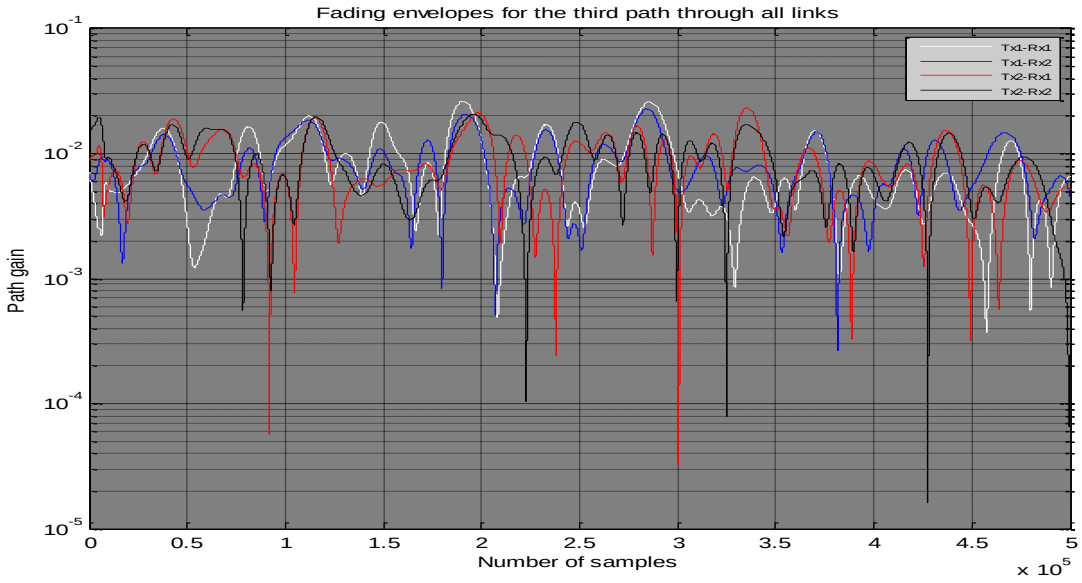

Figure 4.5: Fading envelopes for path3 through all links (2x2Bad urban).

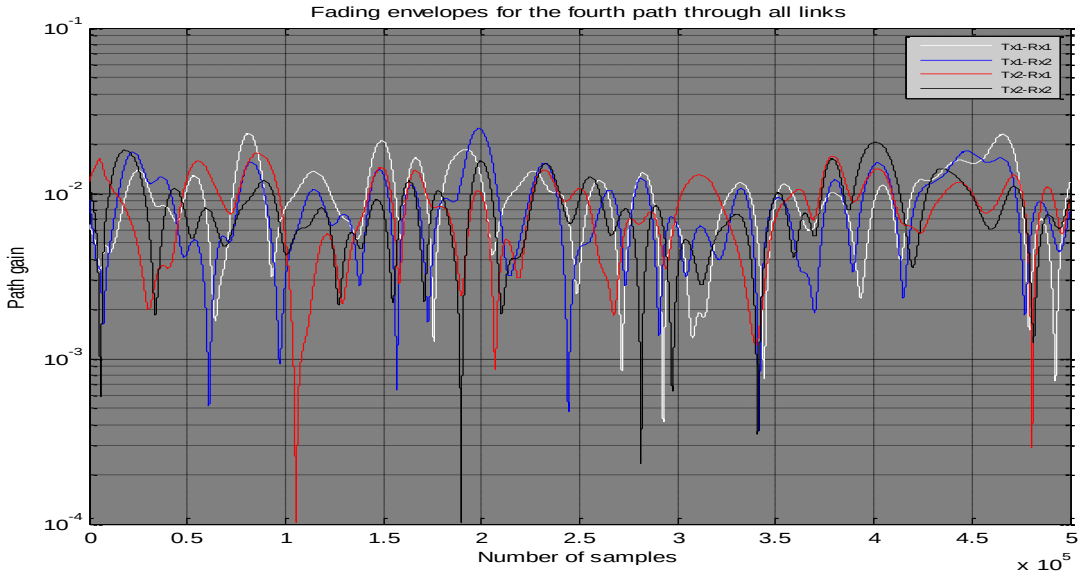

Figure 4.6: Fading envelopes for path4 through all links (2x2Bad urban).

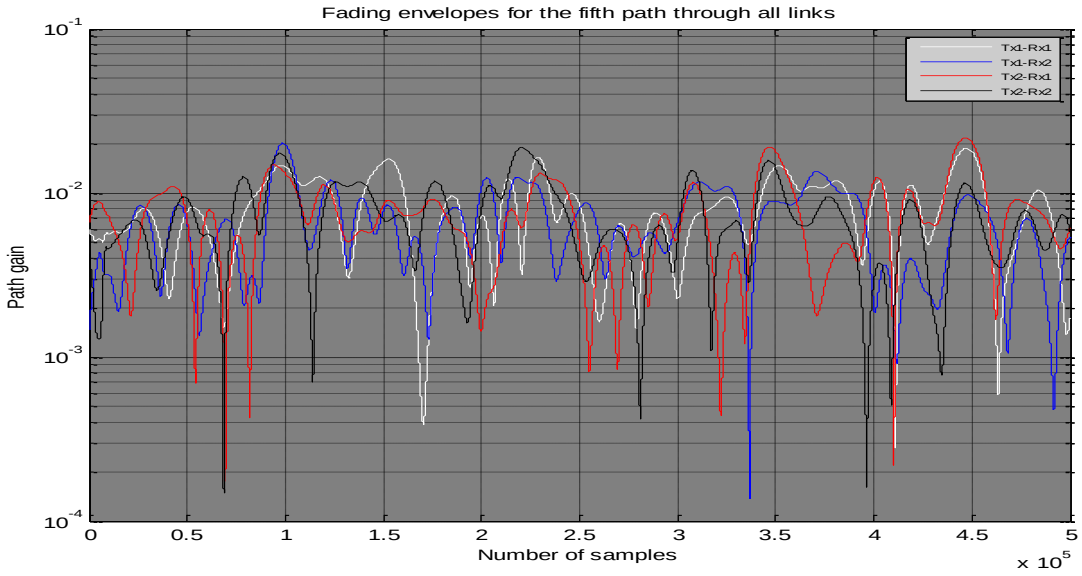

Figure 4.7: Fading envelopes for path5 through all links (2x2Bad urban).

- **Rural macro-cell:**

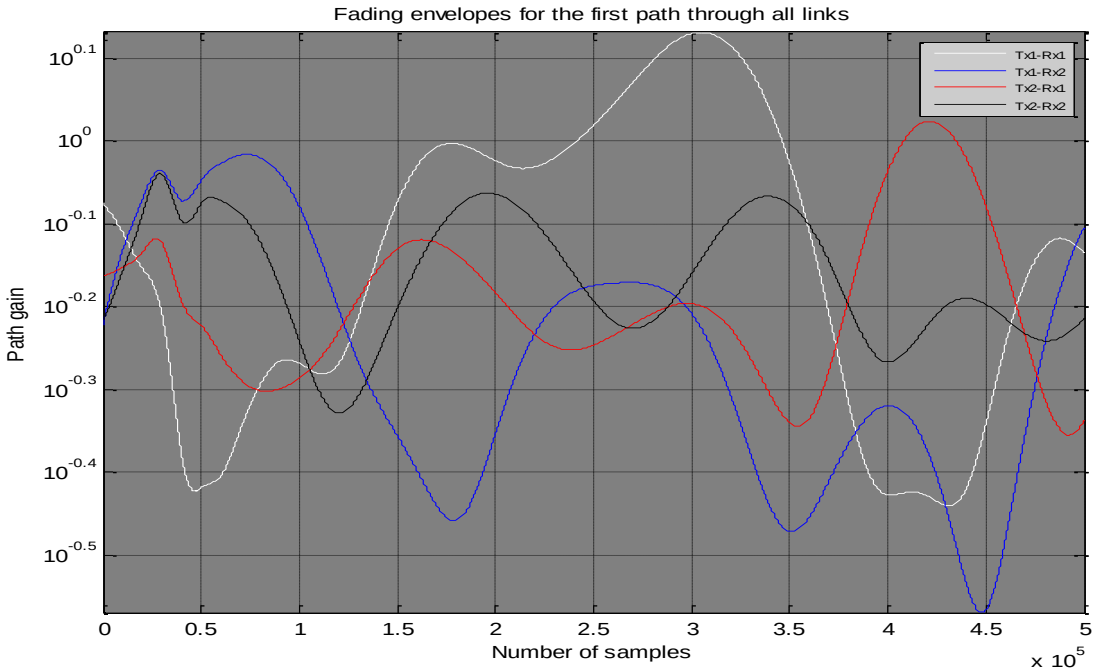

Figure 4.8: Fading envelopes for path1 through all links (2x2Rural).

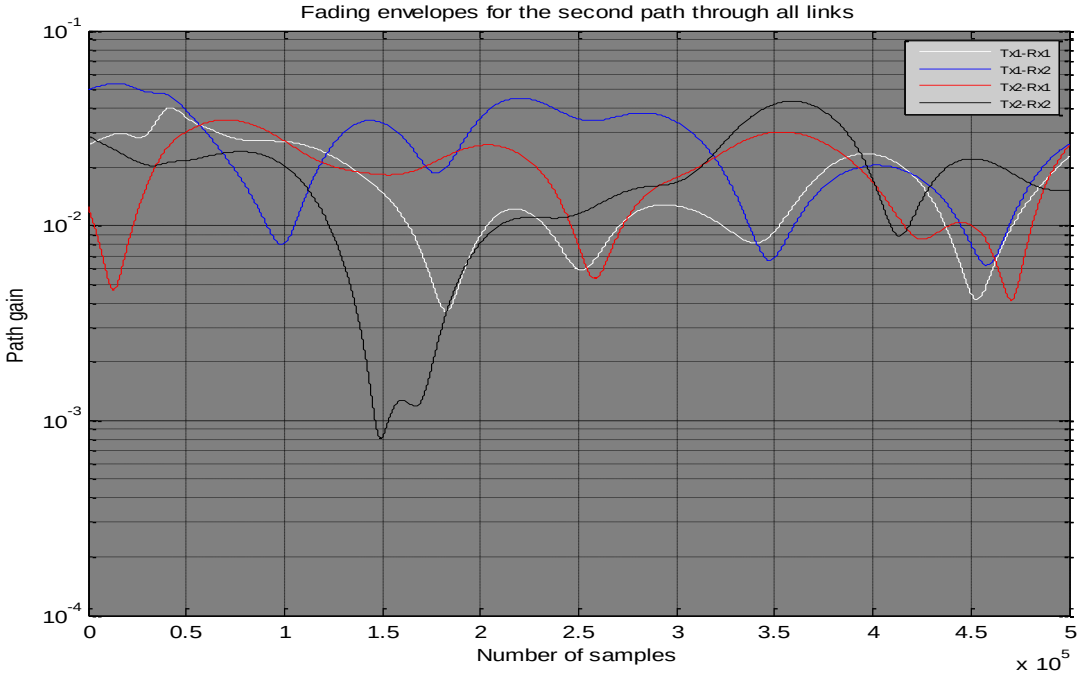

Figure 4.9: Fading envelopes for path2 through all links (2x2Rural).

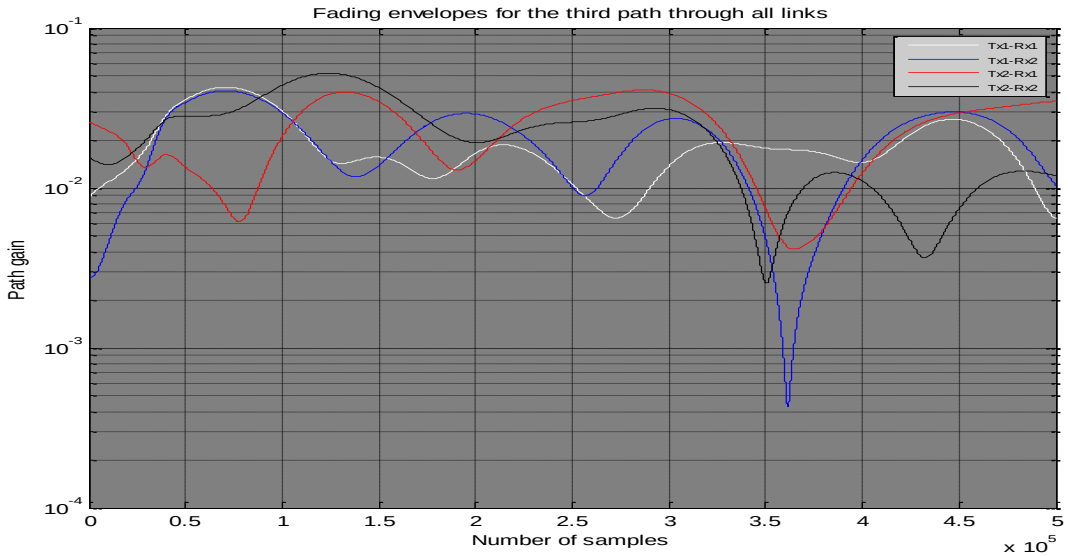

Figure 4.10: Fading envelopes for path3 through all links (2x2Rural).

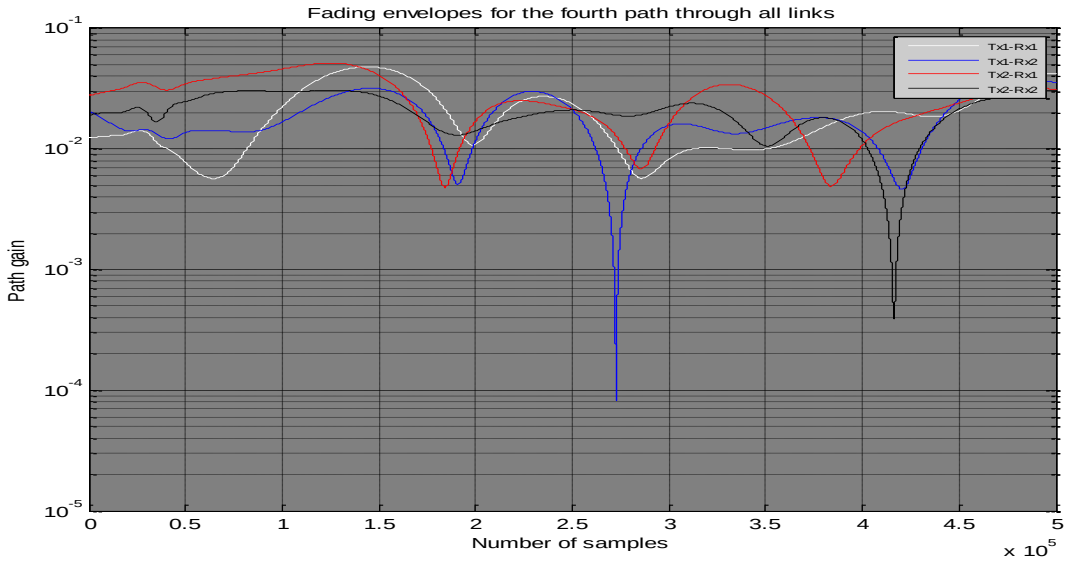

Figure 4.11: Fading envelopes for path4 through all links (2x2Rural).

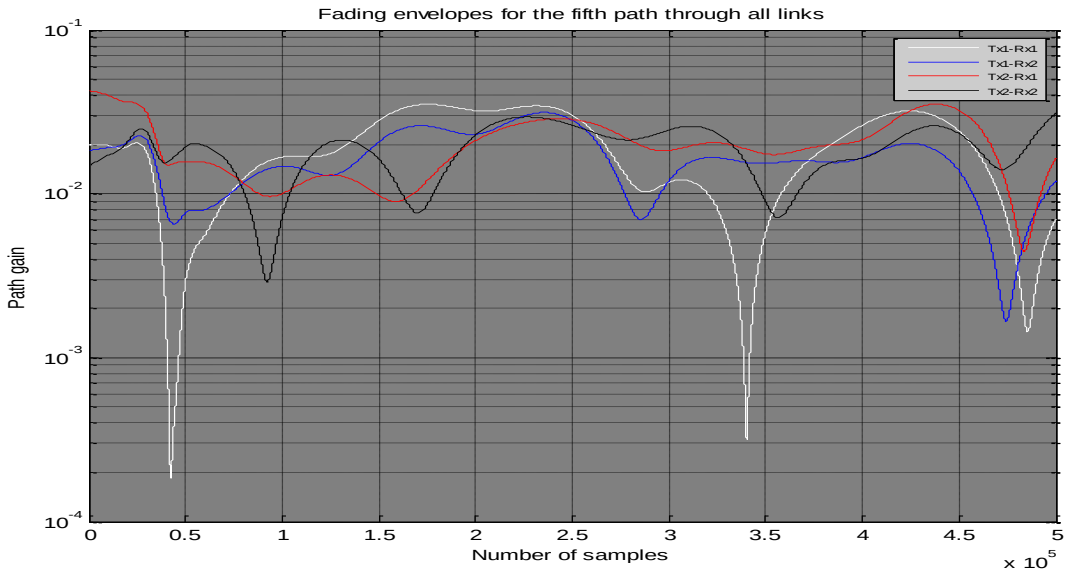

Figure 4.12: Fading envelopes for path5 through all links (2x2Rural).

The graphs above **(4.3 - 4.12)** show the response of the MIMO channel under bad urban and rural macro-cell environments while maintaining: symbol rate=10^3, Doppler shift of 2 for bad urban and 0.4 for rural, and T_x and R_x spacing of 1 λ and 0.5 λ respectively.

Figures **(4.3** and **4.8)** were considered to be LOS components and given a Rician K-factor of 2. This is why they suffer a less fading than the other NLOS components.

From the simulation results above, it can easily be noticed that the channel behavior is more stable in the rural propagation environment than the bad urban scenario. Stability here means low fluctuations and smoother fading envelopes.

4.4. Simulation results for 4x2 MIMO channel model under bad urban environment.

This section shows the simulation results for 4x2 MIMO system configurations under bad urban environments. The influence of the Doppler shift and the symbol rate is also observed and analyzed.

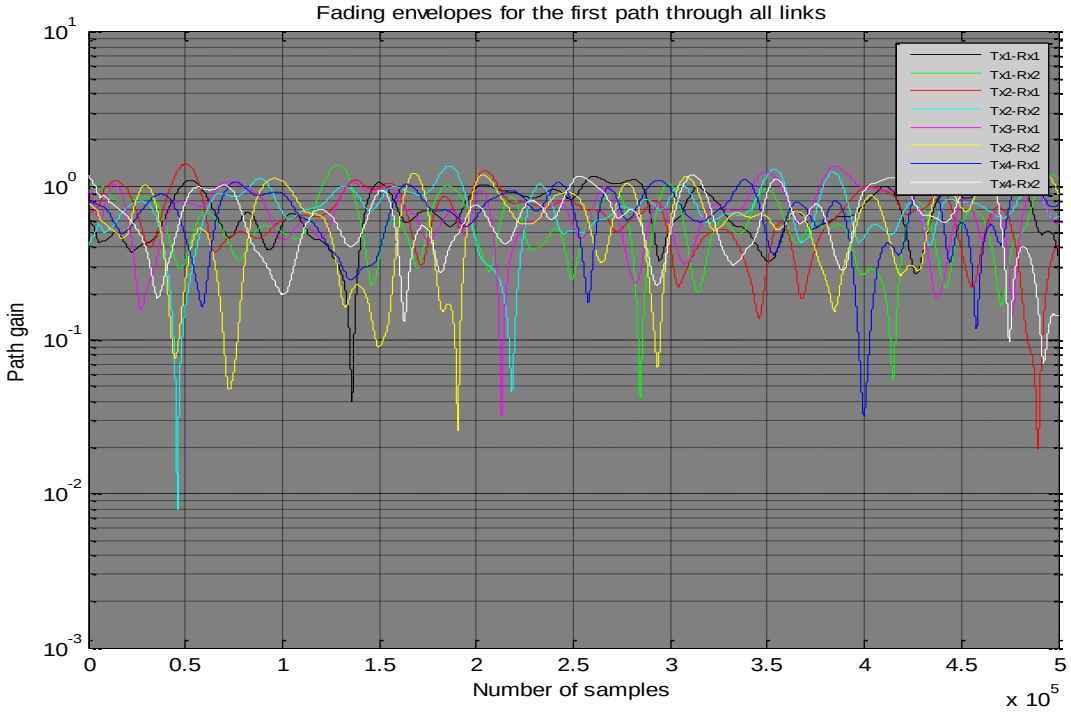

Figure 4.13: Fading envelopes for path1 through all links (4x2Bad Urban).

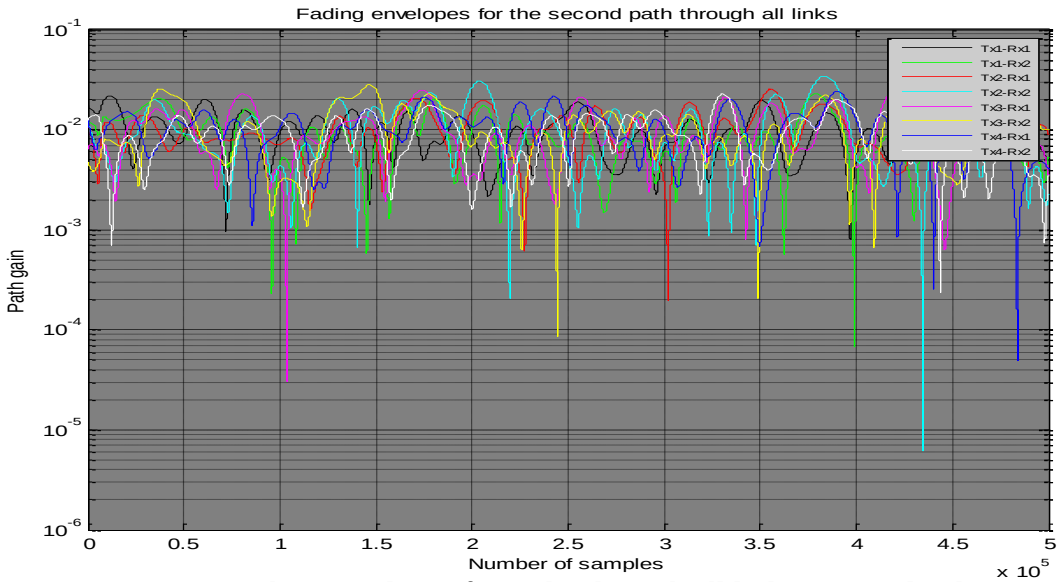

Figure 4.14: Fading envelopes for path2 through all links (4x2Bad Urban).

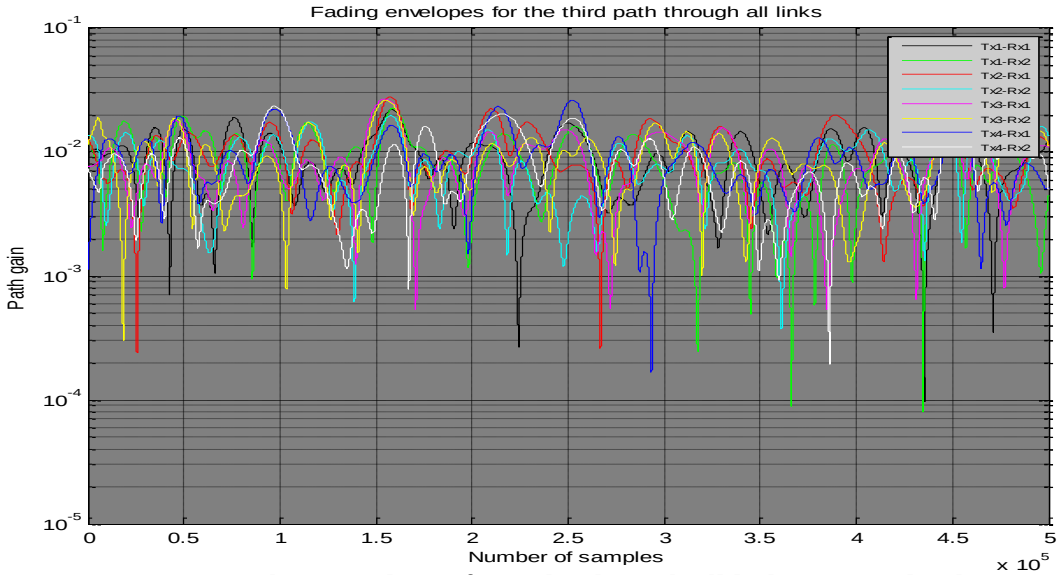

Figure 4.15: Fading envelopes for path3 through all links (4x2Bad Urban).

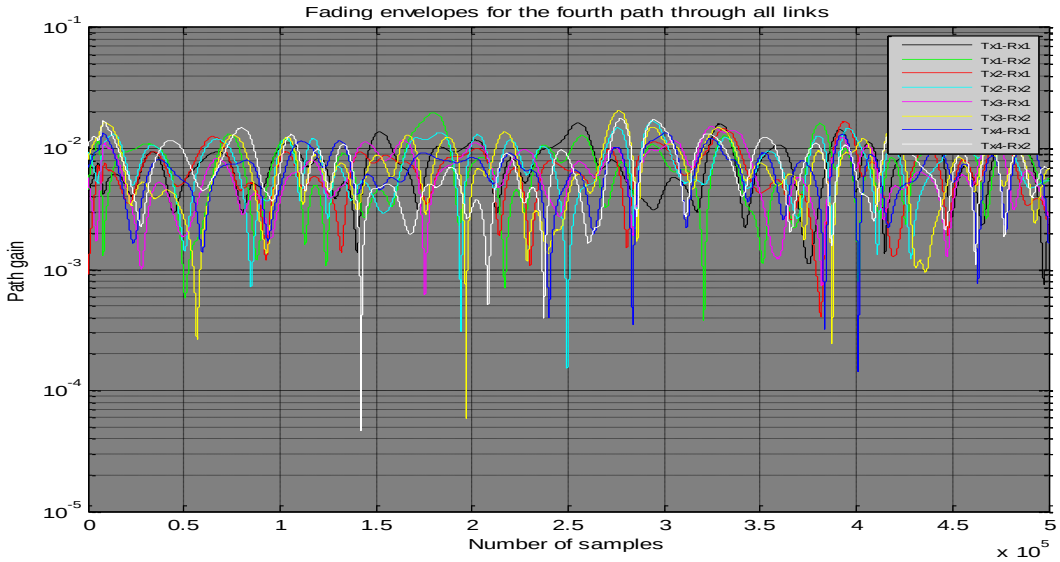

Figure 4.16: Fading envelopes for path4 through all links (4x2Bad Urban).

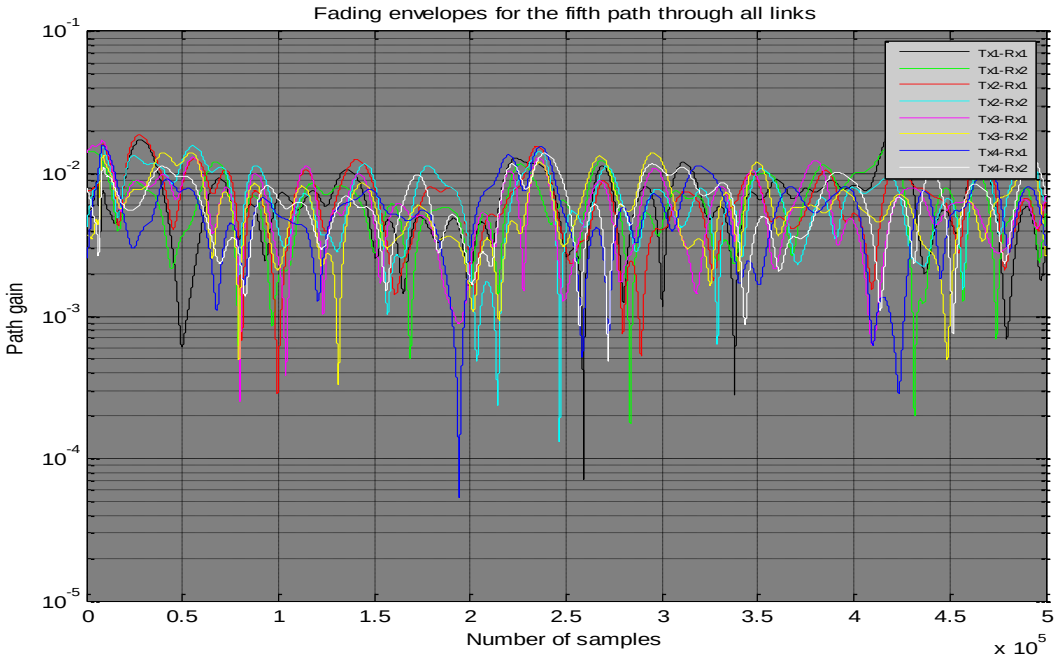

Figure 4.17: Fading envelopes for path5 through all links (4x2Urban).

As a matter of illustration between LOS and NLOS propagating signals, the five paths are observed through Tx4-Rx-2 link as a simulation sample.

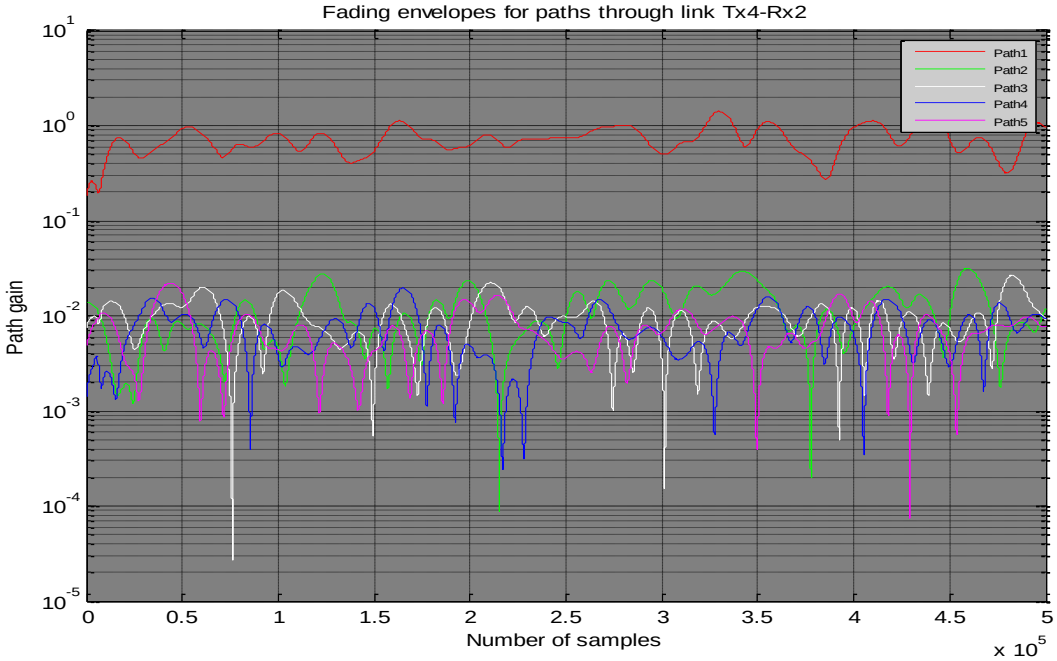

Figure 4.18: Fading envelopes for the five paths through link Tx4-Rx2 (4x2Urban).

In the above figure, the line of sight component is drawn with a red color while the other four components are non-line of sight ones. The level of the fading that the signals examine can be clearly noted in the above figures. It is clear that the LOS

component suffers a much less fading than the NLOS components do. In addition, considering the case of NLOS a more fluctuation in the signal envelopes can be seen.

4.4.1. Observing the effect of changing the Doppler shift, symbol rate, and the antennas spacing.

- ***Symbol rate effect:***

For comparison purpose take figure **(4.17)** as a reference point. Figures **(4.19.A)** and **(4.19.B)** show the fading envelopes of the fifth path through all links when increasing the symbol rate to 10^4 symbol/second and when decreasing its value to 10^2 respectively, considering the bad urban macro cell scenario. Increasing the symbol rate leads to reduced symbol period and as a result the probability of the symbol's transmission within the coherence time will increase, that is the symbol will travel through the channel while it is not varying ,which means the variations of the channel that the symbol will examine will be less, and vice versa when reducing the symbol rate.[31]

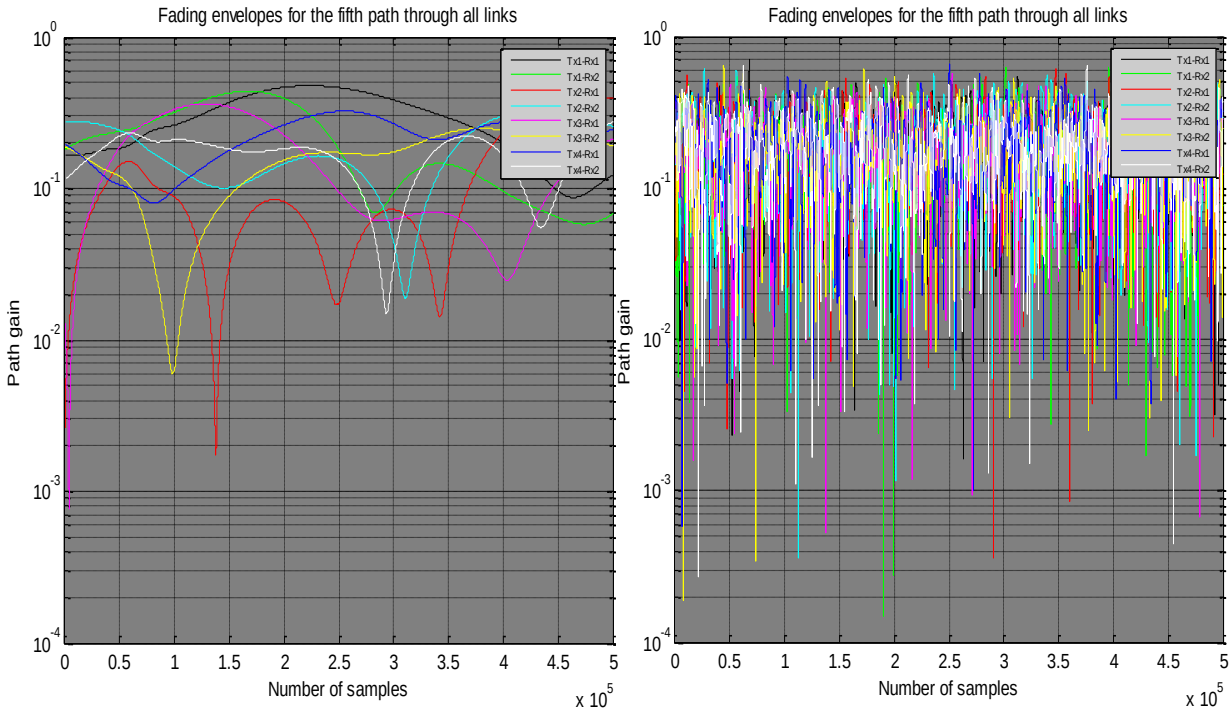

(A) **(B)**

Figure 4.19: Bad urban macro cell behavior at **(A)** 10^4 symbols/sec and **(B)** at 10^2 symbols/sec.

- ***Doppler shift effect:***

For comparison purpose take figure **(4.17)** as a reference point. Figure **(4.20.A)** and **(4.20.B)** show the fading envelopes of the fifth path through all links when reducing the Doppler shift from 2 to 1 and when increasing its value to 3 respectively, considering the bad urban macro cell scenario. Reducing the Doppler shift value from 2 to 1 result in slow variations in the fading envelopes, so more smooth envelopes are found to occur. In reality, this indicates the slowly movements of the transmitter and the receiver, they may be considered almost fixed. Moreover, the probability of line of sight between the transmitter and the receiver is implicitly increases, and vice versa when increasing its value. [34]

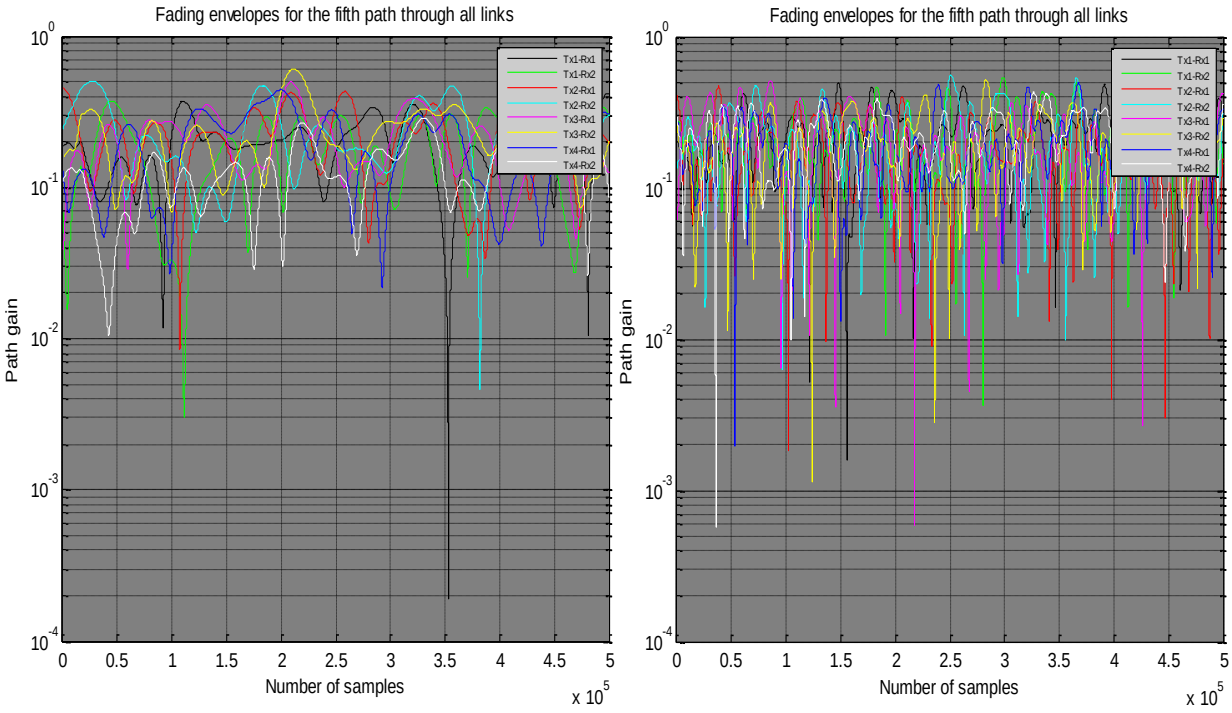

(A) **(B)**

Figure 4.20: Bad urban macro cell behavior at Doppler shift **(A)** at 1 and **(B)** at 3.

4.5. Simulation results for 4x2 MIMO channel model under rural macro-cell.

This section shows the simulation results for 4x2 MIMO system configurations under rural macro-cell environment.

In real environments, correlation among the propagating signals can exist; as a result the system performance will be affected. So, Multiple transmit antennas have to be placed far apart in order to avoid undesired effects such as correlation and changing the beam patterns. Therefore, the effect of receive and transmit antennas spacing on the channel behavior has been investigated.[31]

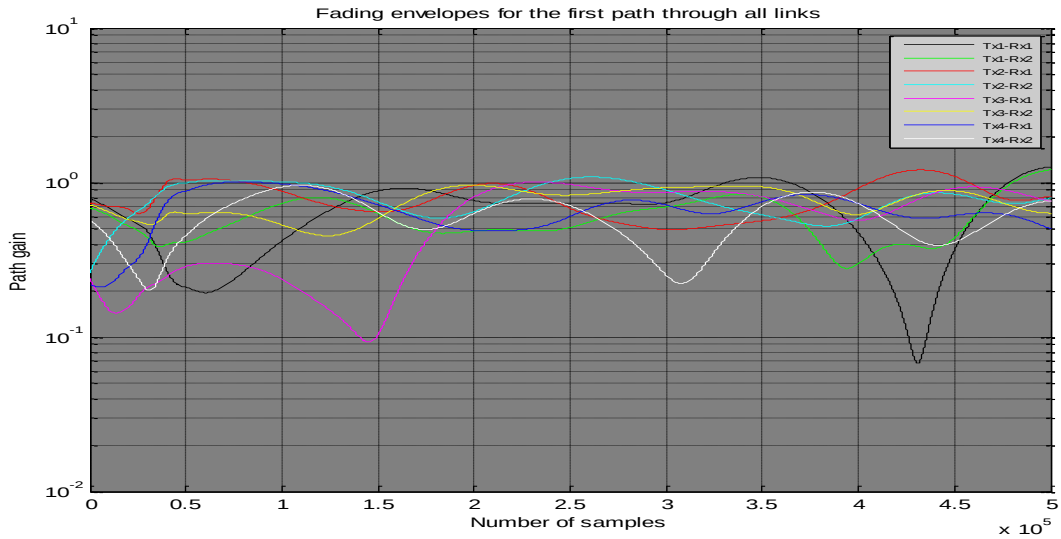

Figure 4.21: Fading envelopes for path1 through all links (4x2 Rural).

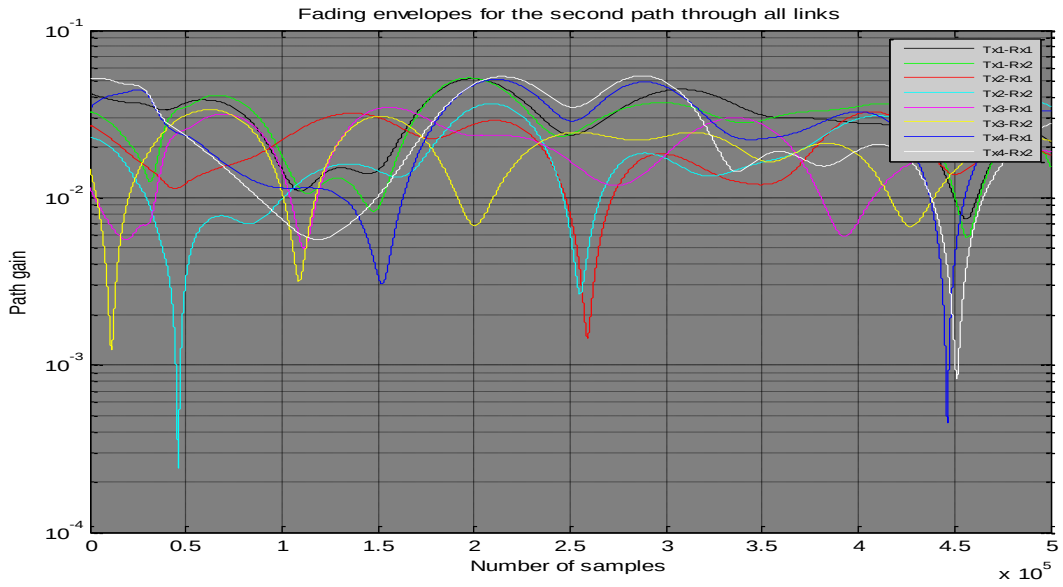

Figure 4.22: Fading envelopes for path2 through all links (4x2 Rural).

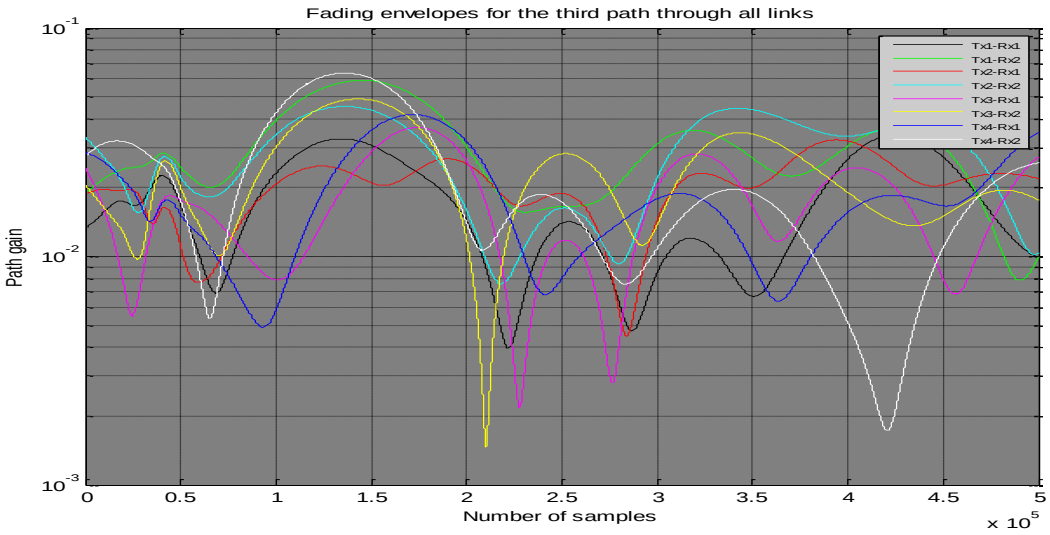

Figure 4.23: Fading envelopes for path3 through all links (4x2 Rural).

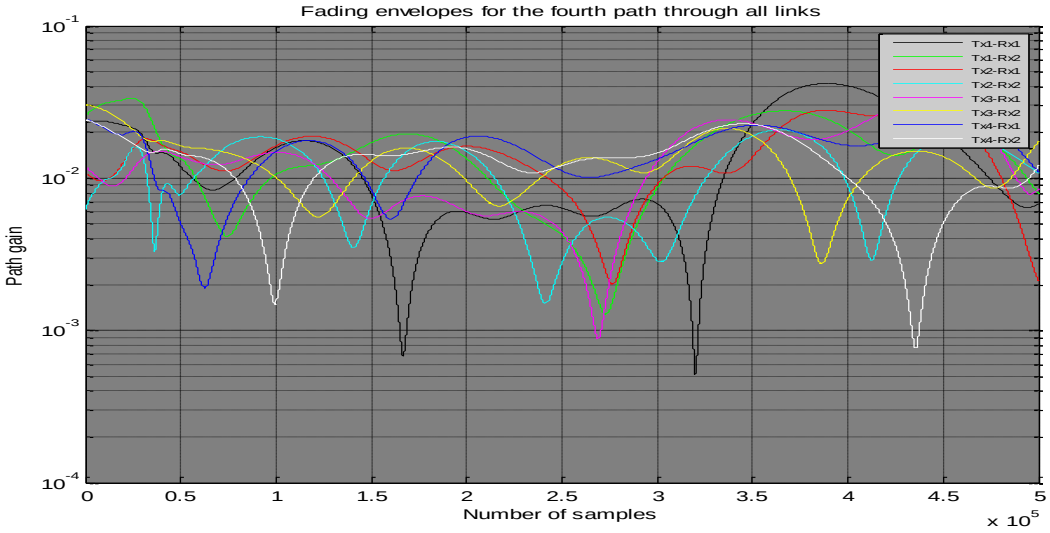

Figure 4.24: Fading envelopes for path4 through all links (4x2 Rural).

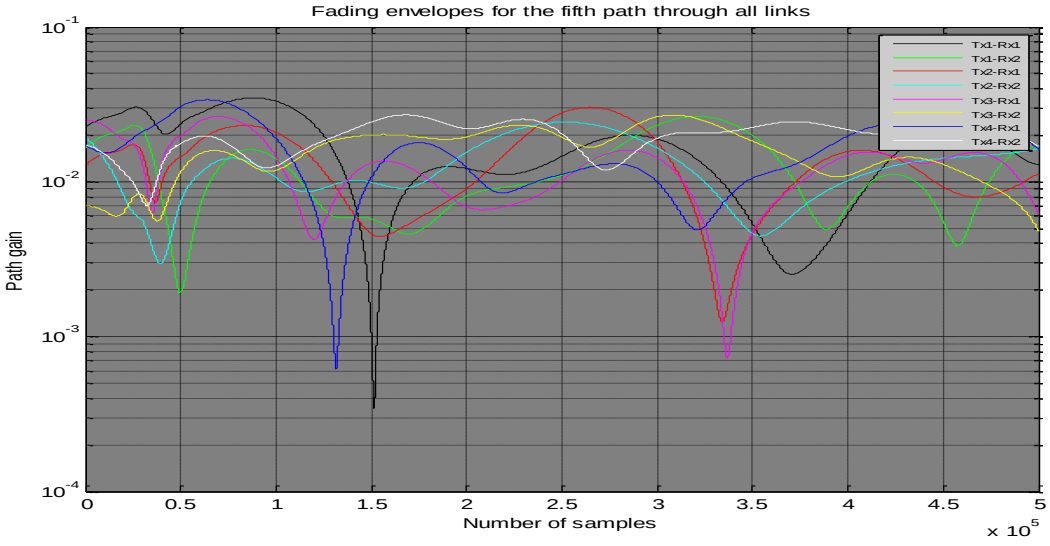

Figure 4.25: Fading envelopes for path5 through all links (4x2 Rural).

- ***Antennas spacing effect:***

For comparison purpose take figure **(4.25)** as a reference point. Considering the rural macro cell scenario, figure **(4.26.A)** shows the fading envelopes of the fifth path when increasing the T_x and R_x spacing from 1λ to 3λ and from 0.5λ to 3λ respectively. While figure **(4.26.B)** shows the effect of decreasing T_x and R_x spacing from 1λ to 0.15λ and from 0.5λ to 0.15λ. The results indicate that by increasing the spacing distance between the T_x and R_x antennas, the performance of the system is almost like an ideal system with independent transmitting and receiving antennas. On the other hand, decreasing the antennas spacing will lead to high correlation between the signals and accordingly results on poor system performance. Thus the more spacing between the antennas, the better MIMO system's performance will be.[31]

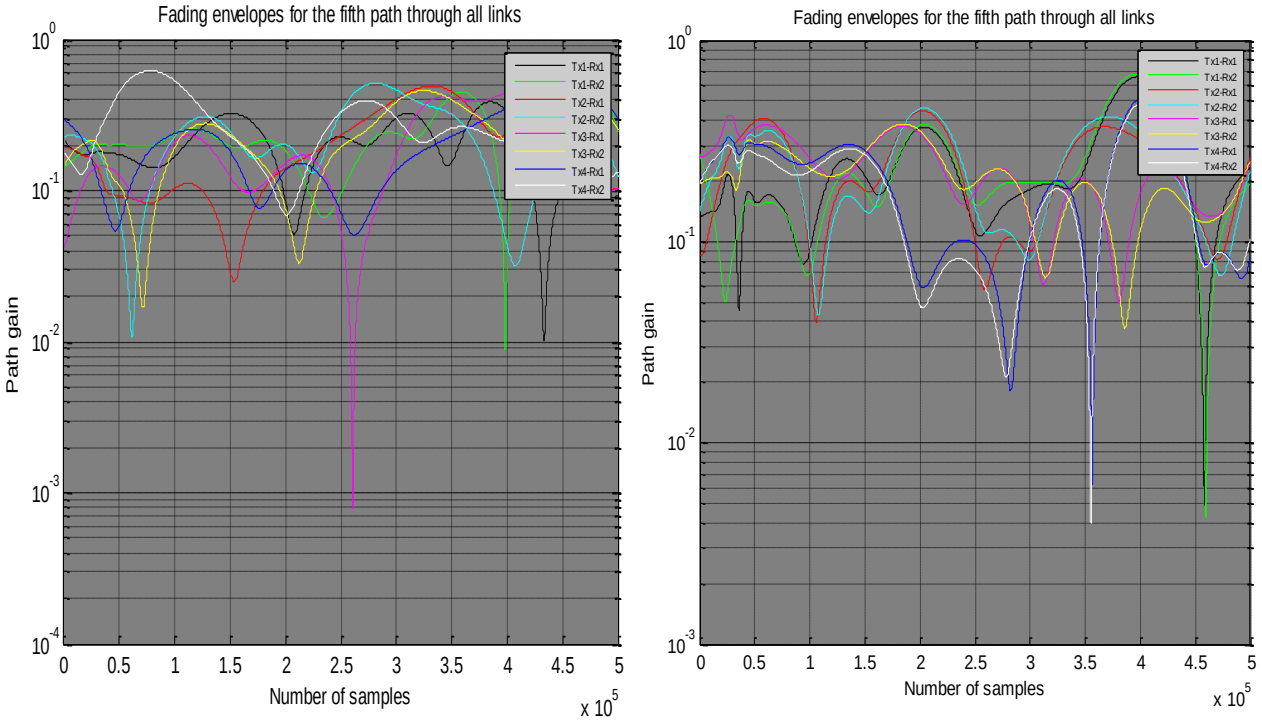

(A) **(B)**

Figure 4.26: Rural macro cell behavior when:

(a) Increasing the Tx and Rx spacing from 1λ to 3λ and from 0.5λ to 3λ respectively.

(b) Decreasing Tx and Rx spacing from 1λ to 0.15λ and from 0.5λ to 0.15λ respectively.

4.6. Simulation results for 8x2 MIMO channel model under Indoor small office scenario.

Throughout this section the behavior of the propagating signals of 8x2 MIMO system in an indoor propagation environment is observed. The response of the channel for all links between the transmit and receive antennas are plotted below.

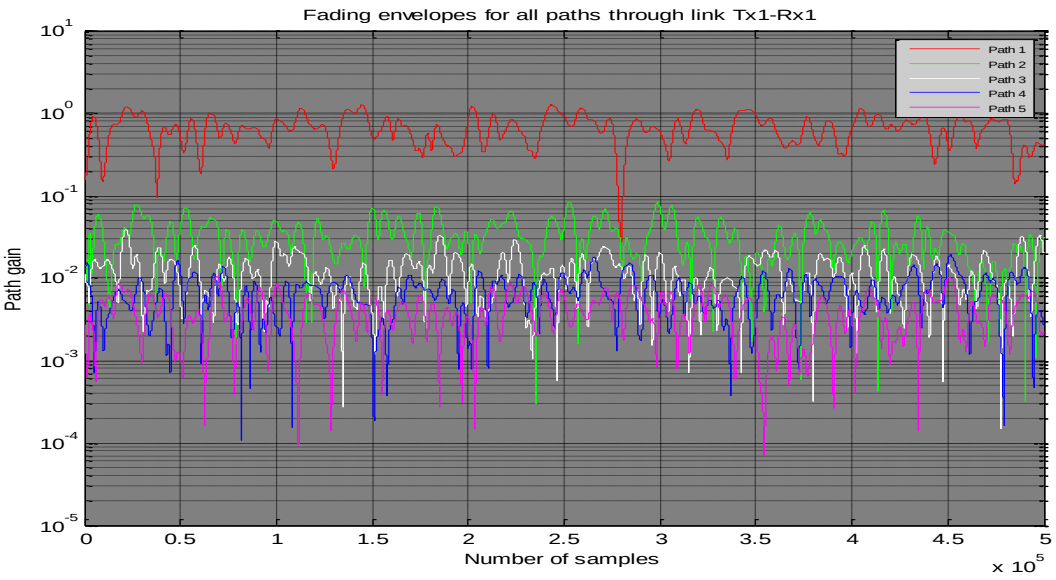

Figure 4.27: Fading envelopes for the five paths through link Tx1-Rx1.

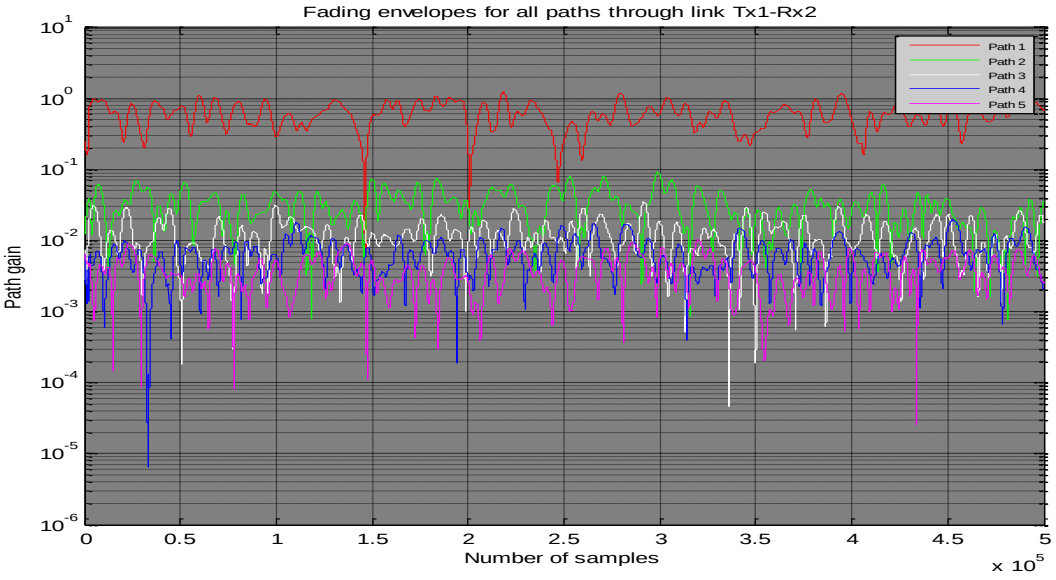

Figure 4.28: Fading envelopes for the five paths through link Tx1-Rx2.

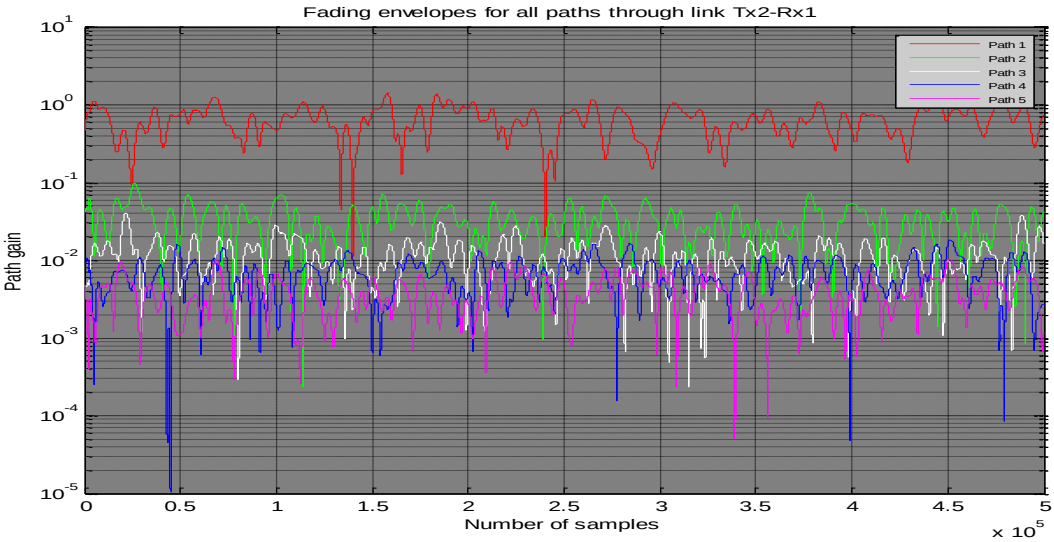

Figure 4.29: Fading envelopes for the five paths through link Tx2-Rx1.

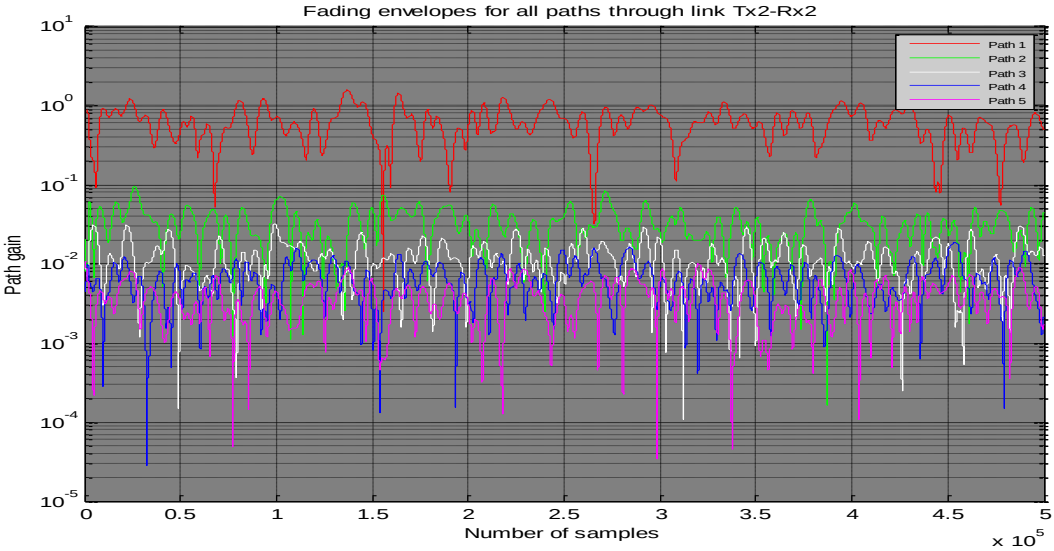

Figure 4.30: Fading envelopes for the five paths through link Tx2-Rx2

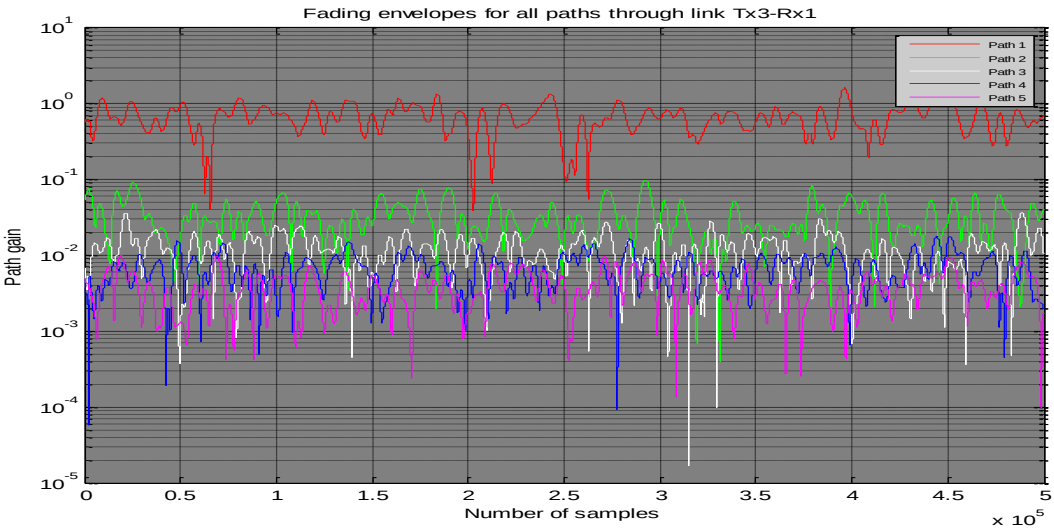

Figure 4.31: Fading envelopes for the five paths through link Tx3-Rx1.

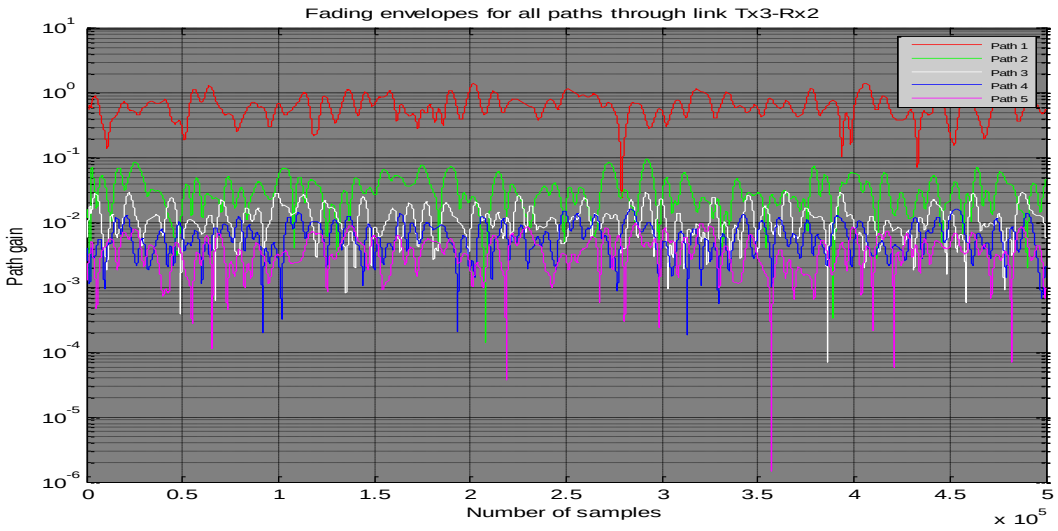

Figure 4.32: Fading envelopes for the five paths through link Tx3-Rx2.

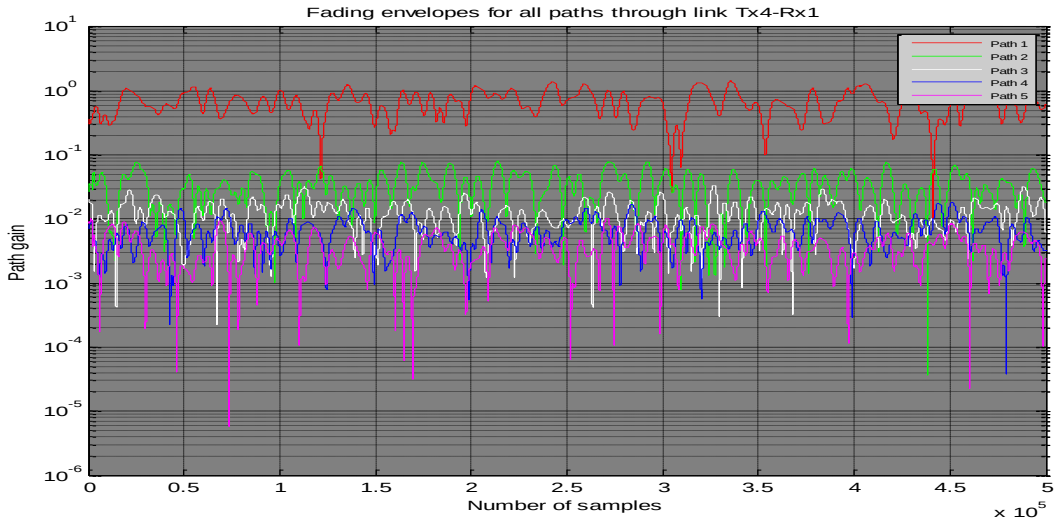

Figure 4.33: Fading envelopes for the five paths through link Tx4-Rx1.

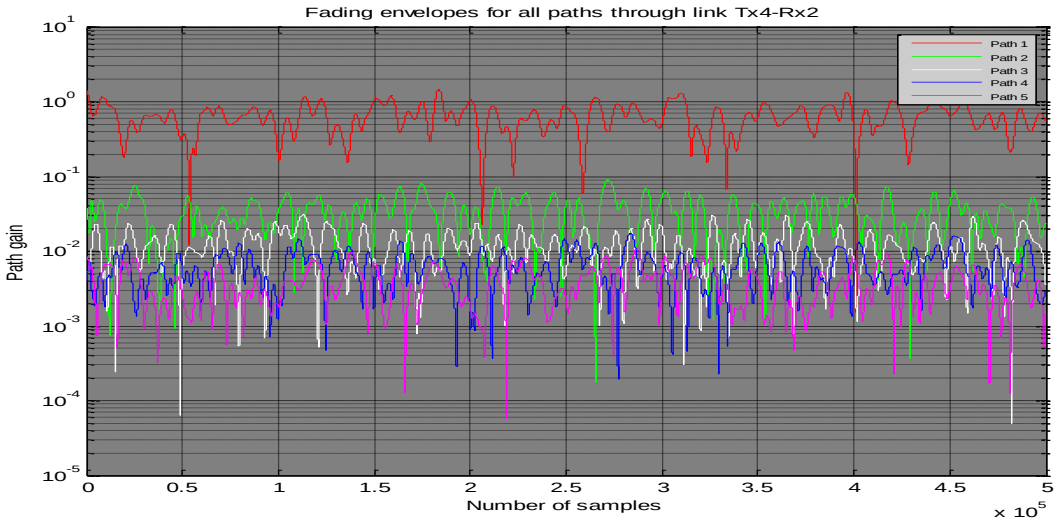

Figure 4.34: Fading envelopes for the five paths through link Tx4-Rx2.

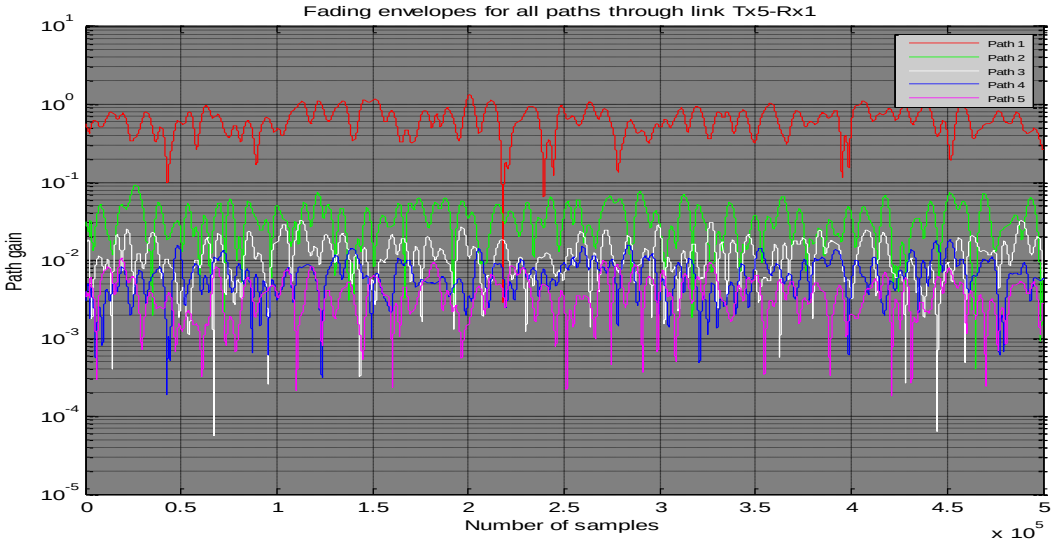

Figure 4.35: Fading envelopes for the five paths through link Tx5-Rx1.

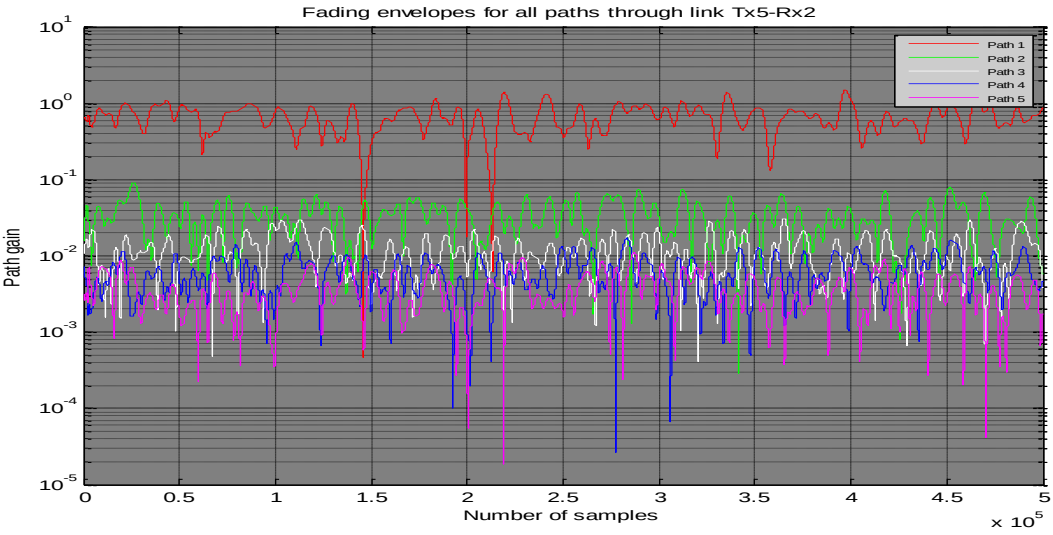

Figure 4.36: Fading envelopes for the five paths through link Tx5-Rx2.

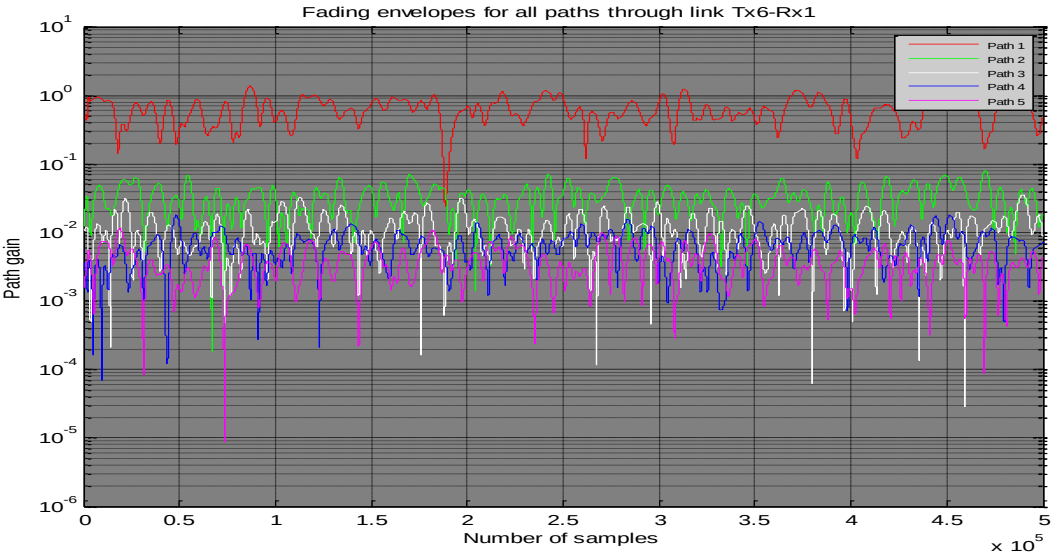

Figure 4.37: Fading envelopes for the five paths through link Tx6-Rx1.

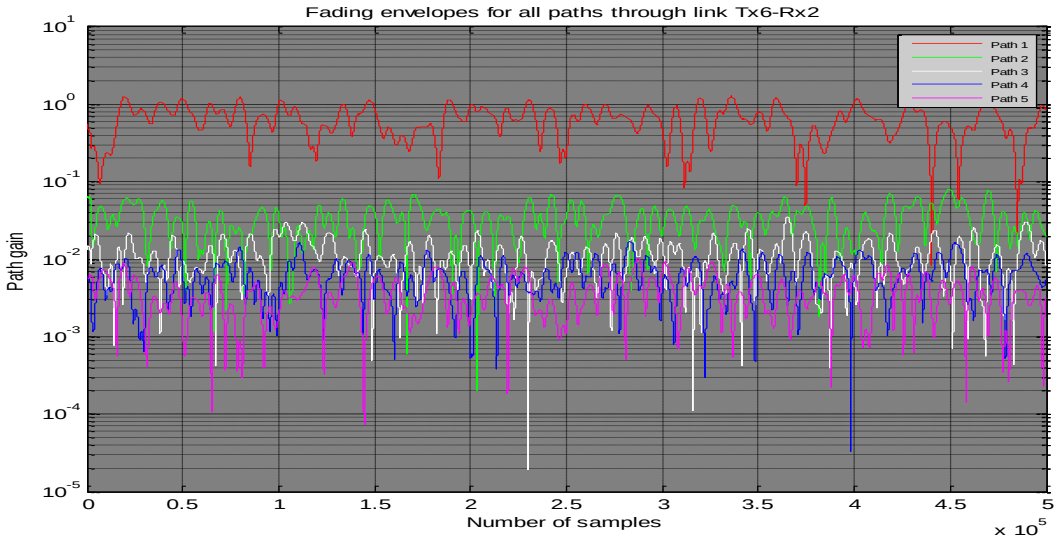

Figure 4.38: Fading envelopes for the five paths through link Tx6-Rx2.

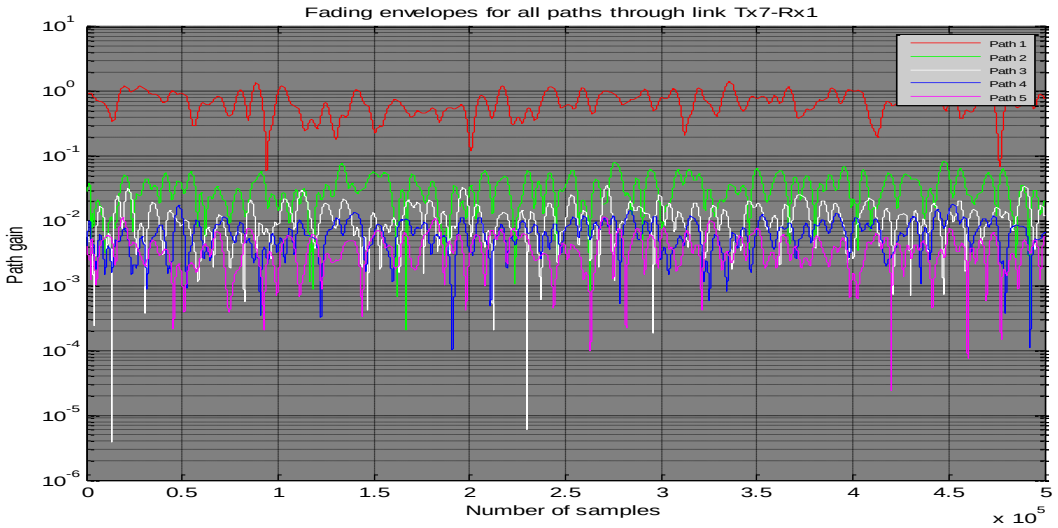

Figure 4.39: Fading envelopes for the five paths through link Tx7-Rx1.

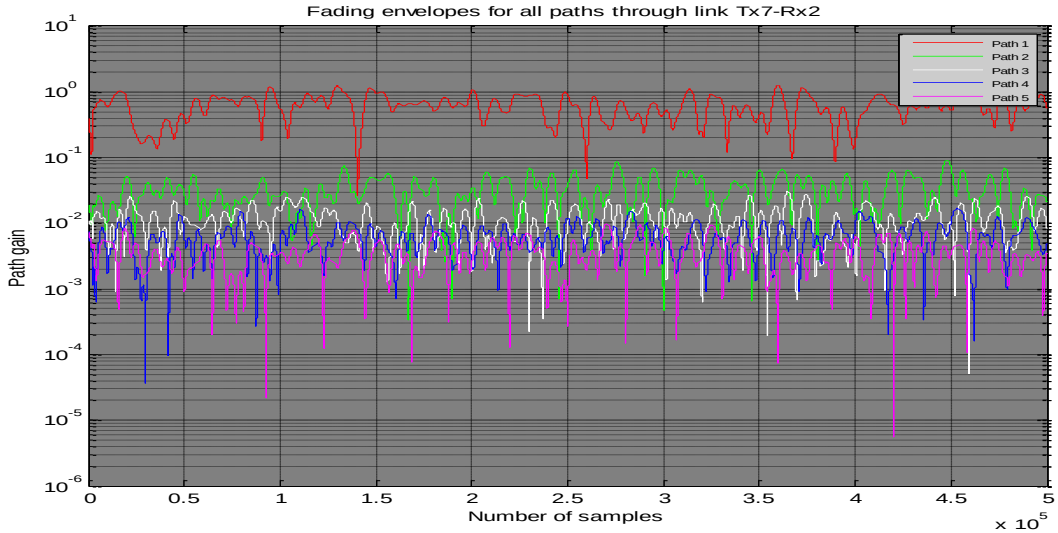

Figure 4.40: Fading envelopes for the five paths through link Tx7-Rx2.

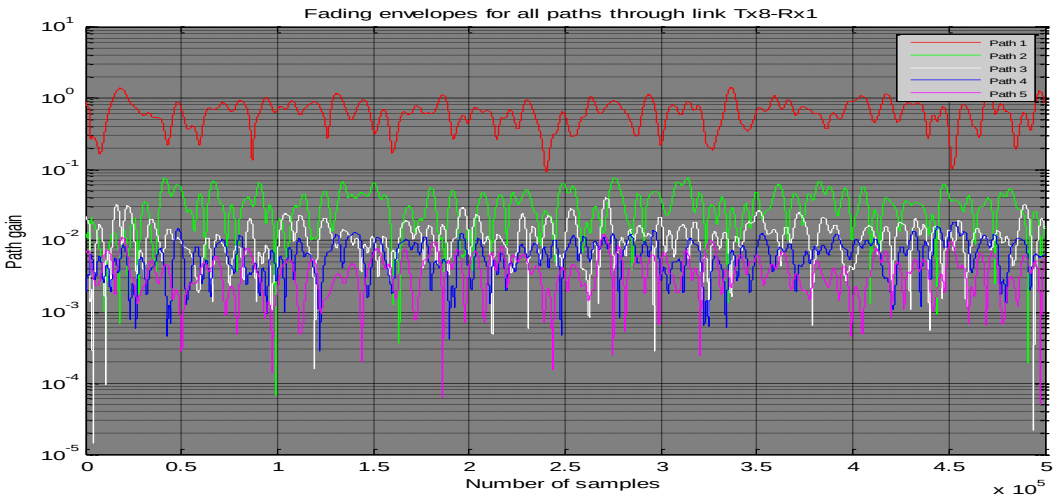

Figure 4.41: Fading envelopes for the five paths through link Tx8-Rx1.

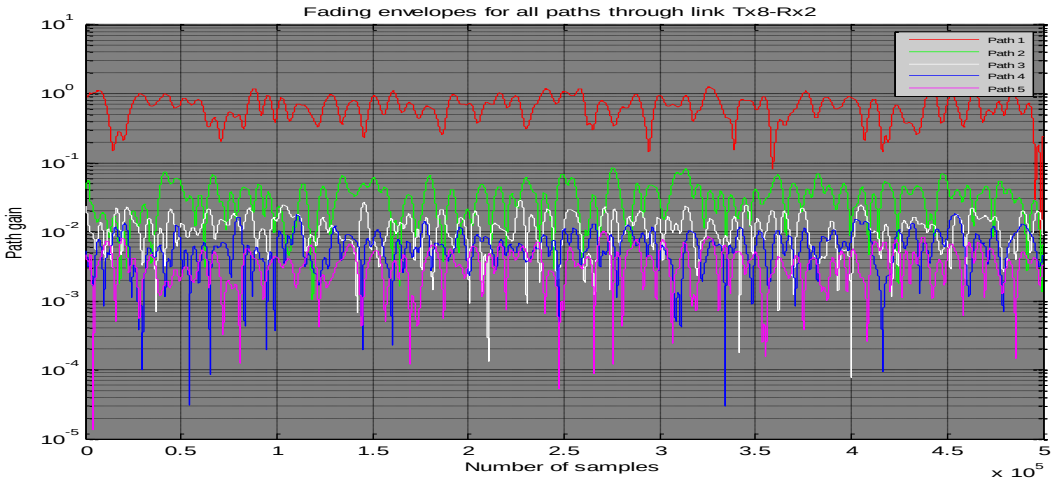

Figure 4.42: Fading envelopes for the five paths through link Tx8-Rx2.

In the simulation results above, red curves correspond to LOS components which clearly appear away from the fading level that NLOS components reach. Except LOS signal, the propagating signals highly fluctuate due to the large amount of reflections in indoor propagation scenario. It can also be noted that the signals suffer a fast and deep fading. Furthermore, the depth of the fades reduces considerably as the distance between the transmitter and the receiver decreases that is; the paths drawn with the green color were assumed to propagate the shortest distances in the simulation process.

4.7. Frequency of operation influence on the path loss.

This section is devoted to illustrate the frequency of operation's effect on the path loss for bad urban and rural macro cells, suburban macro-cell, fixed stationary feeder (roof – top to roof-top), indoor small office, indoor to outdoor, and moving networks considering eight propagating signals from the transmit to the receive antennas. As a simulation sample only two paths were plotted and posted in the upcoming pages, one for the line of sight and another for the non-line of sight cases.

All the simulation results can be obtained by running the Matlab code entitled “effect of frequency on path loss for 8x8 system’’ which is attached in the appendix. The simulation made use of the path loss equations listed in chapter one of this project.

The flowchart below illustrates the simulation process:

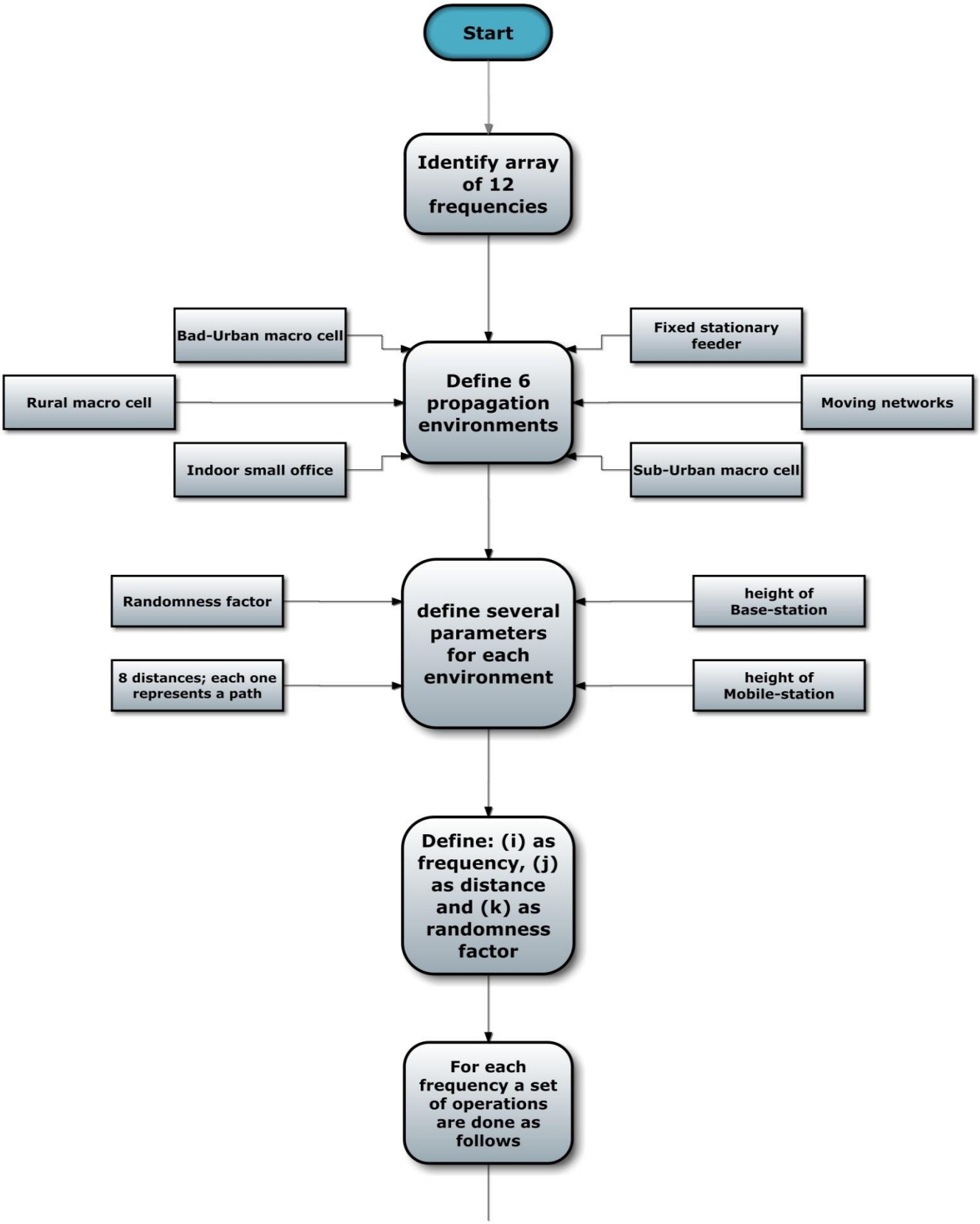

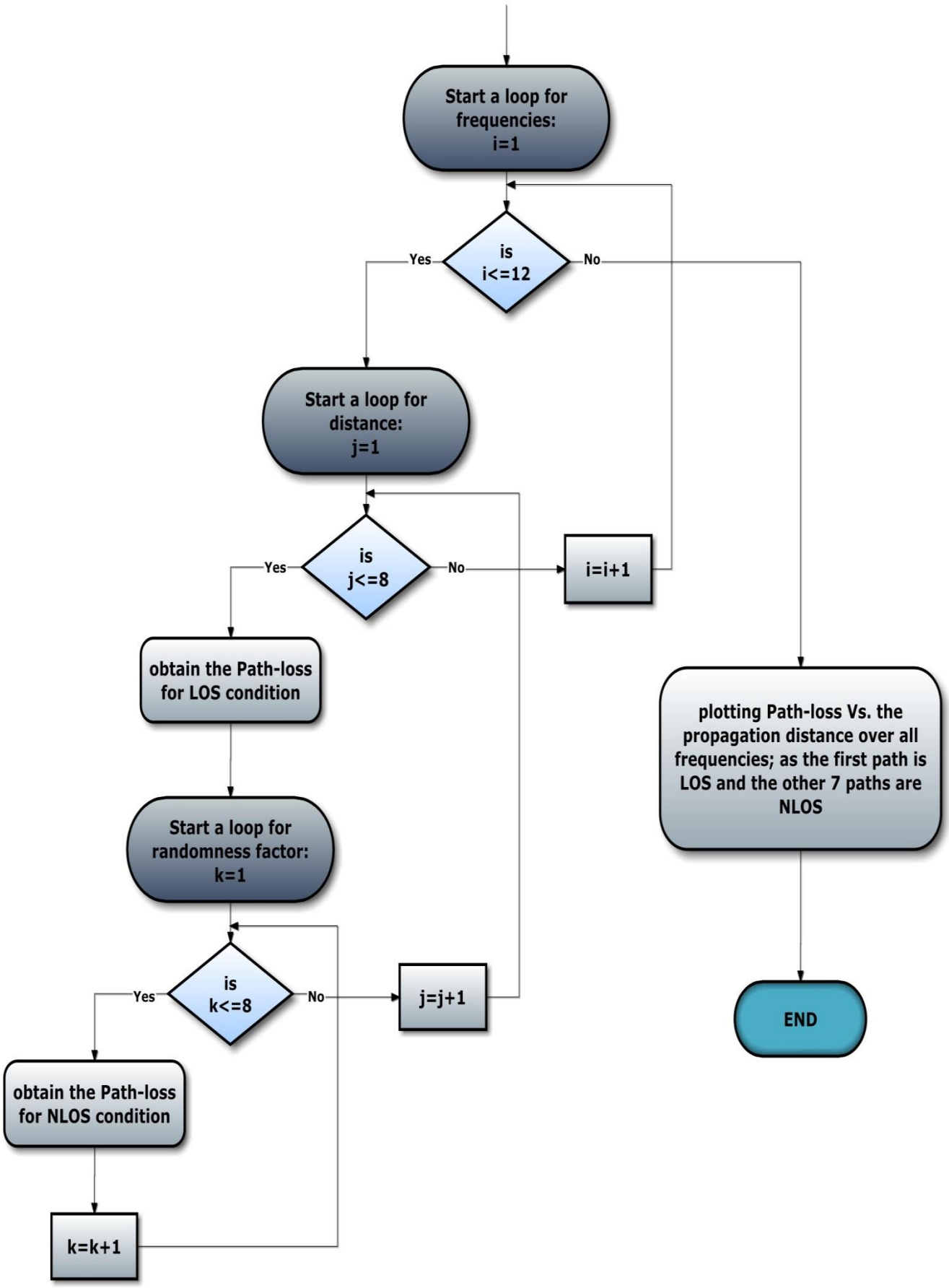

Figure 4.43: flowchart for the simulation process of the frequency of operation influence on path-loss.

Below are the simulation's results samples:

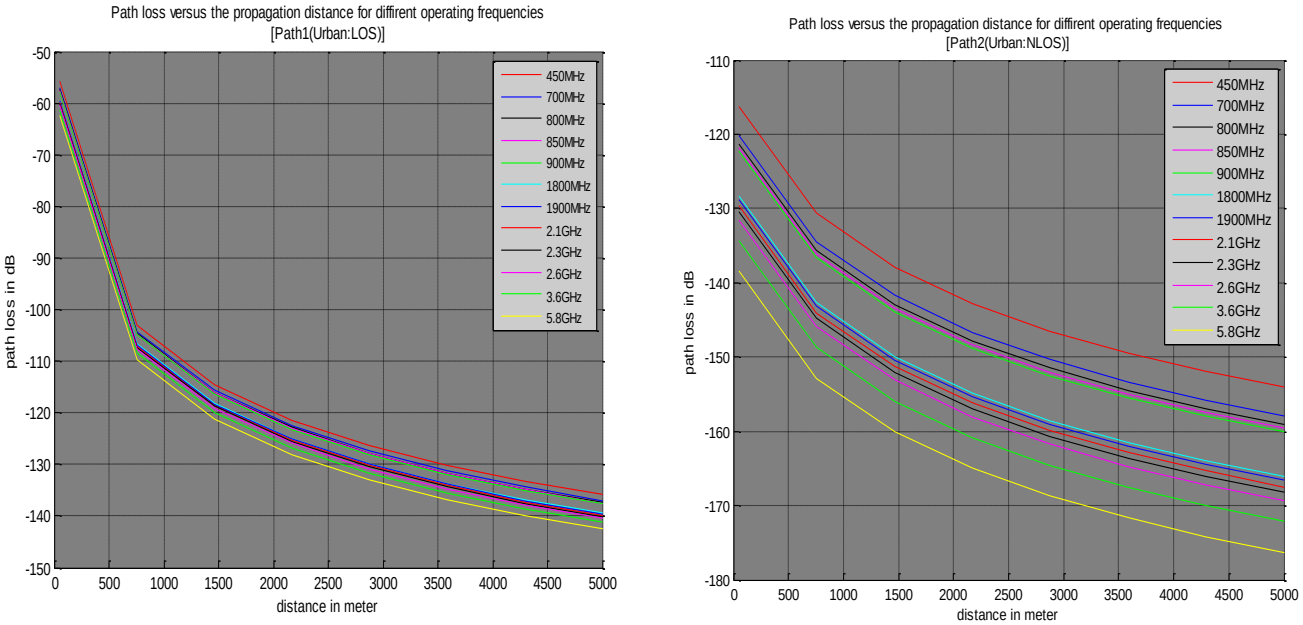

(A) **(B)**

Figure 4.44: Path loss vs. propagation distance for different frequencies of operation for bad urban macro-cell **(A)** LOS **(B)** NLOS.

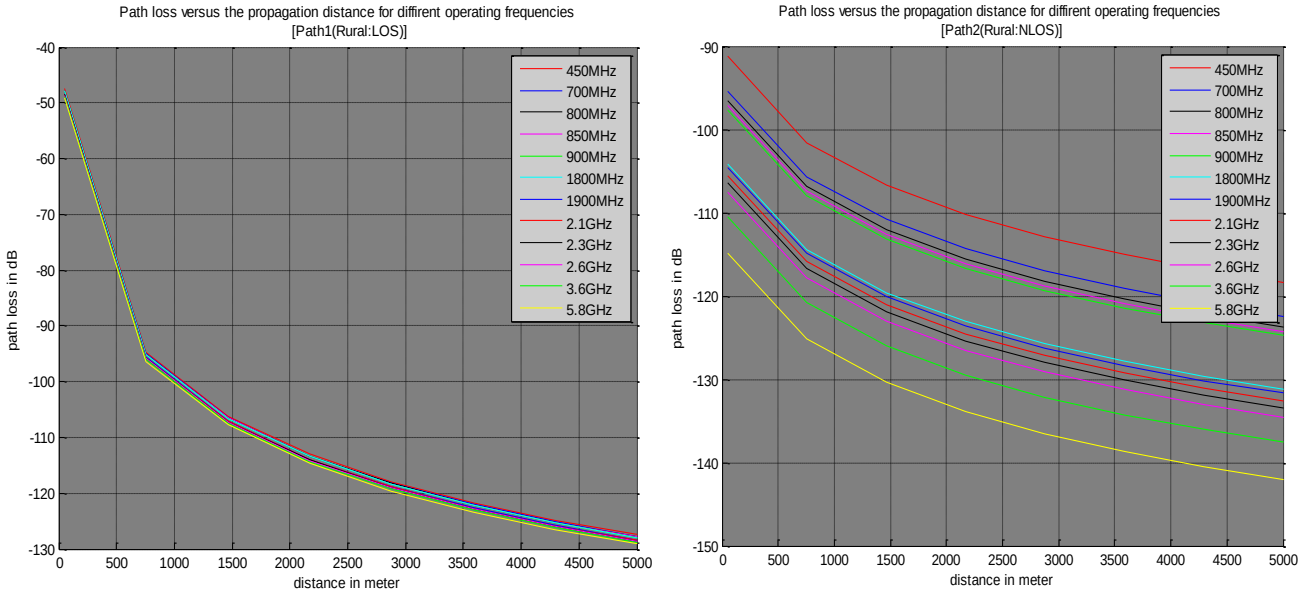

(A) **(B)**

Figure 4.45: Path loss vs. propagation distance for different frequencies of operation for rural macro-cell **(A)** LOS **(B)** NLOS.

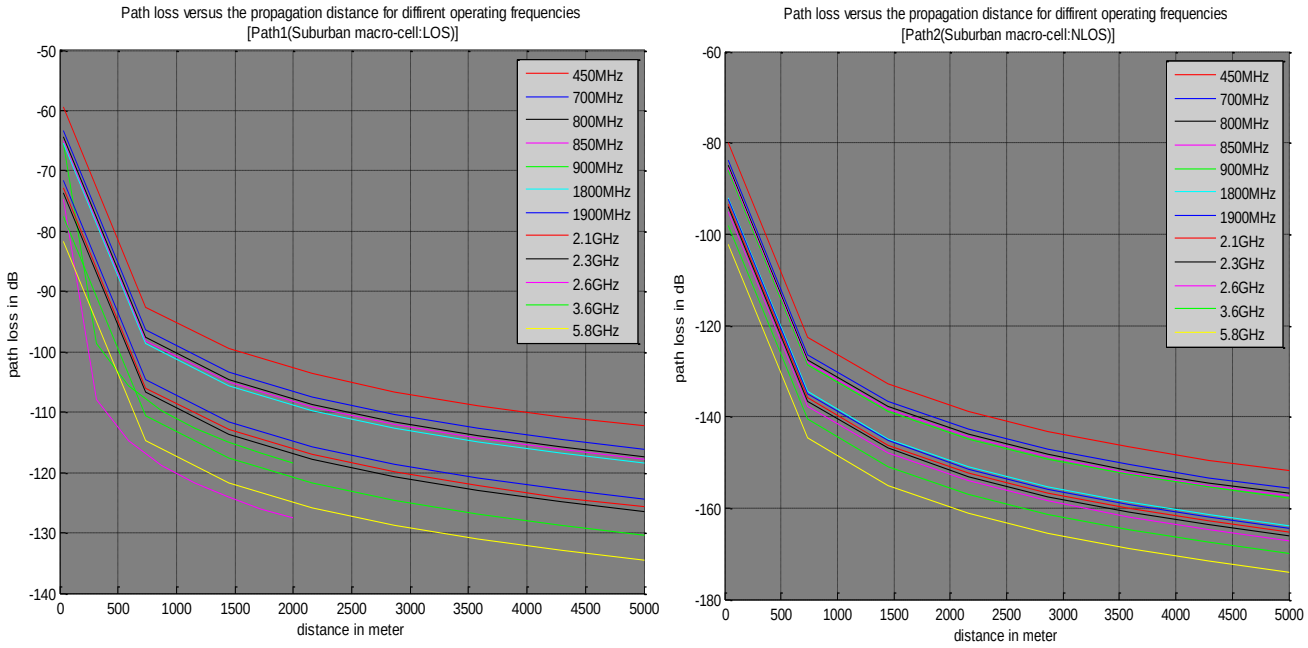

(A) **(B)**

Figure 4.46: Path loss vs. propagation distance for different frequencies of operation for suburban macro-cell **(A)** LOS **(B)** NLOS.

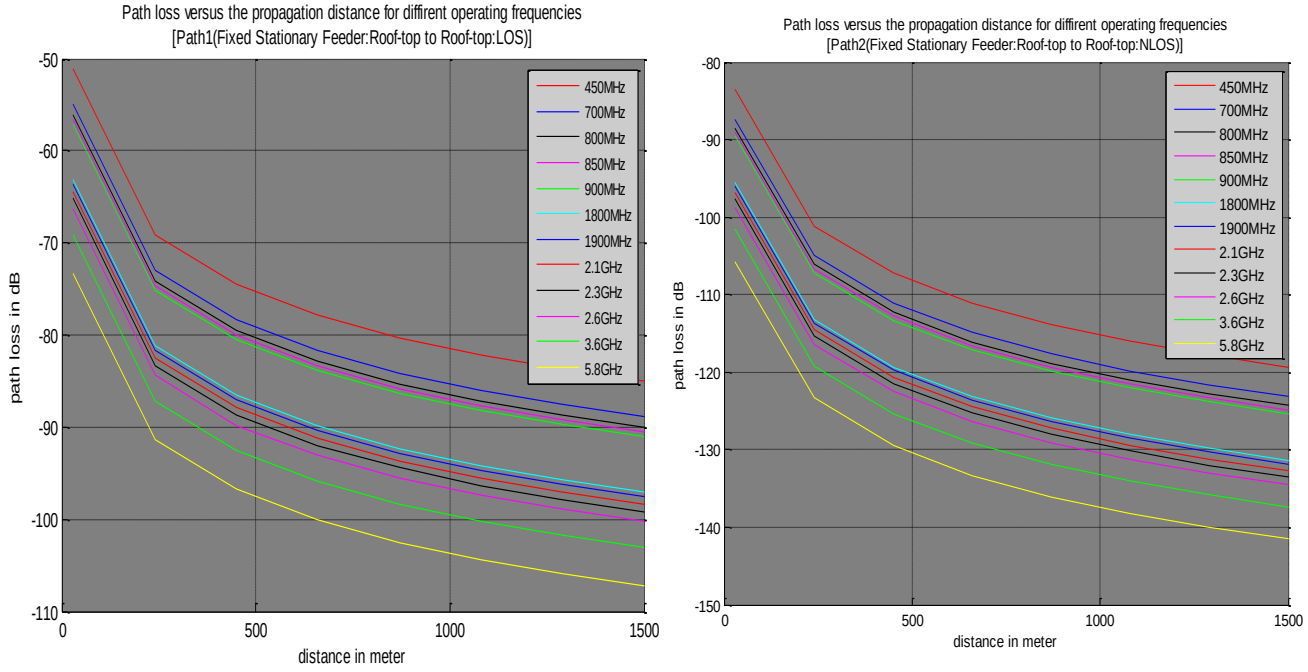

(A) **(B)**

Figure 4.47: Path loss vs. propagation distance for different frequencies of operation for fixed stationary feeder **(A)** LOS **(B)** NLOS.

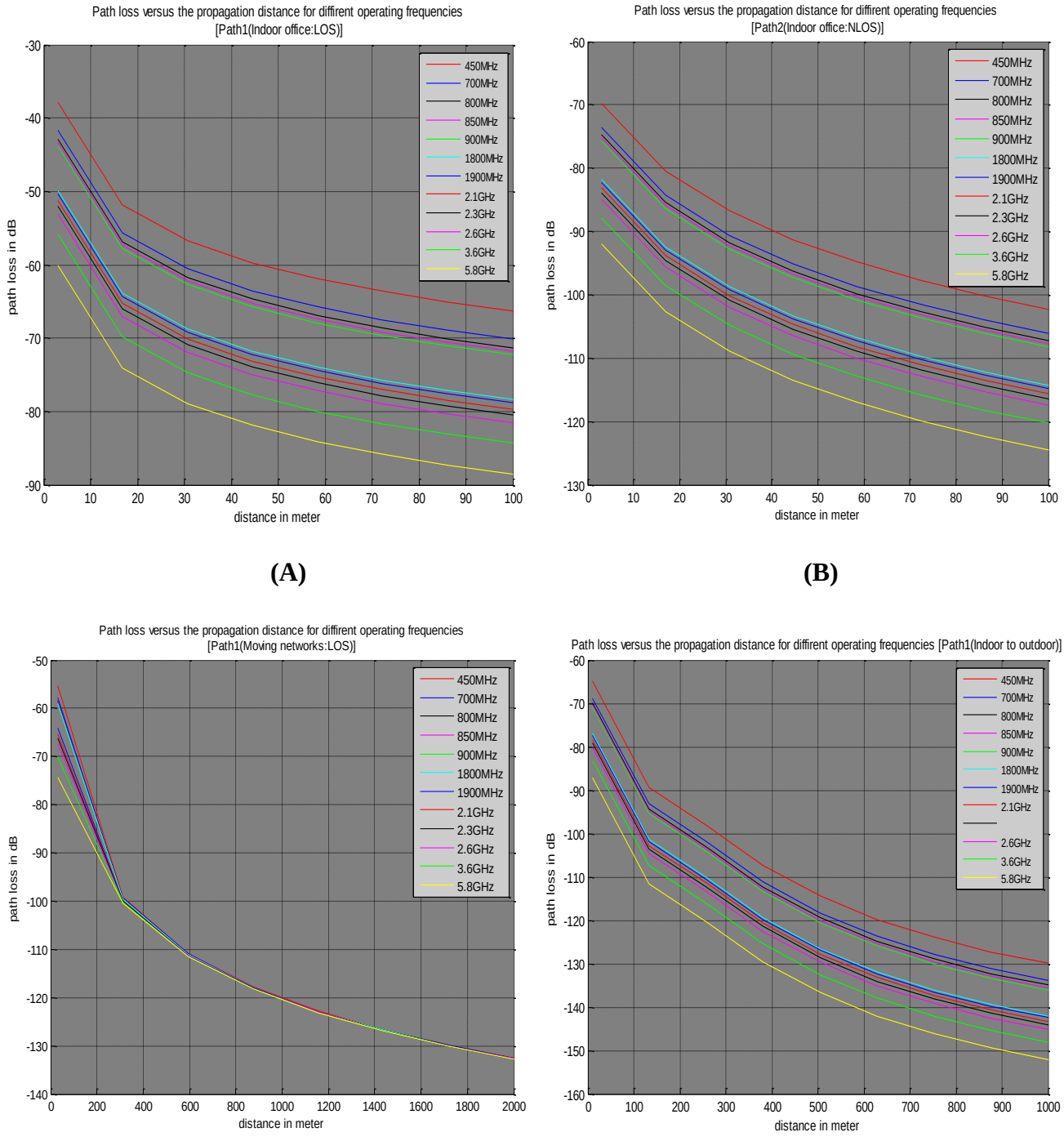

Figure 4.48: Path loss vs. propagation distance for different frequencies of operation for indoor small office **(A)** LOS **(B)** NLOS and **(C)** for LOS moving networks **(D)** for indoor to outdoor.

Based on the previous simulation results, the path loss is highly dependent on the frequency of operation except for the LOS condition of the rural, moving networks and bad urban scenarios, where there is slightly difference between the response of the channel among all the simulated frequencies. Propagation losses caused by operating on high frequency bands are much greater than operating on low frequency bands. For example and considering the non-line of sight case of bad urban scenario, the signal suffers about more 13dB loss when operating on the 3.6 GHz band compared with the 900 MHz at a distance of 1000 meters.

Chapter 5

Conclusions

Chapter contents:

5.1. An overview.

This chapter is devoted to summarize the results obtained during the simulation process and introduces some of suggested ideas in order to develop this work.

5.2. Conclusions.

The following points present the main results of the simulation processes throughout this project:

1. The response of the channel for the aforementioned (4x2), (2x2), and (8x2) MIMO configurations under the three simulated scenarios; bad urban, rural macro-cells, and indoor small office, is apparently different. The channel was noticed to be in its worst state when considering an indoor propagation environment.

2. Rapid fluctuations in the fading envelopes are observed when increasing the Doppler shift value and vice versa when decreasing its value.

3. Increasing the symbol rate will result in low fluctuations in the fading envelopes and high similarity among them, since the probability of the symbol's transmission within the coherence time is increased, and vice versa when decreasing its value.

4. By increasing the spacing between the Tx and Rx antennas an ideal MIMO system performance can be achieved, while decreasing the spacing will lead to a poor performance as a result of the high correlation among the signals.

5. It has been observed that increasing the paths delays will lead to reduce the fading due to ISI's reduction, and vice versa when decreasing their value.

6. It was shown that the path loss that the propagating signals suffer is highly dependent on the frequency of operation, as the frequency band gets higher, the more loss the signal will examine.

5.3. Future work.

Here are some of suggested ideas to be worked on in order to develop this project:

1. Doing simulations for other MIMO systems configurations under more propagation environments.

2. Observing the effect of more scenarios-dependent parameters on the channel behavior.

3. Developing the correlation function by including other related propagation parameters to get more reliable results.

References:

[1]. Theodore s. Rappaport, wireless communications principles and practice, second edition.

[2]. Jivesh Govi and Jivika Govil, "4G Mobile Communication Systems :Turns, Trends and Transition", International Conference on Convergence Information Technology. 2007.

[3]. Pekka Kyosti, Juha Meinila, Lassi Hentila, Xiongwen Zhao, Tommi Jamsa, Christian Schneider, Milan Narandzić, Marko Milojević, Aihua Hong, Juha Ylitalo, Veli-Matti Holappa, Mikko Alatossava, Robert Bultitude, Yvo de Jong, Terhi Rautiainen," WINNER II Channel Models", WINNER, 30/09/2007.

[4]. David Tse, Pramod Viswanath, Fundamentals of wireless communication, Cambridge University press, New York, United stated of America, 2005.

[5]. http://en.wikipedia.org/wiki/Path_loss.

[6]. Pekka Kyosti, Juha Meinila, Lassi Hentila, Xiongwen Zhao, Tommi Jamsa, Christian Schneider, Milan Narandzić, Marko Milojević, Aihua Hong, Juha Ylitalo, Veli-Matti Holappa, Mikko Alatossava, Robert Bultitude, Yvo de Jong, Terhi Rautiainen, " WINNER II interim channel models", 09/02/2007.

[7]. http://en.wikipedia.org/wiki/fading.

[8]. Arogyaswami Paulraj, Rohit Nabar, and Dhananjay Gore, Introduction to space-time wireless communications, Cambridge.

[9].Jim Seymour, Bell Labs, and Alcatel-Lucent,"3GPP mobile broadband innovation", 3G Americas, February 2010.

[10]. Bruno Clerckx, Angel Lozano, Stefania Sesia, Cornelius van Rensburg, and Constantinos B. Papadias, " 3GPP LTE and LTE Advanced", Hindawi Publishing Corporation, 2009.

[11]. Fabio Belloni, "Fading Models", Autumn 2004.

[12]. J.A. Wepman, J.R. Hoffman, L.H. Loe, "Characterization of macro cellular PCS propagation channels in the 1850-1990 MHz band", 3rd Annual International Conference on Universal Personal Communications, 1994.

[13]. Daniel S. Baum, Hassan El-Sallabi, Tommi Jämsä, Juha Meinilä, Pekka Kyösti, Xiongwen Zhao, Daniela Laselva, Jukka-Pekka Nuutinen, Lassi Hentilä, Pertti Vainikainen, Jarmo Kivinen, Lasse Vuokko, Per Zetterberg, Mats Bengtsson, Kai Yu, Niklas Jaldén, Terhi Rautiainen, Kimmo Kalliola, Marko Milojevic, Christian

Schneider, Jan Hansen, " D5.4 Final Report on Link Level and System Level Channel Models", WINNER, v. 1.4, 2005.

[14]. http://www.radio-electronics.com/info/antennas/mimo/formats-siso-simo-miso-mimo.php

[15]. Mohinder Jankiraman, Space-Time Codes and MIMO Systems, Artech House, Boston-London.

[16]. G.J. Foschini and M.J. Gans, "On limits of wireless communications in a fading environment when using multiple antennas", Wireless Pers. Communication, 1998.

[17]. Lajos Hanzo, Osamah Alamri, Mohammed El-Hajjar and Nan Wu, Near-Capacity Multi-Functional MIMO Systems, A John Wiley and Sons Publication, 2009.

[18]. Shuangquan Wang and Ali Abdi, "Statistical Properties of Eigen-Modes and instantaneous Mutual Information in MIMO Time-Varying Rayleigh Channels", IEEE, 2006.

[19]. Daniel W. Bliss, KeithW. Forsythe, and Amanda M. Chan, "MIMO Wireless Communication". Lincon Laboratory Journal, 2005.

[20]. Gilad Bukai, Neri Merhav, "Channel Estimation Using Feedback", IEEE International Symposium on, PP. 1243 – 1247, Israel, 2008.

[21]. Oomke Weikert, Udo Zolzer, "Efficient MIMO Channel Estimation with Optimal Training Sequences", Department of Signal Processing and Communications, University of the Federal Armed Forces Hamburg, Germany,2006.

[22]. David J. Love, Robert W. Heath Jr., Wiroonsak Santipach, Michael L. Honig, " What is the value of limited feedback for MIMO channels?", IEEE Communications Society, Vol .42, PP .54 - 59, 2004.

[23]. Maxime Guillaud, Dirk T.M. Slock, Raymond Knopp, "A practical method for wireless channel reciprocity exploitation through relative calibration ", Signal Processing and Its Applications. Proceedings of the Eighth International Symposium on, Vol .1, PP. 403 - 406, 2005.

[24]. Huseyin Ozcelik, Nicolai Czink, Ernst Bonek, "What Makes a Good MIMO Channel Model?", IEEE Vehicular Technology Conference, 2005.

[25]. Xuedong WANG, Jiandong LI, "A generic channel model for MIMO systems", Intenational Conference on Communication Technology, 2006.

[26]. O. Fernández, M. Domingo, R.P. Torres, "Outdoor to Indoor 2x2 Wideband MIMO Channel Modeling", IEEE, 2009.

[27]. Dovis. Fantini, R. Mondin, M. Savi,"4G Communications Based on High Altitude Stratospheric Platforms:Channel Modeling and Performance Evaluation", IEEE Global Telecommunications Conference,2001.

[28]. Z. Daud, M. Z. A. Abdul Aziz, M. K Suaidi, M.R Che Rose, M. F Abdul Kadir, M.S. R. Mohd Shah, D. Misman " MIMO Channel Characterization and Optimization "Telecommunication Technologies and 2nd Malaysia Conference on Photonics, 2008.

[29]. H. Ge, K. D. Wong, M. Barton, J. C. Liberti, " Statistical Characterization of Multiple-Input Multiple-Output (MIMO) Channel Capacity" , IEEE Wireless Communications and Networking Conference, vol.2 , PP . 789 – 793, 2002.

[30]. Rashmi Verma , Shilpa Mahajan and Vishal Rohila, "Classification of MIMO Channel Model", (networks,2008.ICON 2008. 16th IEEE International Conference on),PP.(1-4),2008.

[31]. Khaled Hijjeh, Ahmed Mujahed, Mohammed Jaber, Suzan Al-Hroub, Narmeen Dawadeh, " Matlab simulation for (4x2) MIMO channel modeling under bad urban and rural macro cell environments", Palestine Cellular Communication Ltd., Palestine Polytechnic University, Palestine, 2011.

Appendix (A):

A1) SUI-1 channel model code:

```
% Creating an array of random numbers
S = RandStream('swb2712', 'Seed', 12345);
% Modulation order
M = 2;
% Identifying a 2-psk modulator
hModem = modem.pskmod(M);
% Input symbol rate
Rsym = 10e3;
% Input bit rate
Rbit = Rsym * log2(M);
% Oversampling factor
Nos = 4;
% Input sample period
ts = (1/Rbit) / Nos;
% Path delays, in seconds
tau = [0 0.4 0.9]*1e-6;
%Average path gains in dB
pdb = [0 -15 -20];
%constructing a rounded Doppler spectrum object with a default
%vector of polynomial coefficients
dop = doppler.rounded;
% Maximum Doppler shift for all paths
fd = 0.5;
%Number of transmit antennas
Nt = 2;
% Number of receive antennas
Nr = 1;
%Correlation coefficient = antenna correlation which defines as the
%envelop correlation coefficient b/w signals received at two antenna
%elements
rho = 0.7;
%MIMO channel object, returns a MIMO channel that models each
%discrete path as an independent Rayleigh fading process
h = mimochan(Nt, Nr, ts, fd, tau, pdb);
%defining the k-factor for the first path since it's Rician, it
%defines the power ratio b\w the direct path and the scattered
%multipath component.
h.KFactor = 4;
%Doppler spectrum of MIMO object
h.DopplerSpectrum = dop;
%Transmit correlation matrix
h.TxCorrelationMatrix = toeplitz([1 rho]);
%After each frame is processed, the channel is not reset: this is
%necessary to preserve continuity across frames. in order to make the
%filter make use of the existing state info. of the channel when
%starting the filtering operation
h.ResetBeforeFiltering = 0;
%This setting is needed to store the path gains.
h.StorePathGains = 1
%the complex path gain vector is stored as the channel filter
%function processess the signal
%Total number of channel samples
```

```
Nsamp = 1.5e6;
%Number of samples per frame
Nsamp_f = 1000;
% Number of frames
Nframes = Nsamp/Nsamp_f;
%defining a zero matrix of size NsampxNr in order to make use of it
%in the frame sequencing process.
out = zeros(Nsamp, Nr);
%defining the three paths
y1 = zeros(Nsamp, Nt);  y2 = zeros(Nsamp, Nt); y3 = zeros(Nsamp, Nt);
%starting a loop to do a set of operations for each frame
for iFrames = 1:Nframes
%moduate the input signal using modulator object hModem
inputSig = modulate(hModem, randi(S, [0 M-1], Nsamp_f, Nt));
%to make a counter of the frames,(first frame contains the samples
%from 1 to 1000 and the second contains the samples from 1001 to 2000
%and so on)
idx = (1:Nsamp_f)+(iFrames-1)*Nsamp_f
%passes the signal through the MIMO channel
out(idx,:) = filter(h, inputSig);
for it = 1:Nt
        % For each transmit antenna, store gains of all three paths
        y1(idx,it) = h.PathGains(:,1,it,1); % for the first path
        y2(idx,it) = h.PathGains(:,2,it,1); % for the second path
        y3(idx,it) = h.PathGains(:,3,it,1); % for the third path
    end
    end
%estimating the power of a signal vs. Frequency, and implicitly
%reducing the noise in the data
Hs = spectrum.welch('Hamming', Nsamp/5, 50);
figure;
%returning a power spectral density object containing the power
%spectral density estimate of the discrete time signal using the
%spectrum object Hs, the PSD is the distribution of power per unit
%frequency
psd(Hs, y2(:,1), 'Fs', 1/ts, 'SpectrumType', 'twosided', 'Centerdc',
true)%

axis([-0.1/10 0.1/10 -80 10]);
legend('Simulation');
f = -fd: 0.01 :fd;
%Parameters of the rounded Doppler spectrum
a = [1 -1.72 0.785];
%the analytical polynomial of the normalized rounded Doppler
%spectrum
Sd=1/(2*fd*(a(1)+a(2)/3+a(3)/5))*(a(1)+a(2)*(f/fd).^2+
a(3)*(f/fd).^4);
%scaling by average path power
Sd = Sd * 10^(-15/10);
hold on;
plot(f(Sd>0)/1e3, 10*log10(Sd(Sd>0)), 'k--');
legend('Simulation', 'Theory');
figure;
psd(Hs, y2(:,2), 'Fs', 1/ts, 'SpectrumType', 'twosided', 'Centerdc',
true)
axis([-0.1/10 0.1/10 -80 10]);
legend('Simulation');
hold on;
plot(f(Sd>0)/1e3, 10*log10(Sd(Sd>0)), 'k--');
legend('Simulation', 'Theory');
figure;
```

```
%using semilogy which is the same as PLOT(...), except a logarithmic
%(base 10) scale is used for the Y-axis
semilogy(abs(y1(:,1)),'b');
hold on; grid on;
semilogy(abs(y1(:,2)),'r');
legend('First transmit link', 'Second transmit link');
title('Fading envelopes for two transmit links of Path 1');
figure;
semilogy(abs(y2(:,1)),'b');
hold on; grid on;
semilogy(abs(y2(:,2)),'r');
legend('First transmit link', 'Second transmit link');
title('Fading envelopes for two transmit links of Path 2');
figure;
semilogy(abs(y3(:,1)),'b');
hold on; grid on;
semilogy(abs(y3(:,2)),'r');
legend('First transmit link', 'Second transmit link');
title('Fading envelopes for two transmit links of Path 3');

% compute the correlation matrices for each path
TxCorrMatrixPath1 = corrcoef(y1(:,1),y1(:,2)).';
TxCorrMatrixPath2 = corrcoef(y2(:,1),y2(:,2)).';
TxCorrMatrixPath3 = corrcoef(y3(:,1),y3(:,2)).';
```

A2) 2x2 MIMO channel model code:

```
clear all
close all
clc

% Creating an array of random numbers
S = RandStream('swb2712', 'Seed', 12345);
% Modulation order
M = 2;
% 2-PSK modulator object
Modulator = modem.pskmod(M);
% Input symbol rate
Symb_R = 10e3;
% Input bit rate
Bit_R = Symb_R * log2(M);
% Oversampling factor
Over_F = 4;
% Input sample period
ts = (1/Bit_R) / Over_F;

% The speed of light
C=3*10^8;
% The frequency in GHZ
F=2.4;

% Constructing a rounded doppler spectrum with a default vector of
% polynomial coefficients
dopp_spec = doppler.rounded;

% Path delays, in seconds
tau =rand(1,5)*1e-6;
% Number of paths
Np = length(tau);

hBS=25;                 % Base station antenna height, in meter
hMS=1.5;                % Mobile station antenna height, in meter

environment_switch=1;  %this variable is defined '1' to run the
%simulation for bad urban and '0' to run the simulation for rural.

if environment_switch==1

ind=1;
for d=[50 55 60 65 70];     % Array of distances in meter
 % Path loss for Bad-Urban macro cell at LOS condition
 PL_LOS(ind)=40*log10(d)+13.47-14*log10(hBS)-14*log10(hMS)+...
     6*log10(F/5)+6;
 % Path loss for Bad-Urban macro cell at NLOS condition
 PL_NLOS(ind)=(44.9-
6.55*log10(hBS))*log10(d)+34.46+5.83*log10(hMS)+...
     20*log10(F/5)+8;
 ind=ind+1;
end
```

```
% Path gains for the five paths of cluster 1
pdb1 = PL_LOS(1)-[PL_LOS(1),PL_NLOS(2),PL_NLOS(3),...
    PL_NLOS(4),PL_NLOS(5)];


for d=[80 85 90 95 100];    % Array of distances in meter
 % Path loss for Bad-Urban macro cell at LOS condition
 PL_LOS(ind)=40*log10(d)+13.47-14*log10(hBS)-14*log10(hMS)+...
     6*log10(F/5)+6;
 % Path loss for Bad-Urban macro cell at NLOS condition
 PL_NLOS(ind)=(44.9-
6.55*log10(hBS))*log10(d)+34.46+5.83*log10(hMS)+...
     20*log10(F/5)+8;
 ind=ind+1;
end

% Path gains for the five paths of cluster 2
pdb2 =PL_LOS(1)-[PL_LOS(6),PL_NLOS(7),PL_NLOS(8),...
    PL_NLOS(9),PL_NLOS(10)];


for d=[110 115 120 125 130];    % Array of distances in meter
 % Path loss for Bad-Urban macro cell at LOS condition
 PL_LOS(ind)=40*log10(d)+13.47-14*log10(hBS)-14*log10(hMS)+...
     6*log10(F/5)+6;
 % Path loss for Bad-Urban macro cell at NLOS condition
 PL_NLOS(ind)=(44.9-
6.55*log10(hBS))*log10(d)+34.46+5.83*log10(hMS)+...
     20*log10(F/5)+8;
 ind=ind+1;
end

% Path gains for the five paths of cluster 3
pdb3 =PL_LOS(1)-[PL_LOS(11),PL_NLOS(12),PL_NLOS(13),...
    PL_NLOS(14),PL_NLOS(15)];


% Total average path gains for all clusters
pdb = 10*log10(10.^(pdb1/10)+10.^(pdb2/10)+10.^(pdb3/10));

% speed of mobile station in m/s
speedms_ms = 0.25;
% Wavelength in meter
wavelength_m = C / (F*10^9);
% Maximum Doppler shift for all paths
fd = speedms_ms / wavelength_m;

else

ind=1;
for d=[50 55 60 65 70];    % Array of distances in meter
 % Free loss
 PLfree=46.4+20*log10(d)+20*log10(F/5);
 % Path loss for Rural macro cell at LOS condition
 PL_LOS(ind)=10.5+40*log10(d)-18.5*log10(hBS)-...
     18.5*log10(hMS)+1.5*log10(F/5)+4;
 % Path loss for Rural macro cell at NLOS condition
 PL_NLOS(ind)=max((55.4+25.1*log10(d)-0.13*log10(hBS-25))*...
     log(d/100)-0.9*(hMS-1.5)+21.3*log10(F/5),PLfree)+8;
```

```
 ind=ind+1;
end

% Path gains for the five paths of cluster 1
pdb1 = PL_LOS(1)-[PL_LOS(1),PL_NLOS(2),PL_NLOS(3),...
    PL_NLOS(4),PL_NLOS(5)];


for d=[80 85 90 95 100];    % Array of distances in meter
 % Free loss
 PLfree=46.4+20*log10(d)+20*log10(F/5);
 % Path loss for Rural macro cell at LOS condition
 PL_LOS(ind)=10.5+40*log10(d)-18.5*log10(hBS)-...
     18.5*log10(hMS)+1.5*log10(F/5)+4;
 % Path loss for Rural macro cell at NLOS condition
 PL_NLOS(ind)=max((55.4+25.1*log10(d)-0.13*log10(hBS-25))*...
     log(d/100)-0.9*(hMS-1.5)+21.3*log10(F/5),PLfree)+8;
 ind=ind+1;
end

% Path gains for the five paths of cluster 2
pdb2 =PL_LOS(1)-[PL_LOS(6),PL_NLOS(7),PL_NLOS(8),...
    PL_NLOS(9),PL_NLOS(10)];


for d=[110 115 120 125 130];    % Array of distances in meter
 % Free loss
 PLfree=46.4+20*log10(d)+20*log10(F/5);
 % Path loss for Rural macro cell at LOS condition
 PL_LOS(ind)=10.5+40*log10(d)-18.5*log10(hBS)-...
     18.5*log10(hMS)+1.5*log10(F/5)+4;
 % Path loss for Rural macro cell at NLOS condition
 PL_NLOS(ind)=max((55.4+25.1*log10(d)-0.13*log10(hBS-25))*...
     log(d/100)-0.9*(hMS-1.5)+21.3*log10(F/5),PLfree)+8;
 ind=ind+1;
end

% Path gains for the five paths of cluster 3
pdb3 =PL_LOS(1)-[PL_LOS(11),PL_NLOS(12),PL_NLOS(13),...
    PL_NLOS(14),PL_NLOS(15)];


% Total average path gains for all clusters
pdb = 10*log10(10.^(pdb1/10)+10.^(pdb2/10)+10.^(pdb3/10));

% speed of mobile station in m/s
speedms_ms = 0.05;
% Wavelength in meter
wavelength_m = C / (F*10^9);
% Maximum Doppler shift for all paths
fd = speedms_ms / wavelength_m;

end


Nt = 2;                 % Number of transmit antennas
Nr = 2;                 % Number of receive antennas
```

```
% Element spacing at the transmit antennas (normalized by the
%wavelength)
TxSpacing = 1;
% Element spacing at the receive antennas (normalized by the
%wavelength)
RxSpacing = 0.5;

% Angular spreads of cluster 1 at transmit side
Angular_spread_Cluster1_Tx = 14.4*ones(1,5);
% Angular spreads of cluster 2 at transmit side
Angular_spread_Cluster2_Tx = 25.4*ones(1,5);
% Angular spreads of cluster 3 at transmit side
Angular_spread_Cluster3_Tx = 29.5*ones(1,5);

% Angular spreads of cluster 1 at receive side
Angular_spread_Cluster1_Rx = 14.4*ones(1,5);
% Angular spreads of cluster 2 at receive side
Angular_spread_Cluster2_Rx = 25.4*ones(1,5);
% Angular spreads of cluster 3 at receive side
Angular_spread_Cluster3_Rx = 25.4*ones(1,5);

% Mean angles of departure of cluster 1
AoD_Cluster1 = 120*rand(1,5);
% Mean angles of departure of cluster 2
AoD_Cluster2 = 150*rand(1,5);
% Mean angles of departure of cluster 3
AoD_Cluster3 = 200*rand(1,5);

% Mean angles of arrival of cluster 1
AoA_Cluster1 = 170*rand(1,5);
% Mean angles of arrival of cluster 2
AoA_Cluster2 = 250*rand(1,5);
% Mean angles of arrival of cluster 3
AoA_Cluster3 = 130*rand(1,5);

% Calculate transmit and receive correlation matrices
[TxCorrelationMatrix1, RxCorrelationMatrix1] = ...
calculateCorrMatrixx(Nt,    Nr,    pdb1,    pdb2,pdb3,    TxSpacing,
RxSpacing,...
Angular_spread_Cluster1_Tx, Angular_spread_Cluster2_Tx,...
Angular_spread_Cluster3_Tx,...
Angular_spread_Cluster1_Rx,Angular_spread_Cluster2_Rx,...
Angular_spread_Cluster3_Rx,...
AoD_Cluster1, AoD_Cluster2,AoD_Cluster3,...
AoA_Cluster1, AoA_Cluster2,AoA_Cluster3);

%MIMO channel object, returns a MIMO channel that models each
%discrete path as an independent Rayleigh fading process.
channel = mimochan(Nt, Nr, ts, fd, tau, pdb);
%Defining the k-factor for the first path since it's Rician, it
%defines the power ratio b\w the direct path and the scattered
%multipath component.
channel.KFactor = 2;
% Doppler spectrum of MIMO object
channel.DopplerSpectrum = dopp_spec;
% Transmit correlation matrix
channel.TxCorrelationMatrix = TxCorrelationMatrix1;
% Receive correlation matrix
channel.RxCorrelationMatrix = RxCorrelationMatrix1;
```

```
% After each frame is processed, the channel is not reset: this is
%necessary to preserve continuity across frames. in order to make the
%filter make use of the existing state info. of the channel when
%starting the filtering operation.
channel.ResetBeforeFiltering = 0;
% This setting is needed to store the path gains (the complex path
gain
%vector is stored as the channel filter function processes the
signal).
channel.StorePathGains = 1;

Nsamp = 1e6/2;                  % Total number of channel samples
Nsamp_f = 1000;                 % Number of samples per frame
Nframes = Nsamp/Nsamp_f;        % Number of frames

%defining a zero matrix of size Nsamp*Nr in order to make use of it
%in the frame sequencing process.
out = zeros(Nsamp, Nr);
%defining all sub-channels(links)
link11 = zeros(Nsamp, Np);  link12 = zeros(Nsamp, Np);
link21 = zeros(Nsamp, Np);  link22 = zeros(Nsamp, Np);

%starting a loop to do a set of operations for each frame
for iFrames = 1:Nframes
    %moduate the input signal using modulator object
    inputSig = modulate(Modulator, randi(S, [0 M-1], Nsamp_f, Nt));
    %to make a counter of the frames,(first frame contains the
samples
    %from 1 to 1000 and the second contains the samples from 1001 to
    %2000 and so on).
    idx = (1:Nsamp_f)+(iFrames-1)*Nsamp_f;
    %passes the signal through the MIMO channel.
    out(idx,:) = filter(channel, inputSig);
    %starting a loop from 1 to number of paths
    for ip = 1:Np
        % For each transmit-receive link, store gains of all paths
        link11(idx,ip) = channel.PathGains(:,ip,1,1);
        link12(idx,ip) = channel.PathGains(:,ip,1,2);
        link21(idx,ip) = channel.PathGains(:,ip,2,1);
        link22(idx,ip) = channel.PathGains(:,ip,2,2);
    end
end

% Plot the fading envelopes using semilogy which is the same as
%PLOT(...), except a logarithmic (base 10) scale is used for the Y-
axis

figure;
semilogy(abs(link11(:,1)),'w');
hold on; grid on;
semilogy(abs(link12(:,1)),'b');
hold on;
semilogy(abs(link21(:,1)),'r');
hold on;
semilogy(abs(link22(:,1)),'k');
legend('Tx1-Rx1','Tx1-Rx2','Tx2-Rx1','Tx2-Rx2');
title('Fading envelopes for the first path through all links');
xlabel('Number of samples');
ylabel('Path gain');
```

```
figure;
semilogy(abs(link11(:,2)),'w');
hold on; grid on;
semilogy(abs(link12(:,2)),'b');
hold on;
semilogy(abs(link21(:,2)),'r');
hold on;
semilogy(abs(link22(:,2)),'k');
legend('Tx1-Rx1','Tx1-Rx2','Tx2-Rx1','Tx2-Rx2');
title('Fading envelopes for the second path through all links');
xlabel('Number of samples');
ylabel('Path gain');

figure;
semilogy(abs(link11(:,3)),'w');
hold on; grid on;
semilogy(abs(link12(:,3)),'b');
hold on;
semilogy(abs(link21(:,3)),'r');
hold on;
semilogy(abs(link22(:,3)),'k');
legend('Tx1-Rx1','Tx1-Rx2','Tx2-Rx1','Tx2-Rx2');
title('Fading envelopes for the third path through all links');
xlabel('Number of samples');
ylabel('Path gain');

figure;
semilogy(abs(link11(:,4)),'w');
hold on; grid on;
semilogy(abs(link12(:,4)),'b');
hold on;
semilogy(abs(link21(:,4)),'r');
hold on;
semilogy(abs(link22(:,4)),'k');
legend('Tx1-Rx1','Tx1-Rx2','Tx2-Rx1','Tx2-Rx2');
title('Fading envelopes for the fourth path through all links');
xlabel('Number of samples');
ylabel('Path gain');

figure;
semilogy(abs(link11(:,5)),'w');
hold on; grid on;
semilogy(abs(link12(:,5)),'b');
hold on;
semilogy(abs(link21(:,5)),'r');
hold on;
semilogy(abs(link22(:,5)),'k');
legend('Tx1-Rx1','Tx1-Rx2','Tx2-Rx1','Tx2-Rx2');
title('Fading envelopes for the fifth path through all links');
xlabel('Number of samples');
ylabel('Path gain');

% Obtain transmit correlation matrices for the five paths
transmit_corr_mat_path1=TxCorrelationMatrix1(:,:,1)
transmit_corr_mat_path2=TxCorrelationMatrix1(:,:,2)
transmit_corr_mat_path3=TxCorrelationMatrix1(:,:,3)
transmit_corr_mat_path4=TxCorrelationMatrix1(:,:,4)
transmit_corr_mat_path5=TxCorrelationMatrix1(:,:,5)
```

```
% Obtain receive correlation matrices for the five paths
receive_corr_mat_path1=RxCorrelationMatrix1(:,:,1)
receive_corr_mat_path2=RxCorrelationMatrix1(:,:,2)
receive_corr_mat_path3=RxCorrelationMatrix1(:,:,3)
receive_corr_mat_path4=RxCorrelationMatrix1(:,:,4)
receive_corr_mat_path5=RxCorrelationMatrix1(:,:,5)

MIMO_channel=channel          % Obtain MIMO channel properties
Doppler_shift=fd              % Obtain the Doppler shift
Path_gain_cluster_1=pdb1      % Obtain the path gains for cluster 1
Path_gain_cluster_2=pdb2      % Obtain the path gains for cluster 2
Path_gain_cluster_3=pdb2      % Obtain the path gains for cluster 3
```

A3) 4x2 MIMO channel model code:

```
clear all
close all
clc

% Creating an array of random numbers
S = RandStream('swb2712', 'Seed', 12345);
% Modulation order
M = 2;
% 2-PSK modulator object
Modulator = modem.pskmod(M);
% Input symbol rate
Symb_R = 10e3;
% Input bit rate
Bit_R = Symb_R * log2(M);
% Oversampling factor
Over_F = 4;
% Input sample period
ts = (1/Bit_R) / Over_F;

% The speed of light
C=3*10^8;
% The frequency in GHZ
F=2.4;

% Constructing a rounded doppler spectrum with a default vector of
% polynomial coefficients
dopp_spec = doppler.rounded;

% Path delays, in seconds
tau =rand(1,5)*1e-6;
% Number of paths
Np = length(tau);

hBS=25;                 % Base station antenna height, in meter
hMS=1.5;                % Mobile station antenna height, in meter

environment_switch=0;  %this variable is defined '1' to run the
%simulation for bad urban and '0' to run the simulation for rural.

if environment_switch==1

ind=1;
for d=[50 55 60 65 70];     % Array of distances in meter
 % Path loss for Bad-Urban macro cell at LOS condition
 PL_LOS(ind)=40*log10(d)+13.47-14*log10(hBS)-14*log10(hMS)+...
     6*log10(F/5)+6;
 % Path loss for Bad-Urban macro cell at NLOS condition
 PL_NLOS(ind)=(44.9-
6.55*log10(hBS))*log10(d)+34.46+5.83*log10(hMS)+...
     20*log10(F/5)+8;
 ind=ind+1;
end
```

```
% Path gains for the five paths of cluster 1
pdb1 = PL_LOS(1)-[PL_LOS(1),PL_NLOS(2),PL_NLOS(3),...
    PL_NLOS(4),PL_NLOS(5)];


for d=[80 85 90 95 100];    % Array of distances in meter
 % Path loss for Bad-Urban macro cell at LOS condition
 PL_LOS(ind)=40*log10(d)+13.47-14*log10(hBS)-14*log10(hMS)+...
     6*log10(F/5)+6;
 % Path loss for Bad-Urban macro cell at NLOS condition
 PL_NLOS(ind)=(44.9-
6.55*log10(hBS))*log10(d)+34.46+5.83*log10(hMS)+...
     20*log10(F/5)+8;
 ind=ind+1;
end

% Path gains for the five paths of cluster 2
pdb2 =PL_LOS(1)-[PL_LOS(6),PL_NLOS(7),PL_NLOS(8),...
    PL_NLOS(9),PL_NLOS(10)];


for d=[110 115 120 125 130];    % Array of distances in meter
 % Path loss for Bad-Urban macro cell at LOS condition
 PL_LOS(ind)=40*log10(d)+13.47-14*log10(hBS)-14*log10(hMS)+...
     6*log10(F/5)+6;
 % Path loss for Bad-Urban macro cell at NLOS condition
 PL_NLOS(ind)=(44.9-
6.55*log10(hBS))*log10(d)+34.46+5.83*log10(hMS)+...
     20*log10(F/5)+8;
 ind=ind+1;
end

% Path gains for the five paths of cluster 3
pdb3 =PL_LOS(1)-[PL_LOS(11),PL_NLOS(12),PL_NLOS(13),...
    PL_NLOS(14),PL_NLOS(15)];


% Total average path gains for all clusters
pdb = 10*log10(10.^(pdb1/10)+10.^(pdb2/10)+10.^(pdb3/10));

% speed of mobile station in m/s
speedms_ms = 0.25;
% Wavelength in meter
wavelength_m = C / (F*10^9);
% Maximum Doppler shift for all paths
fd = speedms_ms / wavelength_m;

else

ind=1;
for d=[50 55 60 65 70];    % Array of distances in meter
 % Free loss
 PLfree=46.4+20*log10(d)+20*log10(F/5);
 % Path loss for Rural macro cell at LOS condition
 PL_LOS(ind)=10.5+40*log10(d)-18.5*log10(hBS)-...
     18.5*log10(hMS)+1.5*log10(F/5)+4;
 % Path loss for Rural macro cell at NLOS condition
 PL_NLOS(ind)=max((55.4+25.1*log10(d)-0.13*log10(hBS-25))*...
     log(d/100)-0.9*(hMS-1.5)+21.3*log10(F/5),PLfree)+8;
```

```
 ind=ind+1;
end

% Path gains for the five paths of cluster 1
pdb1 = PL_LOS(1)-[PL_LOS(1),PL_NLOS(2),PL_NLOS(3),...
    PL_NLOS(4),PL_NLOS(5)];


for d=[80 85 90 95 100];    % Array of distances in meter
 % Free loss
 PLfree=46.4+20*log10(d)+20*log10(F/5);
 % Path loss for Rural macro cell at LOS condition
 PL_LOS(ind)=10.5+40*log10(d)-18.5*log10(hBS)-...
     18.5*log10(hMS)+1.5*log10(F/5)+4;
 % Path loss for Rural macro cell at NLOS condition
 PL_NLOS(ind)=max((55.4+25.1*log10(d)-0.13*log10(hBS-25))*...
     log(d/100)-0.9*(hMS-1.5)+21.3*log10(F/5),PLfree)+8;
 ind=ind+1;
end

% Path gains for the five paths of cluster 2
pdb2 =PL_LOS(1)-[PL_LOS(6),PL_NLOS(7),PL_NLOS(8),...
    PL_NLOS(9),PL_NLOS(10)];


for d=[110 115 120 125 130];    % Array of distances in meter
 % Free loss
 PLfree=46.4+20*log10(d)+20*log10(F/5);
 % Path loss for Rural macro cell at LOS condition
 PL_LOS(ind)=10.5+40*log10(d)-18.5*log10(hBS)-...
     18.5*log10(hMS)+1.5*log10(F/5)+4;
 % Path loss for Rural macro cell at NLOS condition
 PL_NLOS(ind)=max((55.4+25.1*log10(d)-0.13*log10(hBS-25))*...
     log(d/100)-0.9*(hMS-1.5)+21.3*log10(F/5),PLfree)+8;
 ind=ind+1;
end

% Path gains for the five paths of cluster 3
pdb3 =PL_LOS(1)-[PL_LOS(11),PL_NLOS(12),PL_NLOS(13),...
    PL_NLOS(14),PL_NLOS(15)];


% Total average path gains for all clusters
pdb = 10*log10(10.^(pdb1/10)+10.^(pdb2/10)+10.^(pdb3/10));

% speed of mobile station in m/s
speedms_ms = 0.05;
% Wavelength in meter
wavelength_m = C / (F*10^9);
% Maximum Doppler shift for all paths
fd = speedms_ms / wavelength_m;

end


Nt = 4;                 % Number of transmit antennas
Nr = 2;                 % Number of receive antennas
```

```
% Element spacing at the transmit antennas (normalized by the
%wavelength)
TxSpacing = 1;
% Element spacing at the receive antennas (normalized by the
%wavelength)
RxSpacing = 0.5;

% Angular spreads of cluster 1 at transmit side
Angular_spread_Cluster1_Tx = 14.4*ones(1,5);
% Angular spreads of cluster 2 at transmit side
Angular_spread_Cluster2_Tx = 25.4*ones(1,5);
% Angular spreads of cluster 3 at transmit side
Angular_spread_Cluster3_Tx = 29.5*ones(1,5);

% Angular spreads of cluster 1 at receive side
Angular_spread_Cluster1_Rx = 14.4*ones(1,5);
% Angular spreads of cluster 2 at receive side
Angular_spread_Cluster2_Rx = 25.4*ones(1,5);
% Angular spreads of cluster 3 at receive side
Angular_spread_Cluster3_Rx = 25.4*ones(1,5);

% Mean angles of departure of cluster 1
AoD_Cluster1 = 120*rand(1,5);
% Mean angles of departure of cluster 2
AoD_Cluster2 = 150*rand(1,5);
% Mean angles of departure of cluster 3
AoD_Cluster3 = 200*rand(1,5);

% Mean angles of arrival of cluster 1
AoA_Cluster1 = 170*rand(1,5);
% Mean angles of arrival of cluster 2
AoA_Cluster2 = 250*rand(1,5);
% Mean angles of arrival of cluster 3
AoA_Cluster3 = 130*rand(1,5);

% Calculate transmit and receive correlation matrices
[TxCorrelationMatrix1, RxCorrelationMatrix1] = ...
calculateCorrMatrixx(Nt, Nr, pdb1, pdb2,pdb3, TxSpacing,
RxSpacing,...
Angular_spread_Cluster1_Tx, Angular_spread_Cluster2_Tx,...
Angular_spread_Cluster3_Tx,...
Angular_spread_Cluster1_Rx,Angular_spread_Cluster2_Rx,...
Angular_spread_Cluster3_Rx,...
AoD_Cluster1, AoD_Cluster2,AoD_Cluster3,...
AoA_Cluster1, AoA_Cluster2,AoA_Cluster3);

%MIMO channel object, returns a MIMO channel that models each
%discrete path as an independent Rayleigh fading process.
channel = mimochan(Nt, Nr, ts, fd, tau, pdb);
%Defining the k-factor for the first path since it's Rician, it
%defines the power ratio b\w the direct path and the scattered
%multipath component.
channel.KFactor = 2;
% Doppler spectrum of MIMO object
channel.DopplerSpectrum = dopp_spec;
% Transmit correlation matrix
channel.TxCorrelationMatrix = TxCorrelationMatrix1;
% Receive correlation matrix
channel.RxCorrelationMatrix = RxCorrelationMatrix1;
```

```
% After each frame is processed, the channel is not reset: this is
%necessary to preserve continuity across frames. in order to make the
%filter make use of the existing state info. of the channel when
%starting the filtering operation.
channel.ResetBeforeFiltering = 0;
% This setting is needed to store the path gains (the complex path
gain
%vector is stored as the channel filter function processes the
signal).
channel.StorePathGains = 1;

Nsamp = 1e6/2;                  % Total number of channel samples
Nsamp_f = 1000;                 % Number of samples per frame
Nframes = Nsamp/Nsamp_f;        % Number of frames

%defining a zero matrix of size Nsamp*Nr in order to make use of it
%in the frame sequencing process.
out = zeros(Nsamp, Nr);
%defining all sub-channels(links)
link11 = zeros(Nsamp, Np);  link12 = zeros(Nsamp, Np);
link21 = zeros(Nsamp, Np);  link22 = zeros(Nsamp, Np);
link31 = zeros(Nsamp, Np);  link32 = zeros(Nsamp, Np);
link41 = zeros(Nsamp, Np);  link42 = zeros(Nsamp, Np);

%starting a loop to do a set of operations for each frame
for iFrames = 1:Nframes
    %moduate the input signal using modulator object
    inputSig = modulate(Modulator, randi(S, [0 M-1], Nsamp_f, Nt));
    %to make a counter of the frames,(first frame contains the
samples
    %from 1 to 1000 and the second contains the samples from 1001 to
    %2000 and so on).
    idx = (1:Nsamp_f)+(iFrames-1)*Nsamp_f;
    %passes the signal through the MIMO channel.
    out(idx,:) = filter(channel, inputSig);
    %starting a loop from 1 to number of paths
    for ip = 1:Np
        % For each transmit-receive link, store gains of all paths
        link11(idx,ip) = channel.PathGains(:,ip,1,1);
        link12(idx,ip) = channel.PathGains(:,ip,1,2);
        link21(idx,ip) = channel.PathGains(:,ip,2,1);
        link22(idx,ip) = channel.PathGains(:,ip,2,2);
        link31(idx,ip) = channel.PathGains(:,ip,3,1);
        link32(idx,ip) = channel.PathGains(:,ip,3,2);
        link41(idx,ip) = channel.PathGains(:,ip,4,1);
        link42(idx,ip) = channel.PathGains(:,ip,4,2);
    end
end

% Plot the fading envelopes using semilogy which is the same as
%PLOT(...), except a logarithmic (base 10) scale is used for the Y-
axis

figure;
semilogy(abs(link11(:,1)),'k');
hold on; grid on;
semilogy(abs(link12(:,1)),'g');
hold on;
semilogy(abs(link21(:,1)),'r');
hold on;
```

```
semilogy(abs(link22(:,1)),'c');
hold on;
semilogy(abs(link31(:,1)),'m');
hold on;
semilogy(abs(link32(:,1)),'y');
hold on;
semilogy(abs(link41(:,1)),'b');
hold on;
semilogy(abs(link42(:,1)),'w');
legend('Tx1-Rx1','Tx1-Rx2','Tx2-Rx1','Tx2-Rx2','Tx3-Rx1','Tx3-
Rx2',...
    'Tx4-Rx1','Tx4-Rx2');
title('Fading envelopes for the first path through all links');
xlabel('Number of samples');
ylabel('Path gain');

figure;
semilogy(abs(link11(:,2)),'k');
hold on; grid on;
semilogy(abs(link12(:,2)),'g');
hold on;
semilogy(abs(link21(:,2)),'r');
hold on;
semilogy(abs(link22(:,2)),'c');
hold on;
semilogy(abs(link31(:,2)),'m');
hold on;
semilogy(abs(link32(:,2)),'y');
hold on;
semilogy(abs(link41(:,2)),'b');
hold on;
semilogy(abs(link42(:,2)),'w');
legend('Tx1-Rx1','Tx1-Rx2','Tx2-Rx1','Tx2-Rx2','Tx3-Rx1','Tx3-
Rx2',...
    'Tx4-Rx1','Tx4-Rx2');
title('Fading envelopes for the second path through all links');
xlabel('Number of samples');
ylabel('Path gain');

figure;
semilogy(abs(link11(:,3)),'k');
hold on; grid on;
semilogy(abs(link12(:,3)),'g');
hold on;
semilogy(abs(link21(:,3)),'r');
hold on;
semilogy(abs(link22(:,3)),'c');
hold on;
semilogy(abs(link31(:,3)),'m');
hold on;
semilogy(abs(link32(:,3)),'y');
hold on;
semilogy(abs(link41(:,3)),'b');
hold on;
semilogy(abs(link42(:,3)),'w');
legend('Tx1-Rx1','Tx1-Rx2','Tx2-Rx1','Tx2-Rx2','Tx3-Rx1','Tx3-
Rx2',...
    'Tx4-Rx1','Tx4-Rx2');
title('Fading envelopes for the third path through all links');
xlabel('Number of samples');
ylabel('Path gain');
```

```
figure;
semilogy(abs(link11(:,4)),'k');
hold on; grid on;
semilogy(abs(link12(:,4)),'g');
hold on;
semilogy(abs(link21(:,4)),'r');
hold on;
semilogy(abs(link22(:,4)),'c');
hold on;
semilogy(abs(link31(:,4)),'m');
hold on;
semilogy(abs(link32(:,4)),'y');
hold on;
semilogy(abs(link41(:,4)),'b');
hold on;
semilogy(abs(link42(:,4)),'w');
legend('Tx1-Rx1','Tx1-Rx2','Tx2-Rx1','Tx2-Rx2','Tx3-Rx1','Tx3-
Rx2',...
    'Tx4-Rx1','Tx4-Rx2');
title('Fading envelopes for the fourth path through all links');
xlabel('Number of samples');
ylabel('Path gain');

figure;
semilogy(abs(link11(:,5)),'k');
hold on; grid on;
semilogy(abs(link12(:,5)),'g');
hold on;
semilogy(abs(link21(:,5)),'r');
hold on;
semilogy(abs(link22(:,5)),'c');
hold on;
semilogy(abs(link31(:,5)),'m');
hold on;
semilogy(abs(link32(:,5)),'y');
hold on;
semilogy(abs(link41(:,5)),'b');
hold on;
semilogy(abs(link42(:,5)),'w');
legend('Tx1-Rx1','Tx1-Rx2','Tx2-Rx1','Tx2-Rx2','Tx3-Rx1','Tx3-
Rx2',...
    'Tx4-Rx1','Tx4-Rx2');
title('Fading envelopes for the fifth path through all links');
xlabel('Number of samples');
ylabel('Path gain');

% Obtain transmit correlation matrices for the five paths
transmit_corr_mat_path1=TxCorrelationMatrix1(:,:,1)
transmit_corr_mat_path2=TxCorrelationMatrix1(:,:,2)
transmit_corr_mat_path3=TxCorrelationMatrix1(:,:,3)
transmit_corr_mat_path4=TxCorrelationMatrix1(:,:,4)
transmit_corr_mat_path5=TxCorrelationMatrix1(:,:,5)

% Obtain receive correlation matrices for the five paths
receive_corr_mat_path1=RxCorrelationMatrix1(:,:,1)
receive_corr_mat_path2=RxCorrelationMatrix1(:,:,2)
receive_corr_mat_path3=RxCorrelationMatrix1(:,:,3)
receive_corr_mat_path4=RxCorrelationMatrix1(:,:,4)
receive_corr_mat_path5=RxCorrelationMatrix1(:,:,5)
```

```
MIMO_channel=channel          % Obtain MIMO channel properties
Doppler_shift=fd              % Obtain the Doppler shift
Path_gain_cluster_1=pdb1      % Obtain the path gains for cluster 1
Path_gain_cluster_2=pdb2      % Obtain the path gains for cluster 2
Path_gain_cluster_3=pdb2      % Obtain the path gains for cluster 3
```

A4) 8x2 MIMO channel model code:

```
clear all
close all
clc

% Creating an array of random numbers
S = RandStream('swb2712', 'Seed', 12345);
% Modulation order
M = 2;
% 2-PSK modulator object
Modulator = modem.pskmod(M);
% Input symbol rate
Symb_R = 10e3;
% Input bit rate
Bit_R = Symb_R * log2(M);
% Oversampling factor
Over_F = 4;
% Input sample period
ts = (1/Bit_R) / Over_F;

% The speed of light
C=3*10^8;
% The frequency in GHZ
F=2.4;
% speed of mobile station in m/s
speedms_ms = 0.75;
% Wavelength in meter
wavelength_m = C / (F*10^9);
% Maximum Doppler shift for all paths
fd = speedms_ms / wavelength_m;

% Constructing a rounded doppler spectrum with a default vector of
% polynomial coefficients
dopp_spec = doppler.rounded;

% Path delays, in seconds
tau =rand(1,5)*1e-6;
% Number of paths
Np = length(tau);

d=linspace(3,100,15);    % Array of distances in meter
for i=1:15;
 % Path loss for indoor small office at LOS condition
 PL_LOS(i)= 18.7*log10(d(i))+46.8+20*log10(F/5)+3;
 % Path loss for indoor small office at NLOS condition
 PL_NLOS(i)= 36.8*log10(d(i))+43.8+20*log10(F/5)+4;
end

% Path gains for the five paths of cluster 1
pdb1 = PL_LOS(1)-[PL_LOS(1),PL_NLOS(2),PL_NLOS(3),...
    PL_NLOS(4),PL_NLOS(5)];

% Path gains for the five paths of cluster 2
pdb2 =PL_LOS(1)-[PL_LOS(6),PL_NLOS(7),PL_NLOS(8),...
    PL_NLOS(9),PL_NLOS(10)];
```

```
% Path gains for the five paths of cluster 3
pdb3 =PL_LOS(1)-[PL_LOS(11),PL_NLOS(12),PL_NLOS(13),...
    PL_NLOS(14),PL_NLOS(15)];

% Total average path gains for all clusters
pdb = 10*log10(10.^(pdb1/10)+10.^(pdb2/10)+10.^(pdb3/10));


Nt = 8;                 % Number of transmit antennas
Nr = 2;                 % Number of receive antennas

% Element spacing at the transmit antennas (normalized by the
%wavelength)
TxSpacing = 0.5;
% Element spacing at the receive antennas (normalized by the
%wavelength)
RxSpacing = 0.5;

% Angular spreads of cluster 1 at transmit side
Angular_spread_Cluster1_Tx = 14.4*ones(1,5);
% Angular spreads of cluster 2 at transmit side
Angular_spread_Cluster2_Tx = 25.4*ones(1,5);
% Angular spreads of cluster 3 at transmit side
Angular_spread_Cluster3_Tx = 29.5*ones(1,5);

% Angular spreads of cluster 1 at receive side
Angular_spread_Cluster1_Rx = 14.4*ones(1,5);
% Angular spreads of cluster 2 at receive side
Angular_spread_Cluster2_Rx = 25.4*ones(1,5);
% Angular spreads of cluster 3 at receive side
Angular_spread_Cluster3_Rx = 25.4*ones(1,5);

% Mean angles of departure of cluster 1
AoD_Cluster1 = 120*rand(1,5);
% Mean angles of departure of cluster 2
AoD_Cluster2 = 150*rand(1,5);
% Mean angles of departure of cluster 3
AoD_Cluster3 = 200*rand(1,5);

% Mean angles of arrival of cluster 1
AoA_Cluster1 = 170*rand(1,5);
% Mean angles of arrival of cluster 2
AoA_Cluster2 = 250*rand(1,5);
% Mean angles of arrival of cluster 3
AoA_Cluster3 = 130*rand(1,5);

% Calculate transmit and receive correlation matrices
[TxCorrelationMatrix1, RxCorrelationMatrix1] = ...
calculateCorrMatrixx(Nt, Nr, pdb1, pdb2,pdb3, TxSpacing,
RxSpacing,...
Angular_spread_Cluster1_Tx, Angular_spread_Cluster2_Tx,...
Angular_spread_Cluster3_Tx,...
Angular_spread_Cluster1_Rx,Angular_spread_Cluster2_Rx,...
Angular_spread_Cluster3_Rx,...
AoD_Cluster1, AoD_Cluster2,AoD_Cluster3,...
AoA_Cluster1, AoA_Cluster2,AoA_Cluster3);
```

```
%MIMO channel object, returns a MIMO channel that models each
%discrete path as an independent Rayleigh fading process.
channel = mimochan(Nt, Nr, ts, fd, tau, pdb);
%Defining the k-factor for the first path since it's Rician, it
%defines the power ratio b\w the direct path and the scattered
%multipath component.
channel.KFactor = 2;
% Doppler spectrum of MIMO object
channel.DopplerSpectrum = dopp_spec;
% Transmit correlation matrix
channel.TxCorrelationMatrix = TxCorrelationMatrix1;
% Receive correlation matrix
channel.RxCorrelationMatrix = RxCorrelationMatrix1;
% After each frame is processed, the channel is not reset: this is
%necessary to preserve continuity across frames. in order to make the
%filter make use of the existing state info. of the channel when
%starting the filtering operation.
channel.ResetBeforeFiltering = 0;
% This setting is needed to store the path gains (the complex path
gain
%vector is stored as the channel filter function processes the
signal).
channel.StorePathGains = 1;

Nsamp = 1e6/2;                  % Total number of channel samples
Nsamp_f = 1000;                 % Number of samples per frame
Nframes = Nsamp/Nsamp_f;        % Number of frames

%defining a zero matrix of size Nsamp*Nr in order to make use of it
%in the frame sequencing process.
out = zeros(Nsamp, Nr);
%defining all sub-channels(links)
link11 = zeros(Nsamp, Np);  link12 = zeros(Nsamp, Np);
link21 = zeros(Nsamp, Np);  link22 = zeros(Nsamp, Np);
link31 = zeros(Nsamp, Np);  link32 = zeros(Nsamp, Np);
link41 = zeros(Nsamp, Np);  link42 = zeros(Nsamp, Np);
link51 = zeros(Nsamp, Np);  link52 = zeros(Nsamp, Np);
link61 = zeros(Nsamp, Np);  link62 = zeros(Nsamp, Np);
link71 = zeros(Nsamp, Np);  link72 = zeros(Nsamp, Np);
link81 = zeros(Nsamp, Np);  link82 = zeros(Nsamp, Np);

%starting a loop to do a set of operations for each frame
for iFrames = 1:Nframes
    %moduate the input signal using modulator object
    inputSig = modulate(Modulator, randi(S, [0 M-1], Nsamp_f, Nt));
    %to make a counter of the frames,(first frame contains the
samples
    %from 1 to 1000 and the second contains the samples from 1001 to
    %2000 and so on).
    idx = (1:Nsamp_f)+(iFrames-1)*Nsamp_f;
    %passes the signal through the MIMO channel.
    out(idx,:) = filter(channel, inputSig);
    %starting a loop from 1 to number of paths
    for ip = 1:Np
        % For each transmit-receive link, store gains of all paths
        link11(idx,ip) = channel.PathGains(:,ip,1,1);
        link12(idx,ip) = channel.PathGains(:,ip,1,2);

        link21(idx,ip) = channel.PathGains(:,ip,2,1);
        link22(idx,ip) = channel.PathGains(:,ip,2,2);
```

```
        link31(idx,ip) = channel.PathGains(:,ip,3,1);
        link32(idx,ip) = channel.PathGains(:,ip,3,2);

        link41(idx,ip) = channel.PathGains(:,ip,4,1);
        link42(idx,ip) = channel.PathGains(:,ip,4,2);

        link51(idx,ip) = channel.PathGains(:,ip,5,1);
        link52(idx,ip) = channel.PathGains(:,ip,5,2);

        link61(idx,ip) = channel.PathGains(:,ip,6,1);
        link62(idx,ip) = channel.PathGains(:,ip,6,2);

        link71(idx,ip) = channel.PathGains(:,ip,7,1);
        link72(idx,ip) = channel.PathGains(:,ip,7,2);

        link81(idx,ip) = channel.PathGains(:,ip,8,1);
        link82(idx,ip) = channel.PathGains(:,ip,8,2);
    end
end

% Plot the fading envelopes using semilogy which is the same as
%PLOT(...), except a logarithmic (base 10) scale is used for the Y-
axis

figure;
semilogy(abs(link11(:,1)),'r');
hold on; grid on;
semilogy(abs(link11(:,2)),'g');
hold on;
semilogy(abs(link11(:,3)),'w');
hold on;
semilogy(abs(link11(:,4)),'b');
hold on;
semilogy(abs(link11(:,5)),'m');
legend('Path 1','Path 2','Path 3','Path 4','Path 5');
title('Fading envelopes for all paths through link Tx1-Rx1 ');
xlabel('Number of samples');
ylabel('Path gain');

figure;
semilogy(abs(link12(:,1)),'r');
hold on; grid on;
semilogy(abs(link12(:,2)),'g');
hold on;
semilogy(abs(link12(:,3)),'w');
hold on;
semilogy(abs(link12(:,4)),'b');
hold on;
semilogy(abs(link12(:,5)),'m');
legend('Path 1','Path 2','Path 3','Path 4','Path 5');
title('Fading envelopes for all paths through link Tx1-Rx2 ');
xlabel('Number of samples');
ylabel('Path gain');

figure;
semilogy(abs(link21(:,1)),'r');
hold on; grid on;
semilogy(abs(link21(:,2)),'g');
```

```
hold on;
semilogy(abs(link21(:,3)),'w');
hold on;
semilogy(abs(link21(:,4)),'b');
hold on;
semilogy(abs(link21(:,5)),'m');
legend('Path 1','Path 2','Path 3','Path 4','Path 5');
title('Fading envelopes for all paths through link Tx2-Rx1 ');
xlabel('Number of samples');
ylabel('Path gain');

figure;
semilogy(abs(link22(:,1)),'r');
hold on; grid on;
semilogy(abs(link22(:,2)),'g');
hold on;
semilogy(abs(link22(:,3)),'w');
hold on;
semilogy(abs(link22(:,4)),'b');
hold on;
semilogy(abs(link22(:,5)),'m');
legend('Path 1','Path 2','Path 3','Path 4','Path 5');
title('Fading envelopes for all paths through link Tx2-Rx2 ');
xlabel('Number of samples');
ylabel('Path gain');

figure;
semilogy(abs(link31(:,1)),'r');
hold on; grid on;
semilogy(abs(link31(:,2)),'g');
hold on;
semilogy(abs(link31(:,3)),'w');
hold on;
semilogy(abs(link31(:,4)),'b');
hold on;
semilogy(abs(link31(:,5)),'m');
legend('Path 1','Path 2','Path 3','Path 4','Path 5');
title('Fading envelopes for all paths through link Tx3-Rx1 ');
xlabel('Number of samples');
ylabel('Path gain');

figure;
semilogy(abs(link32(:,1)),'r');
hold on; grid on;
semilogy(abs(link32(:,2)),'g');
hold on;
semilogy(abs(link32(:,3)),'w');
hold on;
semilogy(abs(link32(:,4)),'b');
hold on;
semilogy(abs(link32(:,5)),'m');
legend('Path 1','Path 2','Path 3','Path 4','Path 5');
title('Fading envelopes for all paths through link Tx3-Rx2 ');
xlabel('Number of samples');
ylabel('Path gain');

figure;
semilogy(abs(link41(:,1)),'r');
hold on; grid on;
semilogy(abs(link41(:,2)),'g');
```

```
hold on;
semilogy(abs(link41(:,3)),'w');
hold on;
semilogy(abs(link41(:,4)),'b');
hold on;
semilogy(abs(link41(:,5)),'m');
legend('Path 1','Path 2','Path 3','Path 4','Path 5');
title('Fading envelopes for all paths through link Tx4-Rx1 ');
xlabel('Number of samples');
ylabel('Path gain');

figure;
semilogy(abs(link42(:,1)),'r');
hold on; grid on;
semilogy(abs(link42(:,2)),'g');
hold on;
semilogy(abs(link42(:,3)),'w');
hold on;
semilogy(abs(link42(:,4)),'b');
hold on;
semilogy(abs(link42(:,5)),'m');
legend('Path 1','Path 2','Path 3','Path 4','Path 5');
title('Fading envelopes for all paths through link Tx4-Rx2 ');
xlabel('Number of samples');
ylabel('Path gain');

figure;
semilogy(abs(link51(:,1)),'r');
hold on; grid on;
semilogy(abs(link51(:,2)),'g');
hold on;
semilogy(abs(link51(:,3)),'w');
hold on;
semilogy(abs(link51(:,4)),'b');
hold on;
semilogy(abs(link51(:,5)),'m');
legend('Path 1','Path 2','Path 3','Path 4','Path 5');
title('Fading envelopes for all paths through link Tx5-Rx1 ');
xlabel('Number of samples');
ylabel('Path gain');

figure;
semilogy(abs(link52(:,1)),'r');
hold on; grid on;
semilogy(abs(link52(:,2)),'g');
hold on;
semilogy(abs(link52(:,3)),'w');
hold on;
semilogy(abs(link52(:,4)),'b');
hold on;
semilogy(abs(link52(:,5)),'m');
legend('Path 1','Path 2','Path 3','Path 4','Path 5');
title('Fading envelopes for all paths through link Tx5-Rx2 ');
xlabel('Number of samples');
ylabel('Path gain');

figure;
semilogy(abs(link61(:,1)),'r');
hold on; grid on;
semilogy(abs(link61(:,2)),'g');
```

```
hold on;
semilogy(abs(link61(:,3)),'w');
hold on;
semilogy(abs(link61(:,4)),'b');
hold on;
semilogy(abs(link61(:,5)),'m');
legend('Path 1','Path 2','Path 3','Path 4','Path 5');
title('Fading envelopes for all paths through link Tx6-Rx1 ');
xlabel('Number of samples');
ylabel('Path gain');

figure;
semilogy(abs(link62(:,1)),'r');
hold on; grid on;
semilogy(abs(link62(:,2)),'g');
hold on;
semilogy(abs(link62(:,3)),'w');
hold on;
semilogy(abs(link62(:,4)),'b');
hold on;
semilogy(abs(link62(:,5)),'m');
legend('Path 1','Path 2','Path 3','Path 4','Path 5');
title('Fading envelopes for all paths through link Tx6-Rx2 ');
xlabel('Number of samples');
ylabel('Path gain');

figure;
semilogy(abs(link71(:,1)),'r');
hold on; grid on;
semilogy(abs(link71(:,2)),'g');
hold on;
semilogy(abs(link71(:,3)),'w');
hold on;
semilogy(abs(link71(:,4)),'b');
hold on;
semilogy(abs(link71(:,5)),'m');
legend('Path 1','Path 2','Path 3','Path 4','Path 5');
title('Fading envelopes for all paths through link Tx7-Rx1 ');
xlabel('Number of samples');
ylabel('Path gain');

figure;
semilogy(abs(link72(:,1)),'r');
hold on; grid on;
semilogy(abs(link72(:,2)),'g');
hold on;
semilogy(abs(link72(:,3)),'w');
hold on;
semilogy(abs(link72(:,4)),'b');
hold on;
semilogy(abs(link72(:,5)),'m');
legend('Path 1','Path 2','Path 3','Path 4','Path 5');
title('Fading envelopes for all paths through link Tx7-Rx2 ');
xlabel('Number of samples');
ylabel('Path gain');

figure;
semilogy(abs(link81(:,1)),'r');
hold on; grid on;
semilogy(abs(link81(:,2)),'g');
```

```
hold on;
semilogy(abs(link81(:,3)),'w');
hold on;
semilogy(abs(link81(:,4)),'b');
hold on;
semilogy(abs(link81(:,5)),'m');
legend('Path 1','Path 2','Path 3','Path 4','Path 5');
title('Fading envelopes for all paths through link Tx8-Rx1 ');
xlabel('Number of samples');
ylabel('Path gain');

figure;
semilogy(abs(link82(:,1)),'r');
hold on; grid on;
semilogy(abs(link82(:,2)),'g');
hold on;
semilogy(abs(link82(:,3)),'w');
hold on;
semilogy(abs(link82(:,4)),'b');
hold on;
semilogy(abs(link82(:,5)),'m');
legend('Path 1','Path 2','Path 3','Path 4','Path 5');
title('Fading envelopes for all paths through link Tx8-Rx2 ');
xlabel('Number of samples');
ylabel('Path gain');

% Obtain transmit correlation matrices for the five paths
transmit_corr_mat_path1=TxCorrelationMatrix1(:,:,1)
transmit_corr_mat_path2=TxCorrelationMatrix1(:,:,2)
transmit_corr_mat_path3=TxCorrelationMatrix1(:,:,3)
transmit_corr_mat_path4=TxCorrelationMatrix1(:,:,4)
transmit_corr_mat_path5=TxCorrelationMatrix1(:,:,5)

% Obtain receive correlation matrices for the five paths
receive_corr_mat_path1=RxCorrelationMatrix1(:,:,1)
receive_corr_mat_path2=RxCorrelationMatrix1(:,:,2)
receive_corr_mat_path3=RxCorrelationMatrix1(:,:,3)
receive_corr_mat_path4=RxCorrelationMatrix1(:,:,4)
receive_corr_mat_path5=RxCorrelationMatrix1(:,:,5)

MIMO_channel=channel          % Obtain MIMO channel properties
Doppler_shift=fd              % Obtain the Doppler shift
Path_gain_cluster_1=pdb1      % Obtain the path gains for cluster 1
Path_gain_cluster_2=pdb2      % Obtain the path gains for cluster 2
Path_gain_cluster_3=pdb2      % Obtain the path gains for cluster 3
```

A5) Transmit and receive correlation matrices function:

```
function [TxCorrelationMatrix1, RxCorrelationMatrix1] =...
calculateCorrMatrixx(Nt, Nr, pdb1, pdb2,pdb3, TxSpacing,
RxSpacing,...
Angular_spread_Cluster1_Tx, Angular_spread_Cluster2_Tx,...
Angular_spread_Cluster3_Tx,...
Angular_spread_Cluster1_Rx,Angular_spread_Cluster2_Rx,...
Angular_spread_Cluster3_Rx,...
AoD_Cluster1, AoD_Cluster2,AoD_Cluster3,...
AoA_Cluster1, AoA_Cluster2,AoA_Cluster3)

Np = length(pdb1);  % Number of paths

% Concatenated clusters for each path
Angular_spread_Tx = [Angular_spread_Cluster1_Tx;...
    Angular_spread_Cluster2_Tx;Angular_spread_Cluster3_Tx];
AoD = [AoD_Cluster1; AoD_Cluster2;AoD_Cluster3];
Angular_spread_Rx = [Angular_spread_Cluster1_Rx;...
    Angular_spread_Cluster2_Rx;Angular_spread_Cluster3_Rx];
AoA = [AoA_Cluster1; AoA_Cluster2;AoA_Cluster3];

% Maximum number of Tx clusters across all paths
MaxNcTx = size(Angular_spread_Tx, 1);
% Maximum number of Rx clusters across all paths
MaxNcRx = size(Angular_spread_Rx, 1);

% Non-null clusters for each path
validClustersTx = ~isinf(Angular_spread_Tx);
validClustersRx = ~isinf(Angular_spread_Rx);

% Actual number of Tx clusters for each path
NcTx = sum(validClustersTx, 1);
% Actual number of Rx clusters for each path
NcRx = sum(validClustersRx, 1);

% Initialize Tx and Rx correlation matrices
TxCorrelationMatrix1 = zeros(Nt, Nt, Np);
RxCorrelationMatrix1 = zeros(Nr, Nr, Np);

% Loop over number of paths
for ip = 1:Np

    % Calculation of Tx correlation matrices
    Rt_XX = zeros(1, Nt);
    Rt_XY = zeros(1, Nt);

    phi0Tx = AoD(:,ip) * pi/180;
    sigmaTx = Angular_spread_Tx(:, ip) * pi/180;
    delta_theta = 180 * pi/180;

    % Calculation of approximate normalization coefficient(s)
    QTx = calculateQ(NcTx(ip), pdb1(ip), pdb2(ip),pdb3(ip),...
        sigmaTx, delta_theta);

    for ic = 1:MaxNcTx
        if validClustersTx(ic, ip) == 1  % Check if valid cluster
```

```
            if NcTx(ip) == 1
                iq = 1;
            else
                iq = ic;
            end
            Rt_XX = Rt_XX + QTx(iq) * calculateR_XX(Nt, TxSpacing, ...
                                    sigmaTx(ic), phi0Tx(ic), delta_theta);
            Rt_XY = Rt_XY + QTx(iq) * calculateR_XY(Nt, TxSpacing, ...
                                    sigmaTx(ic), phi0Tx(ic), delta_theta);
            end
        end
        TxCorrelationMatrix1(:,:,ip) = toeplitz(Rt_XX + sqrt(-1)* Rt_XY);
        for it = 1:Nt
            % Ensures diagonal elements are exactly 1
            TxCorrelationMatrix1(it,it,ip) = 1;

        end

        % Calculation of Rx correlation matrices
        Rr_XX = zeros(1, Nr);
        Rr_XY = zeros(1, Nr);

        phi0Rx = AoA(:, ip) * pi/180;
        sigmaRx = Angular_spread_Rx(:, ip) * pi/180;

        % Calculation of approximate normalization coefficient(s)
        QRx = calculateQ(NcRx(ip), pdb1(ip), pdb2(ip),pdb3(ip),...
            sigmaRx, delta_theta);

        for ic = 1:MaxNcRx
            if validClustersRx(ic, ip) == 1  % Check if valid cluster
                if NcRx(ip) == 1
                    iq = 1;
                else
                    iq = ic;
                end
                Rr_XX = Rr_XX + QRx(iq) * calculateR_XX(Nr,...
                                          RxSpacing, sigmaRx(ic),...
                                          phi0Rx(ic), delta_theta);
                Rr_XY = Rr_XY + QRx(iq) * calculateR_XY(Nr,...
                                          RxSpacing, sigmaRx(ic),...
                                          phi0Rx(ic),delta_theta);

            end
        end
        RxCorrelationMatrix1(:,:,ip) = toeplitz(Rr_XX + sqrt(-1)* Rr_XY);
        for ir = 1:Nr
            % Ensures diagonal elements are exactly 1
            RxCorrelationMatrix1(ir,ir,ip) = 1;

        end
    end

    function Q = calculateQ(Nc, pdb1, pdb2, pdb3, sigma, delta_theta)

    if Nc == 1
        Q = 1/(1-exp(-sqrt(2)*delta_theta/sigma(sigma>-Inf)));
    elseif Nc == 2
        Q = zeros(1, 2);
```

```
    Q(1) = 1/( 1-exp(-sqrt(2)*delta_theta/sigma(1)) ...
        + (sigma(2)*10^(pdb2/10))/(sigma(1)*10^(pdb1/10)) ...
        * (1-exp(-sqrt(2)*delta_theta/sigma(2)))) ;
    Q(2) = Q(1) * (sigma(2)*10^(pdb2/10)/(sigma(1)*10^(pdb1/10)));
  elseif Nc == 3
     Q = zeros(1, 3);
    Q(1) = 1/( 1-exp(-sqrt(2)*delta_theta/sigma(1)) ...
           + (sigma(2)*10^(pdb2/10))/(sigma(1)*10^(pdb1/10)) ...
           * (1-exp(-sqrt(2)*delta_theta/sigma(2)))) ;
    Q(2) = Q(1) * (sigma(2)*10^(pdb2/10)/(sigma(1)*10^(pdb1/10)));

    Q(3) = Q(2) * (sigma(3)*10^(pdb3/10)/sigma(2)...
           *10^(pdb2/10)/(sigma(1)*10^(pdb1/10)));
end

function R_XX = calculateR_XX(N, spacing, sigma, phi0, delta_theta)

R_XX = zeros(1, N);
R_XX(1,1) = 1;

for n = 2:N
    D = (n-1) * 2*pi* spacing;
    R_XX(1, n) = besselj(0,D);
    mInf = 100;
    sum_m = 0;
    for m = 1:mInf
        sum_m = sum_m + besselj(2*m,D)* 1/((sqrt(2)/sigma)^2+...
            (2*m)^2) *cos(2*m*phi0).* ( sqrt(2)/sigma + ...
            exp(-sqrt(2)/sigma*delta_theta) ...
            * (-sqrt(2)/sigma*cos(2*m*delta_theta) +...
            2*m*sin(2*m*delta_theta) ) );
    end
    R_XX(1, n) = R_XX(1, n) + sum_m * 4/(sqrt(2)*sigma);
end

function R_XY = calculateR_XY(N, spacing, sigma, phi0, delta_theta)

R_XY = zeros(1, N);
R_XY(1,1) = 0;

for n = 2:N
    D = (n-1) * 2*pi* spacing;
    R_XY(1, n) = 0;
    mInf = 100;
    sum_m = 0;
    for m = 0:mInf
        sum_m = sum_m + besselj(2*m+1,D)* 1/((sqrt(2)/sigma)^2+...
            (2*m+1)^2)* sin((2*m+1)*phi0) .* ( sqrt(2)/sigma + ...
            exp(-sqrt(2)/sigma*delta_theta) ...
            * (-sqrt(2)/sigma*cos((2*m+1)*delta_theta) +...
            (2*m+1)*sin((2*m+1)*delta_theta) ) );
    end
    R_XY(1, n) = R_XY(1, n) + sum_m * 4/(sqrt(2)*sigma);
end
```

A6) Effect of frequency on path loss for 8x8 system code:

```
clear all
close all
clc
%*****************************************************************
%The path-loss equations used in this simulation are defined
% in details in D1.1.1 V1.1 ''WINNER II interim channel models''.
%*****************************************************************

%frequencies of operation in GHz.
F=[0.45 0.7 0.8 0.85 0.9 1.8 1.9 2.1 2.3 2.6 3.6 5.8];
%the speed of light.
c=3*10^8;
%defined base station height for bad urban and rural macro-cells
hBS=32;
% mobile station height for bad urban and rural macro-cells
hMS=2;
% a randomness factor to differentiate the multipath components.
randomnessfactor1=300*rand(1,8);
%defined propagation distance for rural and bad urban environments.
d1=linspace(50,5000,8);

%Bad urban micro-cell & Rural:
for i=1:12
    for j=1:8

        %line of sight (LOS) path-loss equation for bad urban
        %macro-cell.
        PL_LOS_urban(j,i)=-1*[40*log10(d1(j))+13.47-14*...
            log10(hBS)-14*log10(hMS)+6*log10(F(i)/5)+6];
        %line of sight (LOS) path-loss equation for Rural macro-cell.
        PL_LOS_rural(j,i)=-1*[10.5+40*log10(d1(j))-18.5*...
            log10(hBS)-18.5*log10(hMS)+1.5*log10(F(i)/5)+4];

     for k=1:8

        %Non-line of sight (NLOS) path-loss equation for bad urban
        %macro-cell.
        PL_NLOS_urban(j,k,i)=-1*[(44.9-6.55*log10(hBS))*...
            log10(d1(j)+(randomnessfactor1(k)))+34.46+5.83*...
            log10(hMS)+20*log10(F(i)/5)+8];
        %free space loss.
        PLfree(j,k,i)=46.4+20*log10(d1(j)+...
            (randomnessfactor1(k)))+20*log10(F(i)/5);
        ru_NLOS(j,k,i)=(55.4+25.1*log10(d1(j)+...
            (randomnessfactor1(k)))-0.13*log10(hBS-25)*...
            log((d1(j)+(randomnessfactor1(k))))/100)-0.9*...
            (hMS-1.5)+21.3*log10(F(i)/5);
        %Non-line of sight (NLOS) path-loss equation for rural
        %macro-cell.
        PL_NLOS_rural(j,k,i)=-1*max(PLfree(j,k,i),ru_NLOS(j,k,i))+8;

     end
    end
end
```

```
%*************************************************************
% Indoor small office:%hBS=1.5;hMS=hBS.
 d2=linspace(3,100,8);randomnessfactor2=20*rand(1,8);
for i=1:12
    for j=1:8
        %line of sight (LOS) path-loss equation for Indoor small
        %office(Room-Corridor).
        PL_LOS_inoff(j,i)=-18.7*log10(d2(j))-46.8-20*log10(F(i)/5)-3;

for k=1:8
        %Non-line of sight (NLOS) path-loss equation for Indoor
        % small office(Room-Corridor).
        PL_NLOS_inoff(j,k,i)= -36.8*log10(d2(j)+...
            randomnessfactor2(k))-43.8-20*log10(F(i)/5)-4;
 end
    end
end


%*************************************************************
%Fixed Stationary Feeder, Moving Network:
randomnessfactor3=100*rand(1,8);%hMS=hBS=25
% defined distance for Fixed Stationary Feeder and Moving networks
% respectively.
d3=linspace(30,1500,8); d4=linspace(30,2000,8);
for i=1:12
    for j=1:8

        %fress space loss
        PLfree(j,i)=46.4+20*log10(d3(j))+20*log10(F(i)/5);
        %Fixed Stationary Feeder: Roof-top to Roof-top path-
loss(LOS).
        PL_LOS_FSF(j,i)= -1*max(PLfree(j,i),(23.5*log10(d3(j)+...
            42.5+20*log10(F(i)/5))))+4;
        %Moving networks; hBS=6;hMS=5.
        PL_LOS_MoNe(j,i)= -1*max(PLfree(j,i),(41.1*log10(d4(j)+...
            17.2+20*log10(F(i)/5))))+3;
for k=1:8

    %Fixed Stationary Feeder: Roof-top to Roof-top path-loss(NLOS).
        PL_NLOS_FSF(j,k,i)=-23.5*log10(d3(j)+...
            randomnessfactor3(k))-57.5-20*log10(F(i)/5)-8;
 end
    end
end


%*************************************************************
%Suburban macro-cell:
d5=linspace(30,1500,8);randomnessfactor4=150*rand(1,8);
hBS=25;hMS=1.5;
for i=1:12
    for j=1:8
        % Suburban macro-cell (LOS) path-loss.
        PL_LOS_Suburban(j,i)=-23.8*log10(d5(j))-41.2-20*...
            log10(F(i)/5)-4;
for k=1:8
        % Suburban macro-cell (NLOS) path-loss.
        PL_NLOS_Suburban(j,k,i)=-1*[(44.9-6.55*log10(hBS))*...
            log10(d5(j)+(randomnessfactor4(k)))+31.46+...
```

```
            5.83*log10(hMS)+20*log10(F(i)/5)+8];
 end
    end
end


%*****************************************************************
%Indoor to outdoor, Outdoor environment is urban:
randomnessfactor5=20*rand(1,8);d6=linspace(10,1000,9);
Dist_in=3;%indoor distance
SW=10;%street width

 for j=1:9
 Dist_out(j)=d6(j)-Dist_in;
 %angle from the BS to the normal of the wall
 Theta(j)= acos(SW/2/Dist_out(j))*180/pi;
 end

    for i=1:12
   for j=1:9
  for k=1:8

 LossIn = 0.5*Dist_in;%indoor loss
 LossWall = 14+15*(1-cos(Theta(j))).^2; %Through wall loss
 %free space loss.
 PLfree(j,k,i)=46.4+20*log10(d6(j)+(randomnessfactor5(k)))+...
     20*log10(F(i)/5);
 % Total loss including Outdoor loss
 LosstTot(j,k,i) = -1*[max((41 + 20*log10(F(i)/5) +...
     22.7*log10(d6(j))+randomnessfactor5(k)), PLfree(j,k,i))+...
     LossIn+LossWall];

  end
   end
    end


%*****************************************************************
%plotting the simulation results for bad urban macero-cell:
figure(1) %LOS
hold on; grid on;
plot (d1,PL_LOS_urban(:,1),'r');plot (d1,PL_LOS_urban(:,2),'b');
plot (d1,PL_LOS_urban(:,3),'k');plot (d1,PL_LOS_urban(:,4),'m');
plot (d1,PL_LOS_urban(:,5),'g');plot (d1,PL_LOS_urban(:,6),'c');
plot (d1,PL_LOS_urban(:,7),'b');plot (d1,PL_LOS_urban(:,8),'r');
plot (d1,PL_LOS_urban(:,9),'k');plot (d1,PL_LOS_urban(:,10),'m');
plot (d1,PL_LOS_urban(:,11),'g');plot (d1,PL_LOS_urban(:,12),'y');
legend('450MHz','700MHz','800MHz','850MHz','900MHz','1800MHz',...
       '1900MHz','2.1GHz','2.3GHz','2.6GHz','3.6GHz','5.8GHz');
title('Path loss versus the propagation distance for diffirent
operating frequencies [Path1(Urban:LOS)]');
xlabel('distance in meter');ylabel('path loss in dB');

figure(2)%NLOS
hold on; grid on;
plot (d1,PL_NLOS_urban(:,2,1),'r');plot(d1,PL_NLOS_urban(:,2,2),'b');
plot (d1,PL_NLOS_urban(:,2,3),'k');plot(d1,PL_NLOS_urban(:,2,4),'m');
plot (d1,PL_NLOS_urban(:,2,5),'g');plot(d1,PL_NLOS_urban(:,2,6),'c');
plot (d1,PL_NLOS_urban(:,2,7),'b');plot(d1,PL_NLOS_urban(:,2,8),'r');
```

```
plot(d1,PL_NLOS_urban(:,2,9),'k');plot(d1,PL_NLOS_urban(:,2,10),'m');
plot(d1,PL_NLOS_urban(:,2,11),'g');
plot(d1,PL_NLOS_urban(:,2,12),'y');
legend('450MHz','700MHz','800MHz','850MHz','900MHz','1800MHz',...
       '1900MHz','2.1GHz','2.3GHz','2.6GHz','3.6GHz','5.8GHz');
title('Path loss versus the propagation distance for diffirent
operating frequencies [Path2(Urban:NLOS)]');
xlabel('distance in meter');ylabel('path loss in dB');

figure(3)%NLOS
hold on; grid on;
plot (d1,PL_NLOS_urban(:,3,1),'r');plot(d1,PL_NLOS_urban(:,3,2),'b');
plot (d1,PL_NLOS_urban(:,3,3),'k');plot(d1,PL_NLOS_urban(:,3,4),'m');
plot (d1,PL_NLOS_urban(:,3,5),'g');plot(d1,PL_NLOS_urban(:,3,6),'c');
plot (d1,PL_NLOS_urban(:,3,7),'b');plot(d1,PL_NLOS_urban(:,3,8),'r');
plot(d1,PL_NLOS_urban(:,3,9),'k');plot(d1,PL_NLOS_urban(:,3,10),'m');
plot(d1,PL_NLOS_urban(:,3,11),'g');
plot(d1,PL_NLOS_urban(:,3,12),'y');
legend('450MHz','700MHz','800MHz','850MHz','900MHz','1800MHz',...
       '1900MHz','2.1GHz','2.3GHz','2.6GHz','3.6GHz','5.8GHz');
title('Path loss versus the propagation distance for diffirent
operating frequencies [Path3(Urban:NLOS)]');
xlabel('distance in meter');ylabel('path loss in dB');

figure(4)%NLOS
hold on; grid on;
plot (d1,PL_NLOS_urban(:,4,1),'r');plot(d1,PL_NLOS_urban(:,4,2),'b');
plot (d1,PL_NLOS_urban(:,4,3),'k');plot(d1,PL_NLOS_urban(:,4,4),'m');
plot (d1,PL_NLOS_urban(:,4,5),'g');plot(d1,PL_NLOS_urban(:,4,6),'c');
plot (d1,PL_NLOS_urban(:,4,7),'b');plot(d1,PL_NLOS_urban(:,4,8),'r');
plot(d1,PL_NLOS_urban(:,4,9),'k');plot(d1,PL_NLOS_urban(:,4,10),'m');
plot (d1,PL_NLOS_urban(:,4,11),'g');
plot (d1,PL_NLOS_urban(:,4,12),'y');
legend('450MHz','700MHz','800MHz','850MHz','900MHz','1800MHz',...
       '1900MHz','2.1GHz','2.3GHz','2.6GHz','3.6GHz','5.8GHz');
title('Path loss versus the propagation distance for diffirent
operating frequencies [Path4(Urban:NLOS)]');
xlabel('distance in meter');ylabel('path loss in dB');

figure(5)%NLOS
hold on; grid on;
plot (d1,PL_NLOS_urban(:,5,1),'r');plot(d1,PL_NLOS_urban(:,5,2),'b');
plot (d1,PL_NLOS_urban(:,5,3),'k');plot(d1,PL_NLOS_urban(:,5,4),'m');
plot (d1,PL_NLOS_urban(:,5,5),'g');plot(d1,PL_NLOS_urban(:,5,6),'c');
plot (d1,PL_NLOS_urban(:,5,7),'b');plot(d1,PL_NLOS_urban(:,5,8),'r');
plot(d1,PL_NLOS_urban(:,5,9),'k');plot(d1,PL_NLOS_urban(:,5,10),'m');
plot (d1,PL_NLOS_urban(:,5,11),'g');
plot (d1,PL_NLOS_urban(:,5,12),'y');
legend('450MHz','700MHz','800MHz','850MHz','900MHz','1800MHz',...
       '1900MHz','2.1GHz','2.3GHz','2.6GHz','3.6GHz','5.8GHz');
title('Path loss versus the propagation distance for diffirent
operating frequencies [Path5(Urban:NLOS)]');
xlabel('distance in meter');ylabel('path loss in dB');

figure(6)%NLOS
hold on; grid on;
plot (d1,PL_NLOS_urban(:,6,1),'r');plot(d1,PL_NLOS_urban(:,6,2),'b');
plot (d1,PL_NLOS_urban(:,6,3),'k');plot(d1,PL_NLOS_urban(:,6,4),'m');
plot (d1,PL_NLOS_urban(:,6,5),'g');plot(d1,PL_NLOS_urban(:,6,6),'c');
plot (d1,PL_NLOS_urban(:,6,7),'b');plot(d1,PL_NLOS_urban(:,6,8),'r');
```

```
plot(d1,PL_NLOS_urban(:,6,9),'k');plot(d1,PL_NLOS_urban(:,6,10),'m');
plot (d1,PL_NLOS_urban(:,6,11),'g');
plot (d1,PL_NLOS_urban(:,6,12),'y');
legend('450MHz','700MHz','800MHz','850MHz','900MHz','1800MHz',...
       '1900MHz','2.1GHz','2.3GHz','2.6GHz','3.6GHz','5.8GHz');
title('Path loss versus the propagation distance for diffirent
operating frequencies [Path6(Urban:NLOS)]');
xlabel('distance in meter');ylabel('path loss in dB');

figure(7)%NLOS
hold on; grid on;
plot (d1,PL_NLOS_urban(:,7,1),'r');plot(d1,PL_NLOS_urban(:,7,2),'b');
plot (d1,PL_NLOS_urban(:,7,3),'k');plot(d1,PL_NLOS_urban(:,7,4),'m');
plot (d1,PL_NLOS_urban(:,7,5),'g');plot(d1,PL_NLOS_urban(:,7,6),'c');
plot (d1,PL_NLOS_urban(:,7,7),'b');plot(d1,PL_NLOS_urban(:,7,8),'r');
plot(d1,PL_NLOS_urban(:,7,9),'k');plot(d1,PL_NLOS_urban(:,7,10),'m');
plot (d1,PL_NLOS_urban(:,7,11),'g');
plot (d1,PL_NLOS_urban(:,7,12),'y');
legend('450MHz','700MHz','800MHz','850MHz','900MHz','1800MHz',...
       '1900MHz','2.1GHz','2.3GHz','2.6GHz','3.6GHz','5.8GHz');
title('Path loss versus the propagation distance for diffirent
operating frequencies [Path7(Urban:NLOS)]');
xlabel('distance in meter');ylabel('path loss in dB');

figure(8)%NLOS
hold on; grid on;
plot (d1,PL_NLOS_urban(:,8,1),'r');plot(d1,PL_NLOS_urban(:,8,2),'b');
plot (d1,PL_NLOS_urban(:,8,3),'k');plot(d1,PL_NLOS_urban(:,8,4),'m');
plot (d1,PL_NLOS_urban(:,8,5),'g');plot(d1,PL_NLOS_urban(:,8,6),'c');
plot (d1,PL_NLOS_urban(:,8,7),'b');plot(d1,PL_NLOS_urban(:,8,8),'r');
plot(d1,PL_NLOS_urban(:,8,9),'k');plot(d1,PL_NLOS_urban(:,8,10),'m');
plot (d1,PL_NLOS_urban(:,8,11),'g');
plot (d1,PL_NLOS_urban(:,8,12),'y');
legend('450MHz','700MHz','800MHz','850MHz','900MHz','1800MHz',...
       '1900MHz','2.1GHz','2.3GHz','2.6GHz','3.6GHz','5.8GHz');
title('Path loss versus the propagation distance for diffirent
operating frequencies [Path8(UIrban:NLOS)]');
xlabel('distance in meter');ylabel('path loss in dB');


%************************************************************
%plotting the simulation results for rural macero-cell:
figure(9)
hold on; grid on;%LOS
plot (d1,PL_LOS_rural(:,1),'r');plot (d1,PL_LOS_rural(:,2),'b');
plot (d1,PL_LOS_rural(:,3),'k');plot (d1,PL_LOS_rural(:,4),'m');
plot (d1,PL_LOS_rural(:,5),'g');plot (d1,PL_LOS_rural(:,6),'c');
plot (d1,PL_LOS_rural(:,7),'b');plot (d1,PL_LOS_rural(:,8),'r');
plot (d1,PL_LOS_rural(:,9),'k');plot (d1,PL_LOS_rural(:,10),'m');
plot (d1,PL_LOS_rural(:,11),'g');plot (d1,PL_LOS_rural(:,12),'y');
legend('450MHz','700MHz','800MHz','850MHz','900MHz','1800MHz',...
'1900MHz','2.1GHz','2.3GHz','2.6GHz','3.6GHz','5.8GHz');
title('Path loss versus the propagation distance for diffirent
operating frequencies [Path1(Rural:LOS)]');
xlabel('distance in meter');ylabel('path loss in dB');

figure(10)%NLOS
hold on; grid on;
plot (d1,PL_NLOS_rural(:,2,1),'r');plot(d1,PL_NLOS_rural(:,2,2),'b');
plot (d1,PL_NLOS_rural(:,2,3),'k');plot(d1,PL_NLOS_rural(:,2,4),'m');
```

```
plot (d1,PL_NLOS_rural(:,2,5),'g');plot(d1,PL_NLOS_rural(:,2,6),'c');
plot (d1,PL_NLOS_rural(:,2,7),'b');plot(d1,PL_NLOS_rural(:,2,8),'r');
plot(d1,PL_NLOS_rural(:,2,9),'k');plot(d1,PL_NLOS_rural(:,2,10),'m');
plot(d1,PL_NLOS_rural(:,2,11),'g');
plot(d1,PL_NLOS_rural(:,2,12),'y');
legend('450MHz','700MHz','800MHz','850MHz','900MHz','1800MHz',...
'1900MHz','2.1GHz','2.3GHz','2.6GHz','3.6GHz','5.8GHz');
title('Path loss versus the propagation distance for diffirent
operating frequencies [Path2(Rural:NLOS)]');
xlabel('distance in meter');ylabel('path loss in dB');

figure(11)%NLOS
hold on; grid on;
plot (d1,PL_NLOS_rural(:,3,1),'r');plot(d1,PL_NLOS_rural(:,3,2),'b');
plot (d1,PL_NLOS_rural(:,3,3),'k');plot(d1,PL_NLOS_rural(:,3,4),'m');
plot (d1,PL_NLOS_rural(:,3,5),'g');plot(d1,PL_NLOS_rural(:,3,6),'c');
plot (d1,PL_NLOS_rural(:,3,7),'b');plot(d1,PL_NLOS_rural(:,3,8),'r');
plot(d1,PL_NLOS_rural(:,3,9),'k');plot(d1,PL_NLOS_rural(:,3,10),'m');
plot (d1,PL_NLOS_rural(:,3,11),'g');
plot (d1,PL_NLOS_rural(:,3,12),'y');
legend('450MHz','700MHz','800MHz','850MHz','900MHz','1800MHz',...
'1900MHz','2.1GHz','2.3GHz','2.6GHz','3.6GHz','5.8GHz');
title('Path loss versus the propagation distance for diffirent
operating frequencies [Path3(Rural:NLOS)]');
xlabel('distance in meter');ylabel('path loss in dB');

figure(12)%NLOS
hold on; grid on;
plot (d1,PL_NLOS_rural(:,4,1),'r');plot(d1,PL_NLOS_rural(:,4,2),'b');
plot (d1,PL_NLOS_rural(:,4,3),'k');plot(d1,PL_NLOS_rural(:,4,4),'m');
plot (d1,PL_NLOS_rural(:,4,5),'g');plot(d1,PL_NLOS_rural(:,4,6),'c');
plot (d1,PL_NLOS_rural(:,4,7),'b');plot(d1,PL_NLOS_rural(:,4,8),'r');
plot(d1,PL_NLOS_rural(:,4,9),'k');plot(d1,PL_NLOS_rural(:,4,10),'m');
plot (d1,PL_NLOS_rural(:,4,11),'g');
plot (d1,PL_NLOS_rural(:,4,12),'y');
legend('450MHz','700MHz','800MHz','850MHz','900MHz','1800MHz',...
'1900MHz','2.1GHz','2.3GHz','2.6GHz','3.6GHz','5.8GHz');
title('Path loss versus the propagation distance for diffirent
operating frequencies [Path4(Rural:NLOS)]');
xlabel('distance in meter');ylabel('path loss in dB');

figure(13)%NLOS
hold on; grid on;
plot (d1,PL_NLOS_rural(:,5,1),'r');plot(d1,PL_NLOS_rural(:,5,2),'b');
plot (d1,PL_NLOS_rural(:,5,3),'k');plot(d1,PL_NLOS_rural(:,5,4),'m');
plot (d1,PL_NLOS_rural(:,5,5),'g');plot(d1,PL_NLOS_rural(:,5,6),'c');
plot (d1,PL_NLOS_rural(:,5,7),'b');plot(d1,PL_NLOS_rural(:,5,8),'r');
plot(d1,PL_NLOS_rural(:,5,9),'k');plot(d1,PL_NLOS_rural(:,5,10),'m');
plot (d1,PL_NLOS_rural(:,5,11),'g');
plot (d1,PL_NLOS_rural(:,5,12),'y');
legend('450MHz','700MHz','800MHz','850MHz','900MHz','1800MHz',...
'1900MHz','2.1GHz','2.3GHz','2.6GHz','3.6GHz','5.8GHz');
title('Path loss versus the propagation distance for diffirent
operating frequencies [Path5(Rural:NLOS)]');
xlabel('distance in meter');ylabel('path loss in dB')

figure(14)%NLOS
hold on; grid on;
plot (d1,PL_NLOS_rural(:,6,1),'r');plot(d1,PL_NLOS_rural(:,6,2),'b');
plot (d1,PL_NLOS_rural(:,6,3),'k');plot(d1,PL_NLOS_rural(:,6,4),'m');
```

```
plot (d1,PL_NLOS_rural(:,6,5),'g');plot(d1,PL_NLOS_rural(:,6,6),'c');
plot (d1,PL_NLOS_rural(:,6,7),'b');plot(d1,PL_NLOS_rural(:,6,8),'r');
plot(d1,PL_NLOS_rural(:,6,9),'k');plot(d1,PL_NLOS_rural(:,6,10),'m');
plot (d1,PL_NLOS_rural(:,6,11),'g');
plot (d1,PL_NLOS_rural(:,6,12),'y');
legend('450MHz','700MHz','800MHz','850MHz','900MHz','1800MHz',...
'1900MHz','2.1GHz','2.3GHz','2.6GHz','3.6GHz','5.8GHz');
title('Path loss versus the propagation distance for diffirent
operating frequencies [Path6(Rural:NLOS)]');
xlabel('distance in meter');ylabel('path loss in dB');

figure(15)%NLOS
hold on; grid on;
plot (d1,PL_NLOS_rural(:,7,1),'r');plot(d1,PL_NLOS_rural(:,7,2),'b');
plot (d1,PL_NLOS_rural(:,7,3),'k');plot(d1,PL_NLOS_rural(:,7,4),'m');
plot (d1,PL_NLOS_rural(:,7,5),'g');plot(d1,PL_NLOS_rural(:,7,6),'c');
plot (d1,PL_NLOS_rural(:,7,7),'b');plot(d1,PL_NLOS_rural(:,7,8),'r');
plot(d1,PL_NLOS_rural(:,7,9),'k');plot(d1,PL_NLOS_rural(:,7,10),'m');
plot (d1,PL_NLOS_rural(:,7,11),'g');
plot (d1,PL_NLOS_rural(:,7,12),'y');
legend('450MHz','700MHz','800MHz','850MHz','900MHz','1800MHz',...
'1900MHz','2.1GHz','2.3GHz','2.6GHz','3.6GHz','5.8GHz');
title('Path loss versus the propagation distance for diffirent
operating frequencies [Path7(Rural:NLOS)]');
xlabel('distance in meter');ylabel('path loss in dB');

figure(16)%NLOS
hold on; grid on;
plot (d1,PL_NLOS_rural(:,8,1),'r');plot(d1,PL_NLOS_rural(:,8,2),'b');
plot (d1,PL_NLOS_rural(:,8,3),'k');plot(d1,PL_NLOS_rural(:,8,4),'m');
plot (d1,PL_NLOS_rural(:,8,5),'g');plot(d1,PL_NLOS_rural(:,8,6),'c');
plot (d1,PL_NLOS_rural(:,8,7),'b');plot(d1,PL_NLOS_rural(:,8,8),'r');
plot(d1,PL_NLOS_rural(:,8,9),'k');plot(d1,PL_NLOS_rural(:,8,10),'m');
plot (d1,PL_NLOS_rural(:,8,11),'g');
plot (d1,PL_NLOS_rural(:,8,12),'y');
legend('450MHz','700MHz','800MHz','850MHz','900MHz','1800MHz',...
'1900MHz','2.1GHz','2.3GHz','2.6GHz','3.6GHz','5.8GHz');
title('Path loss versus the propagation distance for diffirent
operating frequencies [Path8(Rural:NLOS)]');
xlabel('distance in meter');ylabel('path loss in dB');


%*****************************************************************
%plotting the simulation results for Indoor small office:
figure(17)
hold on; grid on;%LOS
plot (d2,PL_LOS_inoff(:,1),'r');plot (d2,PL_LOS_inoff(:,2),'b');
plot (d2,PL_LOS_inoff(:,3),'k');plot (d2,PL_LOS_inoff(:,4),'m');
plot (d2,PL_LOS_inoff(:,5),'g');plot (d2,PL_LOS_inoff(:,6),'c');
plot (d2,PL_LOS_inoff(:,7),'b');plot (d2,PL_LOS_inoff(:,8),'r');
plot (d2,PL_LOS_inoff(:,9),'k');plot (d2,PL_LOS_inoff(:,10),'m');
plot (d2,PL_LOS_inoff(:,11),'g');plot (d2,PL_LOS_inoff(:,12),'y');
legend('450MHz','700MHz','800MHz','850MHz','900MHz','1800MHz',...
'1900MHz','2.1GHz','2.3GHz','2.6GHz','3.6GHz','5.8GHz');
title('Path loss versus the propagation distance for diffirent
operating frequencies [Path1(Indoor office:LOS)]');
xlabel('distance in meter');ylabel('path loss in dB');
```

```
figure(18)%NLOS
hold on; grid on;
plot (d2,PL_NLOS_inoff(:,2,1),'r');plot(d2,PL_NLOS_inoff(:,2,2),'b');
plot (d2,PL_NLOS_inoff(:,2,3),'k');plot(d2,PL_NLOS_inoff(:,2,4),'m');
plot (d2,PL_NLOS_inoff(:,2,5),'g');plot(d2,PL_NLOS_inoff(:,2,6),'c');
plot (d2,PL_NLOS_inoff(:,2,7),'b');plot(d2,PL_NLOS_inoff(:,2,8),'r');
plot(d2,PL_NLOS_inoff(:,2,9),'k');plot(d2,PL_NLOS_inoff(:,2,10),'m');
plot (d2,PL_NLOS_inoff(:,2,11),'g');
plot (d2,PL_NLOS_inoff(:,2,12),'y');
legend('450MHz','700MHz','800MHz','850MHz','900MHz','1800MHz',...
'1900MHz','2.1GHz','2.3GHz','2.6GHz','3.6GHz','5.8GHz');
title('Path loss versus the propagation distance for diffirent
operating frequencies [Path2(Indoor office:NLOS)]');
xlabel('distance in meter');ylabel('path loss in dB');

figure(19)%NLOS
hold on; grid on;
plot (d2,PL_NLOS_inoff(:,3,1),'r');plot(d2,PL_NLOS_inoff(:,3,2),'b');
plot (d2,PL_NLOS_inoff(:,3,3),'k');plot(d2,PL_NLOS_inoff(:,3,4),'m');
plot (d2,PL_NLOS_inoff(:,3,5),'g');plot(d2,PL_NLOS_inoff(:,3,6),'c');
plot (d2,PL_NLOS_inoff(:,3,7),'b');plot(d2,PL_NLOS_inoff(:,3,8),'r');
plot(d2,PL_NLOS_inoff(:,3,9),'k');plot(d2,PL_NLOS_inoff(:,3,10),'m');
plot (d2,PL_NLOS_inoff(:,3,11),'g');
plot (d2,PL_NLOS_inoff(:,3,12),'y');
legend('450MHz','700MHz','800MHz','850MHz','900MHz','1800MHz',...
'1900MHz','2.1GHz','2.3GHz','2.6GHz','3.6GHz','5.8GHz');
title('Path loss versus the propagation distance for diffirent
operating frequencies [Path3(Indoor office:NLOS)]');
xlabel('distance in meter');ylabel('path loss in dB');

figure(20)%NLOS
hold on; grid on;
plot (d2,PL_NLOS_inoff(:,4,1),'r');plot(d2,PL_NLOS_inoff(:,4,2),'b');
plot (d2,PL_NLOS_inoff(:,4,3),'k');plot(d2,PL_NLOS_inoff(:,4,4),'m');
plot (d2,PL_NLOS_inoff(:,4,5),'g');plot(d2,PL_NLOS_inoff(:,4,6),'c');
plot (d2,PL_NLOS_inoff(:,4,7),'b');plot(d2,PL_NLOS_inoff(:,4,8),'r');
plot(d2,PL_NLOS_inoff(:,4,9),'k');plot(d2,PL_NLOS_inoff(:,4,10),'m');
plot (d2,PL_NLOS_inoff(:,4,11),'g');
plot (d2,PL_NLOS_inoff(:,4,12),'y');
legend('450MHz','700MHz','800MHz','850MHz','900MHz','1800MHz',...
'1900MHz','2.1GHz','2.3GHz','2.6GHz','3.6GHz','5.8GHz');
title('Path loss versus the propagation distance for diffirent
operating frequencies [Path4(Indoor office:NLOS)]');
xlabel('distance in meter');ylabel('path loss in dB');

figure(21)%NLOS
hold on; grid on;
plot (d2,PL_NLOS_inoff(:,5,1),'r');plot(d2,PL_NLOS_inoff(:,5,2),'b');
plot (d2,PL_NLOS_inoff(:,5,3),'k');plot(d2,PL_NLOS_inoff(:,5,4),'m');
plot (d2,PL_NLOS_inoff(:,5,5),'g');plot(d2,PL_NLOS_inoff(:,5,6),'c');
plot (d2,PL_NLOS_inoff(:,5,7),'b');plot(d2,PL_NLOS_inoff(:,5,8),'r');
plot(d2,PL_NLOS_inoff(:,5,9),'k');plot(d2,PL_NLOS_inoff(:,5,10),'m');
plot (d2,PL_NLOS_inoff(:,5,11),'g');
plot (d2,PL_NLOS_inoff(:,5,12),'y');
legend('450MHz','700MHz','800MHz','850MHz','900MHz','1800MHz',...
'1900MHz','2.1GHz','2.3GHz','2.6GHz','3.6GHz','5.8GHz');
title('Path loss versus the propagation distance for diffirent
operating frequencies [Path5(Indoor office:NLOS)]');
xlabel('distance in meter');ylabel('path loss in dB')
```

```
figure(22)%NLOS
hold on; grid on;
plot (d2,PL_NLOS_inoff(:,6,1),'r');plot(d2,PL_NLOS_inoff(:,6,2),'b');
plot (d2,PL_NLOS_inoff(:,6,3),'k');plot(d2,PL_NLOS_inoff(:,6,4),'m');
plot (d2,PL_NLOS_inoff(:,6,5),'g');plot(d2,PL_NLOS_inoff(:,6,6),'c');
plot (d2,PL_NLOS_inoff(:,6,7),'b');plot(d2,PL_NLOS_inoff(:,6,8),'r');
plot(d2,PL_NLOS_inoff(:,6,9),'k');plot(d2,PL_NLOS_inoff(:,6,10),'m');
plot (d2,PL_NLOS_inoff(:,6,11),'g');
plot (d2,PL_NLOS_inoff(:,6,12),'y');
legend('450MHz','700MHz','800MHz','850MHz','900MHz','1800MHz',...
'1900MHz','2.1GHz','2.3GHz','2.6GHz','3.6GHz','5.8GHz');
title('Path loss versus the propagation distance for diffirent
operating frequencies [Path6(Indoor office:NLOS)]');
xlabel('distance in meter');ylabel('path loss in dB');

figure(23)%NLOS
hold on; grid on;
plot (d2,PL_NLOS_inoff(:,7,1),'r');plot(d2,PL_NLOS_inoff(:,7,2),'b');
plot (d2,PL_NLOS_inoff(:,7,3),'k');plot(d2,PL_NLOS_inoff(:,7,4),'m');
plot (d2,PL_NLOS_inoff(:,7,5),'g');plot(d2,PL_NLOS_inoff(:,7,6),'c');
plot (d2,PL_NLOS_inoff(:,7,7),'b');plot(d2,PL_NLOS_inoff(:,7,8),'r');
plot(d2,PL_NLOS_inoff(:,7,9),'k');plot(d2,PL_NLOS_inoff(:,7,10),'m');
plot (d2,PL_NLOS_inoff(:,7,11),'g');
plot (d2,PL_NLOS_inoff(:,7,12),'y');
legend('450MHz','700MHz','800MHz','850MHz','900MHz','1800MHz',...
'1900MHz','2.1GHz','2.3GHz','2.6GHz','3.6GHz','5.8GHz');
title('Path loss versus the propagation distance for diffirent
operating frequencies [Path7(Indoor office:NLOS)]');
xlabel('distance in meter');ylabel('path loss in dB');

figure(24)%NLOS
hold on; grid on;
plot (d2,PL_NLOS_inoff(:,8,1),'r');plot(d2,PL_NLOS_inoff(:,8,2),'b');
plot (d2,PL_NLOS_inoff(:,8,3),'k');plot(d2,PL_NLOS_inoff(:,8,4),'m');
plot (d2,PL_NLOS_inoff(:,8,5),'g');plot(d2,PL_NLOS_inoff(:,8,6),'c');
plot (d2,PL_NLOS_inoff(:,8,7),'b');plot(d2,PL_NLOS_inoff(:,8,8),'r');
plot(d2,PL_NLOS_inoff(:,8,9),'k');plot(d2,PL_NLOS_inoff(:,8,10),'m');
plot (d2,PL_NLOS_inoff(:,8,11),'g');
plot (d2,PL_NLOS_inoff(:,8,12),'y');
legend('450MHz','700MHz','800MHz','850MHz','900MHz','1800MHz',...
'1900MHz','2.1GHz','2.3GHz','2.6GHz','3.6GHz','5.8GHz');
title('Path loss versus the propagation distance for diffirent
operating frequencies [Path8(Indoor office:NLOS)]');
xlabel('distance in meter');ylabel('path loss in dB');


%*****************************************************************
%plotting the simulation results for Fixed Stationary Feeder: Roof-
%top to Roof-top:
figure(25)
hold on; grid on;%LOS
plot (d3,PL_LOS_FSF(:,1),'r');plot (d3,PL_LOS_FSF(:,2),'b');
plot (d3,PL_LOS_FSF(:,3),'k');plot (d3,PL_LOS_FSF(:,4),'m');
plot (d3,PL_LOS_FSF(:,5),'g');plot (d3,PL_LOS_FSF(:,6),'c');
plot (d3,PL_LOS_FSF(:,7),'b');plot (d3,PL_LOS_FSF(:,8),'r');
plot (d3,PL_LOS_FSF(:,9),'k');plot (d3,PL_LOS_FSF(:,10),'m');
plot (d3,PL_LOS_FSF(:,11),'g');plot (d3,PL_LOS_FSF(:,12),'y');
legend('450MHz','700MHz','800MHz','850MHz','900MHz','1800MHz',...
'1900MHz','2.1GHz','2.3GHz','2.6GHz','3.6GHz','5.8GHz');
```

```
title('Path loss versus the propagation distance for diffirent
operating frequencies[Path1(Fixed Stationary Feeder:Roof-top to Roof-
top:LOS)]');
xlabel('distance in meter');ylabel('path loss in dB');

figure(26)%NLOS
hold on; grid on;
plot (d3,PL_NLOS_FSF(:,2,1),'r');plot (d3,PL_NLOS_FSF(:,2,2),'b');
plot (d3,PL_NLOS_FSF(:,2,3),'k');plot (d3,PL_NLOS_FSF(:,2,4),'m');
plot (d3,PL_NLOS_FSF(:,2,5),'g');plot (d3,PL_NLOS_FSF(:,2,6),'c');
plot (d3,PL_NLOS_FSF(:,2,7),'b');plot (d3,PL_NLOS_FSF(:,2,8),'r');
plot (d3,PL_NLOS_FSF(:,2,9),'k');plot (d3,PL_NLOS_FSF(:,2,10),'m');
plot (d3,PL_NLOS_FSF(:,2,11),'g');plot (d3,PL_NLOS_FSF(:,2,12),'y');
legend('450MHz','700MHz','800MHz','850MHz','900MHz','1800MHz',...
'1900MHz','2.1GHz','2.3GHz','2.6GHz','3.6GHz','5.8GHz');
title('Path loss versus the propagation distance for diffirent
operating frequencies[Path2(Fixed Stationary Feeder:Roof-top to Roof-
top:NLOS)]');
xlabel('distance in meter');ylabel('path loss in dB');

figure(27)%NLOS
hold on; grid on;
plot (d3,PL_NLOS_FSF(:,3,1),'r');plot (d3,PL_NLOS_FSF(:,3,2),'b');
plot (d3,PL_NLOS_FSF(:,3,3),'k');plot (d3,PL_NLOS_FSF(:,3,4),'m');
plot (d3,PL_NLOS_FSF(:,3,5),'g');plot (d3,PL_NLOS_FSF(:,3,6),'c');
plot (d3,PL_NLOS_FSF(:,3,7),'b');plot (d3,PL_NLOS_FSF(:,3,8),'r');
plot (d3,PL_NLOS_FSF(:,3,9),'k');plot (d3,PL_NLOS_FSF(:,3,10),'m');
plot (d3,PL_NLOS_FSF(:,3,11),'g');plot (d3,PL_NLOS_FSF(:,3,12),'y');
legend('450MHz','700MHz','800MHz','850MHz','900MHz','1800MHz',...
'1900MHz','2.1GHz','2.3GHz','2.6GHz','3.6GHz','5.8GHz');
title('Path loss versus the propagation distance for diffirent
operating frequencies[Path3(Fixed Stationary Feeder:Roof-top to Roof-
top:NLOS)]');
xlabel('distance in meter');ylabel('path loss in dB');

figure(28)%NLOS
hold on; grid on;
plot (d3,PL_NLOS_FSF(:,4,1),'r');plot (d3,PL_NLOS_FSF(:,4,2),'b');
plot (d3,PL_NLOS_FSF(:,4,3),'k');plot (d3,PL_NLOS_FSF(:,4,4),'m');
plot (d3,PL_NLOS_FSF(:,4,5),'g');plot (d3,PL_NLOS_FSF(:,4,6),'c');
plot (d3,PL_NLOS_FSF(:,4,7),'b');plot (d3,PL_NLOS_FSF(:,4,8),'r');
plot (d3,PL_NLOS_FSF(:,4,9),'k');plot (d3,PL_NLOS_FSF(:,4,10),'m');
plot (d3,PL_NLOS_FSF(:,4,11),'g');plot (d3,PL_NLOS_FSF(:,4,12),'y');
legend('450MHz','700MHz','800MHz','850MHz','900MHz','1800MHz',...
'1900MHz','2.1GHz','2.3GHz','2.6GHz','3.6GHz','5.8GHz');
title('Path loss versus the propagation distance for diffirent
operating frequencies[Path4(Fixed Stationary Feeder:Roof-top to Roof-
top:NLOS)]');
xlabel('distance in meter');ylabel('path loss in dB');

figure(29)%NLOS
hold on; grid on;
plot (d3,PL_NLOS_FSF(:,5,1),'r');plot (d3,PL_NLOS_FSF(:,5,2),'b');
plot (d3,PL_NLOS_FSF(:,5,3),'k');plot (d3,PL_NLOS_FSF(:,5,4),'m');
plot (d3,PL_NLOS_FSF(:,5,5),'g');plot (d3,PL_NLOS_FSF(:,5,6),'c');
plot (d3,PL_NLOS_FSF(:,5,7),'b');plot (d3,PL_NLOS_FSF(:,5,8),'r');
plot (d3,PL_NLOS_FSF(:,5,9),'k');plot (d3,PL_NLOS_FSF(:,5,10),'m');
plot (d3,PL_NLOS_FSF(:,5,11),'g');plot (d3,PL_NLOS_FSF(:,5,12),'y');
legend('450MHz','700MHz','800MHz','850MHz','900MHz','1800MHz',...
'1900MHz','2.1GHz','2.3GHz','2.6GHz','3.6GHz','5.8GHz');
```

```
title('Path loss versus the propagation distance for diffirent
operating frequencies[Path5(Fixed Stationary Feeder:Roof-top to Roof-
top:NLOS)]');
xlabel('distance in meter');ylabel('path loss in dB')

figure(30)%NLOS
hold on; grid on;
plot (d3,PL_NLOS_FSF(:,6,1),'r');plot (d3,PL_NLOS_FSF(:,6,2),'b');
plot (d3,PL_NLOS_FSF(:,6,3),'k');plot (d3,PL_NLOS_FSF(:,6,4),'m');
plot (d3,PL_NLOS_FSF(:,6,5),'g');plot (d3,PL_NLOS_FSF(:,6,6),'c');
plot (d3,PL_NLOS_FSF(:,6,7),'b');plot (d3,PL_NLOS_FSF(:,6,8),'r');
plot (d3,PL_NLOS_FSF(:,6,9),'k');plot (d3,PL_NLOS_FSF(:,6,10),'m');
plot (d3,PL_NLOS_FSF(:,6,11),'g');plot (d3,PL_NLOS_FSF(:,6,12),'y');
legend('450MHz','700MHz','800MHz','850MHz','900MHz','1800MHz',...
'1900MHz','2.1GHz','2.3GHz','2.6GHz','3.6GHz','5.8GHz');
title('Path loss versus the propagation distance for diffirent
operating frequencies[Path6(Fixed Stationary Feeder:Roof-top to Roof-
top:NLOS)]');
xlabel('distance in meter');ylabel('path loss in dB');

figure(31)%NLOS
hold on; grid on;
plot (d3,PL_NLOS_FSF(:,7,1),'r');plot (d3,PL_NLOS_FSF(:,7,2),'b');
plot (d3,PL_NLOS_FSF(:,7,3),'k');plot (d3,PL_NLOS_FSF(:,7,4),'m');
plot (d3,PL_NLOS_FSF(:,7,5),'g');plot (d3,PL_NLOS_FSF(:,7,6),'c');
plot (d3,PL_NLOS_FSF(:,7,7),'b');plot (d3,PL_NLOS_FSF(:,7,8),'r');
plot (d3,PL_NLOS_FSF(:,7,9),'k');plot (d3,PL_NLOS_FSF(:,7,10),'m');
plot (d3,PL_NLOS_FSF(:,7,11),'g');plot (d3,PL_NLOS_FSF(:,7,12),'y');
legend('450MHz','700MHz','800MHz','850MHz','900MHz','1800MHz',...
'1900MHz','2.1GHz','2.3GHz','2.6GHz','3.6GHz','5.8GHz');
title('Path loss versus the propagation distance for diffirent
operating frequencies[Path7(Fixed Stationary Feeder:Roof-top to Roof-
top:NLOS)]');
xlabel('distance in meter');ylabel('path loss in dB');

figure(32)%NLOS
hold on; grid on;
plot (d3,PL_NLOS_FSF(:,8,1),'r');plot (d3,PL_NLOS_FSF(:,8,2),'b');
plot (d3,PL_NLOS_FSF(:,8,3),'k');plot (d3,PL_NLOS_FSF(:,8,4),'m');
plot (d3,PL_NLOS_FSF(:,8,5),'g');plot (d3,PL_NLOS_FSF(:,8,6),'c');
plot (d3,PL_NLOS_FSF(:,8,7),'b');plot (d3,PL_NLOS_FSF(:,8,8),'r');
plot (d3,PL_NLOS_FSF(:,8,9),'k');plot (d3,PL_NLOS_FSF(:,8,10),'m');
plot (d3,PL_NLOS_FSF(:,8,11),'g');plot (d3,PL_NLOS_FSF(:,8,12),'y');
legend('450MHz','700MHz','800MHz','850MHz','900MHz','1800MHz',...
'1900MHz','2.1GHz','2.3GHz','2.6GHz','3.6GHz','5.8GHz');
title('Path loss versus the propagation distance for diffirent
operating frequencies[Path8(Fixed Stationary Feeder:Roof-top to Roof-
top:NLOS)]');
xlabel('distance in meter');ylabel('path loss in dB');


%*********************************************************************
%plotting the simulation results for Moving Networks(LOS):
figure(33)
hold on; grid on;%LOS
plot (d4,PL_LOS_MoNe(:,1),'r');plot (d4,PL_LOS_MoNe(:,2),'b');
plot (d4,PL_LOS_MoNe(:,3),'k');plot (d4,PL_LOS_MoNe(:,4),'m');
plot (d4,PL_LOS_MoNe(:,5),'g');plot (d4,PL_LOS_MoNe(:,6),'c');
plot (d4,PL_LOS_MoNe(:,7),'b');plot (d4,PL_LOS_MoNe(:,8),'r');
plot (d4,PL_LOS_MoNe(:,9),'k');plot (d4,PL_LOS_MoNe(:,10),'m');
```

```
plot (d4,PL_LOS_MoNe(:,11),'g');plot (d4,PL_LOS_MoNe(:,12),'y');
legend('450MHz','700MHz','800MHz','850MHz','900MHz','1800MHz',...
'1900MHz','2.1GHz','2.3GHz','2.6GHz','3.6GHz','5.8GHz');
title('Path loss versus the propagation distance for diffirent
operating frequencies[Path1(Moving networks:LOS)]');
xlabel('distance in meter');ylabel('path loss in dB');


%*****************************************************************
%plotting the simulation results for Suburban macro-cell:
figure(34)
hold on; grid on;%LOS
plot (d5,PL_LOS_Suburban(:,1),'r');plot(d5,PL_LOS_Suburban(:,2),'b');
plot (d5,PL_LOS_Suburban(:,3),'k');plot(d5,PL_LOS_Suburban(:,4),'m');
plot (d5,PL_LOS_Suburban(:,5),'g');plot(d5,PL_LOS_Suburban(:,6),'c');
plot (d5,PL_LOS_Suburban(:,7),'b');plot(d5,PL_LOS_Suburban(:,8),'r');
plot(d5,PL_LOS_Suburban(:,9),'k');plot(d5,PL_LOS_Suburban(:,10),'m');
plot (d5,PL_LOS_Suburban(:,11),'g');
plot (d5,PL_LOS_Suburban(:,12),'y');
legend('450MHz','700MHz','800MHz','850MHz','900MHz','1800MHz',...
'1900MHz','2.1GHz','2.3GHz','2.6GHz','3.6GHz','5.8GHz');
title('Path loss versus the propagation distance for diffirent
operating frequencies [Path1(Suburban macro-cell:LOS)]');
xlabel('distance in meter');ylabel('path loss in dB');

figure(35)%NLOS
hold on; grid on;
plot (d5,PL_NLOS_Suburban(:,2,1),'r');
plot (d5,PL_NLOS_Suburban(:,2,2),'b');
plot (d5,PL_NLOS_Suburban(:,2,3),'k');
plot (d5,PL_NLOS_Suburban(:,2,4),'m');
plot (d5,PL_NLOS_Suburban(:,2,5),'g');
plot (d5,PL_NLOS_Suburban(:,2,6),'c');
plot (d5,PL_NLOS_Suburban(:,2,7),'b');
plot (d5,PL_NLOS_Suburban(:,2,8),'r');
plot (d5,PL_NLOS_Suburban(:,2,9),'k');
plot (d5,PL_NLOS_Suburban(:,2,10),'m');
plot (d5,PL_NLOS_Suburban(:,2,11),'g');
plot (d5,PL_NLOS_Suburban(:,2,12),'y');
legend('450MHz','700MHz','800MHz','850MHz','900MHz','1800MHz',...
'1900MHz','2.1GHz','2.3GHz','2.6GHz','3.6GHz','5.8GHz');
title('Path loss versus the propagation distance for diffirent
operating frequencies [Path2(Suburban macro-cell:NLOS)]');
xlabel('distance in meter');ylabel('path loss in dB');

figure(36)%NLOS
hold on; grid on;
plot (d5,PL_NLOS_Suburban(:,3,1),'r');
plot (d5,PL_NLOS_Suburban(:,3,2),'b');
plot (d5,PL_NLOS_Suburban(:,3,3),'k');
plot (d5,PL_NLOS_Suburban(:,3,4),'m');
plot (d5,PL_NLOS_Suburban(:,3,5),'g');
plot (d5,PL_NLOS_Suburban(:,3,6),'c');
plot (d5,PL_NLOS_Suburban(:,3,7),'b');
plot (d5,PL_NLOS_Suburban(:,3,8),'r');
plot (d5,PL_NLOS_Suburban(:,3,9),'k');
plot (d5,PL_NLOS_Suburban(:,3,10),'m');
plot (d5,PL_NLOS_Suburban(:,3,11),'g');
plot (d5,PL_NLOS_Suburban(:,3,12),'y');
legend('450MHz','700MHz','800MHz','850MHz','900MHz','1800MHz',...
```

```
'1900MHz','2.1GHz','2.3GHz','2.6GHz','3.6GHz','5.8GHz');
title('Path loss versus the propagation distance for diffirent
operating frequencies [Path3(Suburban macro-cell:NLOS)]');
xlabel('distance in meter');ylabel('path loss in dB');

figure(37)%NLOS
hold on; grid on;
plot (d5,PL_NLOS_Suburban(:,4,1),'r');
plot (d5,PL_NLOS_Suburban(:,4,2),'b');
plot (d5,PL_NLOS_Suburban(:,4,3),'k');
plot (d5,PL_NLOS_Suburban(:,4,4),'m');
plot (d5,PL_NLOS_Suburban(:,4,5),'g');
plot (d5,PL_NLOS_Suburban(:,4,6),'c');
plot (d5,PL_NLOS_Suburban(:,4,7),'b');
plot (d5,PL_NLOS_Suburban(:,4,8),'r');
plot (d5,PL_NLOS_Suburban(:,4,9),'k');
plot (d5,PL_NLOS_Suburban(:,4,10),'m');
plot (d5,PL_NLOS_Suburban(:,4,11),'g');
plot (d5,PL_NLOS_Suburban(:,4,12),'y');
legend('450MHz','700MHz','800MHz','850MHz','900MHz','1800MHz',...
'1900MHz','2.1GHz','2.3GHz','2.6GHz','3.6GHz','5.8GHz');
title('Path loss versus the propagation distance for diffirent
operating frequencies [Path4(Suburban macro-cell:NLOS)]');
xlabel('distance in meter');ylabel('path loss in dB');

figure(38)%NLOS
hold on; grid on;
plot (d5,PL_NLOS_Suburban(:,5,1),'r');
plot (d5,PL_NLOS_Suburban(:,5,2),'b');
plot (d5,PL_NLOS_Suburban(:,5,3),'k');
plot (d5,PL_NLOS_Suburban(:,5,4),'m');
plot (d5,PL_NLOS_Suburban(:,5,5),'g');
plot (d5,PL_NLOS_Suburban(:,5,6),'c');
plot (d5,PL_NLOS_Suburban(:,5,7),'b');
plot (d5,PL_NLOS_Suburban(:,5,8),'r');
plot (d5,PL_NLOS_Suburban(:,5,9),'k');
plot (d5,PL_NLOS_Suburban(:,5,10),'m');
plot (d5,PL_NLOS_Suburban(:,5,11),'g');
plot (d5,PL_NLOS_Suburban(:,5,12),'y');
legend('450MHz','700MHz','800MHz','850MHz','900MHz','1800MHz',...
'1900MHz','2.1GHz','2.3GHz','2.6GHz','3.6GHz','5.8GHz');
title('Path loss versus the propagation distance for diffirent
operating frequencies [Path5(Suburban macro-cell:NLOS)]');
xlabel('distance in meter');ylabel('path loss in dB');

figure(39)%NLOS
hold on; grid on;
plot (d5,PL_NLOS_Suburban(:,6,1),'r');
plot (d5,PL_NLOS_Suburban(:,6,2),'b');
plot (d5,PL_NLOS_Suburban(:,6,3),'k');
plot (d5,PL_NLOS_Suburban(:,6,4),'m');
plot (d5,PL_NLOS_Suburban(:,6,5),'g');
plot (d5,PL_NLOS_Suburban(:,6,6),'c');
plot (d5,PL_NLOS_Suburban(:,6,7),'b');
plot (d5,PL_NLOS_Suburban(:,6,8),'r');
plot (d5,PL_NLOS_Suburban(:,6,9),'k');
plot (d5,PL_NLOS_Suburban(:,6,10),'m');
plot (d5,PL_NLOS_Suburban(:,6,11),'g');
plot (d5,PL_NLOS_Suburban(:,6,12),'y');
legend('450MHz','700MHz','800MHz','850MHz','900MHz','1800MHz',...
'1900MHz','2.1GHz','2.3GHz','2.6GHz','3.6GHz','5.8GHz');
```

```
title('Path loss versus the propagation distance for diffirent
operating frequencies [Path6(Suburban macro-cell:NLOS)]');
xlabel('distance in meter');ylabel('path loss in dB');

figure(40)%NLOS
hold on; grid on;
plot (d5,PL_NLOS_Suburban(:,7,1),'r');
plot (d5,PL_NLOS_Suburban(:,7,2),'b');
plot (d5,PL_NLOS_Suburban(:,7,3),'k');
plot (d5,PL_NLOS_Suburban(:,7,4),'m');
plot (d5,PL_NLOS_Suburban(:,7,5),'g');
plot (d5,PL_NLOS_Suburban(:,7,6),'c');
plot (d5,PL_NLOS_Suburban(:,7,7),'b');
plot (d5,PL_NLOS_Suburban(:,7,8),'r');
plot (d5,PL_NLOS_Suburban(:,7,9),'k');
plot (d5,PL_NLOS_Suburban(:,7,10),'m');
plot (d5,PL_NLOS_Suburban(:,7,11),'g');
plot (d5,PL_NLOS_Suburban(:,7,12),'y');
legend('450MHz','700MHz','800MHz','850MHz','900MHz','1800MHz',...
'1900MHz','2.1GHz','2.3GHz','2.6GHz','3.6GHz','5.8GHz');
title('Path loss versus the propagation distance for diffirent
operating frequencies [Path7(Suburban macro-cell:NLOS)]');
xlabel('distance in meter');ylabel('path loss in dB');

figure(41)%NLOS
hold on; grid on;
plot (d5,PL_NLOS_Suburban(:,8,1),'r');
plot (d5,PL_NLOS_Suburban(:,8,2),'b');
plot (d5,PL_NLOS_Suburban(:,8,3),'k');
plot (d5,PL_NLOS_Suburban(:,8,4),'m');
plot (d5,PL_NLOS_Suburban(:,8,5),'g');
plot (d5,PL_NLOS_Suburban(:,8,6),'c');
plot (d5,PL_NLOS_Suburban(:,8,7),'b');
plot (d5,PL_NLOS_Suburban(:,8,8),'r');
plot (d5,PL_NLOS_Suburban(:,8,9),'k');
plot (d5,PL_NLOS_Suburban(:,8,10),'m');
plot (d5,PL_NLOS_Suburban(:,8,11),'g');
plot (d5,PL_NLOS_Suburban(:,8,12),'y');
legend('450MHz','700MHz','800MHz','850MHz','900MHz','1800MHz',...
'1900MHz','2.1GHz','2.3GHz','2.6GHz','3.6GHz','5.8GHz');
title('Path loss versus the propagation distance for diffirent
operating frequencies [Path8(Suburban macro-cell:NLOS)]');
xlabel('distance in meter');ylabel('path loss in dB');


%*********************************************************************
%plotting the simulation results for Indoor to outdoor:
figure(42)
hold on; grid on;
plot (d6,LosstTot(:,1,1),'r');plot (d6,LosstTot(:,1,2),'b');
plot (d6,LosstTot(:,1,3),'k');plot (d6,LosstTot(:,1,4),'m');
plot (d6,LosstTot(:,1,5),'g');plot (d6,LosstTot(:,1,6),'c');
plot (d6,LosstTot(:,1,7),'b');plot (d6,LosstTot(:,1,8),'r');
plot (d6,LosstTot(:,1,9),'k');plot (d6,LosstTot(:,1,10),'m');
plot (d6,LosstTot(:,1,11),'g');plot (d6,LosstTot(:,1,12),'y');
legend('450MHz','700MHz','800MHz','850MHz','900MHz','1800MHz',...
'1900MHz','2.1GHz','2.3GHz','2.6GHz','3.6GHz','5.8GHz');
title('Path loss versus the propagation distance for diffirent
operating frequencies [Path1(Indoor to outdoor)]');
xlabel('distance in meter');ylabel('path loss in dB');
```

```
figure(43)
hold on; grid on;
plot (d6,LosstTot(:,2,1),'r');plot (d6,LosstTot(:,2,2),'b');
plot (d6,LosstTot(:,2,3),'k');plot (d6,LosstTot(:,2,4),'m');
plot (d6,LosstTot(:,2,5),'g');plot (d6,LosstTot(:,2,6),'c');
plot (d6,LosstTot(:,2,7),'b');plot (d6,LosstTot(:,2,8),'r');
plot (d6,LosstTot(:,2,9),'k');plot (d6,LosstTot(:,2,10),'m');
plot (d6,LosstTot(:,2,11),'g');plot (d6,LosstTot(:,2,12),'y');
legend('450MHz','700MHz','800MHz','850MHz','900MHz','1800MHz',...
'1900MHz','2.1GHz','2.3GHz','2.6GHz','3.6GHz','5.8GHz');
title('Path loss versus the propagation distance for diffirent
operating frequencies [Path2(Indoor to outdoor)]');
xlabel('distance in meter');ylabel('path loss in dB');

figure(44)
hold on; grid on;
plot (d6,LosstTot(:,3,1),'r');plot (d6,LosstTot(:,3,2),'b');
plot (d6,LosstTot(:,3,3),'k');plot (d6,LosstTot(:,3,4),'m');
plot (d6,LosstTot(:,3,5),'g');plot (d6,LosstTot(:,3,6),'c');
plot (d6,LosstTot(:,3,7),'b');plot (d6,LosstTot(:,3,8),'r');
plot (d6,LosstTot(:,3,9),'k');plot (d6,LosstTot(:,3,10),'m');
plot (d6,LosstTot(:,3,11),'g');plot (d6,LosstTot(:,3,12),'y');
legend('450MHz','700MHz','800MHz','850MHz','900MHz','1800MHz',...
'1900MHz','2.1GHz','2.3GHz','2.6GHz','3.6GHz','5.8GHz');
title('Path loss versus the propagation distance for diffirent
operating frequencies [Path3(Indoor to outdoor)]');
xlabel('distance in meter');ylabel('path loss in dB');

figure(45)
hold on; grid on;
plot (d6,LosstTot(:,4,1),'r');plot (d6,LosstTot(:,4,2),'b');
plot (d6,LosstTot(:,4,3),'k');plot (d6,LosstTot(:,4,4),'m');
plot (d6,LosstTot(:,4,5),'g');plot (d6,LosstTot(:,4,6),'c');
plot (d6,LosstTot(:,4,7),'b');plot (d6,LosstTot(:,4,8),'r');
plot (d6,LosstTot(:,4,9),'k');plot (d6,LosstTot(:,4,10),'m');
plot (d6,LosstTot(:,4,11),'g');plot (d6,LosstTot(:,4,12),'y');
legend('450MHz','700MHz','800MHz','850MHz','900MHz','1800MHz',...
'1900MHz','2.1GHz','2.3GHz','2.6GHz','3.6GHz','5.8GHz');
title('Path loss versus the propagation distance for diffirent
operating frequencies [Path4(Indoor to outdoor)]');
xlabel('distance in meter');ylabel('path loss in dB');

figure(46)
hold on; grid on;
plot (d6,LosstTot(:,5,1),'r');plot (d6,LosstTot(:,5,2),'b');
plot (d6,LosstTot(:,5,3),'k');plot (d6,LosstTot(:,5,4),'m');
plot (d6,LosstTot(:,5,5),'g');plot (d6,LosstTot(:,5,6),'c');
plot (d6,LosstTot(:,5,7),'b');plot (d6,LosstTot(:,5,8),'r');
plot (d6,LosstTot(:,5,9),'k');plot (d6,LosstTot(:,5,10),'m');
plot (d6,LosstTot(:,5,11),'g');plot (d6,LosstTot(:,5,12),'y');
legend('450MHz','700MHz','800MHz','850MHz','900MHz','1800MHz',...
'1900MHz','2.1GHz','2.3GHz','2.6GHz','3.6GHz','5.8GHz');
title('Path loss versus the propagation distance for diffirent
operating frequencies [Path5(Indoor to outdoor)]');
xlabel('distance in meter');ylabel('path loss in dB');

figure(47)
hold on; grid on;
plot (d6,LosstTot(:,6,1),'r');plot (d6,LosstTot(:,6,2),'b');
plot (d6,LosstTot(:,6,3),'k');plot (d6,LosstTot(:,6,4),'m');
```

```
plot (d6,LosstTot(:,6,5),'g');plot (d6,LosstTot(:,6,6),'c');
plot (d6,LosstTot(:,6,7),'b');plot (d6,LosstTot(:,6,8),'r');
plot (d6,LosstTot(:,6,9),'k');plot (d6,LosstTot(:,6,10),'m');
plot (d6,LosstTot(:,6,11),'g');plot (d6,LosstTot(:,6,12),'y');
legend('450MHz','700MHz','800MHz','850MHz','900MHz','1800MHz',...
'1900MHz','2.1GHz','2.3GHz','2.6GHz','3.6GHz','5.8GHz');
title('Path loss versus the propagation distance for diffirent
operating frequencies [Path6(Indoor to outdoor)]');
xlabel('distance in meter');ylabel('path loss in dB');

figure(48)
hold on; grid on;
plot (d6,LosstTot(:,7,1),'r');plot (d6,LosstTot(:,7,2),'b');
plot (d6,LosstTot(:,7,3),'k');plot (d6,LosstTot(:,7,4),'m');
plot (d6,LosstTot(:,7,5),'g');plot (d6,LosstTot(:,7,6),'c');
plot (d6,LosstTot(:,7,7),'b');plot (d6,LosstTot(:,7,8),'r');
plot (d6,LosstTot(:,7,9),'k');plot (d6,LosstTot(:,7,10),'m');
plot (d6,LosstTot(:,7,11),'g');plot (d6,LosstTot(:,7,12),'y');
legend('450MHz','700MHz','800MHz','850MHz','900MHz','1800MHz',...
'1900MHz','2.1GHz','2.3GHz','2.6GHz','3.6GHz','5.8GHz');
title('Path loss versus the propagation distance for diffirent
operating frequencies [Path7(Indoor to outdoor)]');
xlabel('distance in meter');ylabel('path loss in dB');

figure(49)
hold on; grid on;
plot (d6,LosstTot(:,8,1),'r');plot (d6,LosstTot(:,8,2),'b');
plot (d6,LosstTot(:,8,3),'k');plot (d6,LosstTot(:,8,4),'m');
plot (d6,LosstTot(:,8,5),'g');plot (d6,LosstTot(:,8,6),'c');
plot (d6,LosstTot(:,8,7),'b');plot (d6,LosstTot(:,8,8),'r');
plot (d6,LosstTot(:,8,9),'k');plot (d6,LosstTot(:,8,10),'m');
plot (d6,LosstTot(:,8,11),'g');plot (d6,LosstTot(:,8,12),'y');
legend('450MHz','700MHz','800MHz','850MHz','900MHz','1800MHz',...
'1900MHz','2.1GHz','2.3GHz','2.6GHz','3.6GHz','5.8GHz');
title('Path loss versus the propagation distance for diffirent
operating frequencies [Path8(Indoor to outdoor)]');
xlabel('distance in meter');ylabel('path loss in dB');
```

Appendix (B):

Published work:

Here is a scientific paper which is done in this project and it has been officially accepted by the IEEE.

Dear Khaled Hijjeh,

It is our pleasure to congratulate you that your papers,

1. **MATLAB SIMULATIONS ABOUT THE EFFECT OF LOS AND XPD ON ERGODIC CAPACITY OF A MIMO SYSTEM WITH CSI KNOWN AT TRANSMITTER**
2. **MATLAB SIMULATION FOR A MIMO CHANNEL MODELING UNDER BAD URBAN AND RURAL MACRO CELL ENVIRONMENTS**
3. **MATLAB SIMULATION FOR DIVERSITY IN 8 X 2 MIMO SYSTEM USING OSTBC**

have been accepted and nominated for the competition of the awards.

In order to process all the required documents for your VISA application, please fill in the relevant information before 22 May.

All authors should be aware that all papers accepted by the IEEE iWEM2011 must register. Except for the registration, you should also sign the copyright form and mail to iwem2011@gmail.com. Your papers will not appear at proceeding and IEEE Xplore if your registration and copyright form have not completed before 22 May.

The attach file is IEEE copyright form and competition form document, you should fill in it and mail to iwem2011@gmail.com. Please note that all attendants can register for the IEEE iWEM2011 conference at the online registration (http://ikea.myvnc.com/2011iWEM/).

We appreciate your participation. I am looking forward to seeing you soon in Taipei.

Best regards.

Dau-Chyrh Chang

Dau-Chyrh Chang
Fellows of IEEE, IET, and EMA
Chair Professor, Department of Communication Engineering
Director, Communication Research Center
Oriental Institute of Technology
Email:dcchang@mail.oit.edu.tw
Tel:+886-2-77380211 (O), +886-933557928(m)

MATLAB SIMULATION FOR (4x2) MIMO CHANNEL MODELING UNDER BAD URBAN AND RURAL MACRO CELL ENVIRONMENTS

Khaled Hijjeh[(1)], Ahmed Mujahed[(2)], Mohammed Jaber[(2)], Suzan Al-Hroub[(2)], Narmeen Dawadeh[(2)]
(1) Palestine Cellular Communication Ltd., Ramallah, Palestine. E.mail: Khaled.Hijjeh@jawwal.ps
(2) Palestine Polytechnic University, Hebron, Palestine

Abstract- The paper studies the behavior of bad urban and rural channel models for (4x2) MIMO multipath fading channel. The fading envelops for different paths were observed and analyzed manipulating different parameters: changing the symbol rate, doppler shift, and antennas spacing in order to understand the behavior of the MIMO channel so as to ease the deployment of the entire MIMO system. The simulation results shows that the channel behavior is getting better and becomes more stable when increasing the symbol rate and antennas spacing, and at the same time reducing the Doppler shift.

I. INTRODUCTION

Multiple-Input Multiple-Output (MIMO) systems have recently attracted much attention, since it offers significant increases in data throughput without additional bandwidth or transmit power, which cannot be offered by conventional single antenna communication systems. It achieves this by higher spectral efficiency and link reliability. Thereafter, realistic MIMO channel models are required in order to assess the performance of the entire MIMO systems. Currently, Modeling the MIMO channel is receiving significant attention [1][2][3].

This paper discuss MIMO channel behavior for different propagation parameters such as symbol rate, doppler shift, and T_x and R_x antenna spacing under two propagation scenarios; bad urban macro-cell and rural macro-cell. These two channels are described briefly in the following:

- **Bad urban macro-cell scenario:** describes cities with buildings with distinctly inhomogeneous building heights or densities. The inhomogeneity in city structure can be for example due to large water areas separating the built-up areas, or the high-rise skyscrapers in otherwise typical urban environment. Therefore, NLOs components are commonly considered.
- **Rural macro-cell:** represents radio propagation in large areas with low building density. LOS conditions can be expected to be in most of the coverage area because of the height of the base station antenna is much higher than the average building height.

The rest of this paper is organized as follows; Section II introduces the system of the channel model. The results of observing the MIMO channel response for the propagation environments with the two antenna configuration mentioned earlier are discussed in Section III, where Section IV is devoted for the conclusions.

II. SYSTEM MODEL

The paper simulates MIMO system with M_T transmit antennas and M_R receive antennas. The MIMO system's channel $H(\tau, t)$ consists of $h_{i,j}(\tau, t)$ denoting the impulse response between the j^{th} $(j = 1,2,\ldots, M_T)$ transmit antenna and the i^{th} $(i = 1,2,\ldots,M_R)$ receive antenna. Accordingly, the overall MIMO channel can be given as follows:

$$H(\tau,t)=\begin{bmatrix} h_{1,1}(\tau,t) & h_{1,2}(\tau,t) & \cdots & h_{1,M_T}(\tau,t) \\ h_{2,1}(\tau,t) & h_{2,2}(\tau,t) & & h_{2,M_T}(\tau,t) \\ \vdots & & \ddots & \vdots \\ h_{M_R,1}(\tau,t) & h_{M_R,2}(\tau,t) & \cdots & h_{M_R,M_T}(\tau,t) \end{bmatrix}$$

Given that the modulated information signal $s_j(t)$ launched from the j^{th} transmit antenna, the received signal at the i^{th} receive antenna; $y_i(t)$ can be given as

$$y_i(t)=\sum_{j=1}^{M_T} h_{i,j}(\tau,t)*s_j(t),\ \ i=1,2,\ldots.,M_R \quad (1)$$

To formulate the impulse responses $h_{i,j}(\tau,t)$ between the j^{th} and the i^{th} transmit and receive antenna elements the paper referred to the defined path loss formulas in [4] given as follows:

- In the case of the bad urban macro-cell, the path loss equation that has been considered is [4]:

$$PL=44.9-6.55\log_{10}(h_{BS}[m])\log_{10}(d[m])+34.46+5.83\log_{10}(h_{MS}[m])+20\log_{10}\left(\frac{f[GHz]}{5}\right)+8 \quad (2)$$

Where h_{BS} and h_{MS} are the heights of the base station and the mobile station respectively, d is the distance between the T_x and R_x antennas.

- While the path loss equation that has been considered in the case of rural macro-cell is [4]:

$$PL=25.11\log_{10}(d)+\ 55.4-0.13(h_{BS}-25)\log_{10}\left(\frac{d}{100}\right)-0.9(h_{MS}-1.5)+21.3\log_{10}\left(\frac{f_c}{5}\right)+8 \quad (3)$$

Where f_c is the center frequency.

The cross-correlation between the waves impinging on two antenna elements has been studied in numerous references [5][6][7]. It has been shown that the evolution of the correlation coefficient as a function of the distance between the antenna elements mostly depends on the Power Azimuth Spectrum (PAS) and on the radiation pattern of the antenna.

- **Main simulation steps**

1. The simulation process is initialized firstly by setting the main channel parameters.
2. Then, the multipath components were divided into three clusters each with five paths LOS and NLOS.
3. Two path loss models were used;
   a. Bad urban macro-cell and
   b. Rural macro-cell.
4. Transmit and receive correlation matrices for 4x2 system was developed.
5. Finally, a MIMO channel was constructed and the channel behavior being observed for each path while manipulating the symbol rate, doppler shift, and T_x and R_x antenna spacing.

III. RESULTS

As a reference point the following graphs in Figure.(1.a) and (1.b) shows the response of the MIMO channel under bad urban and rural macro-cells environments while maintaining: symbol rate=10^3, doppler shift of 2 for bad urban and 0.4 for rural, and T_x and R_x spacing of 1 λ and 0.5 λ respectively.

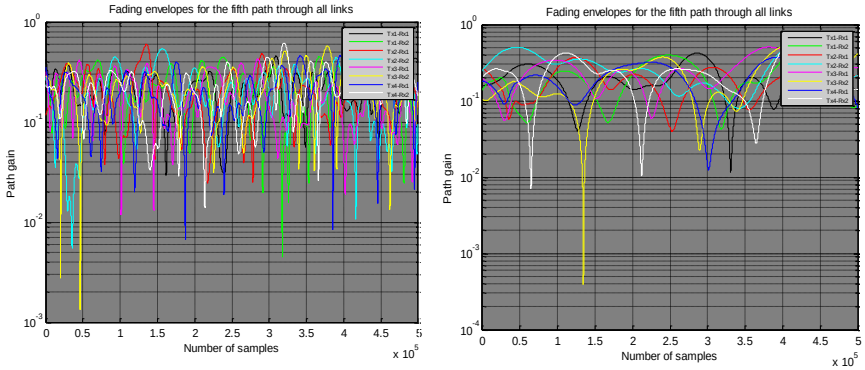

(a) **(b)**

Figure (1)

(a) Bad urban macro cell behavior at original states; symbol rate 10^3, Doppler shift=2, T_x and R_x spacing of 1λ and 0.5 λ
(b) Rural macro cell behavior at original states; symbol rate 10^3, Doppler shift=0.4, T_x and R_x spacing of 1λ and 0.5 λ

- **Observing the effects of changing the symbol rate, doppler shift, and antennas spacing.**

A. Symbol rate effect:

Figures (2.a) and (2.b) shows the fading envelopes of the fifth path through all links when increasing the symbol rate to 10^4 symbol/second and when decreasing its value to 10^2 respectively, considering the bad urban macro cell scenario. Increasing the symbol rate leads to reduced symbol period and as a result the probability of the symbol's transmission within the coherence time will increase, that is the symbol will travel through the channel while it is not varying ,which means the variations of the channel that the symbol will examine will be less, and vice versa when reducing the symbol rate.

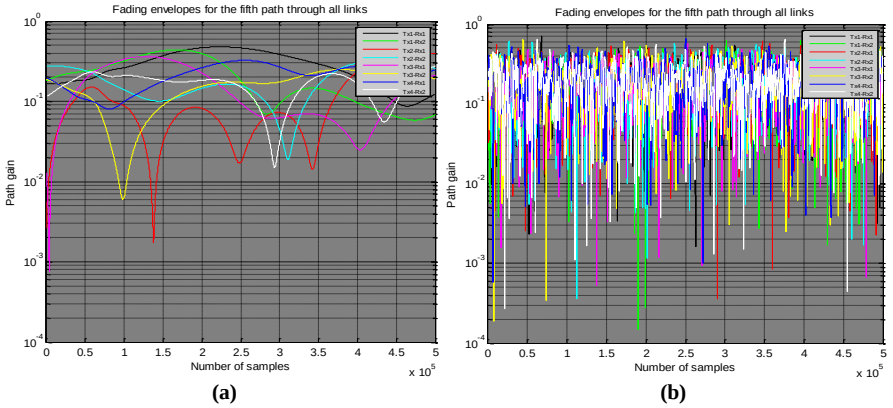

(a) **(b)**

Figure (2)

Bad urban macro cell behavior at **(a)** 10^4 symbols/sec and **(b)** at 10^2 symbols/sec

B. ***Doppler shift effect:***

Figure.(3.a) and (3.b) show the fading envelopes of the fifth path through all links when reducing the Doppler shift from 2 to 1 and when increasing its value to 3 respectively, considering the bad urban macro cell scenario. Reducing the doppler shift value from 2 to 1 result in slow variations in the fading envelopes, so more smooth envelopes are found to occur. In reality, this indicates the slowly movements of the transmitter and the receiver, they may be considered almost fixed. Moreover, the probability of line of sight between the transmitter and the receiver is implicitly increases, and vice versa when increasing its value.

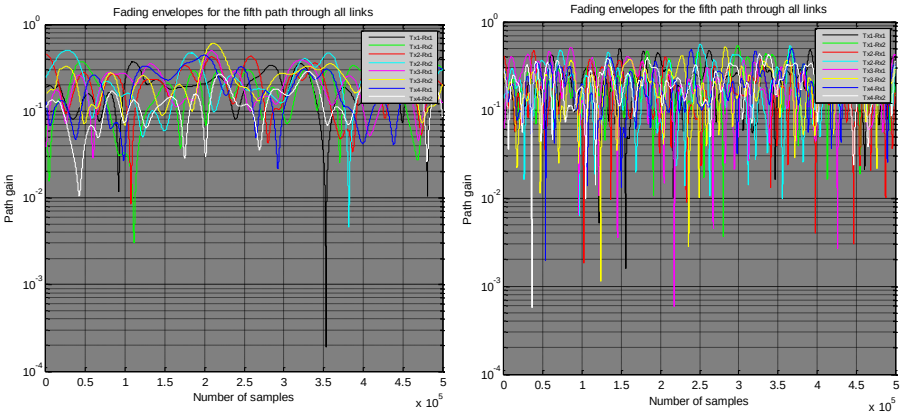

(a) **(b)**

Figure (3)
Bad urban macro cell behavior at doppler shift **(a)** at 1 and **(b)** at 3

C. ***Antennas spacing effect:***

Considering the rural macro cell scenario, figure.(4.a) shows the fading envelopes of the fifth path when increasing the T_x and R_x spacing from 1λ to 3λ and from 0.5λ to 3λ respectively. While figure (4.b) shows the effect of decreasing T_x and R_x spacing from 1λ to 0.15λ and from 0.5λ to 0.15λ. The results indicate that increasing the spacing distance between the T_x and R_x antennas, the performance of the system is almost like an ideal system with independent transmitting and receiving antennas. On the other hand, decreasing the antennas spacing will lead to high correlation between the signals and accordingly results on poor system performance.

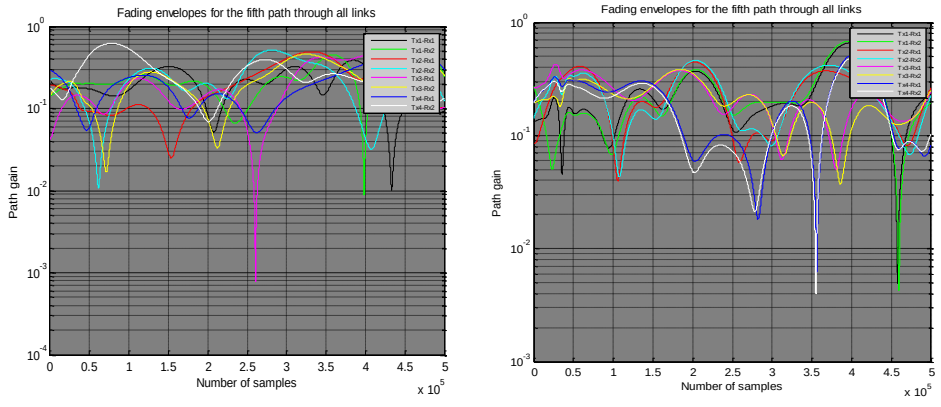

(a) **(b)**

Figure (4) Rural macro cell behavior when:
(c) Increasing the T_x and R_x spacing from 1λ to 3λ and from 0.5λ to 3λ respectively.
(d) Decreasing T_x and R_x spacing from 1λ to 0.15λ and from 0.5λ to 0.15λrespectively.

IV. CONCLUSION

This paper studied through simulation the MIMO channel model that deals with 4x2 configurations under bad urban macro-cell and rural macro-cell environments. The response of the MIMO channel for the two scenarios with different values for symbol rate, doppler shift and spacing between the transmitting and receiving antennas was observed. The simulation results show that the channel behavior is getting better and becomes more stable as increasing the symbol rate, antennas spacing, and reducing the doppler shift.

REFERENCES

[1] G.J. Foschini and M.J. Gans, "On limits of wireless communications in a fading environment when using multiple antennas," Wireless Pers. Communication, 1998.

[2] J. Govi and J. Govil, "4G Mobile Communication Systems: Turns, Trends and Transition", International Conference on Convergence Information Technology. 2007.

[3] A. Paulraj, R. Nabar, and D. Gore, *Introduction to space-time wireless communications*, Cambridge University Press, 2006.

[4] P. Kyosti and others, "WINNER II interim channel models," 2007.

[5] K. I. Pedersen, P. E. Mogensen, and B. H. Fleury, "Spatial Channel Characteristics in Outdoor Environments and their Impact on BS Antenna System Performance," in Proceedings of IEEE Vehicular Technology Conference VTC 1998, Ottawa, Canada, vol. 2, pp. 719–723, 1998.

[6] L. Schumacher, K. I. Pedersen, and P. E.Mogensen, "From antenna spacings to theoretical capacities-Guidelines for simulating MIMO systems", Proc. PIMRC Conf., vol. 2, pp. 587-592, Sep. 2002.

[7] J. Fuhl, A. F. Molisch, and E. Bonek,"Unified Channel Model for Mobile Radio Systems with Smart Antennas," IEEE Proceedings - Radar, Sonar Navigation, vol. 145, pp. 32–41, Feb. 1998.